Benha University
Faculty of Engineering at Shoubra
Surveying Engineering Department

ENHANCEMENT OF GLOBAL GEOPOTENTIAL HARMONIC MODELS FOR EGYPT

A Thesis Submitted in Partial Fulfillment of the Requirements for the M.Sc. Degree in Surveying and Geodesy

Submitted By
Eng. Abd-Elrahim Ruby Abd-Elhamid Hassanain
B.Sc. in Surveying Engineering (2011)

Supervised By

Prof. Ahmed A. Shaker
Prof. of Surveying and Geodesy
Faculty of Engineering at Shoubra
Benha University

Assoc. Prof. Maher M. Amin
Assoc. Prof. of Surveying and Geodesy
Faculty of Engineering at Shoubra
Benha University

Dr. Mervat M. Refaat
Lecturer of Surveying and Geodesy
Faculty of Engineering at Shoubra
Benha University

Cairo – Egypt

2018

Benha University
Faculty of Engineering at Shoubra
Surveying Engineering Department

APPROVAL SHEET

Enhancement of Global Geopotential Harmonic Models for Egypt

A Thesis Submitted in Partial Fulfillment of the Requirements for the M.Sc. Degree in Surveying and Geodesy

Submitted by
Eng. Abd-Elrahim Ruby Abd-Elhamid Hassanain
B.Sc. in Surveying Engineering (2011)

Examiners Committee

Prof. Dr. Ahmed Abdel Sattar Shaker Signature:

Professor of Surveying and Geodesy,
Faculty of Engineering at Shoubra,
Benha University, Cairo, Egypt.

Prof. Dr. Mohamed El Hoseny A. El Tokhey Signature:

Professor of Surveying and Geodesy,
Faculty of Engineering,
Ain Shams University, Cairo, Egypt.

Prof. Dr. Ali Ahmed El-Sagheer Signature:

Professor of Surveying and Geodesy,
Faculty of Engineering at Shoubra,
Benha University, Cairo, Egypt.

Assoc. Prof. Maher Mohamed M. Amin Signature:

Assoc. Professor of Surveying and Geodesy,
Faculty of Engineering at Shoubra,
Benha University, Cairo, Egypt.

Date: 20 / 2 / 2018

Dedication

This thesis is dedicated to my ***parents***; my wife, ***Rasha***, and to my friend, ***Alaa***, who have supported and sustained me during my research. This accomplishment would not have been possible without them. Thank you. Also, this work is dedicated to my kids ***Yaseen*** and ***Jana***.

Abd-Elrahim

Acknowledgements

Without the help of Allah, this work would not be completed nor achieved and any valuable work is a result of efforts of many individuals.

Foremost, it is with immense gratitude that I acknowledge the support and help of my ***Prof. Ahmed Abdel Sattar Shaker***, who is the head of the research team. The door to *Prof. Shaker* office was always open whenever I ran into a trouble spot or had a question about my research.

I would like to express my sincere gratitude to my supervisor ***Assoc. Prof. Maher Mohamed Amin*** for the continuous support for my M.Sc. His guidance helped me in all the time of research and writing of this thesis.

My sincere thanks go to ***Dr. Mervat Mohamed Refaat*** for her special pursuit to bring the gravity data from Ganoub El- Wadi Petroleum Holding Company (Ganope).

I would like to extend my gratitude to ***Prof. Mohamed El Hoseny A. El Tokhey*** and ***Prof. Ali A. El-Sagheer*** for revisions and editing this Thesis. Thanks to ***Prof. Saad Bolbol*** and ***Prof. Abd-allah A. Saad*** for providing me with GPS/Levelling data for the study area.

I would like to acknowledge ***Prof. C.C. Tscherning*** (R.I.P. 1942 – 2014) for providing me the *GRAVSOFT* software. In addition, I would like to very thankful to ***Prof. René Forsberg*** and ***Prof. Tomislav Bašić*** for providing me the *PMITES* program of harmonic analysis by integral techniques and helpful discussions. Thanks much to ***Dr. Josef Sebera*** for sent me a modified version of FORTRAN program Harmonic_Synth_v02.

Finally, large acknowledgment could be presented to *Egyptian General Petroleum Corporation* (EGPC) - Information Center, *Ganope Company* and *Bureau Gravimétrique International* (BGI) for providing me the gravity data for the study area.

Abstract

The aim of this research is to develop a new precise and high-resolution geoid model for Egypt by refining the Global Geopotential Models (GGMs) through a process named tailoring, where the existing spherical harmonic coefficients of geopotential model are fitted to the Egyptian gravity field by integral formulas using an iterative algorithm to improve the accuracy of the obtained harmonic coefficients.

The satellite-only model GOCO05s (complete to degree and order 280) and ultra-high degree geopotential model EGM2008 (complete to degree and order 2190) have been tailored to the Egyptian 5′×5′ mean gravity anomalies in order to select the optimal model that can be used for the reference gravity field for the new geoid model. The results show that both EG1GOC5s and EGTM0818 tailored geopotential models give less and better residual gravity anomalies, where the EGTM0818 tailored model has been improved significantly by about 27% than the EGM2008 model similarly, the EG1GOC5s tailored model better than the GOCO05s model by about 17%.

Gravimetric and combined (gravity and astrogeodetic data) geoids solutions for Egypt have been computed using both tailored geopotential models in the remove-restore technique through Least-squares Collocation (LSC). The computed geoids are fitted to the GPS/levelling stations. The results show that no significant variance between the gravimetric and combined geoids solutions exists. In addition, both combined geoids solutions are given the same accuracy, where RMS ≈ ± 15 cm.

Finally, a comparison between GPS/levelling stations and both $N_{\text{GRAV-A}}$ and $N_{\text{GRAV-B}}$ gravimetric geoids computed by using both EG1GOC5s and EGTM0818 models, respectively, give nearly the same external accuracy, where the RMS of the differences ± 13 cm for $N_{\text{GRAV-A}}$ and ± 15 cm for $N_{\text{GRAV-B}}$. Therefore, we recommend that both tailored geopotential models as reliable models for geoid heights over Egypt.

Table of Contents

List of Figures

List of Tables

List of Abbreviations

ACE	Altimetry Corrected Elevations
AGP	African Gravity Project
ALFs	Associated Legendre Functions
ArcGP	Arctic Gravity Project
BGI	Bureau Gravimétrique International
BVP	Boundary Value Problem
CHAMP	CHAllenging Minisatellite Payload
DMA	Defense Mapping Agency
DOT	Dynamic Ocean Topography
DTM	Digital Terrain Model
DTU	Technical University of Denmark
EAEA	Egyptian Atomic Energy Authority
ECAA	Egyptian Civil Aviation Authority
EG1GOC5s	Tailored Model for Egypt Based on the GOCO05s (N = 280)
EGM	Earth Gravity field Model
EGM08TF	Tailored Model for Egypt Based on the EGM2008 (N =360)
EGM2008	Earth Gravitational Model 2008
EGM96	Earth Gravitational Model 1996
EGPC	Egyptian General Petroleum Corporation
EGSMA	Egyptian Mineral Resources General Authority
EGTM0818	Tailored Model EGM08F plus EGM2008 (361<N <2190)
ENGSN97	Egyptian National Gravity Standardization Net1997
ESA	Egyptian Survey Authority
FFG	Fugro Ground Geophysics
FFT	Fast Fourier Transform
Ganope	Ganoub El- Wadi Petroleum Holding Company
GGMs	Global Geopotential Model(s)

GLOBE	Global Land One-kilometer Base Elevation
GNSS	Global Navigation Satellite System
GOCE	Gravity field and steady-state Ocean Circulation
GOCO	Gravity Observation Combination Consortium
GPC	General Petroleum Company
GPS	Global Positioning System
GRACE	Gravity Recovery And Climate Experiment
GRS	Geodetic Reference System
GSFC	Goddard Space Flight Center
GSHA	Global Spherical Harmonic Analysis
GSHS	Global Spherical Harmonic Synthesis
HARN	High Accurate Reference Network
IAG	International Association of Geodesy
ICESat	Ice, Cloud, and land Elevation Satellite
ICGEM	International Centre for Global Earth Models
IERS	International Earth Rotation and Reference Systems Service
IGFS	International Gravity Field Service
IGS	International Geodynamic Service
IGSN71	International Gravity Standardization Network 1971
LSC	Least Squares Collocation
MSL	Mean Sea Level
NASA	National Aeronautics and Space Administration
N_{COMB-A}	Combined geoid (gravity and astrogeodetic data) for Egypt using LSC and the tailored model EG1GOC5s
N_{COMB-B}	Combined geoid (gravity and astrogeodetic data) for Egypt using LSC and the tailored model EGTM0818
NED-95	New Egyptian Datum 1995
$N_{EG1GOC5s}$	Geoid Model for Egypt Derived from Coefficients of EG1GOC5s

$N_{EGM2008}$	Geoid Model for Egypt Derived from Coefficients of EGM2008
N_{EGM96}	Geoid Model for Egypt Derived from Coefficients of EGM96
$N_{EGTM0818}$	Geoid Model for Egypt Derived from Coefficients of EGTM0818
NGA	National Geospatial-Intelligence Agency
$N_{GOCO05s}$	Geoid Model for Egypt Derived from Coefficients of GOCO05s
N_{GRAV-A}	Gravimetric geoid for Egypt using LSC and the tailored model EG1GOC5s
N_{GRAV-B}	Gravimetric geoid for Egypt using LSC and the tailored model EGTM0818
NGSBN-77	National Gravity Standard Base Network 1977
NIMA	National Imagery and Mapping Agency
NRIAG	National Research Institute of Astronomy and Geophysics
OED	Old Egyptian Datum
OSU	Ohio State University
ppm	part per million
Pty Ltd	Private Company Limited
R.I.P	Rest in Peace
RMS	Root Mean Square
RTM	Residual Terrain Model
SLR	Satellite Laser Ranging
SRI	Survey Research Institutes
SRTM	Shuttle Radar Topography Mission
SST	Sea-Surface Topography
TIM	Time – Wise solution
VLBI	Very-long-baseline interferometry
WGS 84	World Geodetic System 1984
WGS 72	World Geodetic System 1972

Chapter 1

INTRODUCTION

1. INTRODUCTION

1.1 Preamble

Precise geoid determination has been an important research topic in geodesy and geophysics in the past two decades. A geoid is required to define a national vertical datum. In addition, geoid models allow transforming ellipsoidal heights, which are relatively easily determined from GPS observations, into physical heights, which are associated with the Earth's gravity field, without the need for expensive and time-consuming spirit-leveling (Pinon, 2016).

Nowadays, Global Geopotential Models (GGMs) may be used as a reference to support the development of more detailed regional/local geoids or to provide the geoid heights on its own. GGMs are mainly derived from satellite gravity measurements and/or from a combination of a satellite model, terrestrial gravimetry, altimeter-derived gravity data in marine areas, and more recently airborne gravimetry.

The current GGMs may contain long-wavelength errors due to difficulties in collecting and using global gravity data as well as may be different estimation techniques were used to compute different spectral bands of the model (Heck, 1990; Saleh et al. 2013), which in turn affect the geoid heights obtained from these models.

Moreover, their data density is often heterogeneous, with data gaps in mountainous regions, dense vegetation and nearshore or sea ice covered areas, which further degrades the quality of any terrestrially derived gravity field models (Bolkas et al., 2016), whereas data availability and data accuracy can only be enhanced by performing additional observations,

accordingly the resolution of the geopotential models can then be improved by increasing its maximum degree.

In addition, practical studies had proved that the methods of tailoring GGMs (modified the geopotential model to fit local gravity data) have succeeded to upgrade it as a reference model for better regional/local geoid heights solutions see e.g. (Forsberg & Kearsley, 1990; Amin et al., 2005; Abd-Elmotaal, 2008).

In Egyptian territory, a large number of researchers are eager to access to an official precise geoid model for Egypt that agrees with the Egyptian vertical datum e.g. (Alnaggar, 1986; Shaker et al., 1997b; Nassar et al., 2000; Abd-Elmotaal, 2015; Al-Krargy, 2016; El-Ashquer, 2017), more information about geoid modelling trials and efforts in Egypt see this Web https://sites.google.com/site/gomaadawod/geoidofegypt.

Hence, the aim of this investigation is to develop a new precise and high-resolution geoid model for Egypt by refining GGMs through a process named tailoring, where the existing spherical harmonic coefficients of GGMs are fitted to the Egyptian gravity data for better modelling of the Egyptian gravity field. This can be made by computing the differences between local gravity anomalies and those derived from the geopotential models, then the harmonic analysis of the residual gravity anomalies yields correction terms that are added to the original spherical coefficients of the relevant model to give the final modified coefficients of the fitted model.

Several methods of harmonic analysis techniques can be used to estimate the potential coefficients of the tailored geopotential model to the local gravity data such as Integral Formulas (Wenzel,1985; Weber&Zomorrodian,1988); Fast Fourier Transform (Colombo, 1981; Abd-Elmotaal, 2004); Gauss-Legendre Numerical Integration Technique

(Abd-Elmotaal et al. 2013); Least-squares Technique (Heck &Seitz 1991); Least-squares Collocation (Tscherning, 2001); Fast Spherical Collocation (Sanso`&Tscherning, 2003).

In this thesis, we have used the integral formulas, suggested by Weber and Zomorrodian (1988), which is based on a previous investigation made by Wenzel (1985), through an iterative algorithm, to improve the accuracy of the obtained harmonic coefficients and to decrease the residual field.

In order to achieve the objectives of this thesis, the satellite-only model GOCO05s (Mayer et al., 2015) versus ultra-high degree geopotential model EGM2008 (Pavlis et al., 2012) tailored to gravity data in Egypt, in order to select the optimal model that can be used for the reference gravity field for the new Egyptian geoid model.

The first is selected because it signifies unsurpassed satellite-only models, which is based on complete data of the three gravity field mapping missions (CHAMP, GRACE, and GOCE), while the second is picked because it represents one of the best ultra-high degree or resolution model, and usually used as a reference model to assess other the latest development geopotential models.

1.2 Previous Studies

GGMs can usually be refined by a process named tailoring, where the existing spherical harmonic coefficients of GGMs are adjusted, and often extended to higher degrees, using gravity data that may not necessarily have been used in the model.

Therefore, many scholars have tried to compute tailored geopotential models to best suit their specific areas of interest (globally, continental and regionally over a particular region).

For example, Wenzel (1998b) has computed a set of tailored geopotential models for global; Abd-Elmotaal et al. (2015) for Africa; Weber and Zomorrodian (1988) for Iran; Bašić et al. (1990), Kearsley&Forsberg (1990) and Wenzel (1998a) for Europe; Li and Sideris (1994) for Canada; Lu et al. (2000) for China.

In addition, in Egypt, more studies have been conducted for tailoring geopotential models to Egyptian gravity field e.g. (Amin et al., 2003; Abd-Elmotaal, 2006; Abd-Elbaky, 2011; Abd-Elmotaal, 2014). A brief summary of some of the previous studies will be provided as follows:

The GPM98A, GPM98B and GPM98C globally tailored geopotential models have been computed to spherical harmonic degree 1800 (spatial resolution ~11km) and developed by Wenzel (1998b). The GPM98 models are based on the degree-20 expansion of EGM96 and global $5' \times 5'$ mean gravity anomalies collected from surface gravity and altimetry for about 75% of the earth's surface (the remaining areas being filled by larger block size values), where integral formulas in an iterative algorithm (Wenzel, 1985) were applied for the calculation of the higher degree spherical harmonic coefficients (Torge, 2001, p. 281). However, in areas where no local gravity data were available, such as Australia, the GPM98 models provide results that are worse than the degree- 360 expansion of EGM96 (Featherstone & Olliver, 2001). In areas well covered by high-resolution data, this solution provides a relative geoid accuracy of a few cm and gravity anomalies accurate to several 10 μms^{-2} (Torge, 2001, p. 281).

Abd-Elmotaal et al. (2015) have created high-degree tailored reference geopotential model EGM2008 for Africa, complete to degree and order 360 (spatial resolution ~55km), to be used to fill the gravity data

gaps, which are present in the database of the African Geoid Project, before the geoid computation process. This tailored geopotential model will also be updated iteratively. The gravity anomalies (topographically-isostatically) for Africa have been compiled and interpolated to a local data-grid of 30′ × 30′ resolution. This grid has been merged with a global grid of EGM2008-based topographically-isostatically reduced gravity anomalies and used to estimate the potential coefficients of the tailored reference models for Africa by three different techniques. They are the Fast Fourier Transform (FFT), the least-squares.and the Gauss numerical integration techniques. The tailored geopotential models created in this investigation give smaller residual gravity anomalies for Africa. The variance and the range decreased by about 50% compared to the original free air anomalies. The FFT and the Gauss harmonic analysis techniques give quite similar results, which are very close to the least-squares, derived potential coefficients. The tailored geopotential models created within this investigation are more suitable than EGM2008 or recent GRACE/GOCE derived geopotential models for gravity interpolation considering the large data gaps appearing in the African gravity database.

The IFE88E2 regionally tailored geopotential model was developed by Bašić et al. (1990). The IFE88E2 model is based on the OSU86F global geopotential model and has been tailored using only European gravity data through integral formulas in an iterative algorithm over a region bound by $30°N \leq \varphi \leq 73°N$ and $30°W \leq \lambda \leq 46°E$. The maximum spherical harmonic degree of this model is 360 (spatial resolution ~55km), which is the same as the global geopotential model upon which it is based. The model OSU86F has been tailored to Europe using as input data 30′ × 30′ mean free-air gravity anomalies from the Institut für Erdmessung, University of Hannover, Germany, and Kort-og Matrikelstyrelsen, Denmark. The

residual of point free-air anomalies relative to OSU86F and IFE88E2 were evaluated in 1495 points in Scandinavia, where the RMS of the differences were ± 23.4 mGal and ± 18.5 mGal respectively. Especially comparisons of the two models with GPS /levelling data in Europe show an improved accuracy of the IFE88E2 model. The RMS value of the differences relative to OSU86F is ± 0.774 m and decreases to ± 0.322 m for IFE88E2.

The GPM3E97A, GPM3E97B, and GPM3E97C regionally tailored geopotential models for Europe also now supersede the IFE88E2 model by Wenzel (1998a). The respective maximum spherical harmonic degree and order of these models is 1800, 1080 and 720, which equate to spatial resolutions of approximately 11km, 18.5km and 28km, respectively. A variant of the usual tailoring process was used: instead of using gravity data, quasi-geoid heights from the EGG97 European gravimetric quasi-geoid model (Denker & Torge 1998) were used to tailor the EGM96 global geopotential model through integral formulas in an iterative algorithm This tailoring was applied to a region bound by $25°N \leq \varphi \leq 77°N$ and $35°W \leq \lambda \leq 67.4°E$. The EGG97 quasi-geoid heights were taken from a $5' \times 5'$ grid for GPM3E97A, a $10' \times 10'$ grid for GPM3E97B and a $15' \times 15'$grid for GPM3E97. The RMS discrepancy between the input data and quasi-geoid heights computed from GPM3E97A is 0.005rn with 0.295m maximum discrepancy (these results from the lack of resolution of GPM3E97A compared to EGG97).The comparison of GPM3E97A with three sets of high-resolution free-air gravity anomalies has given about half the discrepancies which were obtained with EGM96. The comparison of GPM3E97A with GPS/Ievelling derived height anomalies from three projects in Germany has given RMS residuals from a three parameter bias fit of 11 ... 24 cm for EGM96 and 2.3 ... 3.9 cm for GPM3E97A. This is

only about twice the RMS residuals which have been obtained for the high resolution regional quasi-geoid determination EGG97

The EGM96EGCT and EGM96EGIT regionally tailored geopotential models for Egypt were developed by Amin et al. (2003). The respective maximum spherical harmonic degree and order of both models is 599 and 650, which equates to spatial resolutions of approximately 33km and 31km, respectively. The EGM96EGCT and EGM96EGIT model are based on the EGM96 global geopotential model, and have been tailored using both the least-squares collocation (Tscherning, 2001) and integral formulas in an iterative algorithm , respectively, over a region bound by $22°N \leq \varphi \leq 32°N$ and $25°E \leq \lambda \leq 36°E$. The model EGM96 has been tailored to Egypt using as input a grid $15' \times 15'$ mean geoid height derived from GPS/Ievelling scattered points for EGM96EGCT and a $5' \times 5'$ grid for EGM96EGIT derived from the same GPS/Ievelling scattered points. Both tailored models showed similar improvement in their fitness to the mean geoid height.

Three different tailored geopotential models for Egypt have been created by maintaining the lower harmonics till degree 20, 36 and 72 to their values as of EGM96 model denoted as EGGM06A, EGGM06B, and EGGM06C, respectively, by Abd-Elmotaal (2006). The tailored geopotential models EGGM06 computed to spherical harmonic degree 360. The local gravity anomalies for the Egyptian data window are gridded in $30' \times 30'$ grid using the remove/restore window technique. The local gridded data are merged with the global $30' \times 30'$ gravity anomalies, computed using EGM96 till N = 360, to establish the data set for computing the tailored geopotential models EGGM06. The merged $30' \times 30'$ global field has been then used to estimate the harmonic coefficients of the tailored reference models by an FFT technique).The tailored

geopotential models EGGM06A, EGGM06B and EGGM06C created in this investigation give better residual gravity anomalies. The variance has dropped to its one-third. The range has dropped to its one-half. All three tailored geopotential models developed within the current investigation give practically the same results.

An ultra-high-degree tailored reference geopotential model for Egypt called EGTGM2014, complete to degree and order 2160, has been developed by Abd-Elmotaal (2014), based on the EGM2008 reference geopotential model. The local gravity anomalies for the Egyptian data window are gridded, after removing the effect of the topographic-isostatic masses for the data window as well as the effect of EGM2008 from n = 361 to n = 2160, in 30′ × 30′ grid using kriging interpolation technique. The local gridded data are merged with the global 30′ × 30′gravity anomalies, computed using EGM2008 till N = 360 after removing the effect of the global topographic-isostatic masses using SRTM 30′ × 30′ DHM, to establish the data set for computing the tailored geopotential models. The merged 30' × 30' global field has been then used to estimate the harmonic coefficients of the tailored reference model by an FFT technique, till degree and order 360, using an iterative process to enhance the accuracy of the obtained harmonic coefficients and to minimize the residual field. The higher coefficients (from n = 361 to n = 2160) of EGM2008 has then been restored generating the EGTGM2014 ultra-high-degree tailored geopotential model complete to degree and order 2160. The tailored geopotential model created in this investigation gives better residual gravity anomalies (unbiased and have much less variance). The variance has dropped by about 35 %. Gravimetric geoids for Egypt have been computed using both the EGM2008 and the EGTGM2014 tailored geopotential models in the framework of the window remove-restore technique using the

1D-FFT technique. The computed geoids have been fitted to the GPS/levelling derived geoid by removing a trend surface. Using the EGTGM2014 tailored geopotential model improves the external geoid accuracy by about 20%, and the range of the remaining differences has dropped by about 22 %.

1.3 Problem Statement

The Egyptian vertical control network carried out from 1906 to 1940, in order to unify a precise vertical datum for the irrigation system in Egypt. The Egyptian vertical control does not extant through the whole country; it is limited to the Nile Valley and the Delta, beside few loops in the Eastern Desert (Saad, 1993). Currently, the conventional re-surveying vertical controls are quite impractical since the cost is expensive and time-consuming.

Nowadays, use of global positioning systems such as GPS, GLONASS, and upcoming GALILEO systems for surveying has made it possible to obtain accuracies *a few centimeters* or less in relative positioning mode. However, the height obtained from positioning systems is relative to an ellipsoid. The relationship, which binds the ellipsoidal heights and heights with respect to a vertical datum established from spirit-leveling (Sansò & Sideris, 2013, p., 518), is:

$$H_{Levelling} = h_{GPS} - N_{Model} \tag{1.1}$$

Where h_{GPS} is the ellipsoidal height, $H_{Levelling}$ is the orthometric height and N_{Model} is the geoidal undulation obtained from gravimetric geoid or geoid model derived from GGMs. In practice, the implementation of Eq. (1.1) is more complicated due to numerous factors that affect the accuracy of

orthometric height. Some of these factors include, but are not limited to, the following:

a) The ellipsoidal heights may also suffer from errors due to the fact that most positions are determined differentially, i.e. with respect to a set of reference points (erroneous identification of the reference point) as well as instability of reference station monuments over time due to geodynamic effects and land subsidence. In addition, poorly modeled GPS errors (e.g., tropospheric refraction).
b) GGMs may contain systematic effects and distortions primarily caused by long-wavelength errors due to difficulties in collecting and using global gravity data as well as may be different estimation techniques were used to develop these models. In addition, the absence of the regional/local gravity data from the collected global data, which further degrades the quality of regional/local geoid derived from these models.
c) No *official precise geoid model* (e.g. gravimetric solution) that agrees with the Egyptian vertical datum.

1.4 Thesis objectives

The aim of this research is to develop a new precise and high-resolution geoid model for Egypt by refining the Global Geopotential Models (GGMs) through a process named tailoring, where the existing spherical harmonic coefficients of GGMs are fitted to the Egyptian gravity field. The main objectives of the research include:

a) To select the optimal GGM to be used for the reference gravity field for the new geoid model by a comparison between the satellite-only versus ultra-high degree reference geopotential model tailored to gravity data in Egypt, using integral formulas.

b) To assess the validation and accuracy of the new geoid model, after fitting to the Egyptian vertical datum, using an available GPS/levelling data set over Egypt.

1.5 Importance of research

This research is important for the following reasons:

a) Tailored geopotential models in this research can contribute to the development of Egypt (e.g. natural resources prospection).
b) The geoids determined in this research is a significant case study in high topography regions, such as the southwest corner of Egypt in particular (e.g. plateau al-Gilf al-Kebir) and the Sinai Peninsula in particular (e.g. South of Sinai, RAS-GHARIB, and TABA)
c) The geoids determined in this research agreement with the national vertical datum in Egypt and are linked to the world geocentric reference frame (WGS 84). Consequently, these geoids can be used to save the cost, time and effort of survey works, which are carried out in many national projects (e.g. conversion of geodetic height from GNSS measurements to orthometric height above Mean Sea Level (MSL) without levelling within average accuracy ±17 cm).
d) The remove-compute-restore technique is a well-known method used in FFT, collocation or Stokes ring integration for computing gravimetric geoid. Thereby, it is expected that the tailored geopotential models improve the quality of the gravimetric geoid generation over the Egyptian territory.

1.6 Research Methodology

Research methodology will be divided into two main stages, harmonic analysis, and synthesis techniques as well as geoid modeling, in order to achieve the objectives of this investigation. The main programs used in research methodology have been found in GRAVSOFT (Forsberg and

Tscherning, 2008; http://cct.gfy.ku.dk/software/pyGravsoft-297.zip). In general, the methodology is depicted in Fig. (1.1).

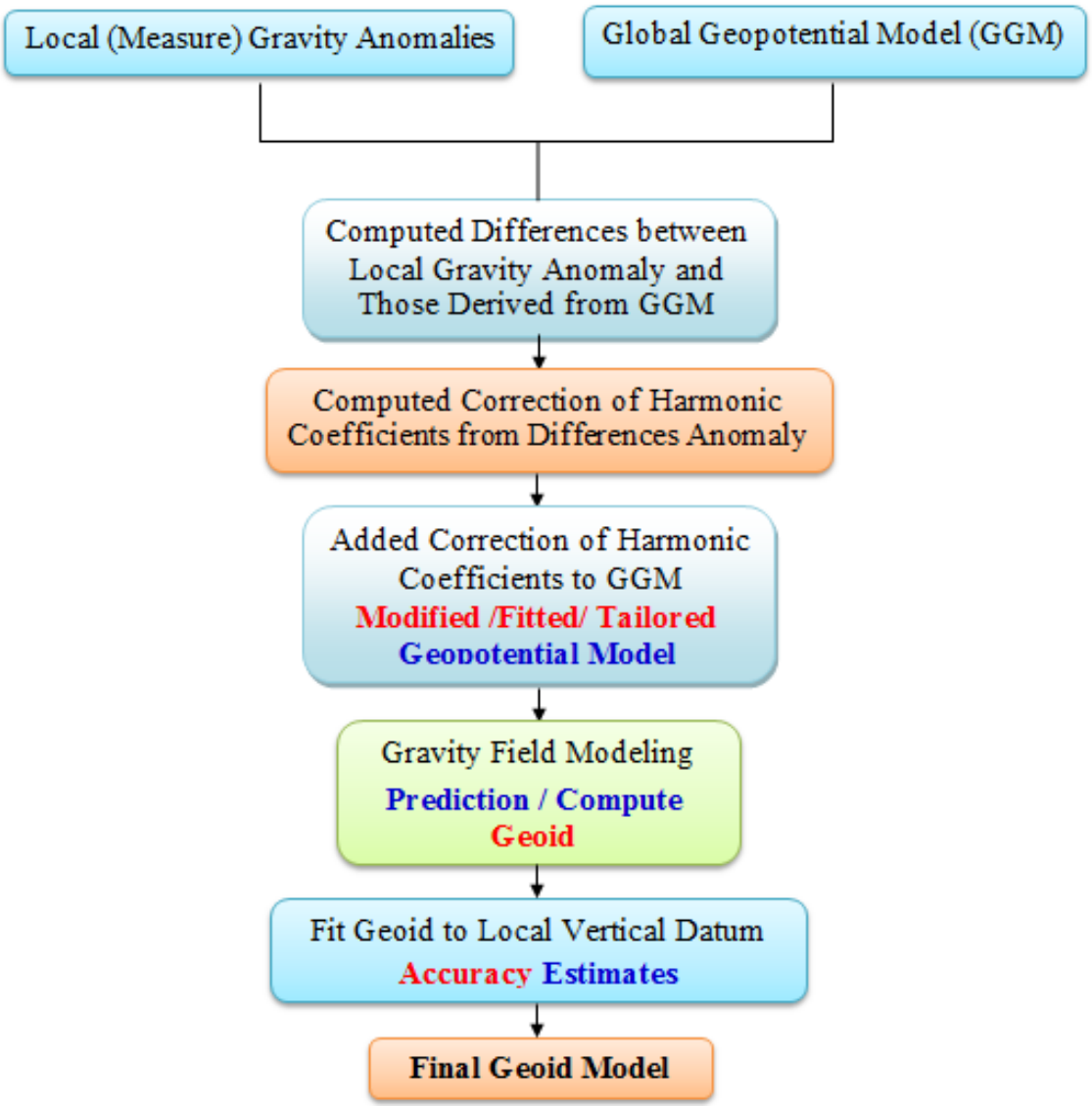

Figure (1.1): Research Methodology

1.7 Outline and structure of Thesis

This thesis is organized into six chapters. The content of those chapters are outlined in the following:

Chapter 1 introduces the research topic and briefly describes the history of trials of tailored global geopotential models to regional/global gravity field and problem statement. The chapter also states the objectives and

importance of this research for the Egyptian territory. In addition, the research methodology and then a hint about each of the following chapters are summarized.

Chapter 2 explains the fundamental concepts of the earth's gravity field determination and the gravity potential computation in terms of spherical harmonics. Moreover, different approaches for reducing the gravity data from the Earth surface to the geoid are explained. In addition, some of the statistical methods used for evaluating the Earth's gravity field models and vertical reference surfaces are introduced. Furthermore, the elastic deformations of the Earth caused by the gravitational action of the Moon and Sun, also known as Earth's tides, are presented, as well as their implications in vertical datum definition. Finally, the history of the Egyptian vertical datum and control network are described.

Chapter 3 describes the basic equation of global spherical harmonic synthesis (functional of the field) and analysis (coefficients of the global gravitational model). In addition, the auxiliary relationships to implement the spherical harmonic analysis and synthesis processes are discussed. Furthermore, computation procedures for tailoring (improving) global gravitational model using integral techniques within an iterative algorithm are present. Finally, the chapter also describes the basic equation of geoid determination by Least-squares collocation (LSC).

Chapter 4 describes in details each of the datasets and the preparation that was undertaken on them before they were used in the computation of tailored Earth geopotential models to gravity data in Egypt for better modelling of the Egyptian gravity field.

Chapter 5 deals with the results and discussion of the practical part of this thesis, where the results of tailoring the satellite-only model versus high

degree reference global geopotential model to gravity data in Egypt. In addition, it presents some of the comparisons between the tailored geopotential models in order to determine the best fit for them that would be considered as a reference model for geoid determination for Egypt. The chapter also presents the validation and the accuracy of the geoid models derived from spherical harmonic coefficients of tailored geopotential models. In addition, gravimetric and combined geoids (gravity and astrogeodetic data) have been computed for Egypt using both tailored geopotential models in the remove-restore technique using the Least-squares collocation (LSC) in order to choose the best ones for the determination of orthometric heights above MSL or geoid heights over Egypt.

Chapter 6 summarizes the outcomes and lists of conclusions obtained from the investigation of the results shown in *chapter 5*, and some recommendations for further future studies are provided.

Chapter 2

THEORETICAL BACKGROUND

2. THEORETICAL BACKGROUND

2.1 Overview

This chapter presents the theoretical basis and methodology required to obtain gravity and gravity potential. The gravitational, centrifugal potentials and Laplace's equation were described, as well as the potential in terms of spherical harmonics. Moreover, various gravity reductions, statistical methods, and vertical datums were discussed in this chapter. Additionally, Earth's tides and its relationship with gravity values, geoid undulations, and ellipsoidal heights were introduced. Finally, the history of the Egyptian vertical datum and control network along some existing defects in the vertical datum of Egypt are described.

2.2 Theory of Gravity Field

2.2.1 Gravitational Potential

Newton's law of universal gravitation (1687) describes the attractive force (F_a) between two particles in the universe with masses of m_1 and m_2 as (Heiskanen & Moritz 1967, p. 1):

$$F_a = -G \frac{m_1 m_1}{l^2} \tag{2.1}$$

This force is directed along the line connecting the two points; where G is the Newton's gravitational constant that has a value of 6.6742 $10^{-11} m^3 kg^{-1} s^{-2}$ (Hofmann-Wellenhof & Moritz, 2005, p.3), l is the distance between the two particles, m_1 and m_2 denotes the mass of approximately the two particles.

2.2.2 Centrifugal Potential

Each point on the surface of the Earth rotates around the *z*-axis at an angular velocity ω and is affected by a centrifugal force (F_c) directed outwards perpendicular to the axis of rotation of the earth as shown in Fig. (2.1). The centrifugal force (F_c) on a unit mass given by (Hofmann-Wellenhof & Moritz, 2005, p.43):

$$F_c = \omega^2 p \tag{2.2}$$

Where *P* is the distance perpendicular to the earth's rotation axis and given by:

$$p = \sqrt{x^2 + y^2} \tag{2.3}$$

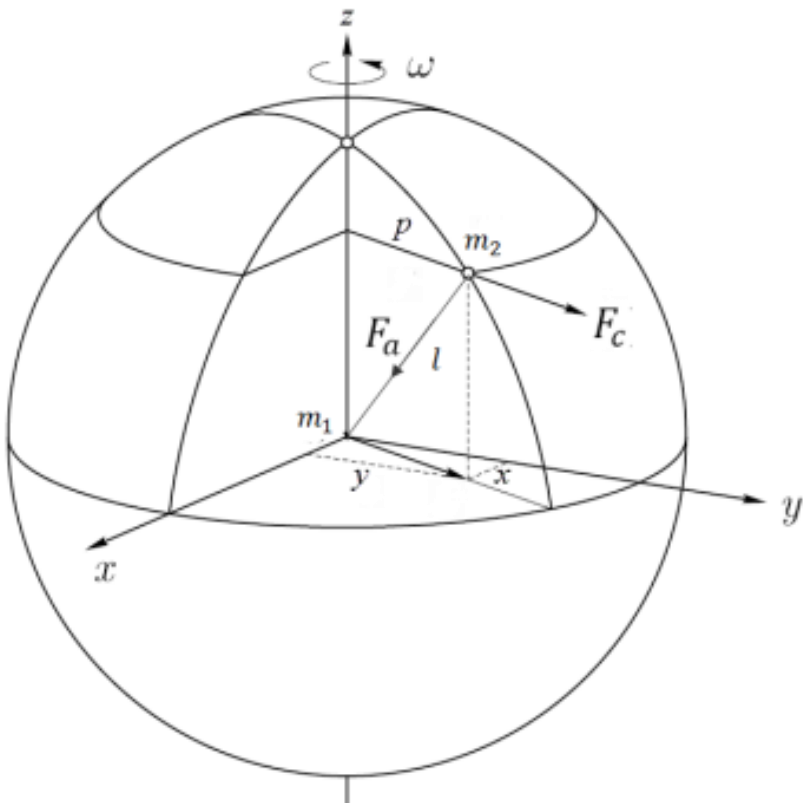

Figure (2.1): Attraction and Centrifugal Force.

The gravity (g) is the force acting on a body at rest on the Earth's surface is the result of gravitational force (F_a) and the centrifugal force (F_c) of the Earth's rotation (Heiskanen & Moritz 1967, p. 46).

Also, the definition of the gravity must include the magnitude and direction, where the magnitude of *g* is called *gravity* in the narrower sense and the direction of *g* is the direction perpendicular to the equipotential surfaces known as *plumb line,* or the vertical, where the equipotential surfaces are surfaces of constant scalar potential such as the geoid.

According to Gauss-Listing definition (Gauss, 1828, p.49) geoid is defined as an equipotential surface of the Earth's geopotential field which assumed to coincide with MSL in a least-squares sense. However, MSL is not an equipotential surface due to numerous meteorological, hydrological, and oceanographic effects.

2.3 Fundamentals of Potential Theory

2.3.1 Potential Theory

The work done when an object is moved from one point to another is independent of the path and is equal to *V*. The potential of gravitation (*V*) is given by (Hofmann-Wellenhof and Moritz, 2005, p.5):

$$V = \frac{Gm}{l} \tag{2.4}$$

When considering the attraction of systems of point masses or solid bodies to one another, as is done in Geodesy, it is easier to deal with the potential than with the three components of the force (*vector*). Thus, by splitting up a larger body into n point masses, $m_1, m_2 \ldots\ldots m_n$, the individual potentials V_i are summed up as (ibid, p.5):

$$V = \frac{Gm_1}{l_1} + \frac{Gm_2}{l_2} + \cdots\cdots\cdots + \frac{Gm_n}{l_n} = G\sum_{i=1}^{n}\frac{m_i}{l_i} \tag{2.5}$$

According to Heiskanen and Moritz (1967, p. 3), the Earth is composed of an infinite number of particles (point masses) distributed continuously over a volume *v* of the earth with density ρ which is given by:

$$\rho = \frac{dm}{dv} \tag{2.6}$$

Where *dm* and *dv* are the differentials of the mass and volume elements respectively, then the gravitational potential Eq. (2.5) of a solid body like the Earth, can be calculated by:

$$V = G \iiint_v \frac{dm}{l} = G \iiint_v \frac{\rho}{l} dv \tag{2.7}$$

The definitions above are the exact representation of the potential of the earth. However, this formulation requires the knowledge of the density ρ. Since the mass distribution in the interior of the earth is definitely not homogeneous, the density can only be approximated. This is insufficient for the determination of the potential *V* (Heuberger, 2005).

2.3.2 Laplace's Equation

The potential *V* of the earth is continuous through the whole space and vanishes at infinity like 1/*l* for $l \rightarrow \infty$. The first derivatives of *V*, that is the force components, are also continued throughout the space, but not so the second derivatives. At points are where density change discontinuously, some second derivatives have a discontinuity. The second derivatives can be written to satisfy Poisson's equation (Hofmann-Wellenhof and Moritz, 2005, p.7):

$$\Delta V = \frac{\partial^2 V}{\partial^2 x} + \frac{\partial^2 V}{\partial^2 y} + \frac{\partial^2 V}{\partial^2 z} = -4\pi G \rho \tag{2.8}$$

Where Δ is called the Laplace operator, the potential *V* satisfies Poisson's equation. But, outside the attracted bodies (earth) in empty space, no masses, the density ρ is zero and then the potential satisfies Laplace's equation, then Eq. (2.8) becomes:

$$\Delta V = 0 \tag{2.9}$$

Hence, the solution of Laplace's equation is harmonic functions. Thus, the potential of gravitation is a harmonic function outside the attraction masses but inside the masses satisfies Poisson's equation.

2.3.3 Potential Expressed in terms of Spherical Harmonics

For global problems, the expansion of the gravitational potential V into spherical harmonics is useful (Torge, 1989, p.28), which is a special solution of Laplace's equation Eq. (2.9). In the exterior space, a representation in terms of spherical coordinates (r, θ, λ) is:

$$V = \frac{GM}{r}\left[1+\sum_{n=2}^{\infty}\left[\frac{a}{r}\right]^{n}\sum_{m=0}^{n}(C_{nm}\cos m\lambda + S_{nm}\sin m\lambda)\, P_{nm}\,(\cos\theta)\right] \qquad (2.10)$$

Where r is geocentric radius, θ is polar distance, λ geodetic longitude, GM $= G\,(M_{earth} + M_{atm})$ is the geocentric gravitational constant referring to the total mass (Earth's body plus atmosphere) and a stands for semi major axis of the earth ellipsoid. The associated Legendre functions (spherical harmonics functions) $P_{nm}(\cos\theta)$ of degree n and order m are given for an argument $t = \cos\theta$ by differentiating $P_{nm}(t)$ m times with respect to t as (Torge, 2001, p.68):

$$P_{nm}(t) = (1-t^2)^{\frac{m}{2}}\,\frac{d^m}{dt^m}\,P_n(t) \qquad (2.11)$$

The expansion into spherical harmonics thus represents a spectral decomposition in field structures of wavelength 360°/n (corresponding to a resolution of 180°/n).

The C_{nm} and S_{nm} are spherical harmonics coefficients given by (ibid, 2001, p.70):

$$C_{n0} = C_n = \frac{1}{M} \iiint_{Earth} \left(\frac{r}{a}\right)^n P_n(\cos\theta)\ dm \qquad m = 0$$

$$\begin{Bmatrix} C_{nm} \\ S_{nm} \end{Bmatrix} = \frac{2}{M} \times \frac{(n-m)!}{(n+m)!} \iiint_{Earth} \left(\frac{r}{a}\right)^n P_{nm}(\cos\theta) \begin{Bmatrix} \cos m\lambda \\ \sin m\lambda \end{Bmatrix} dm \qquad m \neq 0 \tag{2.12}$$

Here *dm* is a mass element and *M* is the earth's mass.

2.4 Gravity Reductions

The topographical effect is one of the most important components in the solution of the geodetic Boundary Value Problem (BVP) and should be treated properly in the determination of a precise geoid. Therefore, gravity (*g*) measured on the physical surface of the earth (terrain/topography) is not directly comparable with normal gravity (γ) referring to the surface of the ellipsoid. A reduction of gravity (*g*) to sea level (geoid) is necessary. Since there are masses above sea level, the reduction methods differ depending on the way how to deal with these topographic masses (Heiskanen &Moritz 1967, p. 126).

Gravity reduction is essentially the same for gravity anomalies (Δg) and gravity disturbances (δg). The classical solution of the geodetic BVP using Stokes's formula to determine the geoid requires the gravity anomalies (Δg) representing boundary values at the geoid. It should be noted that there are two conditions, which should be achieved to use Stokes' formula (Hofrnann-Wellenhof &Moritz, 2005, p. 129). The first condition is that the gravity (*g*) must refer to the geoid. The second condition is that there must be no masses outside the geoid. Hence, the gravity reduction consists of the following steps:-

a) The topographic masses outside the geoid are removed or shifted below the geoid.

b) The gravity station is lowered from the earth's surface (g_p) to the geoid surface (g_{p_o}) as shown in Fig.(2.2).

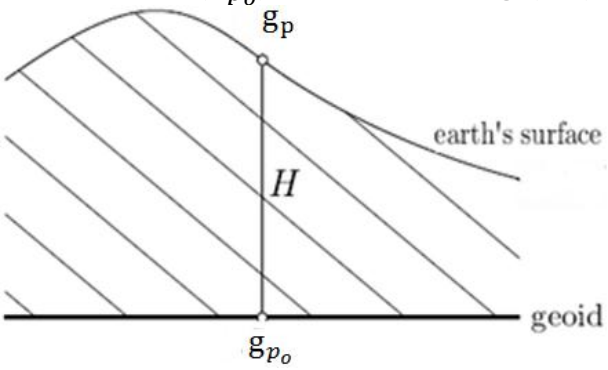

Figure (2.2): Gravity Reductions.

Molodensky's solution is the other fundamental solution to the geodetic BVP. This modern solution gives the quasi-geoid but not a level surface (geoid) as in Stokes's solution. In addition, this approach considers the Earth's surface as the boundary reference surface and overcomes the problem of removing all the topographical masses above the geoid, which is strictly required by Stokes's approach. Molodensky's approach requires both gravity anomalies and the topographical heights be available at the same points but does not require the knowledge of the crust density information. The following sections present some of the gravity reductions methodologies.

2.4.1 Free-Air Reductions

This method reduces the observed gravity on the physical surface of the earth into the geoid surface by assuming that no topographic masses between the surface point (g_p) and its projection on the geoid (g_{p_o}) see Fig.(2.3).

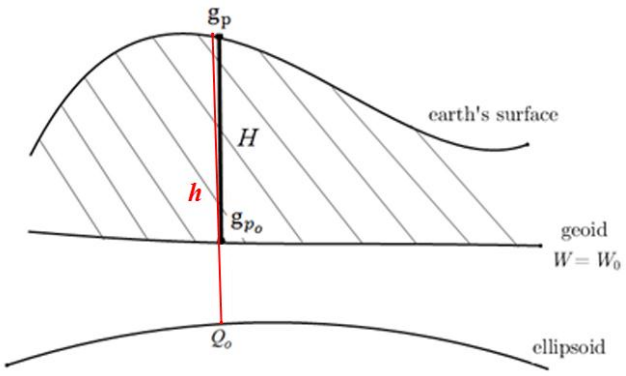

Figure (2.3): Free-air Reductions.

For a theoretically correct reduction of gravity to the geoid, we need the vertical gradient of gravity, the value of gravity on the geoid g_{p_o} according to Taylor expansion (Hofrnann-Wellenhof &Moritz, 2005, p. 134), is equal to:

$$g_{p_o} = g_p - \frac{\partial g}{\partial H} H \ldots\ldots \tag{2.13}$$

Where H is the height of the point above the geoid (orthometric height) and $\frac{\partial g}{\partial H}$ is the vertical gradient of gravity referred to the geoid. Suppose there are no masses above the geoid, are not taken into account, or that such masses have been removed beforehand so that this reduction is indeed carried out in "free-air" and neglecting all terms but the linear one, we have:

$$g_{p_o} = g_p + F \tag{2.14}$$

Where $F = -\frac{\partial g}{\partial H} H$ are free-air reductions to the geoid.

For practical purposes, it is sufficient to use $\frac{\partial \gamma}{\partial h}$ (The normal gradient of gravity referred to the ellipsoid associated with the ellipsoid height h), instead of $\frac{\partial g}{\partial H}$ obtaining (Heiskanen &Moritz, 1967, p. 131):

$$F = -\frac{\partial g}{\partial H} H = -\frac{\partial \gamma}{\partial h} h = +0.3086\, h \quad \text{(mGal)} \quad , \quad for \quad h \ in \ meters \qquad (2.15)$$

Then, from Fig. (2.3) the free air gravity anomalies (Δg_f) is given by the following formula (Heiskanen &Moritz, 1967, p. 293):

$$\Delta g_f = g_{p_o} - \gamma_{Q_o} \qquad (2.16)$$

Where γ_{Q_o} is the normal gravity at point (Q_O) on the ellipsoid.

Theoretical normal gravity (γ_{Q_o}), the magnitude of the gradient of the normal potential function *U*, is given on (at) the surface of the ellipsoid by the closed formula of Somigliana given by (Torge, 2001, p.106):

$$\gamma_{Q_o} = \gamma_e \frac{1 + K \sin^2 \varphi}{(1 - e^2 \sin^2 \varphi)^{1/2}} \quad with \quad K = \frac{b\gamma_p}{a\gamma_e} - 1 \qquad (2.17)$$

Where:

a, b = Semi-major and semi-minor axes of the ellipsoid, respectively.

γ_e, γ_p = Theoretical normal gravity at the equator and poles, respectively.

e^2 = square of the first ellipsoidal eccentricity.

φ = geodetic latitude.

In this study, we used the World Geodetic System 1984 (WGS-84) derived geometric and physical constants was carried out by National Imagery and Mapping Agency (NIMA), currently became National Geospatial-intelligence Agency (NGA), as shown in the Table (2.1).

Table (2.1): WGS 84 Ellipsoid Derived Geometric and Physical Constants. (NIMA, 2004, Tables 3.3 and 3.4, p.3-7)

Parameters	Notation	Value	Unit
Semi-major axis	a	6378137.0	m
Semi-minor Axis	b	6356752.3142	m
First Eccentricity Squared	e^2	0.00669437999014	unitless
Normal gravity at the equator	γ_e	9.7803253359	m s^{-2}
Normal gravity at the Poles	γ_p	9.8321849378	m s^{-2}
Formula Constant	K	0.00193185265241	unitless

2.4.2 Bouguer Reductions

The purpose of the Bouguer gravity reduction is the complete removal of the topographic masses, that is, the masses outside the geoid. Assume the area around the gravity station (*P*) to be completely flat and horizontal see Fig. (2.4) and then let the masses between the geoid and the earth's surface have a constant density (ρ). Then the attraction (*A*) of this so-called Bouguer plate is given by (Hofmann-Wellenhof &Moritz, 2005, p. 135):

$$A_B = 2\pi G\rho H \tag{2.18}$$

Where A_B is the attraction of an infinite Bouguer plate at the point *(P)* on the surface of the earth, *G* is the Universal Constant of Gravitation (cf. Equation 2.1), ρ is the density of topographic masses and *H* is the thickness of the Bouguer plate (height of the point above the geoid).

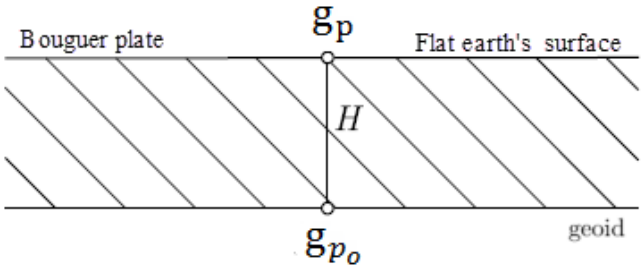

Figure (2.4): Bouguer Reductions.

The Bouguer correction factors for various densities which are used in the anomaly computations:

$$A_B = \left\{ \begin{array}{ll} 0.11195H & , \ with\ \rho = 2.67\ g.cm^{-3} \quad (land) \\ 0.06889H & , \ with\ \rho = 1.643\ g.cm^{-3}\ \text{(Salt Water)} \end{array} \right\} \text{[mGal]} \tag{2.19}$$

where H is elevation in meters

Removing the plate is equivalent to subtracting its attraction Eq. (2.18) from the observed gravity. This is called *incomplete Bouguer reduction*.

Then, the incomplete Bouguer gravity anomalies (Δg_B) can be given by (Heiskanen &Moritz, 1967, p. 131):

$$\Delta g_B = \Delta g_f - A_B \tag{2.20}$$

Note that a truly spherical Bouguer plate can also be used for calculating the gravity anomalies, we would have 4π instead of 2π (Moritz, 1990, p.235). Because of the area around the computation point is not completely flat, and then the value of the attraction of masses of Bouguer plate reduction should be refined by taking into account the deviation of actual topography from the Bouguer plate as (Hofmann-Wellenhof &Moritz, 2005, p. 137):

$$\Delta g_B = \Delta g_f - A_B + A_{TC} \tag{2.21}$$

Equation (2.21) called complete or refined Bouguer reduction, where A_{TC} the classical terrain correction or topographic corrections see Fig. (2.5).

A linear approximation of this correction is presented by Moritz (1968):

$$A_{TC} = \frac{G\rho}{2} \iint_{\sigma} \frac{(H - H_P)^2}{l^3} \, d\sigma \tag{2.22}$$

Where H is the orthometric height of the point for which A_{TC} is calculated, H_P is the height of a roving point P for integration, $d\sigma$ is the infinitesimal surface element, and l is the planar distance from P (Pinon, 2016).

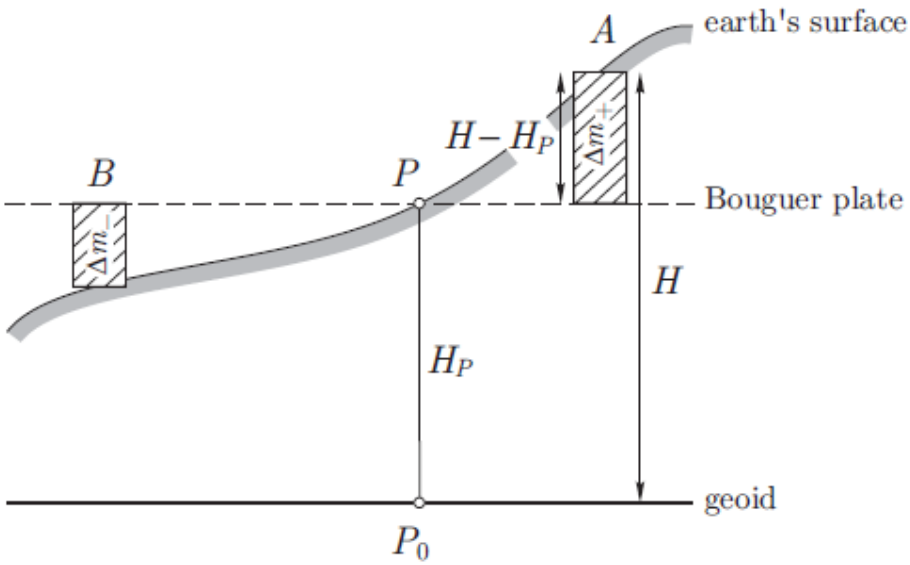

Figure (2.5): Terrain Correction (Hofmann-Wellenhof & Moritz 2005, p. 136).

2.4.3 Isostatic Reduction

In the general concept of isostasy, the topographic mass excesses (*mountains*) and deficiencies (*waters*) are compensated by a corresponding mass distribution in the interior of the Earth (e.g., Torge 2001, p. 339), where the isostatic theory assumes that there is some kind of mass deficiency under mountains so that the systematically negative Bouguer anomalies and may attain large value (Heiskanen & Moritz 1967, p. 133).

There are two main theories about the isostatic compensation applications, one following the Airy-Heiskanen (AH) model and another following the Pratt-Hayford (PH) model. These two models are widely used in applications in geosciences, but the AH model has become a standard in geodetic research.

A. Airy-Heiskanen Isostatic Model

Airy proposed this model, and *Heiskanen* gave it a precise formulation for geodetic purposes and applied it extensively. According to Sansò and Sideris (2013, p.351), this model the mountains are floating on some kind of higher density fluid meaning that there is a mass deficit (*roots*) below mountains and mass surpluses (*anti-roots*) below the oceans. The AH model (Fig. 2.6) is based on the assumptions that the isostatic compensation is complete and local, the density of the mountains is constant and equal to (ρ_o= 2.67 gcm^{-3}), the density of Earth's mantle is equal to (ρ_M= 3.27 gcm^{-3}) and the normal crust thickness T_0 is equal to 30 km (Hofmann-Wellenhof & Moritz, 2005, p.143). Assuming a constant density of (ρ_w= 1.027 gcm^{-3}) for the ocean water, then the condition of floating equilibrium can be written as (Sansò &Sideris, 2013, p.351) for the continental cases:

$$(\rho_M - \rho_0)\, d = \rho_0\, H \tag{2.23}$$

For the oceanic areas:

$$(\rho_M - \rho_0)\, d' = (\rho_0 - \rho_w) H' \tag{2.24}$$

Where in Eq. (2.23) and Eq. (2.24) d is the thickness of the *root*, d' is the thickness of the *anti-root*, H is the height of the topography and H' is the height of the ocean, i.e., the depth. Given the above-mentioned density values for the crust, the mantle and ocean water, Eq. (2.23) and Eq. (2.24) can be written as (Hofmann-Wellenhof & Moritz, 2005, p.143):

$$d = 4.45H \qquad d' = 2.73H' \tag{2.25}$$

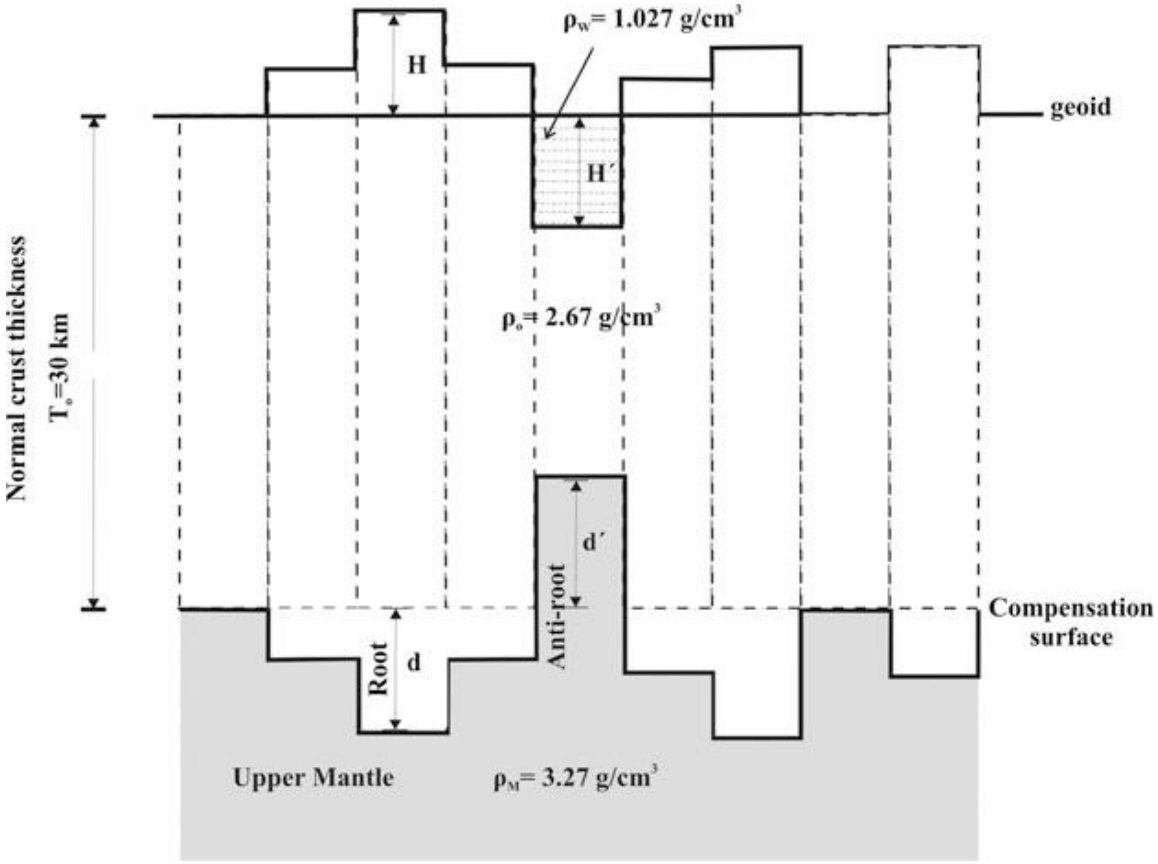

Figure (2.6): Airy-Heiskanen Isostatic Compensation Model (Sansò &Sideris, 2013, p.351)

B. Pratt-Hayford Isostatic Model

This system of compensation was outlined by *Pratt* and put into a mathematical form by *Hayford.* The principle is illustrated in Fig. (2.7).

According to the PH isostatic reduction scheme the topographic masses are distributed between the compensation surface and sea level. Moreover, the PH model assumed that the density beneath the compensation level is constant, while the masses above that level for each column of the cross-section are equal. Within that reduction scheme, the topographic masses are removed along with their isostatic compensation so that what remains is a homogeneous crust layer with constant density and constant depth of compensation (Sansò &Sideris, 2013, p.349).

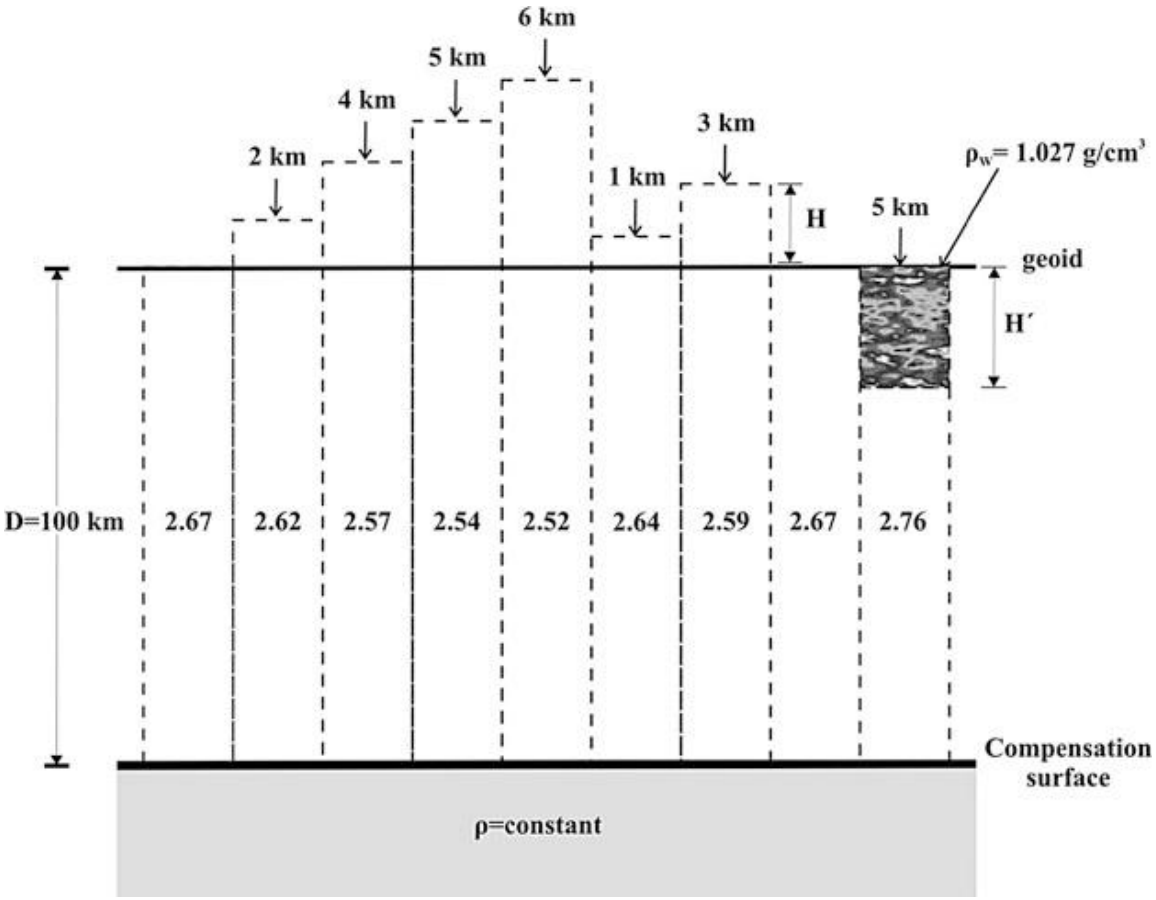

Figure (2.7): Pratt-Hayford Isostatic Compensation Model (Sansò &Sideris, 2013, p.349)

According to Hofmann-Wellenhof and Moritz (2005, p.141), the PH isostatic reduction considers that the level of compensation has a constant and uniform depth *D* assumed equal to 100 km measured from sea level. The topographic masses are delineated into columns of the cross-section with height *D* that allows lateral changes in density in order to

obtain isostatic equilibrium. Considering that a normal column (H = 0) has constant density ρ_o , the continental columns generate densities smaller than ρ_o while the oceanic columns are denser. The equilibrium conditions for the continental of a column of height $D+H$ (H representing the height of the topography) with density $\rho_{cont.}$ satisfies the equation (Sansò &Sideris, 2013, p.350):

$$(D+H)\,\rho_{cont.} = D\rho_0 \tag{2.26}$$

$$\Delta\,\rho_{cont.} = \rho_0 - \rho_{cont.} = \rho_0\,\frac{D}{D+H} \tag{2.27}$$

In the ocean area with density ρ_{ocean} , the density is increased. It given by

$$(D-H')\,\rho_{ocean} + H'\rho_w = D\rho_0 \tag{2.28}$$

$$\Delta\,\rho_{ocean} = \rho_{ocean} - \rho_0 = (\rho_0 - \rho_w)\,\frac{H'}{D-H'} \tag{2.29}$$

The *topographic isostatic reduction* is the difference in the attraction between the topographic masses (A_T) and the compensated masses (A_C) within the depth of the root, where the objective of the topographic-isostatic reduction of gravity is the regularization of the earth's crust (trying to make the earth's crust as homogeneous as possible). Where A_T equals the attraction of Bouguer plate combined with terrain correction ($A_T = A_B - A_{TC}$) and A_C is the attraction of the compensation masses given by Airy-Heiskanen and Pratt-Hayford isostatic model. Finally, the topographic-isostatically reduced gravity on the geoid becomes (Hofmann-Wellenhof & Moritz, 2005, p.147):

$$\Delta g_{TI} = \Delta g_f - A_T + A_C \tag{2.30}$$

2.4.4 Terrain Effects by Residual Terrain Model

The Residual Terrain Model (RTM) is one of the most common mass reduction methods used mainly in the quasi-geoid determination (Sansò &Sideris, 2013, p.366). This reduction method was introduced by Forsberg (1984), wherein this method the contribution of the topography is removed

and restored using a model of the topography equal to the difference between the true topography and a reference elevation surface (smooth mean elevation surface). Therefore, the topographic masses above this reference surface are removed and masses fill up the deficits below this reference surface see Fig. (2.8).

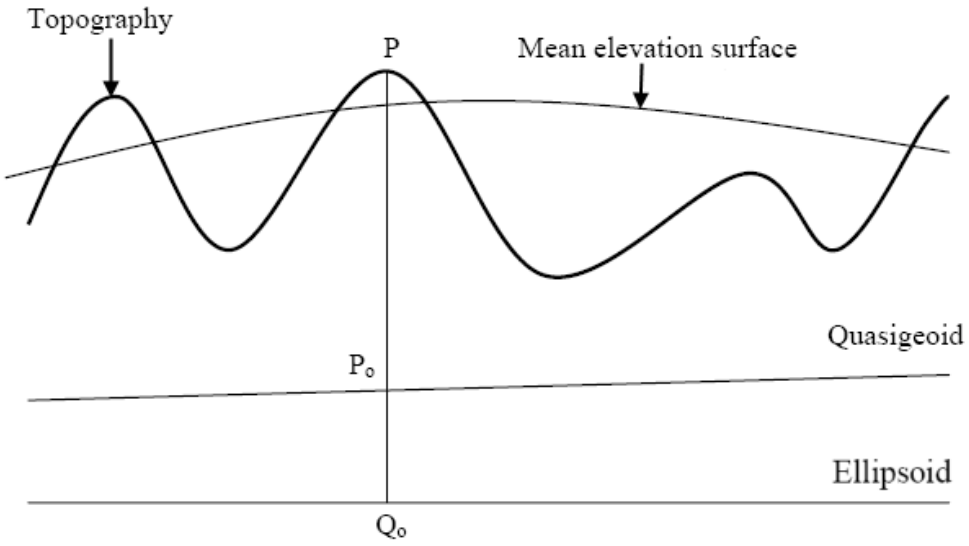

Figure (2.8): The geometry of the RTM reduction.

The reference elevation surface can be constructed by averaging the fine (detailed) resolution topography grid, representing elevations of the area or specially defined through a high-order spherical harmonic expansion of the topography of the earth, and then low-pass filtering the average grid generated by taking moving averages of an appropriate number of adjacent blocks.

According to Forsberg (1984, p. 39), the topographic effect on the gravity of the RTM reduction is computed as:

$$\Delta g_{RTM} = 2\pi G\rho (H - H_{ref}) - A_{TC} \tag{2.31}$$

2.4.5 Molodensky Free-Air Gravity Anomalies

In order to remove *all topographic masses outside the geoid*, it is necessary to know the density of the masses above the geoid. In practice

this involves some kind of an assumption, for instance, putting ρ= 2.67 $g.cm^{-3}$. A second assumption is usually made in the free-air reduction, which is part of the reduction of gravity to the geoid: the actual free-air gravity gradient is assumed to be equal to the normal gradient (cf. section 2.4).

These two assumptions falsify our results, at least theoretically (Heiskanen &Moritz, 1967, p. 290). To avoid this theoretically, Molodensky proposed approach in 1945, replacement of the Earth's surface by the telluroid; and the use of a reference ellipsoid is chosen in the way that it is a normal equipotential surface and has the same normal gravity potential value as the geoid surface with respect to the Earth's gravity field, i.e. $U_o = W_o$ (Molodenskii et al., 1962). The proposed solutions to overcome the above assumptions are; splitting the vertical gradient of gravity $\frac{\partial g}{\partial H}$ into a normal and an anomalous part as (Hofrnann-Wellenhof &Moritz, 2005, p. 120):

$$\frac{\partial g}{\partial H} = \frac{\partial \gamma}{\partial h} + \frac{\partial \Delta g}{\partial h} \tag{2.32}$$

Due to lack of dense gravity coverage required for computing the actual vertical gradient of gravity using Eq. (2.32), it is generally approximated by the normal gradient of gravity $\frac{\partial \gamma}{\partial h}$, setting the anomalous part $\frac{\partial \Delta g}{\partial h}$ equal to zero. Based on this approximation, Eq. (2.13) can be written to second-order as (Balasubramania, 1994, p. 21):

$$g_{P_o} = g_P - \frac{\partial \gamma_{Q_o}}{\partial h} H - \frac{1}{2!} \frac{\partial^2 \gamma_{Q_o}}{\partial h^2} H^2 \tag{2.33}$$

According to Heiskanen &Moritz (1967, p.78 and 79), the first and second derivative of normal gravity can be computed using:

$$\frac{\partial \gamma}{\partial h} = -\frac{2\gamma}{a}(1 + f + m - 2f\sin^2\varphi) \tag{2.34}$$

$$\frac{\partial^2 \gamma}{\partial h^2} = \frac{6\gamma}{a^2} \tag{2.35}$$

Where *m* is given by (Hofmann-Wellenhof &Moritz, 2006, p.70):

$$m = \frac{\omega^2 a^2 b}{GM} \tag{2.36}$$

Where *f* is the flattening, *a* is the semi-major axis, *b* is semi-minor axis, ω is angular velocity and *GM* is a geocentric gravitational constant of the reference ellipsoid.

Substituting the values for the first and second derivative of normal gravity in Eq. (2.33), we can write the free-air gravity anomaly Eq. (2.16) as:

$$\Delta g_c = g_p - \gamma_{Q_o}\left[1 - 2(1 + f + m - 2f\sin^2\varphi)\frac{H}{a} + 3\left(\frac{H}{a}\right)^2\right] \tag{2.37}$$

Where Δg_c are called the free-air gravity anomaly in the classical approach. In the Molodensky approach, the gravity anomaly is the difference between the actual gravity as measured on the ground and the normal gravity on the telluroid defined as (cf. Figure 2.9):

$$\Delta g_M = g_P - \gamma_Q \tag{2.38}$$

Where g_p is the gravity observed at the surface point *P* and the γ_Q is the normal gravity at the corresponding point *Q* on the telluroid.

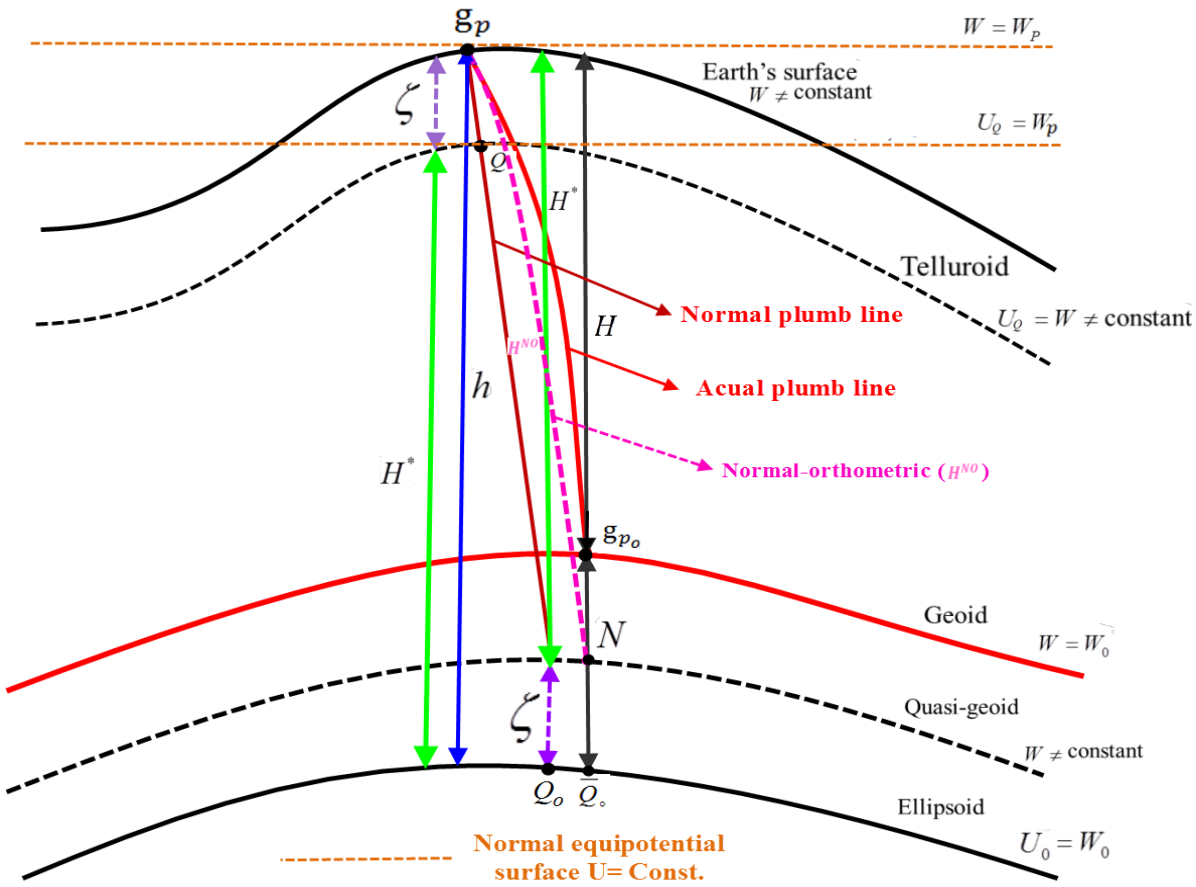

Figure (2.9): The Reference Surfaces and Height Systems.

From Fig.(2.9), the telluroid is an auxiliary surface obtained by the point-wise projection of points P on the Earth's surface along the straight-line ellipsoidal normal to points Q that have the same gravity potential value in the normal gravity field U_Q as the original points P in the Earth's gravity field W_P, i.e., $U_Q = W_P$. As such, the telluroid is not an equipotenial surface without physical meaning coinciding with the ellipsoid on the oceans.

The normal gravity at the point Q is computed from the normal gravity at the ellipsoid γ_{Q_o} by the normal free-air reduction using (Hofrnann-Wellenhof &Moritz, 2005, p. 298):

$$\gamma_Q = \gamma_{Q_o} + \frac{\partial \gamma_{Q_o}}{\partial h} H^* + \frac{1}{2!} \frac{\partial^2 \gamma_{Q_o}}{\partial h^2} H^{*2} + \ldots \qquad (2.39)$$

Where H^* is the normal height of the point *P*. and γ_{Q_o} normal gravity computing using Eq. (2.17).

A direct formula for computing γ_Q at *Q* is also given by (ibid, 2005, p. 298) as:

$$\gamma_Q = \gamma_{Q_o}\left[1 - 2(1 + f + m - 2f\sin^2\varphi)\frac{H^*}{a} + 3\left(\frac{H^*}{a}\right)^2\right] \qquad (2.40)$$

From Eq. (2.38) and Eq. (2.40) we write the Molodensky free-air gravity anomalies as:

$$\Delta g_M = g_P - \gamma_{Q_o}\left[1 - 2(1 + f + m - 2f\sin^2\varphi)\frac{H^*}{a} + 3\left(\frac{H^*}{a}\right)^2\right] \qquad (2.41)$$

In this study, the normal height H^* of the gravity station is generally unavailable, so the orthometric height *H* is used instead. Table (2.2) show that the value of quantities appearing in above equation (NIMA, 2004, Tables 3.1 and 3.4).

Table (2.2): Numerical Values of Some Parameters of WGS 84 Ellipsoid.

Parameters	Notation	Value	Unit
Semi-major axis	*a*	6378137.0	*m*
Flattening	*f*	0.003352810664745	*unitless*
$m=\omega^2 a^2 b/GM$	*m*	0.003449786506841	*unitless*

2.5 Statistical Methods Used For Evaluating Models

2.5.1 Spectral Analysis of Earth's Gravitational Models

Since the main interest in using Earth's gravitational model is in gravity field determination, it has been decided to validate the product models in this Thesis, with respect the accuracy they provide in gravity anomalies.

The Earth's gravitational model can be expressed in a spherical harmonic series where the potential coefficients are $\overline{C}_{nm}$ and $\overline{S}_{nm}$ their standard deviations are $\sigma_{\overline{C}_{nm}}$ and $\sigma_{\overline{S}_{nm}}$ (errors associated for each coefficient), respectively, then the signal and error degree variances for each model, per degree, can be computed.

The signal degree variances (spectral power) represent the amount of the signal contained (amplitude) in each degree or up to a specific degree, while the error degree variances represent the error of the model up to a specific degree. The scaled signal and error degree variances for the various quantities related to the gravity field can be computed as follows (Vergos at al., 2006):

a) For gravity anomalies:

$$\sigma_n^2(\Delta g) = \left(\frac{GM(n-1)}{a}\right)^2 \left(\frac{a^2}{R^2}\right)^{n+1} \sum_{m=0}^{n} (\overline{C}^2_{nm} + \overline{S}^2_{nm}) \qquad (2.42)$$

$$\varepsilon^2_{\sigma_n(\Delta g)} = \left(\frac{GM(n-1)}{a}\right)^2 \left(\frac{a^2}{R^2}\right)^{n+1} \sum_{m=0}^{n} (\sigma^2_{\overline{C}nm} + \sigma^2_{\overline{S}nm}) \qquad (2.43)$$

b) For geoid heights:

$$\varepsilon^2_{\sigma_n(N)} = \left(\frac{GM}{\gamma a}\right)^2 \left(\frac{a^2}{R^2}\right)^{n+1} \sum_{m=0}^{n} (\sigma^2_{\overline{C}nm} + \sigma^2_{\overline{S}nm}) \qquad (2.44)$$

Where *GM* is the geocentric gravitational constant, *R* is mean earth radius, *a* stands for the scaling factor associated with the coefficients, *n*, and *m* are the degree and order of the harmonic expansion.

For example, using Eq. (3.42) and Eq. (3.43) the signal and error amplitudes in terms of gravity anomaly per degree of the solved-for spherical harmonic coefficients for the high degree reference model EGM2008, EGM96 (Lemoine et al., 1998) and the satellite-only gravity field model GOCO05s, which are used in this investigation, are shown in Fig. (2.10). In addition, Fig. (2.11) show gravity anomaly cumulative Root Mean Square (RMS) and geoid error. The error degree amplitudes are the formal ones, i.e. resulting from the adjustment. The computations were carried out using the FORTRAN GRAVSOFT program *degv.for* (not shown in Python Launcher).

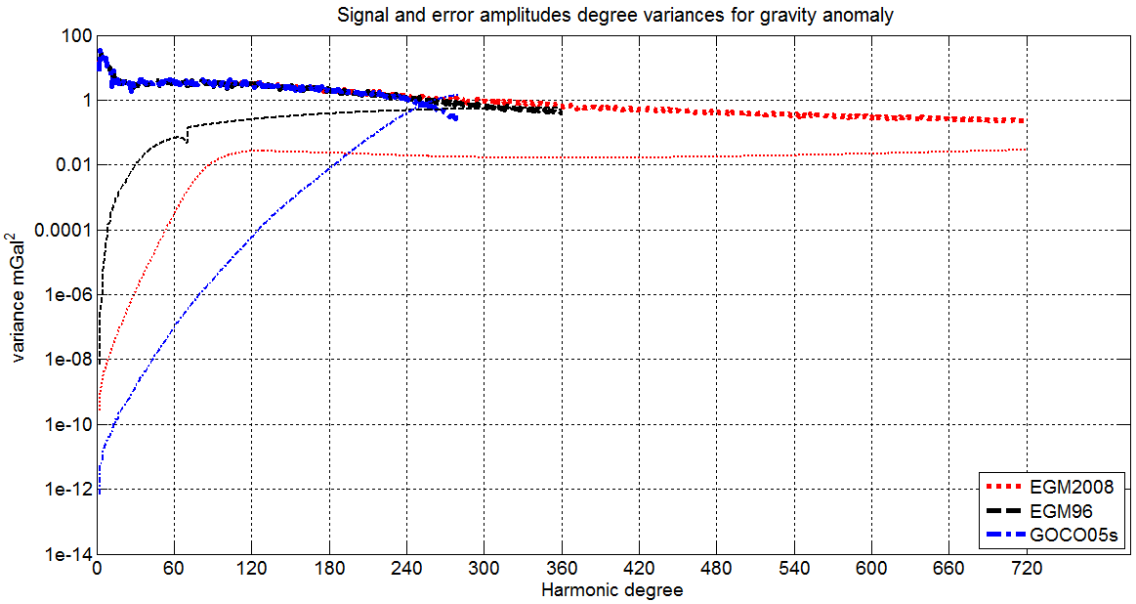

Figure (2.10): Signal (thick lines) and error (thin lines) amplitudes per degree in terms of gravity anomaly for the geopotential harmonic model EGM2008 (Dotted), EGM96 (Dashed) and GOCO05s (Dash-dot).

From Fig. (2.10) it is concluded that the GOCO05s model has the same power as EGM2008 and EGM96 up to its maximum degree of expansion (n=240). In addition, Its error is smaller than the model EGM96 up to n=240 and EGM2008 up to n=190.

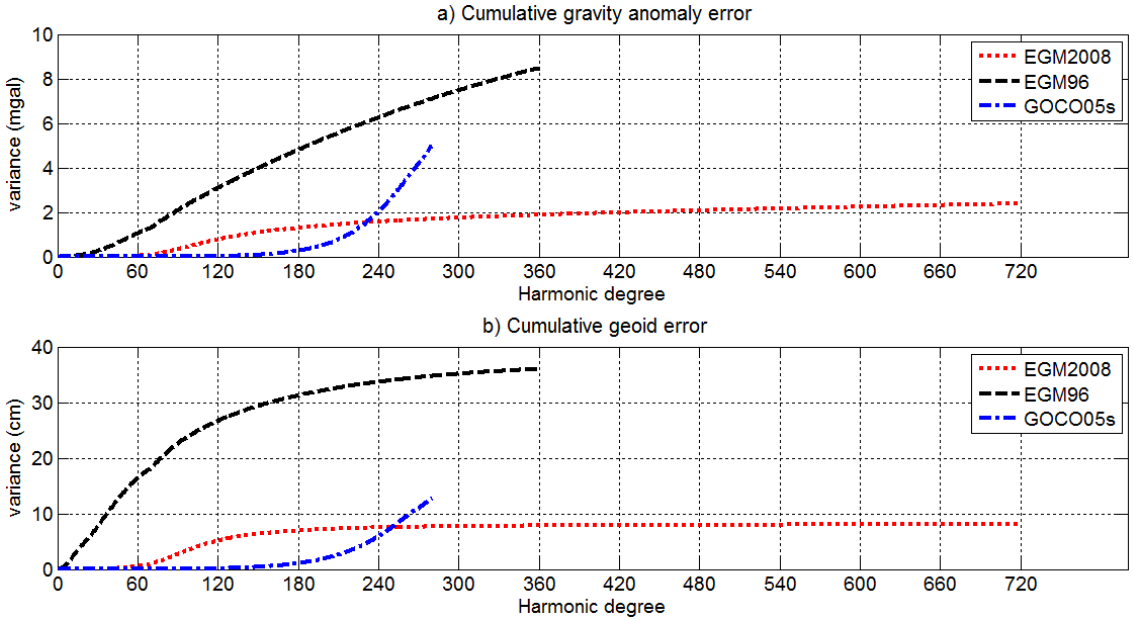

Figure (2.11) Cumulative RMS of Gravity Anomaly and Geoid Error.

Furthermore, from Fig. (2.11a) it can be seen that the satellite-only model GOCO05s offers ±2 mGal accuracy up to n=240 for anomaly while it reaches the ±5 mGal level at n=280. In addition, the GOCO05s more accurate than EGM96. Moreover, the GOCO05s more precise than EGM2008 at n=180, where the RMS decreased from ± 1.30 mGal for EGM2008 to ± 0.27 mGal for GOCO05s, which is due to the use of a longer time-series of CHAMP, GRACE and GOCE data in its development. Besides, the accuracy of the EGM2008 model is an improvement from degree n=240 to the maximum degree compared to both models GOCO05s and EGM96.

Similarly, from Fig. (2.11b) it can be seen that the GOCO05s gives the best geoid accuracies of ± 1 cm than both models EGM2008 and EGM96, up to degree n=180, where EGM2008 and EGM96 give ± 7 cm and ± 31 cm, respectively. From the analysis given so far, the satellite-only model GOCO05s is the best model that is developed from satellite data alone at n=180, while the best-combined model is EGM2008, where EGM2008 gives ± 8 cm at maximum degree.

2.5.2 Local Empirical Covariance Functions

The empirical covariance functions are great importance for studies of the earth's gravity field. The performance of the gravity field is reflected in these functions. The magnitude of the variations and the roughness of the field are described (Knudsen, 1988, p.1).

This kind of information is important and has to be taken into account when gravity field related quantities are estimated from a set of observations. The method of least squares collocation (Moritz, 1980), is widely used for this purpose. When studies of the gravity field take place in local areas, the use of high degree Global Geopotential Harmonic Models (GGMs) is very important. Estimations of gravity field related quantities are carried out relative to GGMs using the residual gravity field (observations) and the local empirical covariance function see e.g. (Fashir & Kadir 1998).

The determination of a local empirical covariance function was discussed by Goad et al. (1984). They arrived at the following definition of a local covariance function: "A local covariance function is a special case of a global covariance function where the information content of wavelengths longer than the extent of the local area has been removed, and the information outside, but nearby, the area is assumed to vary in a manner similar to the information within the area" (Knudsen, 1988, p.1). The gravity anomaly covariance function for gravity anomalies in two points *P* and *Q* estimation using the following formula as (Sansò &Sideris, 2013, p.321):

$$\mathrm{C}(\psi) = \mathrm{C}ov(P,Q) = \frac{1}{M}\sum_{n=1}^{M}\Delta g(\mathrm{P})\ \Delta g(\mathrm{Q}) \qquad (2.45)$$

Where M is the number of products from the i^{th} an interval $\Delta\psi$ of spherical distance. In a local area, we will implicitly regard all data outside the area

as having the same statistical characteristics as the data in the area; so that we may estimate the empirical covariance function by taking an interval of spherical distance (also denoted the sampling interval size).

$$\psi_i - \frac{\Delta\psi_i}{2} \quad \leq \quad \psi_i \quad \leq \quad \psi_i + \frac{\Delta\psi_i}{2} \tag{2.46}$$

For the local gravity anomaly covariance functions, there are three essential parameters (Fashir &Kadir 1998; Amin et al., 2002), these are the covariance (C_0), the correlation length (α) and the first crossing zero- point ($\psi°_1$) as shown in Fig. (2.12).

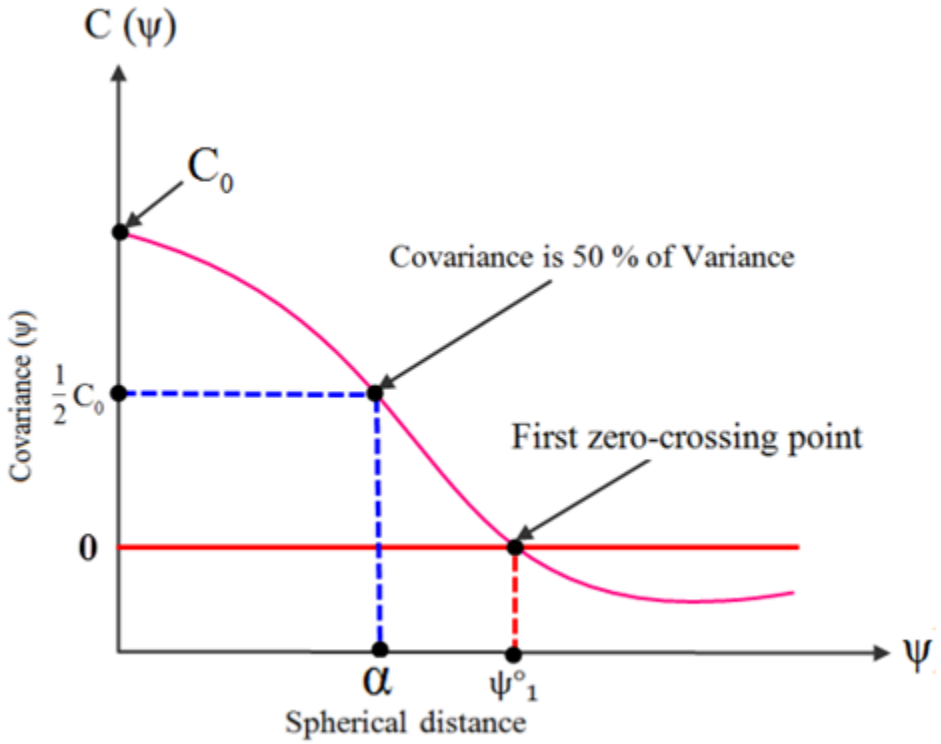

Figure (2.12): Essential parameters of covariance function

a) **The covariance (C_0) :** This is the value of covariance function C (ψ) when the spherical distance (ψ) between the point *P* and *Q* is equal to zero.

$$C_0 = C(\psi) = C(0) \qquad at \quad \psi = 0 \tag{2.47}$$

The covariance defines the statistical correlation of gravity anomalies and the average product of the anomalies at constant

distances of 0', 2', 4', etc. For practical purposes, it's the variance of the residual gravity anomalies in square mGal at $\psi = 0$.

b) **The correlation length (α):** This is the value of the argument for which C (ψ) has decreased to half of its value at $\psi = 0$.

$$C(\alpha) = \frac{1}{2} C_0 \tag{2.48}$$

The correlation length (α) is used to determine the most appropriate shape of covariance function of the residual field, which approximates the maximum distance between the correlated data points.

c) **The first zero-crossing point (ψ°_1):** In theory, the first zero-crossing point (ψ°_1) of the empirical covariance function of the reduced gravity anomalies up to degree *N* of geopotential harmonic model should be located at distance by the rule of thumb as (Arabelos &Tscherning, 2010):

$$\psi_1^\circ = \frac{180^o}{(2 \times N)} \tag{2.49}$$

For example: for degree 360 and 2190 of geopotential harmonic model, the appearance of (ψ°_1) located nearly at distances 15.0′ and 2.5′ minute, respectively. In another word, according to Meissl (1971), Tscherning (1974) and Rapp (1977a), the first zero-crossing point represents how many spectral full degrees have been actually removed from the used harmonic model as follows:

$$N = \frac{180^o}{(\psi_1^\circ)} \tag{2.50}$$

After maximal degree Eq. (2.50) the model may not give reliable information in the area (Tscherning et al., 2001). Equation (2.49) and (2.50) presupposes that the data should be error-free and reduced to an error-free gravitational model.

2.6 Vertical reference surfaces

The choice of the vertical reference surface (vertical datum) is guided by the choice of height system, i.e. orthometric heights use the geoid; normal heights the telluroid; normal-orthometric heights the quasi-geoid and ellipsoidal heights the ellipsoid. In other words, a vertical datum (zero height surfaces) is a reference surface to which the vertical coordinates of points are referred. All of these reference surfaces can be defined either globally or regionally, such that they approximate the entire Earth's surface or some specified region, respectively. With no official global vertical datum definition, most countries or regions today use regional vertical datums as a local reference height system (Fotopoulos, 2003).

The regional vertical datums are to average sea level observations over approximately 19 years (or more precisely, ~18.6 years, which corresponds to the longest tidal component period) for one or more fundamental tide gauge. This average sea level value is known as mean sea level (MSL) and the local MSL was assumed to coincide with the geoid (Sansò and Sideris 2013, p., 521).

However, this assumption is clearly false; today it is well known that differences between the local MSL and the geoid of approximately ±2m can be reached (Rapp, 1995). This difference is caused by the sea dynamics and other meteorological processes, such as changes in seawater temperature, salinity, atmospheric pressure, the wind blows, water currents, etc. (Pugh, 1987), and it is called Sea-Surface Topography (SST) or Dynamic Ocean Topography (DOT).

2.6.1 Global Vertical Datum

A global vertical datum can be defined as a height reference surface for the whole Earth, which referred to a unique global equipotential surface (e.g.

the global geoid). There are several arguments indicating the practical significance of global vertical datum definition (Heck & Rummel, 1990):-

a) Monitoring sea level changes on various time and space scales will become an important challenge for geodesy and oceanography in near future.
b) A globally consistent system of calibration points is required for future satellite altimetry and gradiometry missions.
c) Providing an alternative to local vertical datums, which may have systematic biases between the spirit levelling datasets from different regions and national gravity data centers.
d) Comparison between the results of geodetic levelling and oceanographic procedures for determining sea surface slopes over large distances requires a consistent vertical datum system along the whole coastline segment under consideration.

Another area where a global vertical datum has been deemed necessary is for global change applications, such as instantaneous sea surface models, polar ice-cap volume monitoring, post-glacial rebound and land subsidence studies. These applications require a global view of the Earth with measurements not only on land but over the oceans as well (Fotopoulos, 2003). An accurate datum connection across the globe requires very accurate geoid determination over varying wavelengths (depending on the spatial distance between regional height systems) as well as consistency between regions.

Other strategies offered for solving the global vertical datum problem include purely oceanographic approach, the use of satellite altimetry combined with geostrophic levelling, geodetic boundary value problem, and satellite positioning (GNSS) combined with gravimetry (Sansò and Sideris 2013, p., 523).

2.6.2 Local Vertical Datum

The geoid is a level surface described by the Earth's gravity field and there are an infinite number of level surfaces of the Earth's gravity field, and therefore, it is required to identify which one will be used as the vertical reference surface. There are two practical methods to assess the vertical datum of a levelling network; the first one is defining a constant value of Earth's gravity potential, $W = W_o = \text{constant}$ (abstract option) and the second one whereby the chosen vertical datum gives a specific approximation of the MSL surface (Vaníček, 1991, p. 83). Most countries or regions have chosen the second method to define the height of a benchmark with respect to the local MSL. According to Sansò and Sideris (2013), the following steps need to establish the vertical datum of a levelling network see Fig. (2.13):-

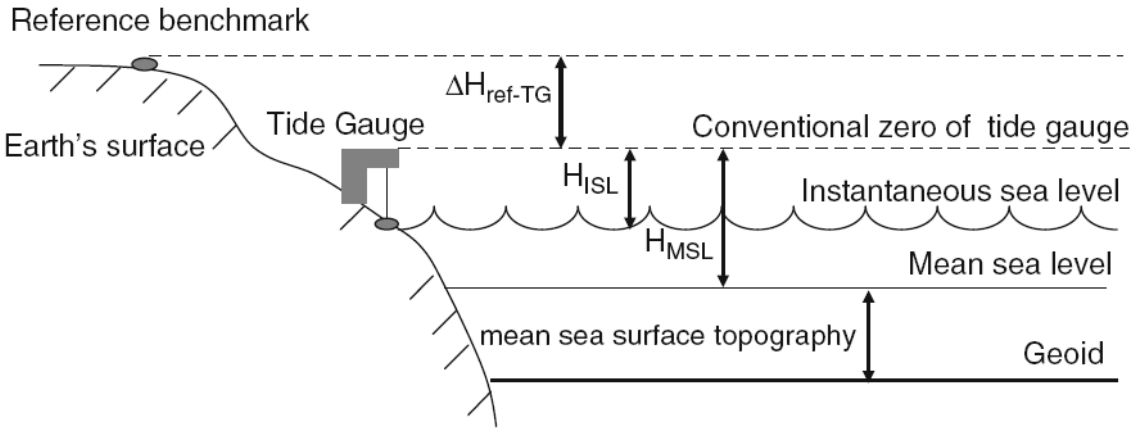

Figure (2.13): Establishment of a reference benchmark height (source: Sansò & Sideris, 2013, p., 521).

a) A tide gauge must continuously record the instantaneous sea level height observations (H_{ISL}).
b) All the H_{ISL} values from a certain period of time are averaged in order to obtain the local MSL (H_{MSL}).
c) The height of the benchmark is measured with respect to the tide gauge (ΔH_{ref-TG}).

d) The height of the benchmark (H_{ref}) is calculated by:

$$H_{ref} = H_{MSL} + \Delta H_{ref-TG} \tag{2.51}$$

Levelling begins from this benchmark and reference heights are accumulated by measuring height differences along levelling lines. The accuracy of the reference benchmark height derived in this manner is dependent on the precision of the height difference ΔH_{ref-TG} and the value for MSL H_{ISL}.

For highly accurate heights such as those needed for a cm-level vertical datum, the tide gauges cannot be assumed to be vertically stable because land motion at tide gauges is a source of systematic error, which causes distortion in the height network if it is not corrected for. In other words, the tide gauge's observations should be averaged for at least 18.6 years for obtaining the local MSL value, because of the high correlation between the tides and the Earth's notation, which requires 18.6 years to complete a full cycle. However, it should be noted that the effect of the local SST is not neglected in Eq. (2.51).

It should be noted that due to the fact that many techniques are used together to define the vertical reference surfaces, it is required that all the measurements are referred to the same tidal system. The tidal system concept will be described in the next section.

2.7 Earth Tides

The definition of the vertical datum zero level is also affected by the phenomenon of Earth tides, which involves of an elastic deformation of the terrestrial globe caused by the gravitational action of the Moon and Sun (Melchior, 1974, p. 275). The tidal deformation consists of two parts: permanent and periodic (Ekman, 1989). The first part is latitude-dependent (and to a smaller extent in the height), while the second part is time-

dependent (e.g. diurnal and semi-diurnal variations). There are three systems for dealing with these permanent tidal effects: (Ekman 1989, Rapp et al., 1991):-

a) Tide-free (or nontidal) system, where all direct and indirect effects of the sun and moon are removed.
b) Mean- tide system, where the periodic tidal deformation is removed but the permanent tidal effects (both direct and indirect) are kept not removed or, equivalently, this system would exist in the presence of the sun and the moon.
c) Zero- tide system, where the permanent direct effects of the sun and moon are removed, but the indirect effect component related to the elastic deformation of the Earth is retained.

The International Association of Geodesy (IAG) Resolution Number 16 adopted in 1983 at the General Assembly in Hamburg (IAG, 1984) states that *"the indirect effect due to the permanent yielding of the Earth should be not removed and the need for the uniform treatment of tidal corrections for various geodetic quantities such as gravity and station positions"* (Tscherning, 1984). The fundamentals supporting this resolution have not changed. The zero-tide system is an adequate tide system applicable gravity field quantities both gravity acceleration and gravity potential of the rotating and deforming Earth.

However, this endorsement has not been universally adopted. For example, the definition of the International Gravity Standardization Net 1971 (IGSN71, Morelli et al., 1972) gravity system is in terms of the mean tide system (Poutanen et al., 1996), while EGM2008 and EGM96 have been produced in terms of the tide-free system because the majority of the source data for these appeared to be in terms of that system. Regarding 3-D positioning, the tide-free approach seems to have entered the 3-D reference

frames more or less by accident (not by design), through the processing programs of the observations (VLBI, SLR, GPS), that apparently happened, although the recommendations of International Earth Rotation and Reference Systems Service (IERS) processing standards for adopting the mean (≡zero) system (McCarthy & Petit, 2004). The IERS's recommendations were strongly opposed by 3-D positioning users since it would have abruptly changed the coordinates of the stations by at least 10 cm (Mäkinen &Ihde, 2009).

According to Ekman (1989), the treatment of the permanent tides must be taken into account in the following cases:-

a) Comparison of different height or gravity systems (e.g. two neighbor countries).
b) Computation of land uplift from two levelling within a country.
c) Study of mean sea level, i.e. SST.
d) Comparison of GPS heights with spirit levelling heights.
e) Computation of geoid heights using Stokes' formula or other moths.

To do this we need to be able to transform one kind of gravity to another or one kind of height to another. Equations to transform gravity observations, height differences, heights above the ellipsoid, and geoid heights between tidal systems were presented in Ekman (1989). Using the subscripts m, n, and z to denote the mean-tide, non-tidal or tide-free and zero-tide system respectively the relations for gravity observations (g) are given by:

$$\left.\begin{aligned} g_m - g_z &= -30.4 + 91.2\ \sin^2\varphi \\ g_z - g_n &= (\delta - 1)(-30.4 + 91.2\ \sin^2\varphi\ ) \\ g_m - g_n &= \delta(-30.4 + 91.2\ \sin^2\varphi\ ) \end{aligned}\right\} \qquad (\mu Gal) \qquad (2.52)$$

Where φ is the latitudes of stations and δ is the so-called tidal gravimetric factor usually taken as 1.16.

In order to transform height differences (ΔH) between the three tide systems are given by:

$$\left.\begin{aligned} \Delta H_m - \Delta H_z &= 29.6\ (\sin^2\varphi_N - \sin^2\varphi_S) \\ \Delta H_z - \Delta H_n &= 29.6\,(\gamma - 1)(\sin^2\varphi_N - \sin^2\varphi_S) \\ \Delta H_m - \Delta H_n &= 29.6\,\gamma\,(\sin^2\varphi_N - \sin^2\varphi_S) \end{aligned}\right\} \qquad (cm) \qquad (2.53)$$

Where φ_N and φ_Z are the latitudes of the northern and southern stations, respectively and γ notes the direct gravitational attraction usually taken as 0.68.

To transform a GPS height (h) of the non-tidal crust to a GPS height of the zero (≡mean) crust we should add as (Kotsakis et al., 2012):

$$h_z \equiv h_m = h_n + k^*\,(9.9 - 29.6\,\sin^2\varphi) \qquad (cm) \qquad (2.54)$$

Where k^* is the conventional (second-degree) Love number that is approximately equal to 0.62 (Ekman, 1989).

Finally, the tidal relationships between geoid undulations (N) are the following:

$$\left.\begin{aligned} N_m - N_z &= (9.9 - 29.6\sin^2\varphi) \\ N_z - N_n &= k\,(9.9 - 29.6\sin^2\varphi) \\ N_m - N_n &= (1+k)(9.9 - 29.6\sin^2\varphi) \end{aligned}\right\} \qquad (cm) \qquad (2.55)$$

Where k the potential *Love number* is usually taken as 0.3 (Melchior, 1983).

2.8 History of the Egyptian Vertical Datum and Control Networks

2.8.1 The Egyptian Vertical Datum

The vertical datum of the precise levelling network in Egypt has been set as MSL at Alexandria harbor. It was taken as the mean between the daily readings of high and low water level during the years 1898 to 1906. These were the only available recorded observations when the survey

department undertook the levelling in 1906 (Cole, 1939). According to the permanent tide considerations (cf. section 2.7), the vertical datum of Egypt is a mean- tide system.

An investigation has been carried out to study the variation of MSL at Alexandria in relation to the meteorological elements, namely wind speed and pressure. This study used real data of monthly average water level from 1962 to 1966, and the results show that an increase of 11.2 cm was detected in the definition of the vertical datum of Egypt (Sharaf El-Din & Rifat, 1968). Recently, from 1944 to 2003 the mean sea level at Alexandria MSL is 11.6 cm over the 1906 old definition of MSL (Mohamed, H.F., 2005).

2.8.2 The First-order vertical Networks in Egypt

The Egyptian vertical control networks do not extant through the whole country; it is limited to the Nile Valley and the Delta, beside few loops in the Eastern Desert Fig. (2.14). The first-order network of precise levelling in Egypt was carried out by the Survey Authority of Egypt in the years of 1906 to 1912 in order to establish the fundamental benchmarks over the whole country, so that the irrigation department's engineers could control systems of levels and refer them to a single standard datum (Cole, 1939). The reference datum adopted by Survey of Egypt was mean sea level at Alexandria harbor. A network of eleven closed loops covering the whole area of the delta, and two single lines joining this network to Alexandria and Suez have been established, too. By 1936 the whole delta has not only been re-observed, but many new lines have been added too, forming a new network of 32 closed loops. Hence, the leveling lines have reached Wadi-Halfa, the southern boundary of Egypt (Cole, 1944).

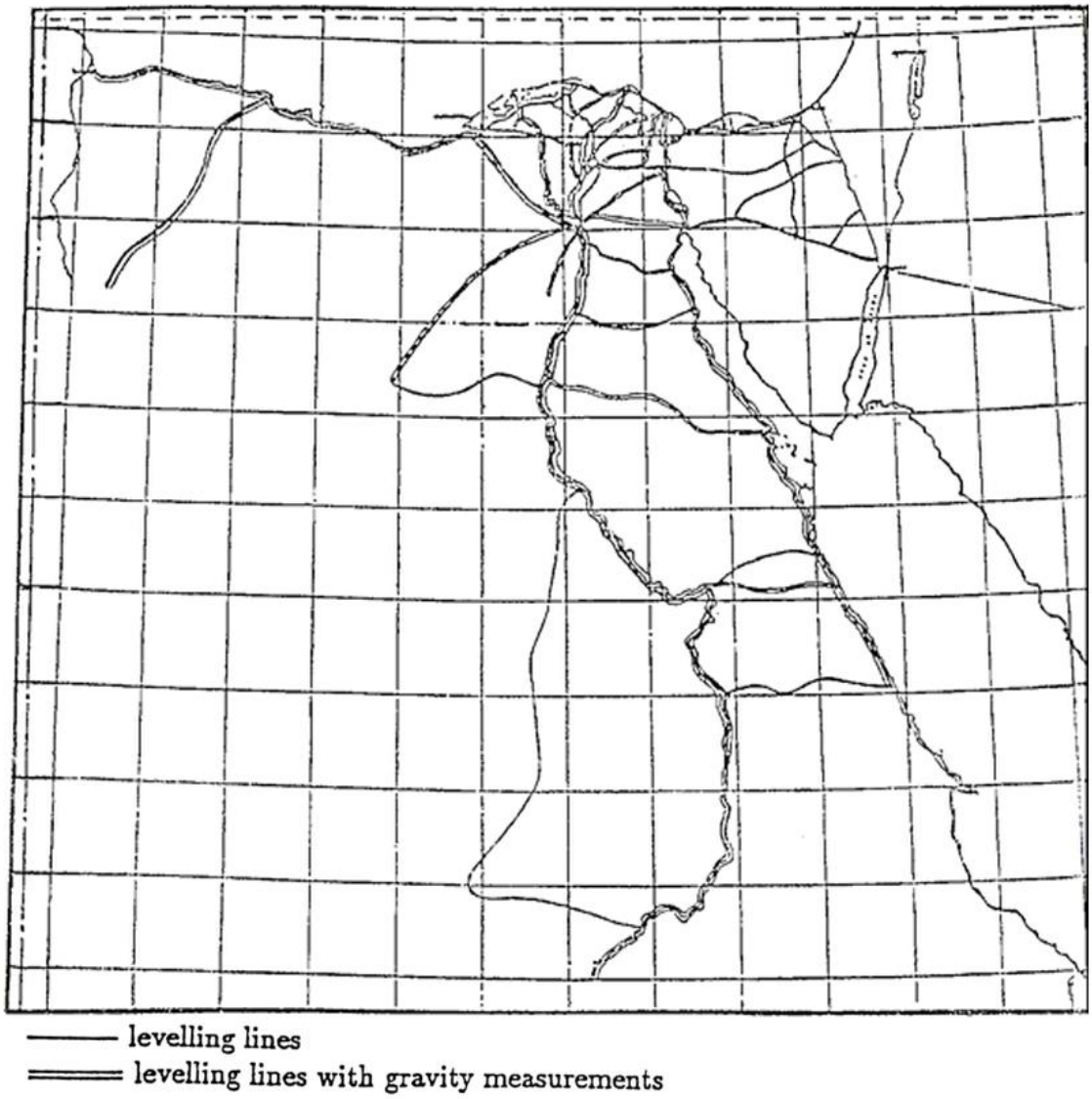

Figure (2.14): The First-order Levelling Network in Egypt (Saad, A., 1993).

2.8.3 Defects in the Vertical Datum of Egypt

Based on the previous sections, it can be concluded that there exist several shortages in the vertical datum of Egypt (Saad, A., 1993; Mohamed, H.F., 2005) such as:-

a) The first remarkable problem is that the vertical datum of Egypt has been established on the determination of MSL from only one tide gauge (not a physical measurement).

b) The determination of MSL has been carried out using the method of averaging daily high and low water level for eight years. This technique is not the optimum method for such a determination.

c) The effects of meteorological quantities on the recorded sea level readings have not been taken into account.
d) The MSL has been assumed to be coinciding with the geoid surface, which is not true as long as the Sea Surface Topography (SST) has not been considered.

Thus, these shortcomings will significantly affect the accuracy of the vertical control network in Egypt. In addition, the systematic and random errors in differential levelling.

For Example, according to Nassar et al. (1997); the deviation of the MSL from the geoid is approximately ±1.0 m (SST), which implies that in geodetic practice this does not cause problems because height differences are the quantity of interest. However, in oceanography, the absolute heights are very important.

However, various investigations have been performed to study these defects and propose solutions to overcome them see e.g. (Nassar, 1981; Shaker, 1990; Saad, A., 1993; El-Shazly, 1995 and Mohamed, H.F., 2005).

Chapter 3

SPHERICAL HARMONIC ANALYSIS AND SYNTHESIS

3. SPHERICAL HARMONIC ANALYSIS AND SYNTHESIS

3.1 Overview

This chapter introduced the theory and procedures required for tailor process. In addition, the basic equations of global spherical harmonic synthesis and analysis and their auxiliary relationships were presented. Moreover, the procedure for improving global gravitational model using integral techniques within an iterative algorithm is described. Finally, the chapter also describes the basic equation of geoid determination by 3D Least-squares collocation (LSC).

3.2 Basic Equations

The actual gravitational potential V in spherical harmonic is given by (Rapp, 1982, p.1):

$$V = \frac{GM}{r}\left[1+\sum_{n=2}^{\infty}\left[\frac{a}{r}\right]^n \sum_{m=0}^{n}(\overline{C}_{nm}\cos m\lambda + \overline{S}_{nm}\sin m\lambda)\,\overline{P}_{nm}\,(\sin\overline{\varphi})\right] \qquad (3.1)$$

Where GM is the geocentric gravitational constant, r is geocentric radius, a stands for the scaling factor associated with the coefficients, λ geodetic longitude, $\overline{\varphi}$ is the geocentric latitude, n and m are the maximum degree and order of the harmonic expansion, $\overline{C}_{nm}$ and $\overline{S}_{nm}$ are the fully normalized geopotential coefficients, and $\overline{P}_{nm}(\sin\overline{\varphi})$ denotes the associated fully normalized Legendre functions.

The disturbing potential quantities (T) is equal to differences between the actual potential (V) and the normal potential (U) at the same point, the normal potential computes on the surface of the ellipsoid. The disturbing potential quantities can be expressed as (ibid., p. 1):

$$T(r,\bar{\varphi},\lambda) = V(r,\bar{\varphi},\lambda) - U(r,\bar{\varphi},\lambda) \tag{3.2}$$

The normal gravitational potential of the mean earth's ellipsoid, given by (Torge, 1989, p. 37):

$$U = \frac{GM_{\circ}}{r}\left[1+\sum_{n=2}^{\infty}\left[\frac{a}{r}\right]^{n}\bar{C}^{u}_{n0}\bar{P}_{nm}\ (\sin\bar{\varphi})\right] \tag{3.3}$$

The parameters $GM_{\circ}$ are the mass of the reference ellipsoid and $\bar{C}^{u}_{n0}$ denote as the fully normalized harmonic coefficients implied by the reference equipotential ellipsoid. Because of the symmetry features postulated in the mean earth's ellipsoid, only even zonal spherical harmonics $\bar{C}^{u}_{2n,0}$ (Heiskanen & Moritz, 1967, p.72) appear in Eq. (3.3). The even degree zonal harmonic coefficients very quickly converge toward zero, so that Eq. (3.3) may normally be truncated after n = 6.

The disturbing potential can be expressed in spherical harmonic expansion by inserting Eq. (3.1) and Eq. (3.3) into Eq.(3.2) as (Rapp, 1982, p.2):

$$T(r,\bar{\varphi},\lambda) = \frac{(GM - GM_{\circ})}{r} + \frac{GM}{r}\left[\sum_{n=2}^{\infty}\left[\frac{a}{r}\right]^{n}\sum_{m=0}^{n}(\bar{C}^{*}_{nm}\cos m\lambda + \bar{S}_{nm}\sin m\lambda)\,\bar{P}_{nm}\ (\sin\bar{\varphi})\right] \tag{3.4}$$

Where $\bar{C}^{*}$ is the difference between the actual coefficients $\bar{C}_{nm}$ and those implied by the reference equipotential ellipsoid, $\bar{C}^{u}_{n0}$ one may write the following relation for $\bar{C}^{*}$:

$$\begin{aligned} \bar{C}^{*}_{n0} &= \bar{C}_{n0} - \bar{C}^{u}_{n0} && if\ \ m = 0 \\ \bar{C}^{*}_{n0} &= \bar{C}_{nm} && if\ \ m \neq 0 \end{aligned} \tag{3.5}$$

This difference is computed to correct the zonal coefficients of the spherical harmonic gravity.

Also, in most cases, we assume GM is equal to $GM_{\circ}$ so that Eq. (3.4) becomes:

$$T(r,\bar{\varphi},\lambda) = \frac{GM}{r}\left[\sum_{n=2}^{\infty}\left[\frac{a}{r}\right]^{n}\sum_{m=0}^{n}(\bar{C}^{*}_{nm}\cos m\lambda + \bar{S}_{nm}\sin m\lambda)\,\bar{P}_{nm}\,(\sin\bar{\varphi})\right] \tag{3.6}$$

3.3 Spherical Harmonic Analysis and Synthesis Techniques

Spherical harmonic analysis and synthesis processes have been revolutionized the development and use of very high-degree Global Gravitational Model (GGM), which is a mathematical approximation to the external gravitational potential of an attracting body.

3.3.1 Global Spherical Harmonic Synthesis

Global Spherical Harmonic Synthesis (GSHS) is the computation of the numerical values of various quantities related to GGM (functionals of the field), given the position of the evaluation point, such height anomalies, gravity anomalies, deflections of the vertical….etc.

In this thesis, the gravity anomaly (Δg) is used, which is can be expressed as (Rapp, 1982, p.4):

$$\Delta g(r,\bar{\varphi},\lambda) = \frac{\partial T}{\partial r} + \frac{1}{\gamma}\frac{\partial \gamma}{\partial r}T(r,\bar{\varphi},\lambda) \tag{3.7}$$

Where γ is the normal gravity on the surface of the ellipsoid described in section (2.4.1), using the spherical approximation, we may write as (Hofmann-Wellenhof &Moritz, 2005, p. 96):

$$\frac{1}{\gamma}\frac{\partial \gamma}{\partial r} = -\frac{2}{r} \tag{3.8}$$

Then Eq. (3.7) becomes:

$$\Delta g(r,\bar{\varphi},\lambda) = -\frac{\partial T}{\partial r} - \frac{2}{r}T(r,\bar{\varphi},\lambda) \tag{3.9}$$

Inserting Eq. (3.6) into Eq. (3.9), the expression for the gravity anomaly (Δg) becomes in spherical harmonics:

$$\Delta g\,(r,\bar{\varphi},\lambda) = \frac{GM}{r^2}\left[\sum_{n=2}^{\infty}(n-1)\left[\frac{a}{r}\right]^n \sum_{m=0}^{n}(\bar{C}^{*}_{nm}\cos m\lambda + \bar{S}_{nm}\sin m\lambda)\,\bar{P}_{nm}(\sin\bar{\varphi})\right] \quad (3.10)$$

The height anomaly and quasi-geoid height are the same, where the height anomaly (ζ) is the distance (measured along the straight-line ellipsoidal normal) between the Earth's surface and the telluroid and the quasi-geoid height (ζ) is the separation between the ellipsoid and the quasi-geoid (cf. Figure 2.7). The quasi-geoid is a non-equipotential surface of the Earth's gravity field and thus has no physical meaning. The height anomaly or quasi-geoid height can be given by the generalized Bruns formula (Bruns, 1878) defined by (Heiskanen & Moritz, 1967, p.293):

$$\zeta\,(r,\bar{\varphi},\lambda) = \frac{T(r,\bar{\varphi},\lambda)}{\gamma} \quad (3.11)$$

Inserting Eq. (3.6) into Eq. (3.11) gives:

$$\zeta(r,\bar{\varphi},\lambda) = \frac{GM}{\gamma r}\left[\sum_{n=2}^{\infty}\left[\frac{a}{r}\right]^n \sum_{m=0}^{n}(\bar{C}^{*}_{nm}\cos m\lambda + \bar{S}_{nm}\sin m\lambda)\,\bar{P}_{nm}(\sin\bar{\varphi})\right] \quad (3.12)$$

Where γ is the normal gravity on the surface of the ellipsoid, the geoid height or usually called geoid undulation is the separation between the reference ellipsoid and the geoid (cf. Figure 2.7)

The geoid height can be given by rewritten formula Eq. (3.11) to become:

$$N\,(\bar{\varphi},\lambda) = \frac{T(\bar{\varphi},\lambda)}{\gamma} \quad (3.13)$$

Here, the anomalous potential *T* evaluated inside masses at sea level (where $r = 0$). However, inside the topography *T* is a non-harmonic function, so N is different from ζ, vice versa in Eq. (3.11). Quasi-geoid coincides reasonably closely with the geoid; up to about 3.4 m in the Himalayas Mountains (Rapp, 1997).

The basic formula for conversion of the height anomaly (ζ) to the geoid height (N) is the well-known equation (Heiskanen & Moritz 1967, p. 326). Conventionally, the height h above the ellipsoid is given by (cf. Figure 2.7).

$$h = H + N \tag{3.14}$$

According to the Molodensky approach (cf. section 2.4.5), the ellipsoid height given by;

$$h = H^* + \zeta \tag{3.15}$$

From these two equations we get:

$$N - \zeta = H^* - H \tag{3.16}$$

This means that the difference between the geoid height N and the height anomaly ζ is equal to the difference between the normal height H^* and the orthometric height H. Since ζ is also the undulation of the quasi-geoid, this difference is also the distance between geoid and quasi-geoid. The normal height and orthometric height are defined by:

$$H = \frac{C}{\bar{g}} \quad , \qquad H^* = \frac{C}{\bar{\gamma}} \tag{3.17}$$

Where C is the geopotential number, $\bar{g}$ is the mean gravity along the plumb line between geoid and earth's surface, and $\bar{\gamma}$ is the mean normal gravity along the normal plumb line between ellipsoid and telluroid. By eliminating C between these two equations, we readily find:

$$H^* - H = \frac{\bar{g} - \bar{\gamma}}{\bar{\gamma}} H \tag{3.18}$$

This is also the distance between the geoid and the quasi-geoid:

$$N = \zeta + \frac{\bar{g} - \bar{\gamma}}{\bar{\gamma}} H \tag{3.19}$$

The term $\bar{g} - \bar{\gamma}$ is approximately equal to the Bouguer anomaly (Hofmann-Wellenhof and Moritz, 2005, p.326); then geoid height or geoid undulation (N) becomes:

$$N(\bar{\varphi},\lambda) = \zeta(r,\bar{\varphi},\lambda) + \frac{\Delta g_B}{\bar{\gamma}} H \qquad (3.20)$$

Where Δg_B are the Bouguer anomaly described in section (2.4.2), and H is the orthometric height

3.3.2 Global Spherical Harmonic Analysis

Global Spherical Harmonic Analysis (GSHA) is extracted the gravitational information from the analysis of the terrestrial data and perturbations of a low Earth orbiter, in a fashion similar to other existing satellite missions. In another word, GSHA seeks the contrary of GSHS, where the function of the field (Synthesis) itself is known from measurements such as gravity anomalies, while the needed quantities are the coefficients of Global Gravitational Model (GGM).

In this thesis, we will use Integral Techniques for harmonic analysis, where the quadrature procedure for estimating spherical harmonic coefficients may be computed from gravity anomalies Eq. (3.10) by employing the orthogonality relationships for fully normalized spherical harmonic functions as (Torge, 1989, p. 44):

$$\begin{Bmatrix} \bar{C}_{nm} \\ \bar{S}_{nm} \end{Bmatrix} = \frac{1}{4\pi} \iint_{\sigma} \frac{r^2}{GM} \left(\frac{r}{a}\right)^n \frac{1}{n-1} \Delta g(\mathrm{r},\theta,\lambda) \begin{Bmatrix} \cos m\lambda \\ \sin m\lambda \end{Bmatrix} \bar{P}_{nm}(\cos\theta)\, d\sigma \qquad (3.21)$$

Where σ is a unit sphere and $d\sigma$ is surface area element and θ polar distance, can simply be expressed in terms of the geocentric latitude $\bar{\varphi}$ as (Torge, 2001, p. 33):

$$\theta = 90^o - \bar{\varphi} \qquad (3.22)$$

The application of Eq. (3.21) requires that the gravity anomaly is given continuously over the surface of the sphere, which is unfortunately not the case for any real data set. We will discuss in detail later how it is used Eq. (3.21) in order to achieve the objectives of this investigation (cf. section 3.5).

3.4 Auxiliary Relationships

To implement the equations discussed in the previous section a number of additional quantities are needed. These are now discussed.

3.4.1 The Reference Potential Coefficients

To implement the basic equations in Eq. (3.1) till Eq. (3.15), the initial computations hypothesis is that the origin of the coordinates system, i.e. the centre of the reference ellipsoid, coincides with the centre of the gravity of the Earth, i.e. the geocentre, and the mass of the reference ellipsoid is considered to be equal to the mass of the Earth, in this way the zero and first order spherical harmonic coefficients are all zero.

We used the values of the Geodetic Reference System 1984 (WGS-84) to define an equipotential reference ellipsoid (NIMA, 2004, Tables 3.1, p.3-5) as shown in the Table (3.1).

Table (3.1): WGS-84 Four Defining Parameters.

Parameters	Notation	Value	Unit
Semi-major axis	a	6378137.0	m
Reciprocal of Flattening	1/f	298.257223563	unitless
Angular velocity	ω	$7292115.0 \times 10^{-11}$	rad/sec
Geocentric gravitational constant	GM	$3.986004418 \times 10^{14}$	$m^3\ s^{-2}$

3.4.2 Permanent Tide System of Harmonic Coefficients

The potential field and the normal potential field can be defined under three different permanent tide systems (cf. section 2.7), it is mandatory that they refer to the same permanent tide system in order to compute geoid undulations through the generalized Bruns equation (Smith, 1998). In addition, In order to compare different harmonic coefficient, it is mandatory that they refer to the same permanent tide system. The effect of changing a permanent tide system is seen only in the second-degree zonal

coefficient $\overline{C}_{2,0}$ (geopotential model) term or $\overline{C}^{*}_{2,0}$ (normal potential field). Conversion between different permanent tide systems involves according to the following equation (Losch & Seufer, 2003):

$$C_{2,0}^{(\text{mean tide})} = C_{2,0}^{(\text{zero tide})} - 1.390 \times 10^{-8} \tag{3.23}$$

$$C_{2,0}^{(\text{mean tide})} = C_{2,0}^{(\text{tide free})} - 1.807 \times 10^{-8} \tag{3.24}$$

Equations (3.23) and (3.24) also agree with the results found in (Melbourne et al, 1983).

3.4.3 The Degree Zonal Coefficients of Reference Potential

The degree zonal harmonics of the equipotential earth's ellipsoid J_n are explicitly defined (Rapp, 1982, p. 7):

$$\begin{aligned} J_2 &= \frac{2}{3}\left[f(1-\frac{f}{2}) - \frac{m}{2}(1-\frac{2f}{7}+\frac{11f^2}{49}) \right] \\ J_4 &= -\frac{4f}{35}(1-\frac{f}{2})\left[7f(1-\frac{f}{2}) - 5m(1-\frac{2f}{7}) \right] \\ J_6 &= \frac{4f^2}{21}(6f-5m) \end{aligned} \tag{3.25}$$

Here *m* is given by (Torge, 1980, p. 58):

$$m = \frac{\omega^2 a^3 (1-f)}{GM} \tag{3.26}$$

The degree zonal harmonic coefficients J_n are related to the fully normalized coefficients of the reference ellipsoid $\overline{C}^{u}_{n}$ through the following relationship (Rapp, 1982, P. 7):

$$\overline{C}^{u}_{n} = \frac{J_2}{\sqrt{2n+1}} \tag{3.27}$$

3.4.4 The Geocentric Radius and Latitude

The geocentric radius *r* can easily be expressed by:

$$r = \sqrt{x^2 + y^2 + x^2} \tag{3.28}$$

Where *x, y,* and *z* are the Geodetic Cartesian Coordinates given by (Rapp, 1981, p.47):

$$\begin{bmatrix} x \\ y \\ z \end{bmatrix} = \begin{bmatrix} (\rho + h)\cos\varphi\cos\lambda \\ (\rho + h)\cos\varphi\sin\lambda \\ \left[\rho(1-e^2) + h\right]\sin\varphi \end{bmatrix} \tag{3.29}$$

Where ρ is the radius of curvature in the prime vertical plane, given by:

$$\rho = \frac{a}{(1 - e^2\sin^2\varphi)^{1/2}} \tag{3.30}$$

Here *h* stands for the ellipsoidal height, φ is the geodetic latitude (should be with respect to an ellipsoid, whose center is at the center of mass of the earth) and *e* is the first eccentricity of the ellipsoid.

The geocentric latitude $\bar{\varphi}$, given by (Rapp, 1982, p.8):

$$\bar{\varphi} = \tan^{-1}\frac{z}{\sqrt{x^2 + y^2}} \tag{3.31}$$

3.4.5 The Fully Normalized Associated Legendre Functions

The fully normalized associated Legendre functions (ALFs), denotes as $\bar{P}_{nm}$ is critical to any calculation involving spherical harmonic expansions. ALFs can be computed from the conventional associated Legendre functions, denote as, P_{nm} by (Torge, 1991, p.26):

$$\bar{P}_{nm}(\cos\theta) = \sqrt{k(2n+1)\frac{(n-m)!}{(n+m)!}}\,P_{nm}(\cos\theta), \quad \mathrm{k}\begin{cases} 1 & for \;\; m = 0 \\ 2 & for \;\; m \neq 0 \end{cases} \tag{3.32}$$

We should be using one of an algorithm, which achieves the speed and the stability and accuracy of the procedure. These can be found in, for

example, Holmes and Featherstone (2002), Colombo (1981) and Paul (1978).

Here, we reproduce one method from Colombo (1981) according to (Rapp, 1982, p.9 -10) as Abd-Elbaky (2011). For convenience; the fully normalized associated Legendre functions are computed as a lower triangular matrix where the rows correspond to degree n and the columns correspond to order m.

Firstly, some elements are computed:

$$\bar{P}_{0,0}(\cos\theta) = 1 \tag{3.33}$$

$$\bar{P}_{1,0}(\cos\theta) = \sqrt{3}\cos\theta \tag{3.34}$$

$$\bar{P}_{1,1}(\cos\theta) = \sqrt{3}\sin\theta \tag{3.35}$$

Then, the diagonal elements corresponding to the diagonal passing through the $n = m$ location. We have:

$$\bar{P}_{n,n}(\cos\theta) = \sqrt{\frac{2n+1}{2n}}\sin\theta \;\; \bar{P}_{n-1,n-1}(\cos\theta)$$

$$\bar{P}_{n,n} = \begin{bmatrix} \bar{P}_{0,0} & & & & \\ & \bar{P}_{1,1} & & & \\ & & \bar{P}_{2,2} & & \\ & & & \ddots & \\ & & & & \bar{P}_{n,n} \end{bmatrix} \tag{3.36}$$

Then the following element is computed:

$$\bar{P}_{n+1,n}(\cos\theta) = \sqrt{2n+3}\,\cos\theta \;\; \bar{P}_{n,m}(\cos\theta)$$

$$\bar{P}_{n,n} = \begin{bmatrix} \bar{P}_{0,0} & & & & \\ \bar{P}_{1,0} & \bar{P}_{1,1} & & & \\ & \bar{P}_{2,1} & \bar{P}_{2,2} & & \\ & & \ddots & \ddots & \\ & & & \bar{P}_{n,n-1} & \bar{P}_{n,n} \end{bmatrix} \tag{3.37}$$

With $n = m$. Then the following recursive relationship is used to calculate the remaining values of $\bar{P}_{nm}$ $n \geq 2$, $(n-2) \geq m \geq 0$.

$$\bar{P}_{n,m}(\cos\theta) = \sqrt{\frac{(2n-1)(2n+1)}{(n-m)(n+m)}}\cos\theta \;\; \bar{P}_{n-1,m}(\cos\theta) - \sqrt{\frac{(2n+1)(n+m-1)(n-m-1)}{(2n-3)(n+m)(n-m)}}\;\bar{P}_{n-2,m}(\cos\theta) \tag{3.38}$$

$$\bar{P}_{n,n} = \begin{bmatrix} \bar{P}_{0,0} & & & & & \\ \bar{P}_{1,0} & \bar{P}_{1,1} & & & & \\ \bar{P}_{2,0} & \bar{P}_{2,1} & \bar{P}_{2,2} & & & \\ \bar{P}_{3,0} & \bar{P}_{3,1} & \ddots & \ddots & & \\ \vdots & \cdots & \ddots & \ddots & \ddots & \\ \bar{P}_{n,0} & \cdots & \cdots & \bar{P}_{n,n-2} & \bar{P}_{n,n-1} & \bar{P}_{n,n} \end{bmatrix}$$

3.4.6 The Calculation of Laplace Surface Harmonic Functions

The generation of $\cos m\lambda$ and $\sin m\lambda$ is done through the following recursion relationships:

$$\begin{aligned} \cos m\lambda &= 2\cos\lambda\cos(m-1)\lambda - \cos(m-2)\lambda \\ \sin m\lambda &= 2\cos\lambda\sin(m-1)\lambda - \sin(m-2)\lambda \end{aligned} \tag{3.39}$$

3.5 Procedure for Improving Global Gravitational Model

After describing the basic equations, we will now discuss in more details the approach of improving a geopotential model using additional gravity data, this process named tailoring. Originally, the approach goes back to an investigation in Kaula (1966), Rapp (1967) and has been further studied by Wenzel (1985).

In this study, we have used the integral formulas for harmonic analysis computation suggested by Weber and Zomorrodian (1988), which is based on a previous investigation made by Wenzel (1985) and refined by Bašić (1990) and Kearsley and Forsberg (1990), through an iterative algorithm, to improve the accuracy of the obtained harmonic coefficients and to decrease the residual field

The basic assumption is that; the additional data have not been used in the development of the geopotential model. The main idea is then to add small correction terms to the original spherical harmonic coefficients to get the new harmonic coefficients (tailored geopotential model) such as

$$\begin{Bmatrix} \overline{C}_{nm} \\ \overline{S}_{nm} \end{Bmatrix}_{Tailored\ \ Model} = \begin{Bmatrix} \overline{C}_{nm} \\ \overline{S}_{nm} \end{Bmatrix}_{Original\ Model} + \begin{Bmatrix} \delta\overline{C}_{nm} \\ \delta\overline{S}_{nm} \end{Bmatrix}_{Corrections} \qquad (3.40)$$

We will rewrite Weber and Zommorrodian (1988) technique in the following steps:-

STEP 0: Start $\overline{C'}_{nm}$ and $\overline{S'}_{nm}$ fully normalized spherical harmonic coefficients of start geopotential coefficients (actual model).

STEP 1: A mean gravity anomaly can be computed from the actual model (start model) as follows (Rapp, 1977b):

$$\overline{\Delta g'} = \frac{GM}{r^2}\sum_{n=2}^{n^{max}}(n-1)\left[\frac{a}{r}\right]^n \beta_n \sum_{m=0}^{n}(\overline{C'}_{nm}\cos m\lambda + \overline{S'}_{nm}\sin m\lambda)\,\overline{P_{nm}}(\cos\theta) \qquad (3.41)$$

Where β_n are the Pellinen smoothing functions and can be viewed as a de-smoothing operator that tries to take into account that frequencies are damped out by taking the average to obtain the mean anomaly. The β_n function can be computed using the following expression:

$$\beta_n = \frac{1}{1-\cos\psi_o}\frac{1}{\sqrt{2n+1}}\left[P_{n-1}(\cos\psi_o) - P_{n+1}(\cos\psi_o)\right] \qquad (3.42)$$

Where ψ_o is the radius of a spherical cap with the same size as the area of integration. A recurrence procedure for the computation of the β_n can be found in Sjöberg (1980).

STEP 2: Comparing the mean gravity anomalies derived from the start model Eq. (3.41) with mean gravity anomalies ($\overline{\Delta g}$), derived from local gravity data, yields differences:

$$\delta\,\overline{\Delta g'} \;=\; \overline{\Delta g} \;-\; \overline{\Delta g'} \tag{3.43}$$

STEP 3: The differences gravity anomalies Eq. (3.43) can be expanded in spherical harmonics as Eq. (3.21), yields correction as follows:

$$\begin{Bmatrix} \delta\,\overline{C'_{nm}} \\ \delta\,\overline{S'_{nm}} \end{Bmatrix} = \frac{1}{4\pi} \iint_{\sigma} \frac{r^2}{GM} \left(\frac{r}{a}\right)^n \frac{1}{\beta_n (n-1)} \; \delta\overline{\Delta g'} \; \begin{Bmatrix} \cos m\lambda \\ \sin m\lambda \end{Bmatrix} \bar{P}_{nm}(\cos\theta)\; d\sigma \tag{3.44}$$

- *Note that:* in the local area the mean gravity anomalies values given over small parts of the sphere bounded by meridians λ= constant and parallels θ = constant, outside this boundaries, mean values is equal to zero, then the numerical evaluation of Eq. (3.44) with respect to a limited number of surface elements $\Delta\sigma$ of the unit sphere; becomes:

$$\begin{Bmatrix} \delta\,\overline{C'_{nm}} \\ \delta\,\overline{S'_{nm}} \end{Bmatrix} = \frac{1}{4\pi} \sum_{i=1}^{k} \frac{r_i^2}{GM} \left(\frac{r_i}{a}\right)^n \frac{1}{\beta_{n,i} (n-1)} \; \delta\overline{\Delta g'_i} \iint_{\Delta\sigma_i} \begin{Bmatrix} \cos m\lambda \\ \sin m\lambda \end{Bmatrix} \bar{P}_{nm}(\cos\theta)\; d\sigma \tag{3.45}$$

Where k is the number of differences occurring between model and terrestrial anomalies, and a splitting of the integral extended over the area of integration $\Delta\sigma$:

$$\iint_{\Delta\sigma_i} \begin{Bmatrix} \cos m\lambda \\ \sin m\lambda \end{Bmatrix} \bar{P}_{nm}(\cos\theta)\; d\sigma = \int_{\lambda_{W_i}}^{\lambda_{E_i}} \begin{Bmatrix} \cos m\lambda \\ \sin m\lambda \end{Bmatrix} d\lambda \int_{\theta_{N_i}}^{\theta_{S_i}} \bar{P}_{nm}(\cos\theta) \sin\theta \, d\theta \tag{3.46}$$

Where θ_N ,θ_S , λ_W and λ_E are the boundaries of the integration area.

STEP 4: Coefficients of the modified potential model (tailored geopotential model) are consequently defined using Eq. (3.40) through:

$$\begin{Bmatrix} \overline{C''}_{nm} \\ \overline{S''}_{nm} \end{Bmatrix}_{Tailored\ \ Model} = \begin{Bmatrix} \overline{C'}_{nm} \\ \overline{S'}_{nm} \end{Bmatrix}_{Original\ Model} + \begin{Bmatrix} \delta\,\overline{C'_{nm}} \\ \delta\,\overline{S'_{nm}} \end{Bmatrix}_{Corrections} \tag{3.47}$$

STEP 5: Again, mean anomalies from tailored geopotential model can be evaluated in analogy to (3.41):

$$\overline{\Delta g''} = \frac{GM}{r^2}\sum_{n=2}^{n\,max}(n-1)\left[\frac{a}{r}\right]^n \beta_n \sum_{m=0}^{n}(\overline{C''}_{nm}\cos m\lambda + \overline{S''}_{nm}\sin m\lambda)\,\overline{P_{nm}}(\cos\theta) \tag{3.48}$$

STEP 6: Then the differences gravity anomalies may once again be formed as defined in analogy to Eq. (3.41):

$$\delta\,\overline{\Delta g''} = \overline{\Delta g} - \overline{\Delta g''} \tag{3.49}$$

However, due to the limited degree of the expansion Eq. (3.48) and due to the approximation through Eq. (3.42), the differences Eq. (3.49) do not vanish completely.

STEP 7: Repeat the steps 3, 4, 5 and 6 until two successive iteration steps give practically the same harmonic coefficients, or alternatively, no practical change in the residual field between two successive iteration steps happens.

Newly, a huge amount of global gravity field data is available. This has improved the resolution of the developed earth global geopotential models (GGMs), where each gravitational observable gives a normal equation in terms of the unknown geopotential coefficients (Abd-Elbaky, 2011).

Thus, a huge system of normal equations is formed, which needs a special technique. Since the early 1980s several methods of harmonic

analysis techniques can be used to estimate the potential coefficients of the geopotential models such as; Colombo (1981) has introduced an effective and fast technique for the harmonic analysis of complete grids of a single data type using Fast Fourier Transform (FFT) and has written two subroutines for harmonic analysis and synthesis, called HARMIN and SSYNTH, referring to a surface of the sphere.

In addition, Tscherning (2001) has presented a method for estimation of spherical harmonic coefficients of the (anomalous) gravity potential from various kinds of gravity field data by using Least-squares collocation (LSC), applied in program GEOCOL. As it is known that LSC requires that as many equations as the number of observations are solved. However, the computational effort may be dramatically reduced if the data are associated with points located equi-distantly on parallels. An implementation of LSC, which takes advantage of this property, is called Fast Spherical Collocation (FSC) (Sanso`& Tscherning, 2003), implemented in program SPHGRIC.

Finally, Abd-Elmotaal (2004) presented a modified technique which used Colombo's (1981) technique with iterative and scaling process for the harmonic analysis of data on the surface of both the sphere and on the ellipsoid. The main idea of this technique, implemented in the HRCOFITR program, is performed using Colombo's main subroutines HARMIN and SSYNTH.

3.6 Geoid Determination by Least-Squares Collocation

3.6.1 Basic Equation for Least-Squares Collocation

The basic equation**s** for the application of LSC for the geoid computation were given in Tscherning (2002), Sadiq, M. et al (2009) and

Tscherning (2013). In addition, the theoretical background is described in full detail by Moritz (1980).

The basic observation equation for LSC is:

$$y_i = L_i(T_{LSC}) + e_i + A_i^T X \tag{3.50}$$

Where y_i a vector of n observations, L_i is a vector of any linear functional associating anomalous potential (T) with the observation (cf. section 3.3), e_i is a vector of errors, X is an *m-vector* of parameters such as bias (N_0) or datum-shift (ΔX, ΔY, and ΔZ), and A_i^T is a $n \times m$ matrix relating the n observations and the m-vector of parameters (partial differential between observations and parameters).

For example of linear functional associating anomalous potential (T) see Eq. (3.7). The estimate functions of local approximation of the anomalous potential $\tilde{T}_{LSC}$ are then equal to the constants multiplied by the covariance between the observations and the value of the anomalous potential in a point, P:

$$T_{LSC}(P) = \sum_{i=1}^{N} b_i \quad \mathrm{cov}_i(T(p), L_i) \tag{3.51}$$

The constants (b_i) are computed by solving one or two system of normal equations:

$$(b_i) = \left\{\mathrm{cov}(L_i, L_j) + \sigma_{ij}\right\}^{-1} . \{y_i\} = \bar{C}^{-1} . y_i \tag{3.52}$$

Where $\mathrm{cov}(L_i, L_j) = C_{ij}$ are the covariance between two quantities, σ_{ij} is the variance-covariances of the errors and $\bar{C}$ are the variance covariance of the observations equal to $n \times n$ matrix, $\mathrm{cov}_i(T(P), L_i) = C_{Pi}$ is the covariance between the *i-th* observation and the value of T in a point P.

In case also parameters *X* have to be estimated, then an estimate of $\tilde{T}_{LSC}$ and of the (*M*) parameters are obtained by:

$$T_{LSC}(P) = \{C_{Pi}\}^T \ \overline{C}^{-1} \ \{y - A^T \ X\} \tag{3.53}$$

$$X = \left(A^T \ \overline{C}^{-1} A + W\right)^{-1} \ \left(A^T \ \overline{C}^{-1} y\right) \tag{3.54}$$

Where *W* is the a-priori weight matrix for the parameters (generally the *zero matrices*). The mean square error of the parameter vector becomes:

$$m_X^2 = \left(A^T \ \overline{C}^{-1} A + W\right)^{-1} \tag{3.55}$$

The associated error estimates of an estimated quantity *L* ($\tilde{T}$):

$$m_L^2 = \sigma_L^2 - H \ \{\text{cov}(L, L_i)\} + H \ A \ m_x^2 \ (H \ A)^T \tag{3.56}$$

$$H = \{\text{cov}(L_i, L_j)\}^T \ \overline{C}^{-1} \tag{3.57}$$

Where $\sigma_L^2 = cov(L, L)$ the square norm (or variance) of a functional *L*

Finally, the properties of the general solution expressed by Eq. (3.51), Eq. (3.53) and Eq. (3.54) can be summarized as the following (Moritz, 1980):-

a) The result is independent of the number of the signal quantities to be estimated.
b) Both observed and estimated quantities can be heterogeneous, provided that all required covariances are known.
c) The method is invariant with respect to linear transformation of the data or of the results.
d) The solution is optimal in the sense that it gives most accurate results obtainable on the basis of the given data.

3.6.2 Covariance Function Estimation and Representation.

In order to perform LSC, we should have been a model of covariance function to the success for application of LSC. An often used approach is to

compute empirical covariances (cf. section 2.5.2). Subsequently, these values might be fitted to a pre-selected model covariance functions.

The well-known Tscherning-Rapp (1974, p. 29) covariance function model was used for the above LSC solutions, where the required auto and cross-covariance functions were computed as follows (Tscherning, 2013):

$$Cov\ (\psi, r_P, r_Q) = \alpha \sum_{i=2}^{N} (\sigma_i^{\ err})^2 \left(\frac{\overline{R^2}}{r_P r_Q} \right)^{i+1} P_i\ (cos\psi_{PQ}) + \sum_{i=N+1}^{\infty} \frac{A}{(i-1)\ (i-2)\ (i+B)} \left(\frac{R_B^2}{r_P r_Q} \right)^{i+1} P_i(cos\psi_{PQ}) \qquad (3.58)$$

Where P and Q are two points having a spherical distance ψ_{PQ} and r_P, r_Q are the geocentric radial distances of points P and Q, α is a scale factor, σ_i^{err} are the error degree variances (cf. section 2.5.1), $\bar{R}$ is the mean radius of the earth, P_i are the Legendre polynomials, A is a constant in units of $(m/s)^4$, R_B is the radius of the Bjerhammar-sphere and B an integer number. If a spherical harmonic series expansion (EGM) is used as in this study, B is typically put equal to a small number *like 4*, while in the original work it was put equal to *24* (ibid., 2013), so that the low-degree degree-variances could be modelled appropriately.

Chapter 4

DATA PREPARATION

4. DATA PREPARATION

4.1 Overview

In this chapter, the necessary data will be described and prepared to realize the geopotential model that would be considered as reference for precise gravity field modeling in Egypt. This has been done by improving geopotential models for gravity field in Egypt using tailor process.

The datasets include the satellite-only model GOCO05s, high degree reference model EGM2008, and older reference model EGM96. In addition, Digital Terrain Model DTM2006.0, available gravity data, GPS/levelling surveys projects and deflections of the vertical data in Egypt. Moreover, the main programs used for the harmonic analysis and synthesis are described.

Furthermore, Molodensky free-air gravity anomalies defined on the Earth's surface are provided and then the EGM96 is used to detect the gross errors that exist in these anomalies. The chapter also shows the methodology of estimate the Egyptian 5 arc-minute mean free-Air anomalies, which are required to estimate the new harmonic coefficients of the tailored geopotential models GOCO05s and EGM2008 for the Egyptian territory.

4.2 Global Geopotential Models (GGMs)

Current Global Geopotential Models (GGMs) of the Earth's gravitational field can be divided among three primary classes (Featherstone, 2002):-

a) Satellite-only GGMs derived from derived from the tracking of artificial Earth satellites (the analysis of satellite-based gravity observations).

b) Combined GGMs, derived from a combination of a satellite-only model, terrestrial gravimetry, satellite altimeter-derived gravity data in marine areas, and (more recently) airborne gravimetry.

   This combined solution generally enables the maximum degree of harmonic expansion of the GGMs to be increased due to the higher resolution of the terrestrial data.

c) Tailored GGMs, derived from a refinement of existing (satellite or combined) global geopotential models using higher resolution gravity data that may have not necessarily been used in the model.

The GGMs were obtained from the International Centre for Global Earth Models (ICGEM) Web page (http://icgem.gfz-potsdam.de/home), which is one of the six centers of the International Gravity Field Service (IGFS) of the IAG. In addition, geopotential models will be made available with four components:-

a) The set of coefficients (usually called "Cnm" and "Snm") from degree 2 to maximum degree "N".
b) The adopted gravity-mass constant value used when creating the model= Gravitational Constant (GM).
c) An equatorial scale factor or reference radius "a".
d) The permanent tide system of the model.

In this study, we chose the satellite-only GOCO05s and high degree reference model EGM2008 to fit (tailor) the Egyptian gravity field in order to determine the best of them that would be considered as a reference model for precise gravity field modeling in Egypt.

The first is selected because it signifies unsurpassed satellite-only models, which is based on complete data of the three gravity field mapping missions, while the second is picked because it represents one of the best

ultra-high degree or resolution model, and usually used as a reference model to assess other recent models.

In addition, the global geopotential model EGM96, the predecessor of the EGM2008 model, are used to detect the gross errors that exist in the Egyptian gravity data (observed gravity points) and validation of the geoid models, which are derived from the spherical harmonic coefficients of tailored geopotential models. In the following sections, GOCO05s, EGM2008, and EGM96 models are described in details.

4.2.1 The satellite-Only Gravity Field Model GOCO05s

The satellite-only gravity model GOCO05s is a combination solution based on 4 years of GOCE gravity gradient data (ITSG-Grace2014s model), 10.5 years of GRACE, Kinematic orbits (8 satellites) and Satellite Laser Ranging (SLR) (6 satellites), resolved up to degree/order 280 of a harmonic series expansion (spatial resolution ~72 km), made by the Gravity Observation Combination Consortium (GOCO, http://www.goco.eu/).

The combined solution, consisting of the lower degree portion of GOCO05s (n<120) was estimated from GRACE data, GOCE-TIM5 gradiometer observations for the degree (120 < n < 260) and kaula regularized for the degree (n > 260) more information's see (Mayer et al., 2015). The model is available via http://inas.tugraz.at/GOCO. Table (4.1) show that the main parameters of the GOCO05s model.

Table (4.1): Parameters of Earth Gravity Field Model GOCO05s.

Parameters	GOCO05s	Unit
Gravitational Constant (GM)	$3.986004415 \times 10^{14}$	$m^3\ s^{-2}$
Reference Radius (a)	6378136.3	m
2^{nd} Degree Zonal Coefficient ($\bar{C}_{2,0}$)	$-4.841694552725 \times 10^{-4}$	unitless
Maximum degree (n)	280	unitless
Tide-System	Tide-zero	unitless

4.2.2 Earth Gravitational Model 2008

The high degree Earth Gravitational Model 2008 (EGM2008) released by the United States (US) National Geospatial-intelligence Agency (NGA) (EGM2008, http://earth-info.nga.mil/GandG/wgs84/gravitymod/egm2008/index.html).

The reference model EGM2008 was developed by combining the best available GRACE-derived satellite-only model, with the most comprehensive compilation of a global 5 arc minute equiangular grid of area-mean free-air gravity anomalies. EGM2008 is complete to spherical harmonic degree and order 2159 but contains additional spherical harmonic coefficients to degree 2190 and order 2159, which corresponds to a spatial resolution of 5 arc minutes (approximately 9 km depending on latitude). Overviews about the main parameters of EGM2008 are shown in Table (4.2).

Table (4.2): Parameters of Earth Gravity Field Model EGM2008.

Parameters	EGM2008	Unit
Gravitational Constant (GM)	$3.986004415 \times 10^{14}$	$m^3\ s^{-2}$
Reference Radius (a)	6378136.3	m
2^{nd} Degree Zonal Coefficient ($\bar{C}_{2,0}$)	$-0.484165143790815 \times 10^{-3}$	unitless
Maximum degree (n)	2190	unitless
Tide-System	Tide-free	unitless

The available gravity anomaly data that were necessary for the computation of the 5 arc-minute area mean values to develop the EGM2008 model, divide into three sub-divisions (see Pavlis et al., [2012, sections 3.5]), as shown in Fig. (4.1a):-

a) Areas without any restrictions [are colored green in Fig. (4.1a)], most of this area is ocean areas, where the altimetry-derived gravity anomalies data.

b) Areas where gravity anomaly data are either unavailable, or too sparse, or too inaccurate, to support the estimation of 5 arc-minute area mean values [are colored red in Fig. (4.1a)], the domains of these data cover approximately 12.0 percent of the Earth's land area and are located in Africa, South America, and Antarctica.

c) Areas where the gravity anomaly data available were of proprietary nature. In agreement with the co-owners of these data, their use was only permitted at a resolution corresponding to 15 arc-minute area mean values. The domain of these data covers approximately 42.9 % of the total land area [are colored gray in Fig. (4.1a)].

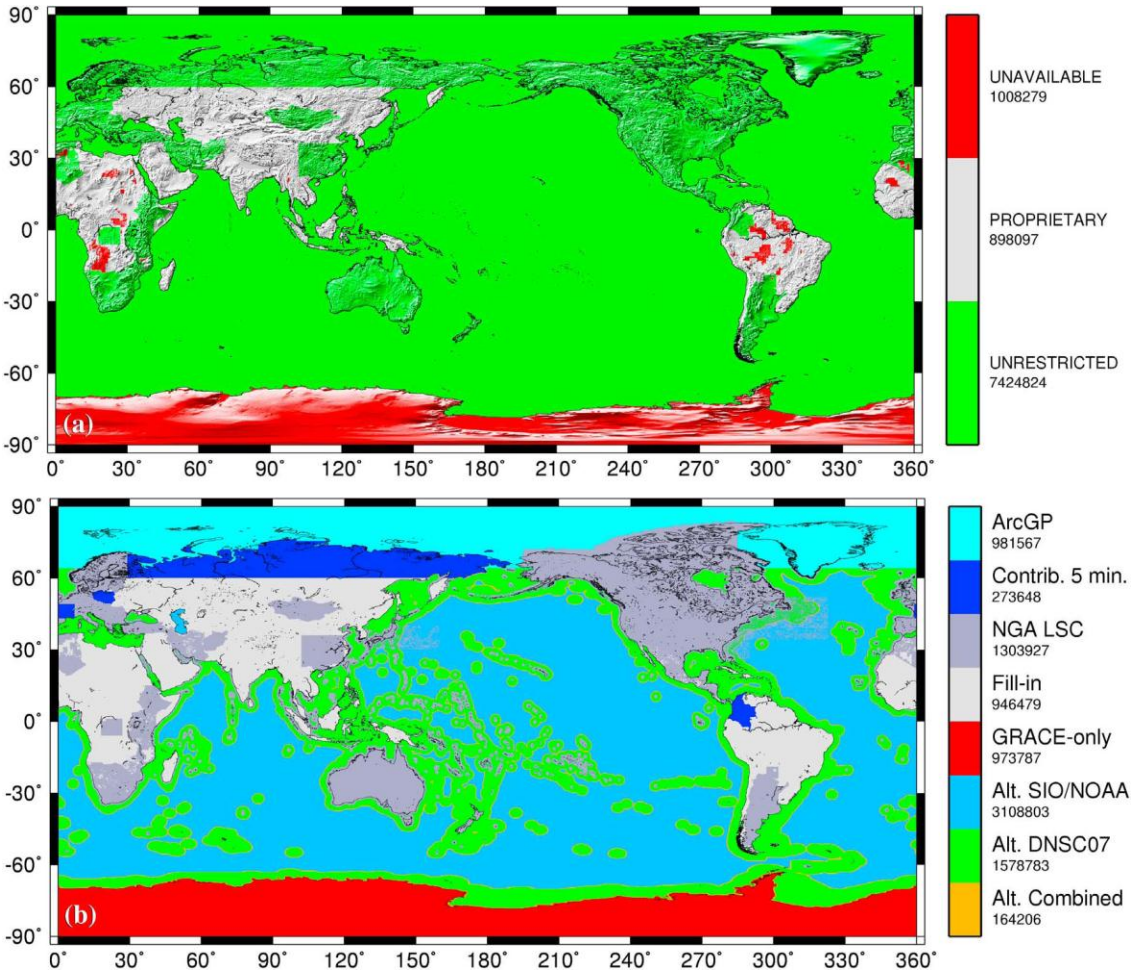

Figure (4.1): Geographic Display of the 5 Arc-minute Anomalies Used to Develop the EGM2008 model: (a) Data Availability. (b) Data Source Identification [source: Pavlis et al., 2012, Fig.(3)].

Table (4.3) summarizes the statistics of these merged data and Fig. (4.1b) show data source identification.

Table (4.3): Statistics of the 5 Arc-minute Anomaly Data Selected by the Merging Procedure Used to Develop the EGM2008 Model, Unit is mGal [source: Pavlis et al., 2012, Table (2)].

Data Source	Percent Area	Minimum	Maximum	RMS	RMS σ
ArcGP	3.0	−192.0	281.8	30.2	3.0
Altimetry	63.2	−361.8	351.1	28.4	3.0
Terrestrial	17.6	−351.9	868.4	41.2	2.8
Fill-in	16.2	−333.0	593.5	46.8	7.6
Non Fill-in	83.8	−361.8	868.4	31.6	2.9
All Source (Global)		−361.8	868.4	34.5	4.1

Over areas where only lower resolution gravity data were available, their spectral content was supplemented with the gravitational information obtained from the global set of Residual Terrain Model (RTM) implied gravity anomalies to support the estimation of 5 arc-minute area-mean for the solution of EGM2008. The specific details of the implementation of this approach are given by Pavlis et al. (2007).

Over areas without adequate gravity anomaly data (unavailable), the 5 arc-minute grid was filled with composite “fill-in” values, computed from the low degree part of GGM02S ($n < 60$), augmented with the EGM96 coefficients for degrees 61 to 360, and further augmented with coefficients of the topographic-isostatic potential for degrees 361 to 2159, (see Pavlis et al., [2012, sections 3.5] for details).

Accordingly, and from Fig. (4.1), Egypt is located in the gray area (lower resolution) and a small part in the red area (unavailable data) as shown in Fig. (4.2).

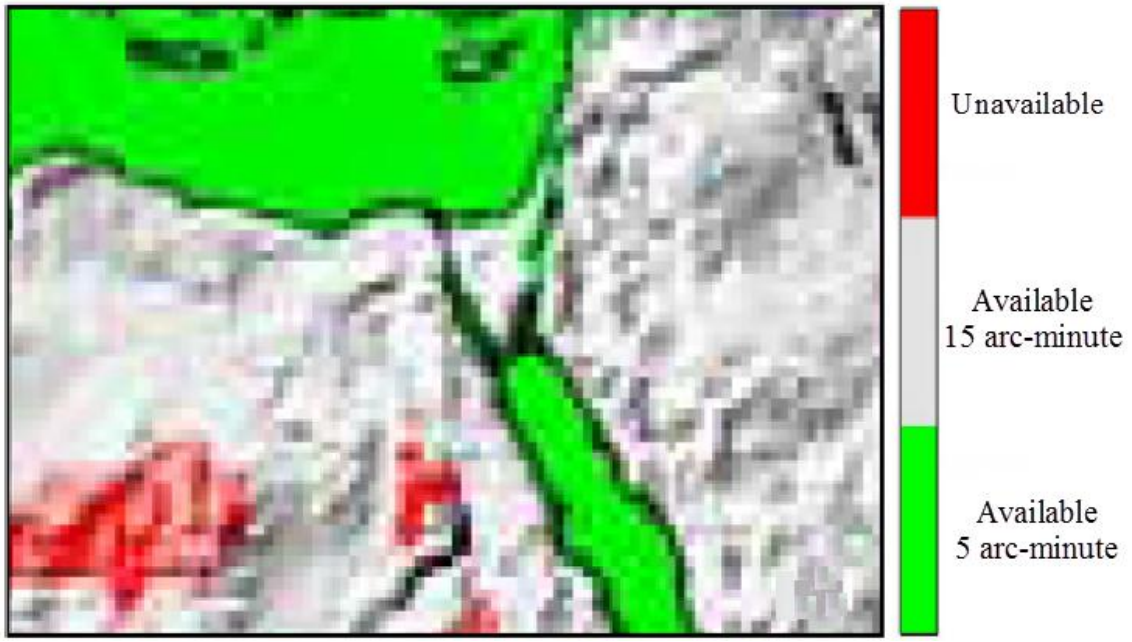

Figure (4.2): Data Availability for Egypt Used to Develop The EGM2008 Model [source: subset from Fig. (4.1)].

4.2.3 Earth Gravitational Model 1996

The Earth Gravitational Model 1996 (EGM96, https://cddis.nasa.gov/926/egm96/egm96.html), had been developed collaboratively by NASA Goddard Space Flight Center (GSFC), NGA, and The Ohio State University (OSU). EGM96 is a spherical harmonic model of the Earth's gravitational field up to degree and order 360, and its resolution is 30 arc minutes (approximately 55 km at the equator). EGM96 was a composite solution in which different estimation techniques were used to compute different spectral bands of the model.

The composite solution, consisting of (a) the lower degree portion of EGM96 (up to degree 70), was estimated from the combination of the satellite-only model EGM96S, with 30 arc minutes area-mean gravity anomalies; (b) a block diagonal solution from degree 71 to 359, and (c) the quadrature solution at degree 360.

Over areas without adequate gravity anomaly data, the 30 arc-minute grid used in EGM96 was filled with composite "fill-in" values, computed from the low degree part of EGM96S (involved the analysis of various types of satellite tracking data from 40 satellites), augmented with coefficients of the topographic-isostatic potential based on global digital topographic database JGP95E (see Lemoine et al. [1998, sections 7.2 and 8.3] for details). Finally, the main parameters of gravity field model EGM96 are shown in Table (4.4).

Table (4.4): Parameters of Earth Gravity Field Model EGM96.

Parameters	EGM96	Unit
Gravitational Constant (GM)	$3.986004415 \times 10^{14}$	$m^3\ s^{-2}$
Reference Radius (a)	6378136.3	m
2^{nd} Degree Zonal Coefficient ($\bar{C}_{2,0}$)	$-0.484165371736 \times 10^{-3}$	unitless
Maximum degree (n)	360	unitless
Tide-System	Tide-free	unitless

The development of the gravitational model EGM96 critically depended on the availability of accurate and complete gravity anomaly data. The estimation of 30' mean gravity anomalies from terrestrial, airborne and altimetry data was carried out by the US Defense Mapping Agency (DMA). On Oct. 1, 1996, DMA was folded into the National Imagery and Mapping Agency (NIMA) until 2004, which later became National Geospatial-intelligence Agency (NGA).

The computation of 30' mean free-air anomalies by NGA is based on Least-Squares Collocation (LSC), which is a technique that combines heterogeneous data types to optimally estimate gravimetric quantities and their errors and it is described in some detail in Kenyon and Pavlis (1996) and Trimmer and Manning (1996).

Five files containing 30 arc minute area-mean gravity anomalies were used in the merging process that produced the final merged 30 arc minutes area-mean gravity anomaly file, which used to develop the EGM96

(see Lemoine et al. [1998, sections 8.3] for details). These were based on: files (A): Terrestrial and (B): Altimetry 30 arc-minute gravity anomalies from NGA, file (C): Terrestrial 30 arc-minute gravity anomalies from OSU, file (D): Terrestrial 1° arc-minute gravity anomalies from NGA (were "split up" in order to define a 30 arc-minute) and file (E): Composite topographic–isostatic 30 arc-minute values. Table (4.5) summarizes the overall statistics of this files and Fig. (4.3) illustrates the geographic locations and source of the merged 30 arc-minute area-mean gravity anomalies. In addition, these files available via anonymous FTP to ftp://cddis.gsfc.nasa.gov/ (cd to the directory pub/egm96/gravity_data/).

Table (4.5): Statistics of the 30 Arc-minute Anomaly Data Selected by the Merging Procedure Used to Develop The EGM96 Model, Unit is mGal [source: Lemoine et al., 1998, p.8-20].

	File A NGA terr.	File B NGA alt.	File C OSU terr.	File D´ "Split-up"	File E "Fill-in"
Number of values	86740	146042	1064	6500	18854
Percentage of area	30.68	66.14	0.11	0.74	2.33
Minimum value	–214.4	–300.3	–153.6	–184.6	–170.3
Maximum value	399.5	328.0	301.7	263.6	170.3
Mean value	4.2	–2.4	8.6	9.4	0.8
RMS value	35.2	25.6	56.7	49.1	28.0
RMS stand. dev.	5.4	1.7	16.9	35.7	36.0

Accordingly, from Fig. (4.3), and referring to Table (4.5), most of Egypt is located in green area file (A), blue area file (B) and a small part in gray area file (D) as shown in Fig. (4.4). This data obtained from African Gravity Project (AGP) (Fairhead & Watts, 1989; Merry, 2003; Merry et al., 2005).

AGP was one of the primary sources of gravity information over Africa, Along with the NGA collections. In 1986, the AGP began with GETECH company, lining up support with 16 sponsors, including major contributions from NGA.

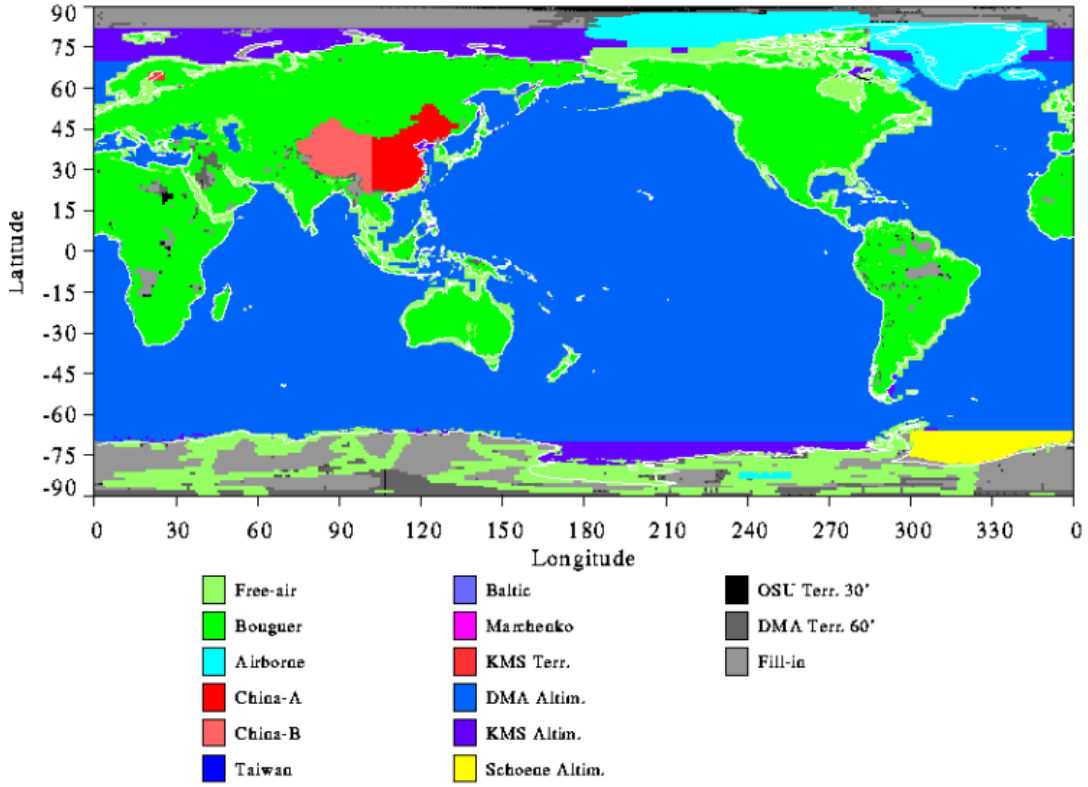

Figure (4.3): Geographic Locations and Identification of Merged 30 Arc-minute Gravity Anomalies Used to Develop The EGM96. (Source: Lemoine et al., 1998, p.8-21).

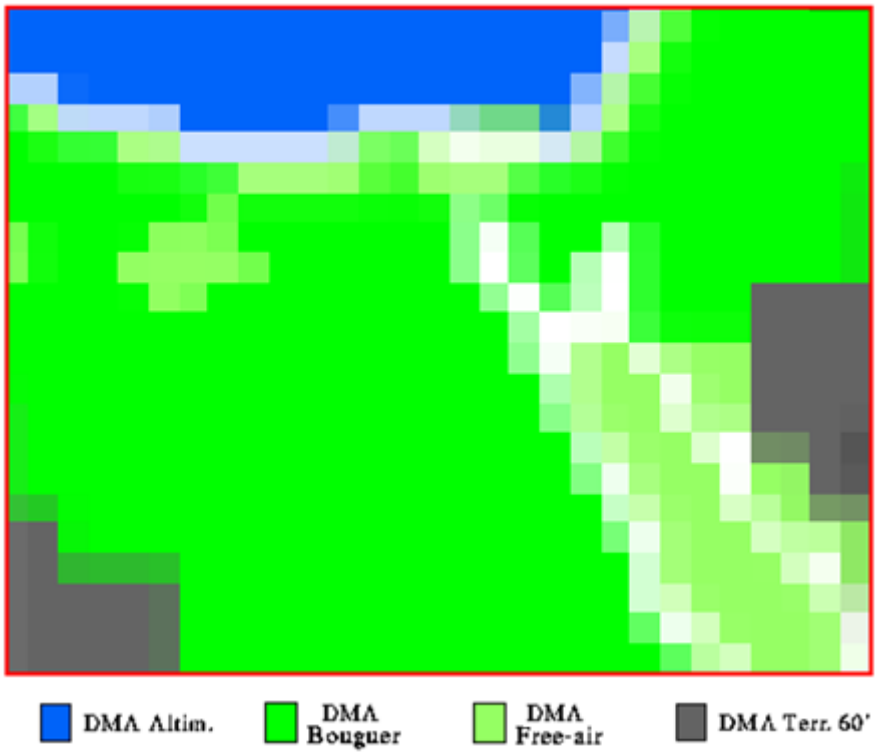

Figure (4.4): Data Source Used to Develop The EGM96 Model for Egypt [source: subset from Fig. (4.3)].

The objective of AGP was to collect all the available gravity data over Africa in an organized manner rather than on a country-by-country basis for oil exploration and scientific investigations. The final published report was produced by GETECH in 1988 with the distribution to the sponsors of free-air and Bouguer gravity files and maps, together with detailed documentation on the gravity processing, map details, and survey specifications (Fairhead & Watts, 1989).

The accuracy of AGP data in land values, which are controlled by the positioning and elevations of the gravity stations, ranged from 1 to 5 mGal and the marine gravity accuracy, which is highly dependent on the ship's navigation, ranged from 3 to 15 mGal (see Lemoine et al., [1998], sections 3.2.4, for details). Fig. (4.5) shows that the distribution of Egyptian gravity data, which used in AGP. These data can be obtained through GETECH Group company (http://www.getech.com/gravandmagmap/) and University of Leeds (https://www.leeds.ac.uk)

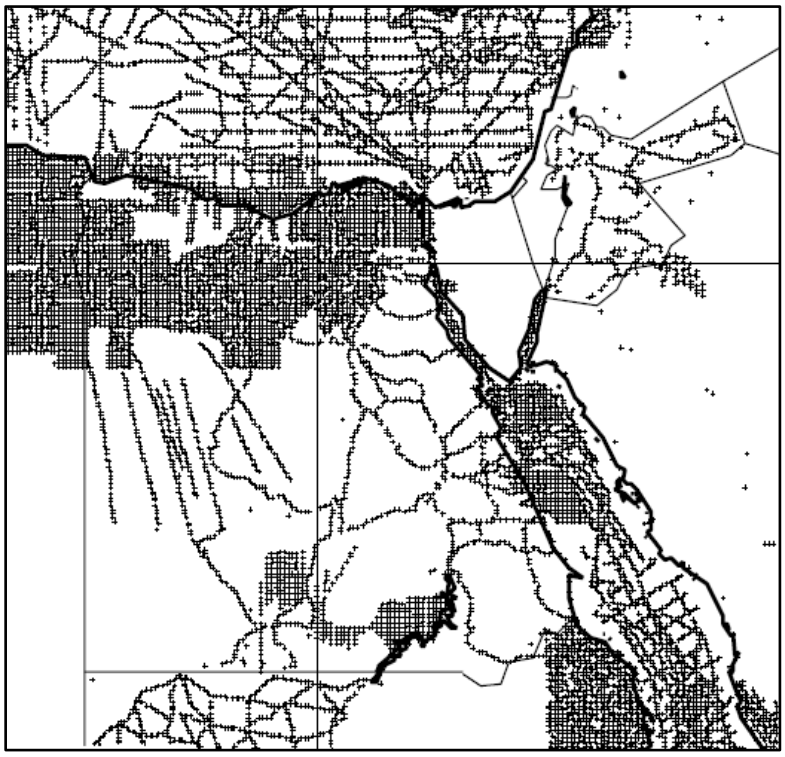

Figure (4.5): Distribution of Egyptian Gravity Data in African Gravity Project. [Source: Fairhead at el., 1997, subset from Fig. (1)].

4.3 Digital Terrain Model (DTM)

In this investigation, the term Digital Topographic Model (DTM) will be used here to identify data sets providing additional information pertaining to different terrain types. In addition, DTM will be used in following computations:-

a) The harmonic coefficients of the tailored (modified) geopotential model are obtained at the surface of gravity information.
b) Conversion of height anomaly to geoid undulation terms, as described in section (3.3.1).

In order to achieve that, we will use a high-resolution Digital Topographic Model DTM2006.0 (Pavlis et al., 2007) described as follows.

4.3.1 The Digital Topographic Model DTM2006.0

DTM2006.0 model contains fully-normalized spherical harmonic coefficients of the elevation $\overline{HC}_{nm}$ and $\overline{HS}_{nm}$ in units of meters, complete to degree and order 2190. Positive heights for land areas above MSL and negative depths for ocean areas (or land areas below MSL), can be expanded in surface spherical harmonics as:

$$H_{DTM\,2006.0} = \sum_{n=0}^{N_{max}} \sum_{m=0}^{n} (\overline{HC}_{nm} \cos m\lambda + \overline{HS}_{nm} \sin m\lambda)\, \bar{P}_{nm}\ (\sin \bar{\varphi}) \qquad (4.1)$$

In addition, DTM2006.0 model was formed specifically to support the development of EGM2008 and it is identical to the Global Digital Terrain Model DTM2002 (Saleh & Pavlis, 2002) in terms of database structure and information content. Where, DTM2002 combines elevations from Global Land One-kilometer Base Elevation (GLOBE) (Hastings and Dunbar, 1999), altimetry/geoid model-derived elevations from Altimetry Corrected Elevations (ACE) and from GSFC over Greenland and Antarctic database, and bathymetry from the predictions of Smith and Sandwell (1997) from altimetry data and ship depth soundings. DTM2006.0 was

compiled by overlying the Shuttle Radar Topography Mission (SRTM) data (Werner, 2001) over the data of DTM2002. In addition to the SRTM data, DTM2006.0 contains ice elevations derived from Ice, Cloud, and land Elevation Satellite (ICESat) laser altimeter data over Greenland and over Antarctica. Over the ocean, DTM2006.0 contains essentially the same information as DTM2002. The DTM2006.0 model is available via http://earth-info.nga.mil/GandG/wgs84/gravitymod/egm2008/first_release.html.

In this study, the DTM2006.0 model, complete to degree and order 2190, has been used to create a 5′×5′ mean heights for Egypt Fig. (4.6) by using harmonic_synth program (Holmes & Pavlis, 2006), in the area bounded by latitudes 21º to 33º and longitudes 24º and 38º, and Table (4.6) shows the statistics of this heights without marine areas.

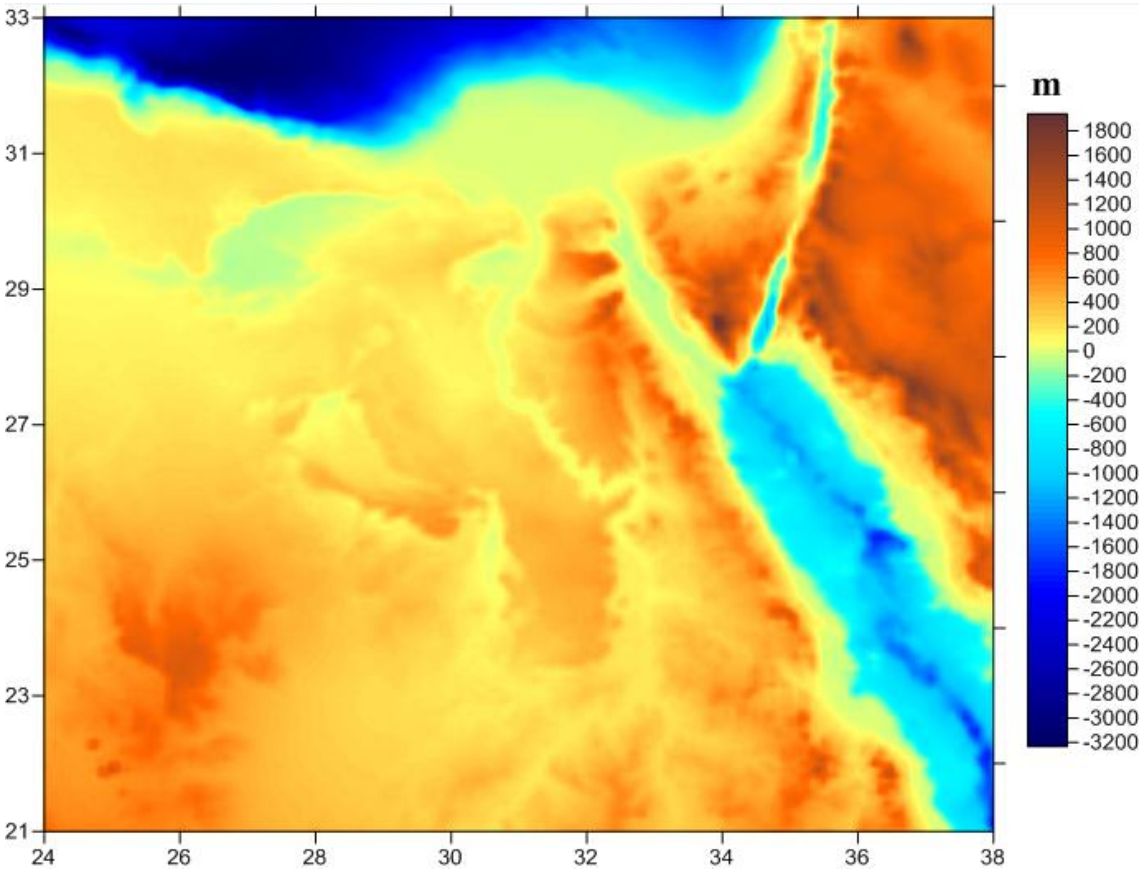

Figure (4.6): The 5′×5′ Mean Heights for Egypt Derived by Using DTM2006.0 Model Complete to Degree and Order 2190.

Table (4.6): Statistics of a 5′ × 5′ (24505 values) Mean Height for Egypt Derived by Using DTM2006.0 (height for marine areas = 0).

Height (H) Egypt	Mean	Standard dev.	Minimum	Maximum
	m	m	m	m
DTM2006.0	310.105	300.149	-414.891	1939.625

4.4 Available Gravity Data Sources in Egypt

The used gravity data sets in this study are collected in the form of point gravity (observed), where the point gravity have been obtained from various local and international organizations such as Ganoub El- Wadi Petroleum Holding Company (Ganope), National Research Institute of Astronomy and Geophysics (NRIAG), Survey Research Institutes (SRI), General Petroleum Company (GPC), Egyptian Survey Authority (ESA) and Bureau Gravimétrique International (BGI). These data will be described in details in the following sections.

4.4.1 Ganoub El- Wadi Petroleum Holding Company

Ganoub El- Wadi Petroleum Holding Company (Ganope) has provided us about 3926 gravity stations with standard deviation 0.01 mGal, of Mesaha Concession located in the southern part of the Western Desert of Egypt, through information center of Egyptian General Petroleum Corporation (EGPC) (EGPC, http://www.egpc.com.eg/). The gravity survey of Mesaha Concession is comprised of 11 lines along East-West of varying length with a nominal spacing of 400 m and along North-South 3 lines of varying length with a nominal spacing of 1000 m as shown in Fig (4.4). The relative gravity measurements of these data were made using Scintrex CG-3 and CG-5 Gravity Meters, while the positioning information was acquired using Trimble 4000 and Trimble 350 receivers. The final data is supplied in a WGS84 horizontal datum and all elevation data in the field

was processed on the WGS84 ellipsoid and then converted to MSL using the EGM96 geoid model (FFG Pty Ltd., 2009).

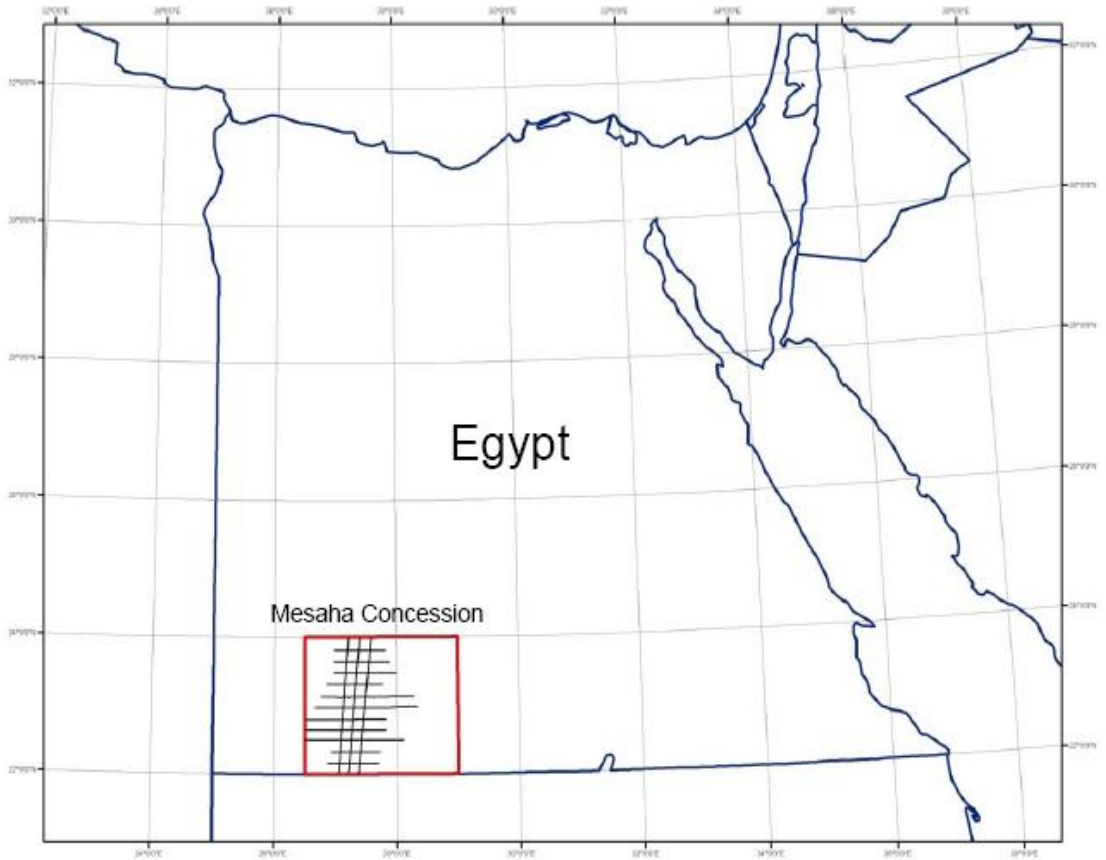

Figure (4.7): Distribution of Mesaha Gravity Survey. (FFG Pty Ltd., 2009)

4.4.2 National Research Institute of Astronomy and Geophysics

The National Research Institute of Astronomy and Geophysics (NRIAG) has observed several small gravity networks as a part of complex geodetic networks serve for the detection of crustal deformation. Most of these loops are concentrated in the active crustal movement Zone of Aswan Lake (Groten & Tealeb, 1995) about 198 gravity stations and other 35 gravity stations with known orthometric heights, were made available with standard deviation 0.02 mGal. In addition, 115 gravity stations near the Southern boundary of Egypt with accuracy 0.2 mGal. Moreover, Network consisting of 11 gravity stations with standard deviation 0.01 mGal was established in 1995 around greater Cairo area along with their spirit

levelling orthometric heights were provided by the same Institute (Hassouna, 2003). Finally, all gravity stations provided by NRIAG about 359 with known WGS-84 geodetics coordinates as shown in Fig (4.8).

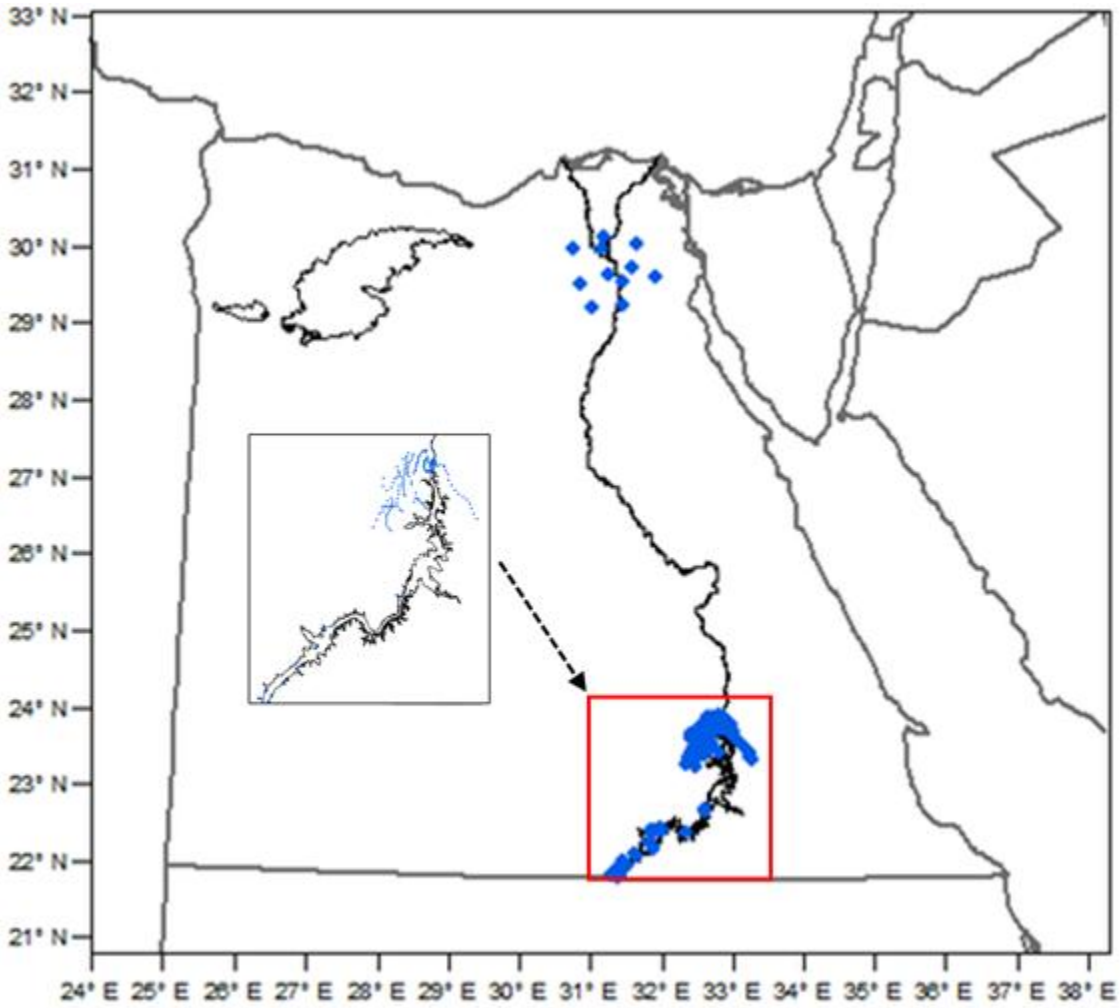

Figure (4.8): Distribution of NRIAG Gravity Data.

4.4.3 Survey Research Institutes

In 1994, SRI has initiated a project for re-calibrating and updating the Egyptian national gravity network. The Egyptian National Gravity Standardization Net (ENGSN97) is a project initiated in late 1994 between Survey Research Institutes (SRI) as the executive counterpart with the cooperation of the General Petroleum Company (GPC) and the Egyptian Academy of Scientific Researchers and Technology as the financial and supervisory organization for re-calibrating and updating the Egyptian

national gravity network. The ENGSN97 network serves as the precise national gravity datum in Egypt.

ENGSN97 consists of 5 absolute gravity stations (observed in a joint effort between the Egypt's Survey Research Institute (SRI) and NGA and 145 relative gravity stations connected to those absolute gravity points with standard deviation range from 0.01 to 0.050 mGal as shown in Fig (4.9). The precise coordinates of almost all of the ENGSN97 points have been observed by static GPS on WGS-84, while their orthometric heights are obtained by precise leveling.

Hence, each gravity stations of the ENGSN97 precisely have a three-dimensional geodetic position (latitude, longitude, and geodetic height) from GPS data, as well as vertical position made by the orthometric height from precise levelling. The standard deviation of the final solution of the ENGSN97 network is range from 0.002 to 0.048 mGal (Dawod, 1998).

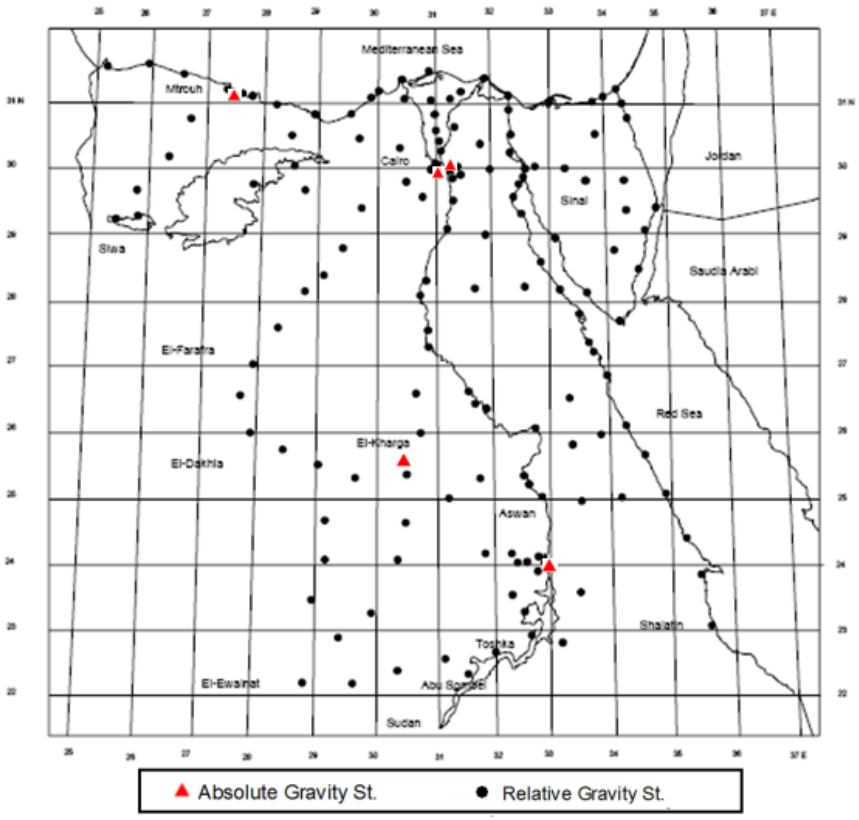

Figure (4.9) Egyptian National Gravity Standardization Network 1997. (Dawod, 1998)

4.4.4 General Petroleum Company

A ten-year project (1974 - 1984) for the compilation of gravity maps of Egypt has resulted in the National Gravity Standard Base Net (NGSBN-77). This project was executed and supervised by the General Petroleum Company (GPC) under the auspices of the Egyptian Academy of Sciences and Technology (Kamel & Nakhla, 1987). The NGSBN-77 consists of 71 stations with standard deviation range from 0.01 to 0.18 mGal and includes the existing stations of the International Gravity Standardization Net (IGSN71) in Egypt (11 stations) as shown in Fig (4.10). The standard error of the adjusted IGSN71 gravity values was less than ± 0.1 mGal (Morelli et al.1972).

The distributed of NGSBN-77 is well all over the country and the geographical coordinates were determined by connecting these stations with the Egyptian Triangulation Network, which based on the Old Egyptian Datum (OED) and the corresponding elevations are determined by tacheometry (El-Tokhey, 1993). The coordinates of about 20 stations located in inaccessible areas, in the western desert and Sinai, were interpolated from governmental topographic maps.

In addition, The General Petroleum Company (GPC) has carried out some gravimetric surveys along the Western Desert and along the Nile about 950 stations for Petroleum Exploration (Hassouna, 2003) as shown in Fig (4.10). The locations of these data were available on the OED, whereas the other portion was given on the WGS72 global datum and the heights were interpolated from the topographic maps. The standard deviation of these data have been estimated to be ±1.0 mGal (El-Tokhey, 1993).

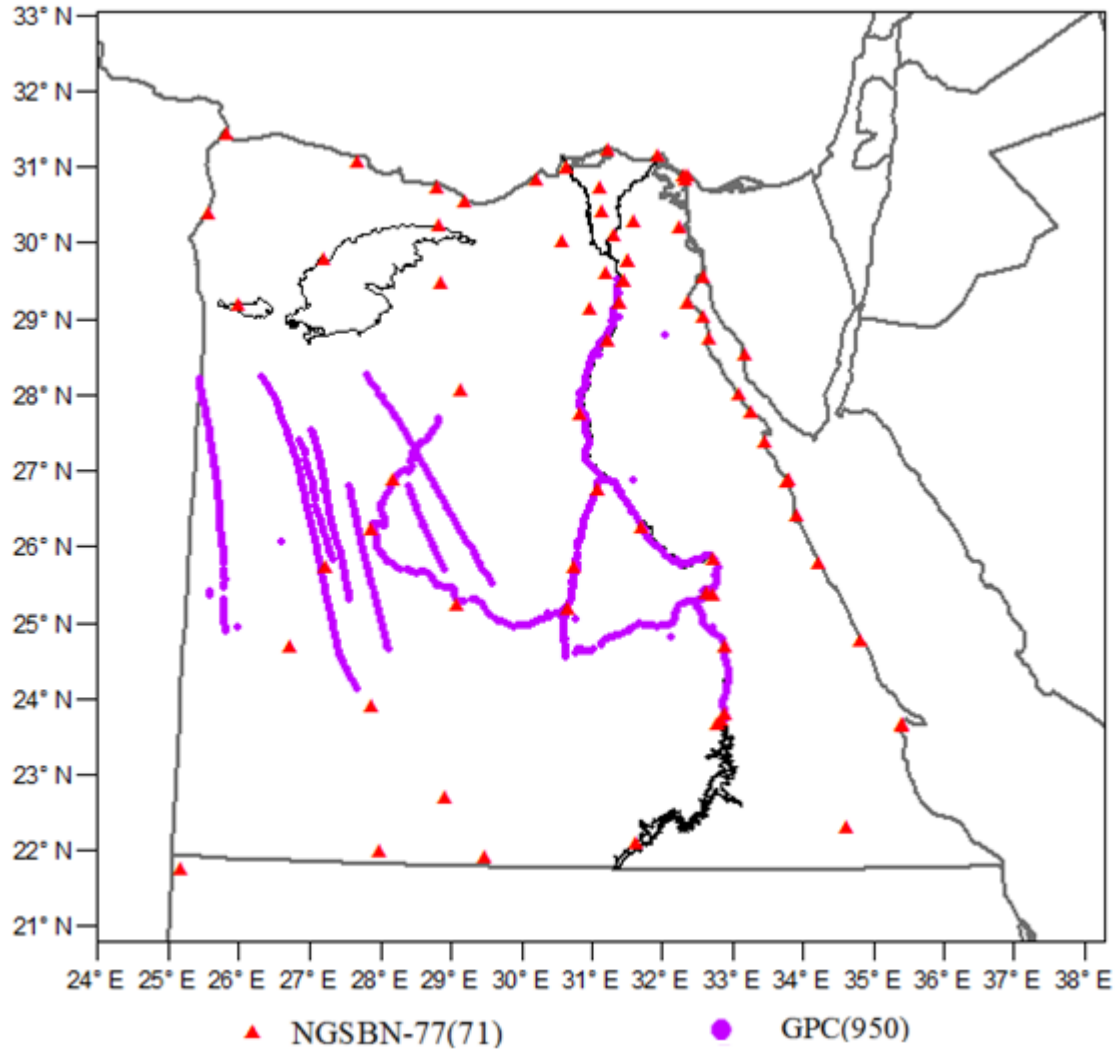

Figure (4.10): Distribution of GPC Gravity Data.

4.4.5 Egyptian Survey Authority

About 190 gravity stations with estimated standard errors ±0.4 mGal (El-Tokhey, 1993) observed by the Egyptian Survey Authority (ESA) were made available. This data is observed along the first order leveling lines and concentrated in the Northern part of Egypt. Furthermore, about 72 gravity stations with average accuracy 0.068 mGal along the first order leveling lines are available from (Youssef, 1970). The geodetic coordinates of these stations are given in the OED and the heights above MSL are observed by spirit levelling as shown in Fig (4.11).

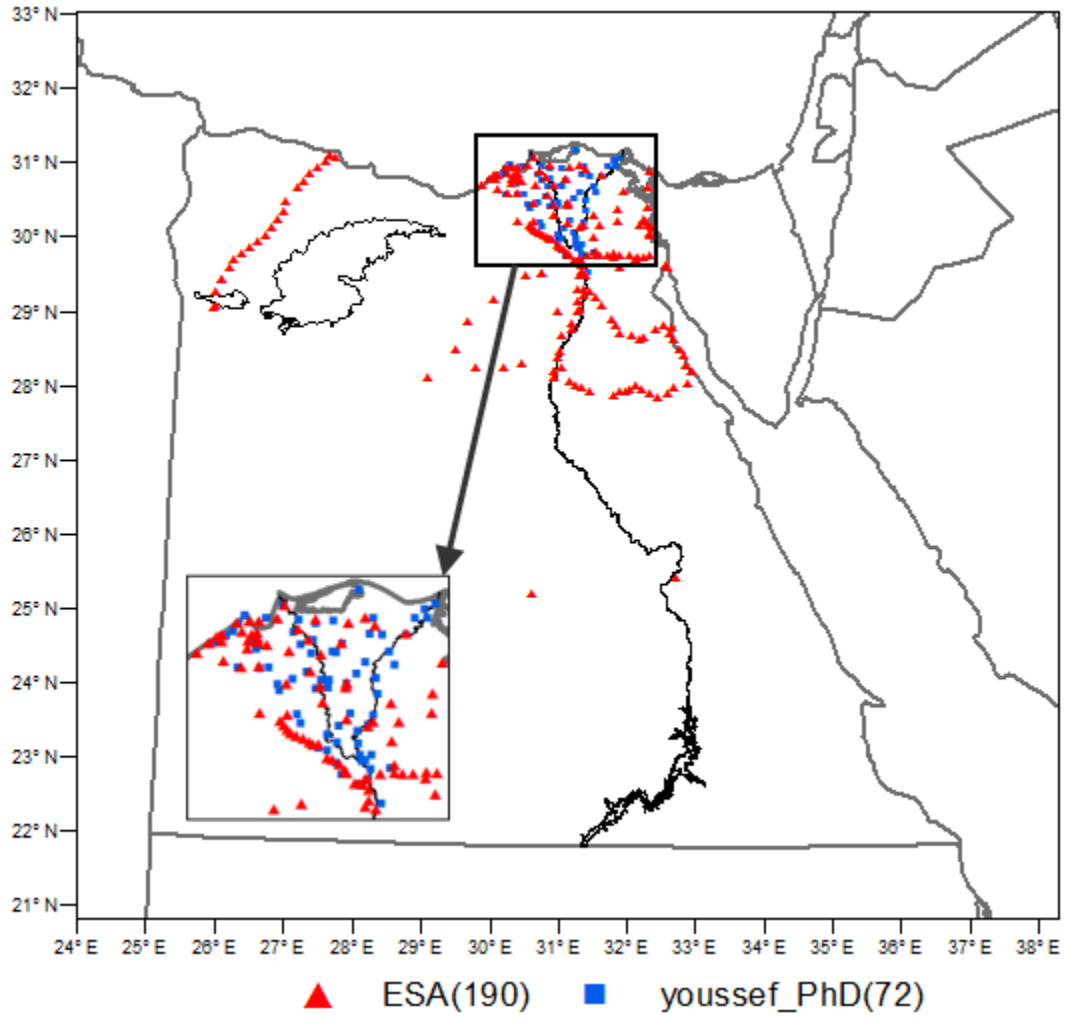

Figure (4.11): Distribution of ESA Gravity Data.

4.4.6 Bureau Gravimétrique International

The Bureau Gravimétrique International (BGI) database, which now contains over 12 million of observations compiled and computerized from land, marine and airborne gravity measurements, has been extensively used for the definition of Earth gravity field models. Fig. (4.12) depicts the distribution of available measurements (over lands and oceans) in the database of BGI. These data accessible from the BGI website http://bgi.obs-mip.fr/ (cd to the directory /data-products/Gravity-Databases/) for any public or private user.

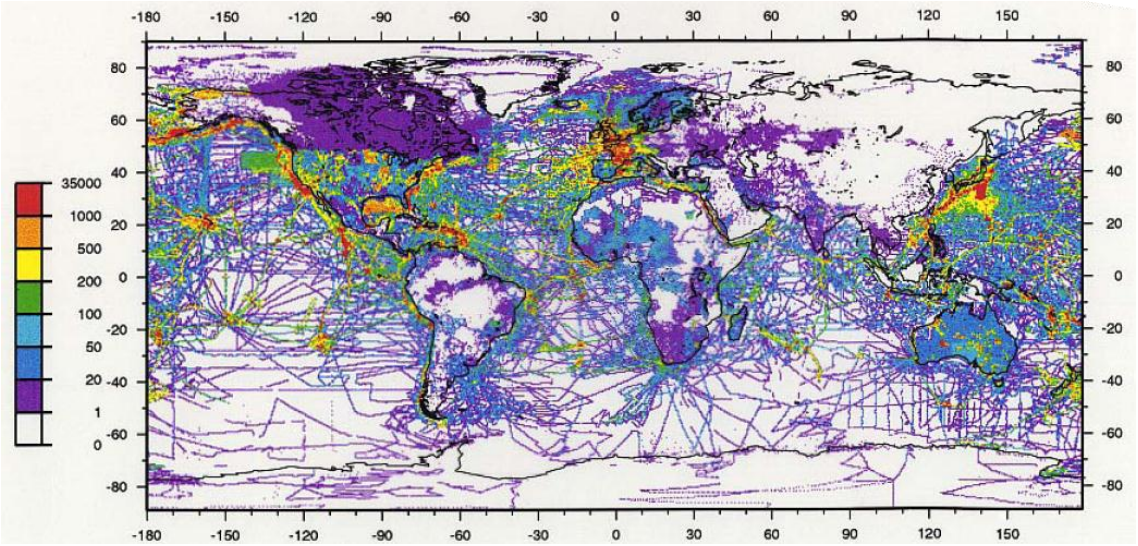

Figure (4.12): Distribution of Available Measurements of Gravity in the Database of BGI. (Balmino G.at el., 1999).

The available BGI dataset in Egyptian Territory cover the window $22^{o} \leq \varphi \leq 32^{o}$ and $25^{o} \leq \lambda \leq 37^{o}$ have 68241 gravity stations (590 in land and 67651 in marine) with known WGS-84 geodetic coordinates. This data is included in 335 points located in Egypt. In addition, some points located in neighboring countries such as Saudi Arabia 15 points (latitude 21.0° to 23.0° and longitude 25.0° to 37.0°) and Sudan 240 points (latitude 22.0° to 32.0° and longitude 34.0° to 37.0°), as shown in Fig (4.13). The standard deviation of BGI dataset in Egypt is estimated 0.2 mGal in Land and from 5.0 to 10.0 mGal at the sea.

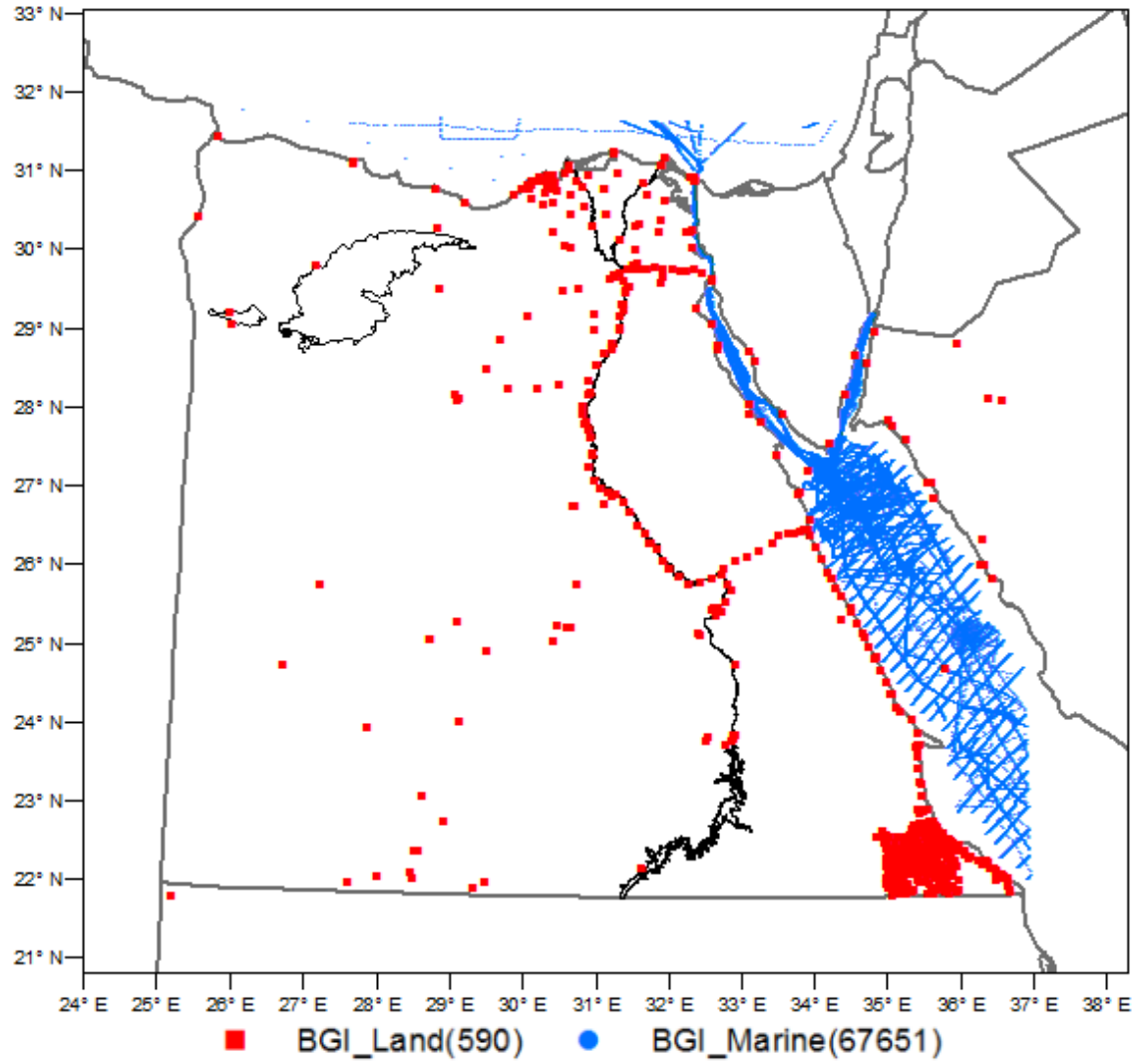

Figure (4.13): Distribution of BGI Gravity Data.

Fig. (4.14) and Table (4.7) show the geographic locations and summarizes the overall of available gravity data for Egypt, respectively, which was explained previously and will be used in this study.

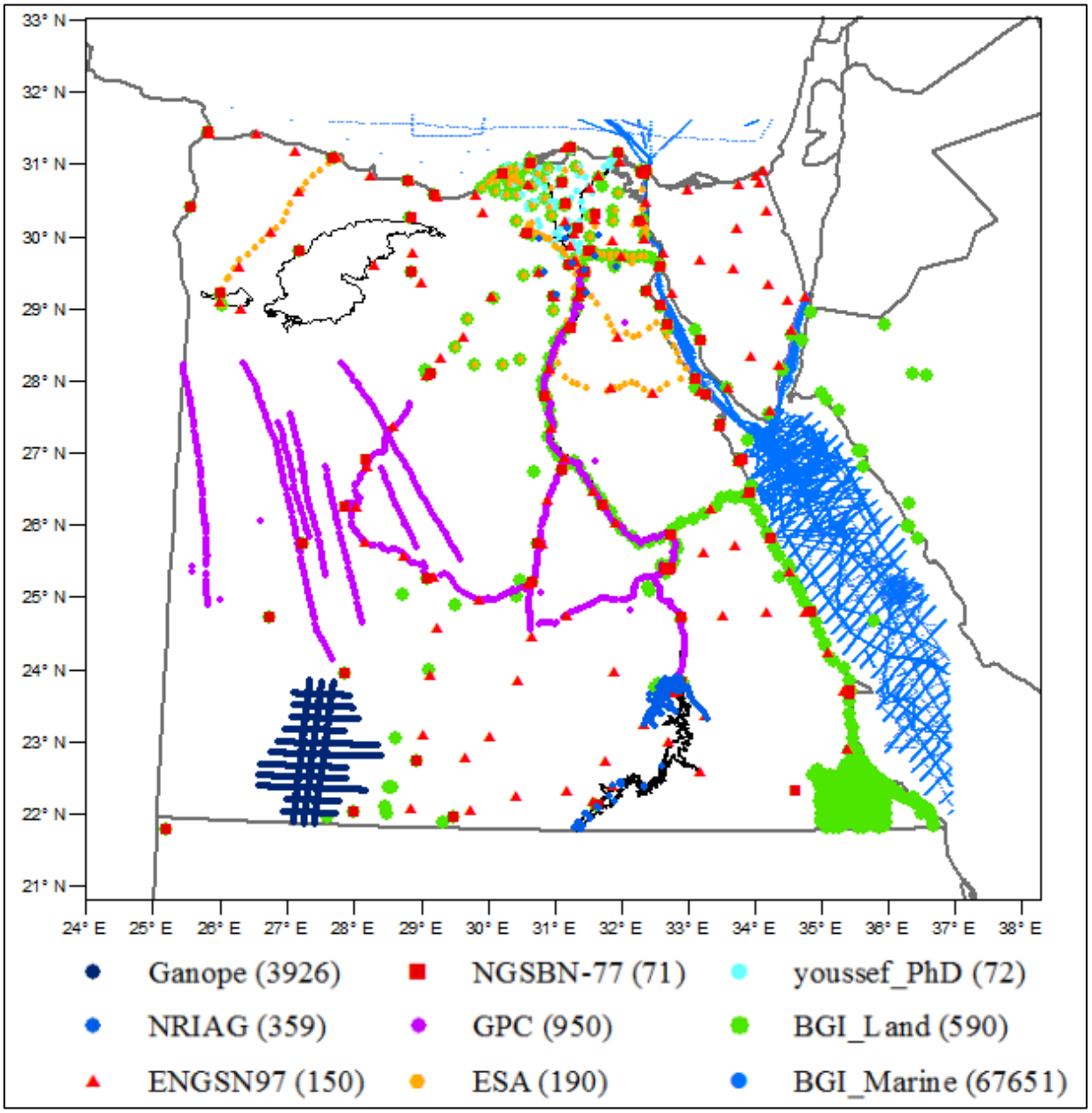

Figure (4.14): Geographic Locations of Available Gravity Data for Egypt.

Table (4.7): Summarizes Overall of Available Gravity Data for Egypt.

Source	Location	No. of point	Accuracy (mGal)	Reference
Ganope	Southwest	3926	0.01	(FFG Pty Ltd., 2009)
NRIAG	Aswan	233	0.02	(Groten and Tealeb, 1995)
	South	115	0.20	(Hassouna,2003)
	Cairo	11	0.01	
SRI	Egypt, ENGSN97	150	0.002-0.048	(Dawod, 1998).
GPC	Egypt,NGSB N-77	71	0.01 - 0.18	(Kamel and Nakhla, 1987)
	The Western Desert and along the Nile	950	±1.0	(El-Tokhey, 1993)
ESA	Along first order leveling + Delta	190	±0.40	
Youssef (Ph.D.)		72	0.068	(Youssef, 1970)
BGI	Along Nile+ Delta+ Southeast	590	0.20	http://bgi.obs-mip.fr/
	The Red Sea and Mediterranean	67651	5.0 -10.0	
Total points 73959 a set of 6308 land and 67651 marine gravity data				

4.5 Deflections of the Vertical

The available astronomic observations were observed by ESA at the 1st order triangulation network. The ESA observed the astronomic latitude (Φ) at 133 stations. In addition, the ESA observed 14 astronomic latitude (Φ) and longitudes (Λ) at Laplace stations. The observing program was based on observing four to six pairs of stars in one or two nights, using Repsold theodolite (Hassouna, 2003). The geodetic coordinates of these stations given relative to the Old Egyptian Datum (OED) and the heights were determined using trigonometric leveling (El-Tokhey, 1993; Hassouna, 2003).

According to Shaker (1986), the astronomical system depends on the direction of the vertical (actual gravity field) and the geodetic system depends on the direction of the ellipsoidal normal (normal gravity field), and then the difference between the two directions is the well-known deflection of the vertical θ. It has two components; a north-south component ξ and an east-west component η, where ξ is the meridian deflection of the vertical (*Ksi*) and η is the prime-vertical deflection of the vertical (*Eta*). The two components were performed using the well-known relations (Hassouna, 2003) see Fig.(4.15):

$$\xi = \Phi - \varphi$$
$$\eta = (\Lambda - \lambda)\cos(\varphi) \tag{4.2}$$

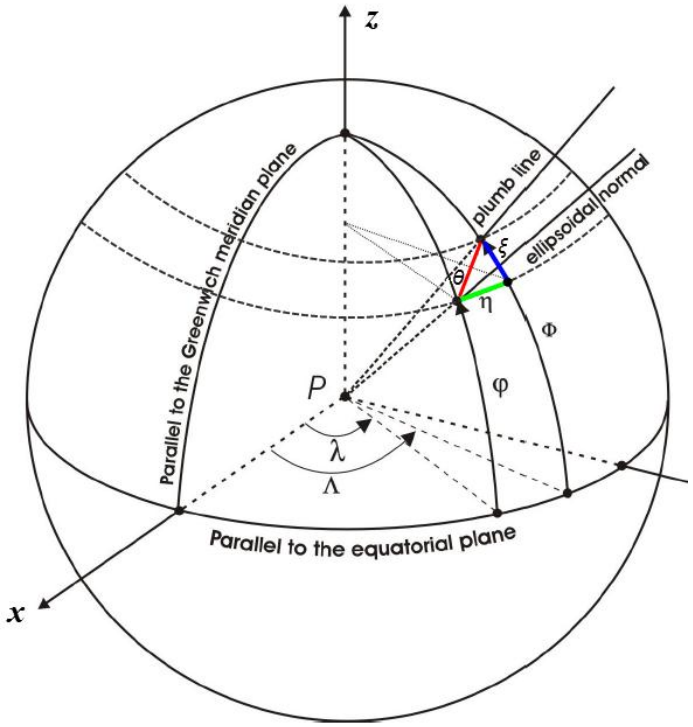

Figure (4.15): Deflection of The Vertical and its Components.

Fig. (4.16) shows the distribution of the available components of deflections of the vertical in Egypt.

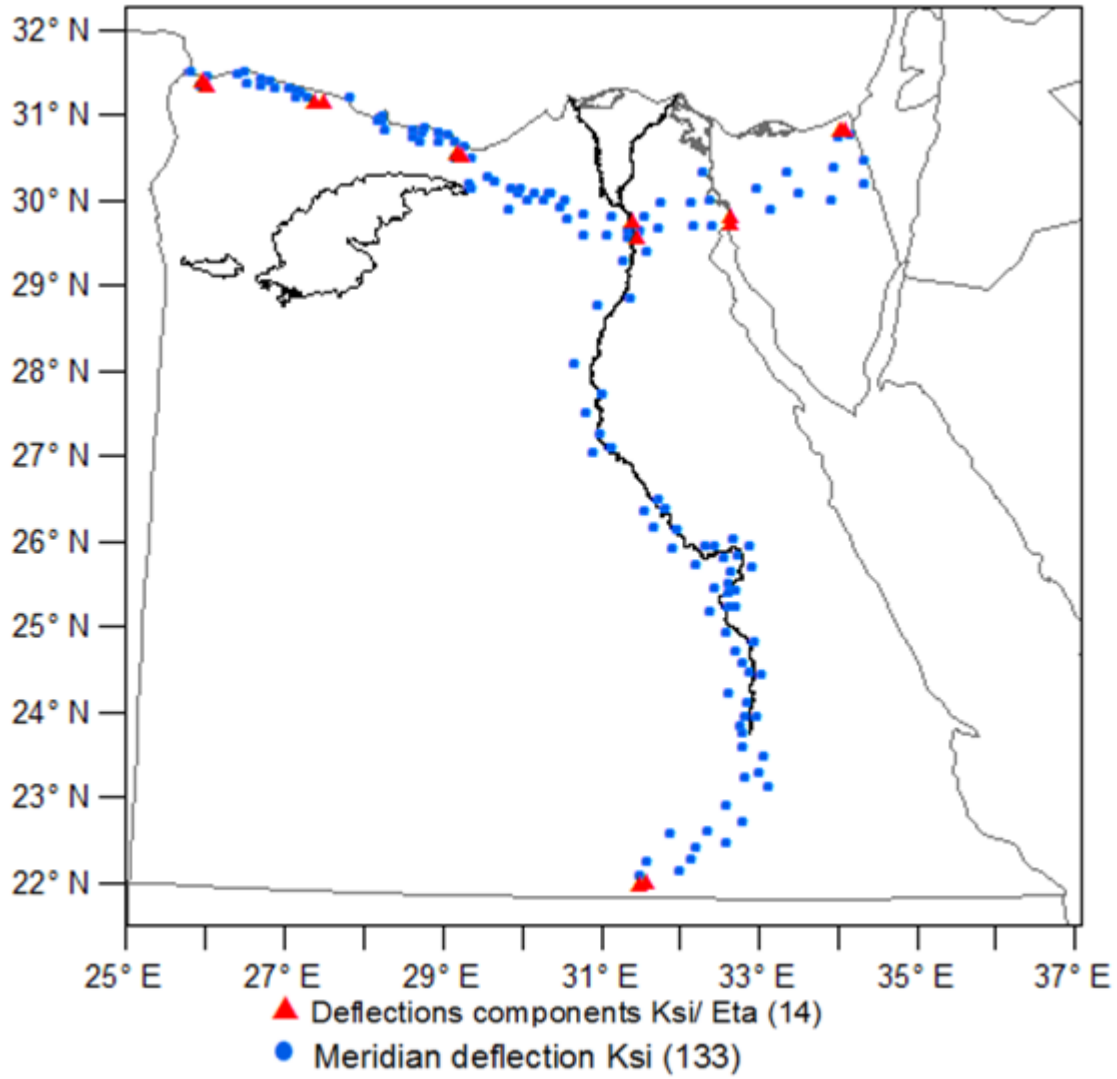

Figure (4.16): Components of Deflections of The Vertical Data in Egypt.

4.6 GPS/Levelling Data

The major GPS/levelling surveys projects, which have been used in this study described as follows (Shaker et al., 2000):-

a) Project 1; the aim of this project was establishing a precise geodetic control network in different sites in Egypt. In the way of doing that, 21 primary stations of ESA were observed (to connect the new work to the national first order net) with dual frequency GPS receivers and tied to 4 IGS stations. A few stations of these projects were used in this study about three stations as shown in Fig. (4.17).

b) Project 2; The Egyptian Civil Aviation Authority (ECAA) made a GPS national network (20 stations). The work in this network is nearly done in the specification of the HARN project and it's divided into three Sub-Nets, which are located in 18 airports distributed along the boundary and the center of Egypt and 9 navigational aids stations out Side the airports (Kamal, O., 2010). The GPS observations of this network are observed three times, every time continued 24 hours, with duration of three weeks apart between every session with dual frequency GPS receivers. Also, this network is tied to IGS and HARN stations with precise ephemeris during the data processing. Besides, ECAA were establishing at each airport small network consists of three to six GPS station ties to the previous network. Finally, 81 GPS stations (in and around the airports) were constructed formational and International Civil Aviation Services. The orthometric heights of all stations (except navigational aids) are measured relative to the Mean Sea Level (MSL) using the ESA benchmarks (first and second order levelling network), which is closed to each airport through a precise levelling loop. The ECAA project was performed from 1996 to 1998. Six stations of these projects were used in this study as shown in Fig. (4.17).

The orthometric heights of all stations (project 1&2) are measured relative to MSL using the ESA benchmarks (Bolbol, S. & Saad, A., 2017)

c) Project 3; The High Accurate Reference Network (HARN) project, made by the Egyptian surveying Authority (ESA) in 1995. The aim of this project is to form the New Egyptian Datum 1995 (NED-95) for furnish a nationwide GPS skeleton for surveying and mapping applications. The HARN network consists of 30 stations covers the area of Egypt in very good geodetic accurate network geometry with

an average spacing of approximately 200 km. In this network, the GPS observations are observed using dual frequency GPS receivers, the observation sessions were long enough and tied to International Geodynamic Service (IGS) and precise ephemeris is used in the processing in order to obtain a high accuracy estimate. The relative precision level of HARN is about 1: 1:10,000,000 or 10 part per million (ppm). Unfortunately, only 17 stations of HARN have observed an orthometric height refers to the national vertical datum in Egypt as shown in Fig. (4.18). Also, these stations connect to the Egyptian Triangulation Network. The other 13 stations (located in remote areas) have no observed orthometric heights and therefore, no undulations could be obtained for these stations (El-Ashquer et al., 2016).

In each of the above three GPS project, the WGS84 reference frame was utilized to be the basic datum of the produced coordinates which were gained directly from GPS.

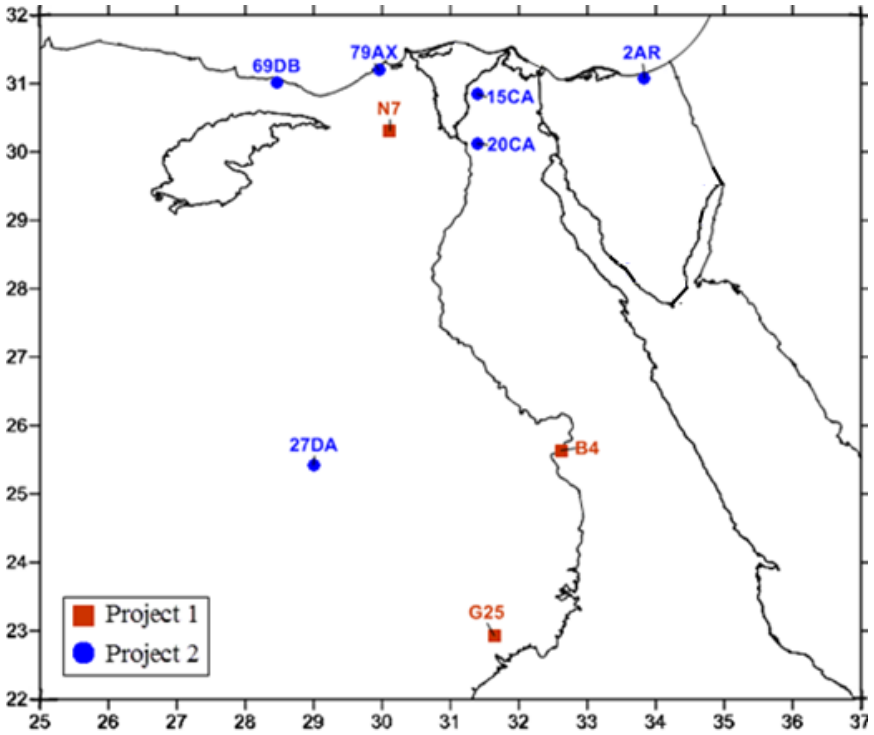

Figure (4.17): Distribution of GPS Stations with a known Orthometric Height of Project 1 and 2.

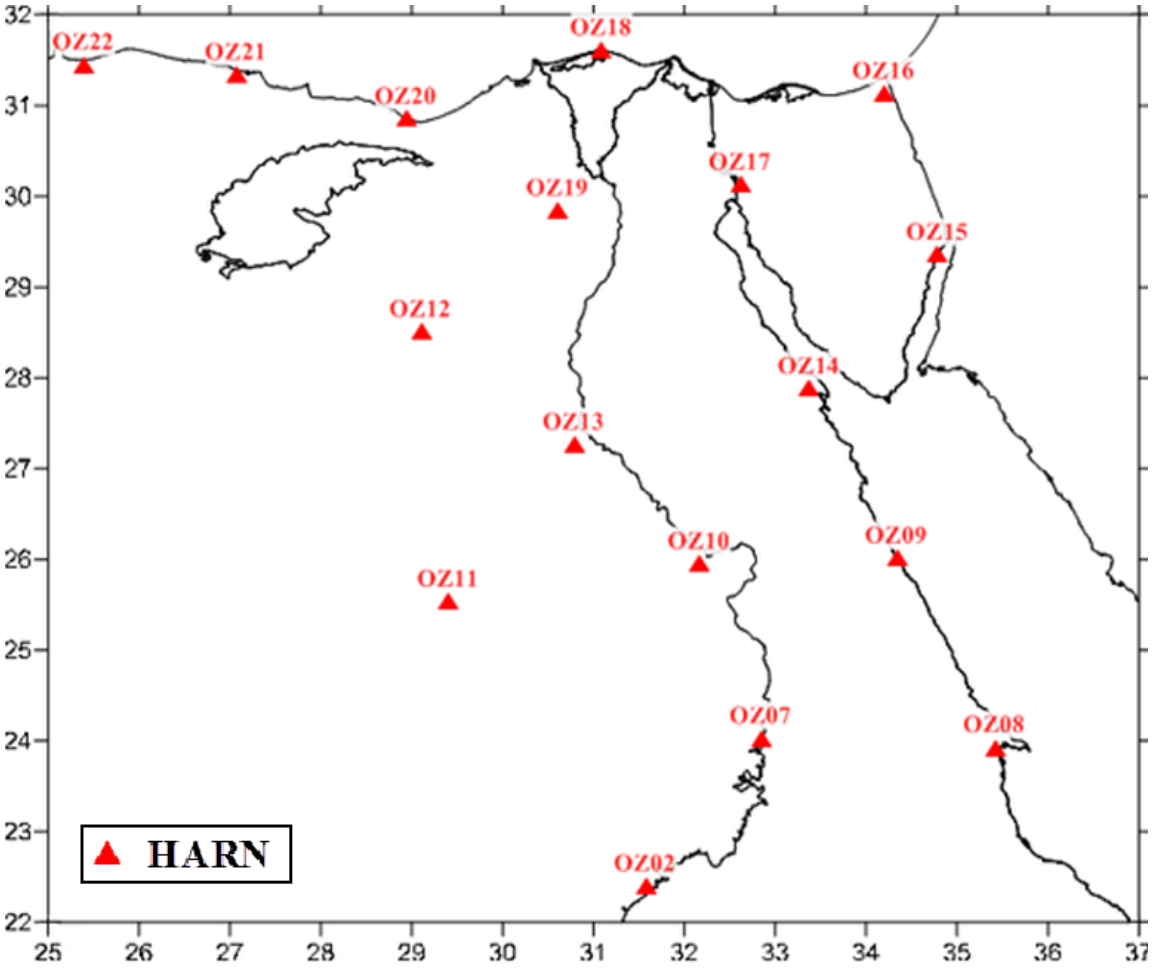

Figure (4.18): Distribution of GPS Stations with a known Orthometric Height of Project 3.

4.7 Programs

4.7.1 GRAVSOFT

GRAVSOFT consists of a rather large suite of FORTRAN programs, which have evolved over many years to tackle many different problems of physical geodesy. The roots of the oldest program – the general collocation program GEOCOL – date back to 1973 (Forsberg **&** Tscherning, 2008). Fig. (4.19) show the main program's package of GRAVSOFT software.

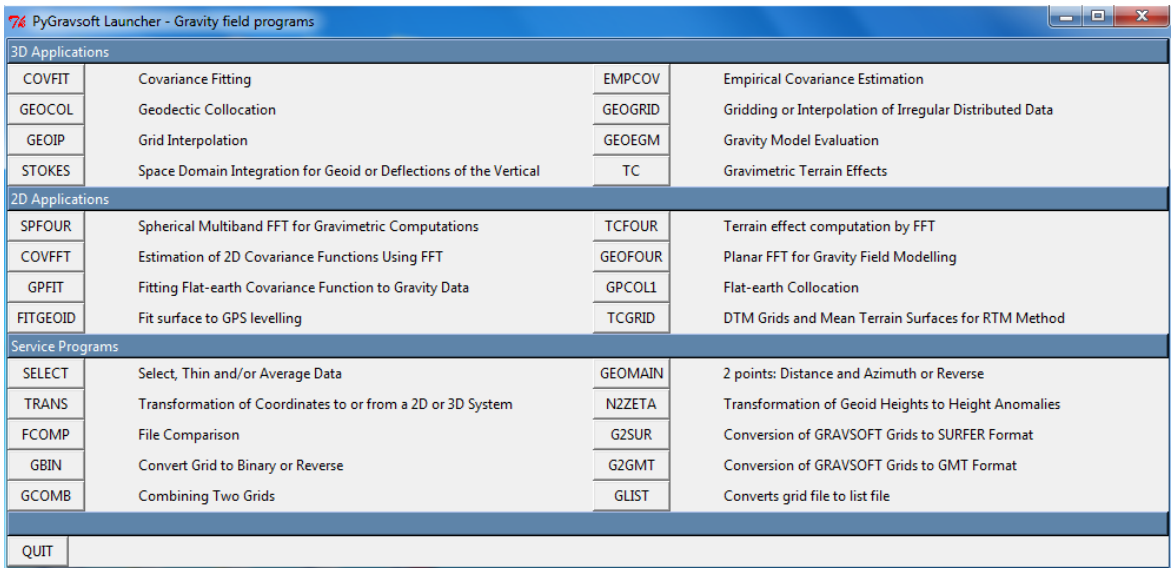

Figure (4.19) Main Programs Package of GRAVSOFT Software.

GEOCOL is the primary function of the program is the computation of an approximation to the anomalous potential of the earth, T, using stepwise least squares collocation. The program may also be used for the evaluation of a spherical harmonic series and corrections to a set of spherical harmonics may also be computed and compared to a reference set see Tscherning (2001). In this study, we used version 17 of GEOCOL called GEOCOL17.

4.7.2 PMITES

The program PMITES, one of GRAVSOFT package, is used for fitting a spherical harmonic expansion to local gravity data. The main routine of PMITES is GEOPMI create by Wenzel (1985) and slightly modified by Weber and Zomorrodian (1988), where GEOPMI is used for the computation of new or correction of existing spherical harmonic potential coefficients by means of mean free air anomalies using integral formulas within an iterative algorithm. This version of routine GEOPMI is limited to a maximum degree and order 360.

Finally, it has been a unification of the four parameters Table (3.1), which are used to define the Geodetic Reference System (GRS) to be used for synthesis and analysis computations in main programs GEOCOL17 and PMITES.

4.8 Preparation and Pre-Processing of Data Set

In the following sections, we present, the preparation and pre-processing of the above data set used to fit the model.

4.8.1 Preparation of Global Geopotential Models

According to section (2.7), the definition of IGSN71 gravity datum is the mean-tide system the same as the vertical datum of Egypt (cf. section 2.8.1). Also, the EGM96 and EGM2008 are classified as a tide-free system and GOCO05s is a zero tide system. Consequently, in order to compare different geopotential harmonic coefficient, it is mandatory that they refer to the same permanent tide system that is the mean tide system the same as gravity and vertical datum of Egypt. This will be discussed later (cf. section 3.4.2). Also, this could be made by converting the models from zero-tide and tide-free coefficients to the mean-tide system, where the second degree zonal coefficient of the models are modified, which describes the flattening of the equipotential surfaces of the gravity field, by using Eq.(3.23) and Eq. (3.24) as given in Table (4.8).

Table (4.8): Second-degree Zonal Coefficient of EGM96, GOCO05s and EGM2008 in Mean - tide system.

Model	Second Degree Zonal Coefficient ($\bar{C}_{2,0}$) [Mean- tide]	Unit
EGM96	- 0.484183441736000E-03	unitless
GOCO05s	- 0.484183355272500E-03	
EGM2008	- 0.484183213790815E-03	

4.8.2 Preparation of Gravity Anomaly

In total, we have processed 73959 points a set of 6308 terrestrial and 67651 marine gravity data as given in Table (4.7). All these gravity data are referring to IGSN-71 gravity datum and World Geodetic System 1984 (WGS 84) horizontal datum, which are the basic datums for all computations in the current work. The transformation of geodetic coordinates of gravity data from the OED and WGS72 into WGS 84 (Hassouna, 2003) made by using the seven transformation parameters El-Tokhey (2000) and (Leick, 1990), respectively.

Important steps in order to obtain the local Egyptian gravity anomaly from observed gravity data, which were previously explained in section (4.4) and summarized in Table (4.7), include:-

1. The Molodensky formula used to compute (point) free-air gravity anomalies, recall from Section (2.4.5)
2. Atmospheric Gravity Correction (δg_A) is a correction that is added to observed gravity recommended by the International Association of Geodesy (IAG, 1971). It is necessary because the WGS 84 earth's gravitational constant (*GM*) value includes the mass of the atmosphere. It is given by (Dimitrijevich, 1987, p. 4):

$$\delta g_{A} = \begin{cases} 0.87 \cdot e^{-0.116 \cdot H^{1.046}} & mGal \quad for \quad H \geq 0 \\ 0.87 & mGal \quad for \quad H < 0 \end{cases} \qquad (4.3)$$

Where *H* is the orthometric elevation above Mean Sea Level (MSL) of the observation point in kilometers, then the Molodensky free-air gravity anomalies Eq.(2.33) becomes:

$$\Delta g = g_P - \gamma_{Q_o} \left[1 - 2(1 + f + m - 2f \sin^2 \varphi) \frac{H}{a} + 3 \left(\frac{H}{a} \right)^2 \right] + \delta g_{A} \qquad (4.4)$$

Notes that the gravity data have been collected by different organizations with different accuracy and it’s likely to be

contaminated with several types of errors, such as vertical, horizontal and gravity datum. It also may contain gross errors and duplicated values. Therefore, the free-air gravity anomalies have been checked to remove these errors and duplicated points in a consistent manner.

3. A scheme for gross error detection has been carried out. Generally, any data that differ from the mean by more than ±3σ can be considered as blunders or outliers and removed from a data set (Wolf & Ghilani, 2006, p.44):

$$\text{Acceptable data be within specified limits} = Mean \pm 3\sigma \qquad (4.5)$$

In order to apply the criterion for rejection of outliers Eq. (4.5), some a priori known reference model, here EGM96 (cf. section 4.2.3), should be selected [where most of the Egyptian gravity anomaly have been used to develop this model see Fig. (4.5) and Fig. (4.14)]. EGM96 used to compute the free-air gravity anomalies at the observational points, then at each point the two values; the actual and the model free-air gravity anomalies are to be compared to get residuals, then any single residual that differs from the mean residual by more than ±3σ (σ: standard deviation of the residuals) can be reject.

4. The duplicated points are found in the BGI data Fig. (4.13) with the NGSBN-77 Fig. (4.10) and ESA data Fig. (4.11). In addition, the big marine data from BGI. A FORTRAN program DUPLICATES (http://cct.gfy.ku.dk/auvergne/duplicates.f) was written to search for observations which were closer than a given input parameter by Tscherning in 2009. Values which were detected as duplicates were removed and output to a new dataset.

After performing the steps (1–4), wherein steps (4) assume that the minimum distance between the gravity anomalies point in the land area is 3″ sec (approximately 90 m) and for the marine area is 5′ minute (approximately 9 km), a set of 6311 point gravity anomalies were selected (5739 in Land and 572 at Marine) as given in Table (4.9), statistics of this selection as given in Table (4.10) and the distribution as shown in Fig (4.20).

Table (4.9): Remove and Clean Data-set of Egyptian Point Gravity Anomalies.

Gravity type	No. of points	Remove data - set	Clean data-set
Land	6308	569	5739
Marine	67651	67079	572
Total points	73959	67648	6311

Table (4.10): Statistics of the selection Egyptian Point Gravity Anomalies.

Free-air gravity anomalies (Δg)	NO. of point	Minimum	Maximum	Mean	Standard dev.
		mGal	mGal	mGal	mGal
Land	5739	-81.669	70.459	2.795	14.121
Marine	572	-73.349	76.124	-3.023	16.127
Total points	6311	-81.669	76.124	2.267	14.410

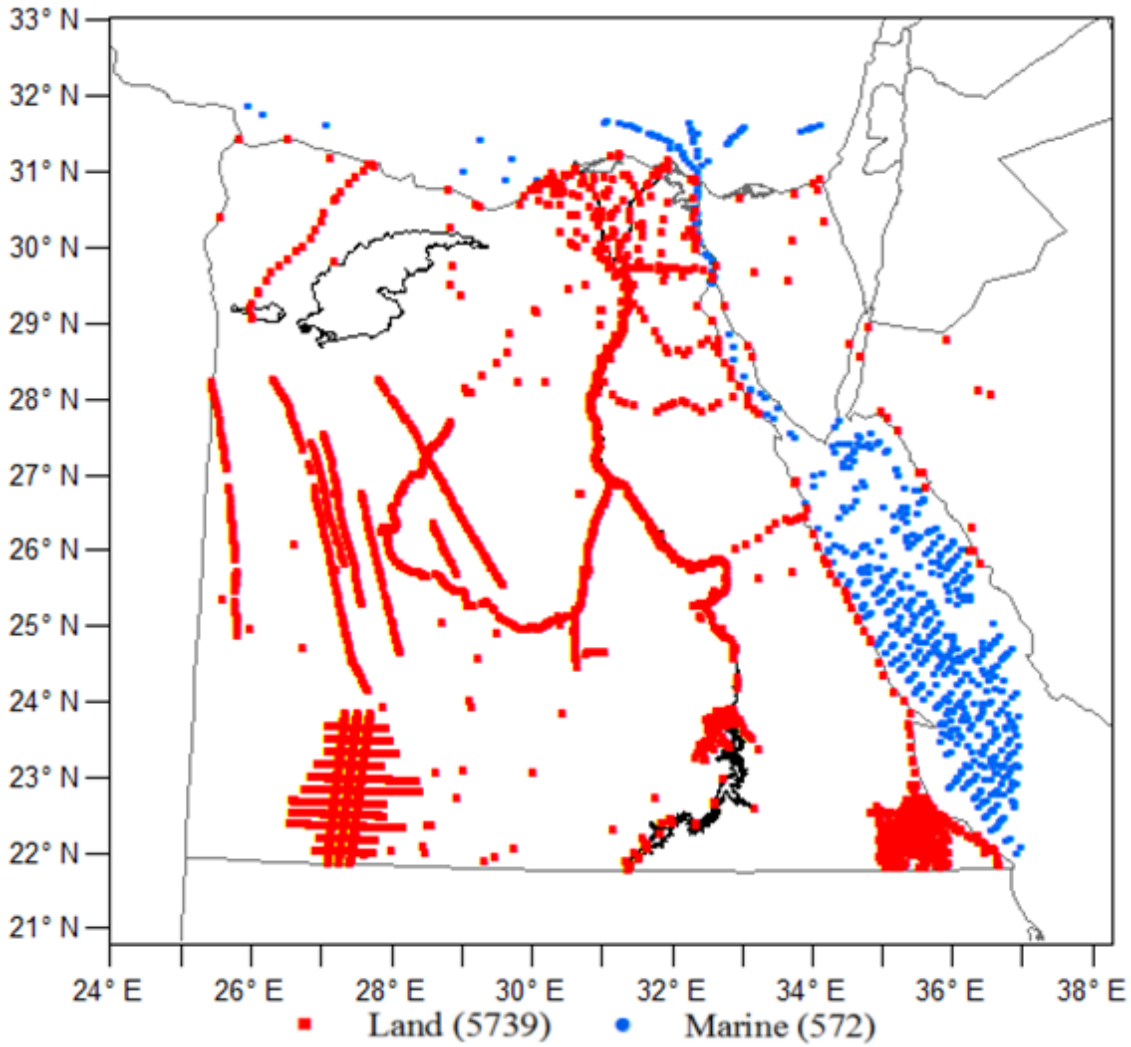

Figure (4.20): Distribution of the Local Egyptian Free-air Gravity Anomalies.

Since the approach described in section (3.5) requires that the gravity anomalies should be computed on a regular grid (mean value) for harmonic analysis computation. So, the Egyptian point gravity anomalies Fig. (4.20) are gridded to the 5′×5′ arc-minute mean free-air gravity anomalies ($\overline{\Delta g}$) in order to achieve the maximum degree of the tailored geopotential model.

In another word, for tailoring of the EGM2008 model, The Egyptian free-air anomalies data were compiled in the form of 5'×5' area mean values corresponding to the resolution of EGM2008. The computation of the local 5'×5' area mean values will be described in the next section.

4.8.3 Estimate the Egyptian 5 arc-minute Mean Anomaly

From Fig. (4.14) the distributions of point gravity are very poor on land; many areas are empty, Sinai, Eastern, and Western deserts. The distribution of the gravity points at the Red Sea is better than that at the Mediterranean Sea. So, we synthesized 5 arc-minute gravity anomalies values ($\overline{\Delta g}$) through a fast quadrant-search Least Squares Collocation (LSC) prediction algorithm through the program GEOGRID.

In order to perform LSC used the remove-compute-restore technique. This technique may sufficiently result in the creation of a high-resolution gravity database in a grid format or the densification of a test area with scarce gravity coverage. Where long wavelength trends are removed from the local free-air anomalies using the contributions of EGM96 from degrees 2 to 360 and augmented with the EGM2008 coefficients from degrees 361 to 2190, then LSC prediction is applied to the residuals data (stochastic field points) and finally, the effects of the mentioned contributions are restored back to the estimated quantities.

The fundamental formula for using LSC to predict 5 arc-minute mean free-air gravity anomalies and their associated errors using point free-air gravity anomalies are given by the well-known expressions as (Kenyon & Pavlis, 1996):

$$\overline{\Delta g}_{5'} = C_{\overline{\Delta g}\Delta g} \cdot \left(C_{\Delta g \Delta g} + V\right)^{-1} \cdot L + RES(\,mean\,) \tag{4.6}$$

$$M^2\left(\overline{\Delta g}_{5'}\right) = C_{\overline{\Delta g}\,\overline{\Delta g}} - C_{\overline{\Delta g}\Delta g} \cdot \left(C_{\Delta g \Delta g} + V\right)^{-1} \cdot C_{\Delta g\,\overline{\Delta g}}$$

Where : –

$\overline{\Delta g}_{5'} = 5'$ *mean free-air gravity anomaly.*

$L = \Delta g - \Delta g_{\,EGM\,96}\big|_{2 \le n \le 360} - \Delta g_{\,EGM\,2008}\big|_{361 \le n \le 2190}$

$\Delta g =$ *Molodensky point free-air gravity anomaly.*

$\Delta g_{\,EGM\,96}\big|_{2 \le n \le 360} =$ *Contribution of* $EGM\,96$ *from degrees* 2 *to* 360.

$\Delta g_{EGM\,2008}\big|_{361\le n\le 2190} = Contribution\ of\ EGM\,2008\ from\ degrees\ 361\ to\ 2190.$

$V = noise\ covariance\ matrix\ (diagonal)\ of\ point\ free\text{-}air\ gravity\ anomalies.$

$RES(mean) = \overline{\Delta g}_{EGM\,96}\big|_{2\le n\le 360} + \overline{\Delta g}_{EGM\,2008}\big|_{361\le n\le 2190}$ *Restore step*

$C_{\Delta g\Delta g} = signal\ covariance\ matrix\ of\ point\ free\text{-}air\ gravity\ anomalies.$

$C_{\overline{\Delta g}\Delta g} = signal\ cross\ covariance\ matrix\ between\ 5'\ mean\ and$
$free\text{-}air\ gravity\ anomalies.$

$M^2\left(\overline{\Delta g}_{5'}\right) = error\ variance\ of\ 5'\ mean\ gravity\ anomaly.$

$C_{\overline{\Delta g}\,\overline{\Delta g}} = signal\ covariance\ between\ 5'\ mean\ gravity\ anomalies\ .$

The covariance modeling consists of calculating empirical covariances from the reduced anomaly data and then fitting a 2nd order Markov analytical covariance model to the empirical covariance given by (Forsberg & Tscherning, 2008, p.38):

$$\mathrm{cov}(\psi) = C_0\ (1+\frac{\psi}{\alpha}).e^{(\frac{-\psi}{\alpha})} \qquad (4.7)$$

Where ψ is the spherical distance between the interpolation and computation points, C_0 is the variance of the residual gravity anomalies in square mGal (covariance scale) and α is the correlation length. When using the program GEOGRID the variance C_0 is found automatically from data and the parameter α determined from the correlation length specified by the user or this is the value of the argument for which Cov (ψ) has decreased to half of its value at $\psi = 0$.

Finally in this research, using the analytical covariance model Eq. (4.7), the value of the correlation length was set to 12.0 km and 20 closest neighbors in each quadrant around a prediction point (with noise 1.0 mGal). The LSC solution resulted in the 5'×5' of the local mean free-air gravity anomalies ($\overline{\Delta g}$) bounded by $21^o \le \varphi \le 33^o$ and $24^o \le \lambda \le 38^o$ are shown in Fig. (4.21) and statistics are given in Table (4.11).

Table (4.11): Statistics of The Egyptian 5'×5' Mean Free-air Gravity Anomalies.

Gravity Anomalies		Mean	Standard dev.	Minimum	Maximum
NO. of Value	24505	mGal	mGal	mGal	mGal
The Egyptian mean free-air anomalies ($\overline{\Delta g}$)		5.482	28.367	-216.298	218.099

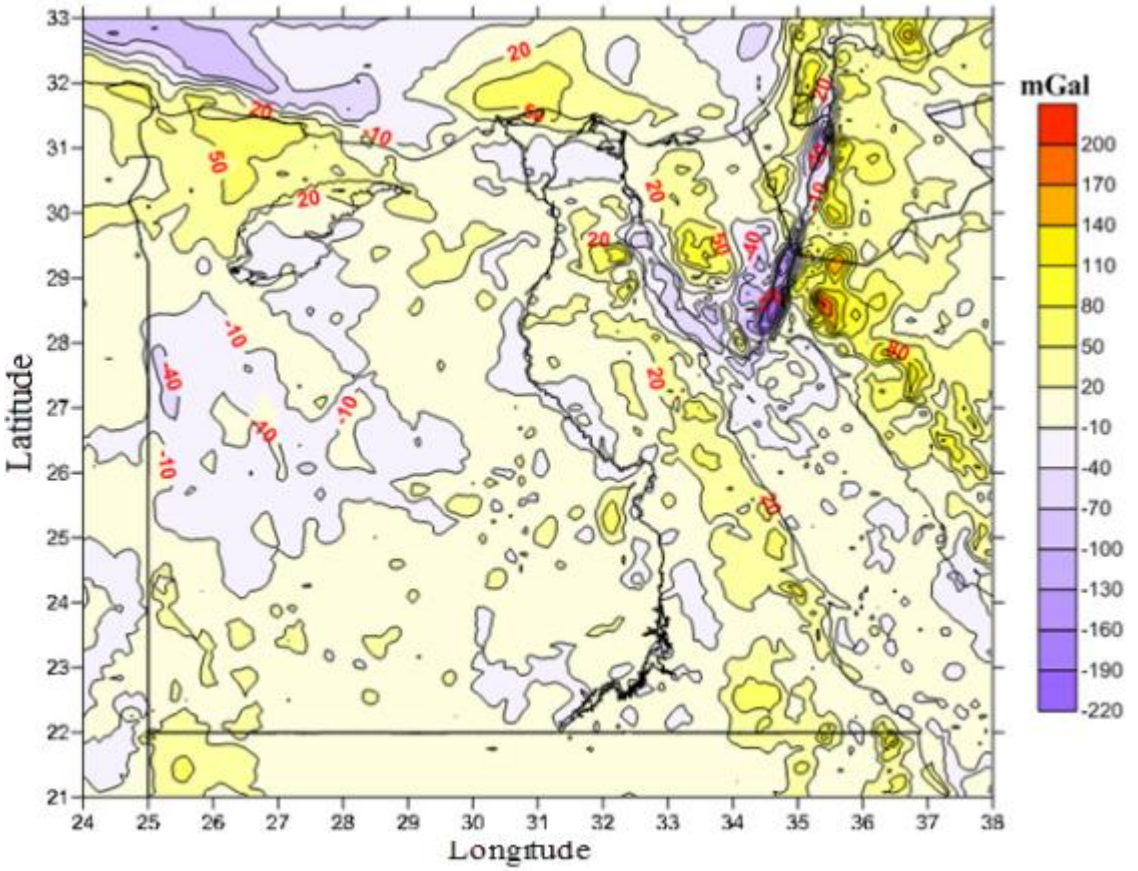

Figure (4.21): The Egyptian 5'×5' Mean Free-air Gravity Anomalies Interpolated by Least Squares Collocation.

We now check the quality of the grid by using it to calculate the original values used to create the grid using the program GEOIP, Fig. (4.22) shows that the histogram of residuals between the gravity anomalies control points (original values) and those derived from the 5 arc-minute mean gravity anomalies.

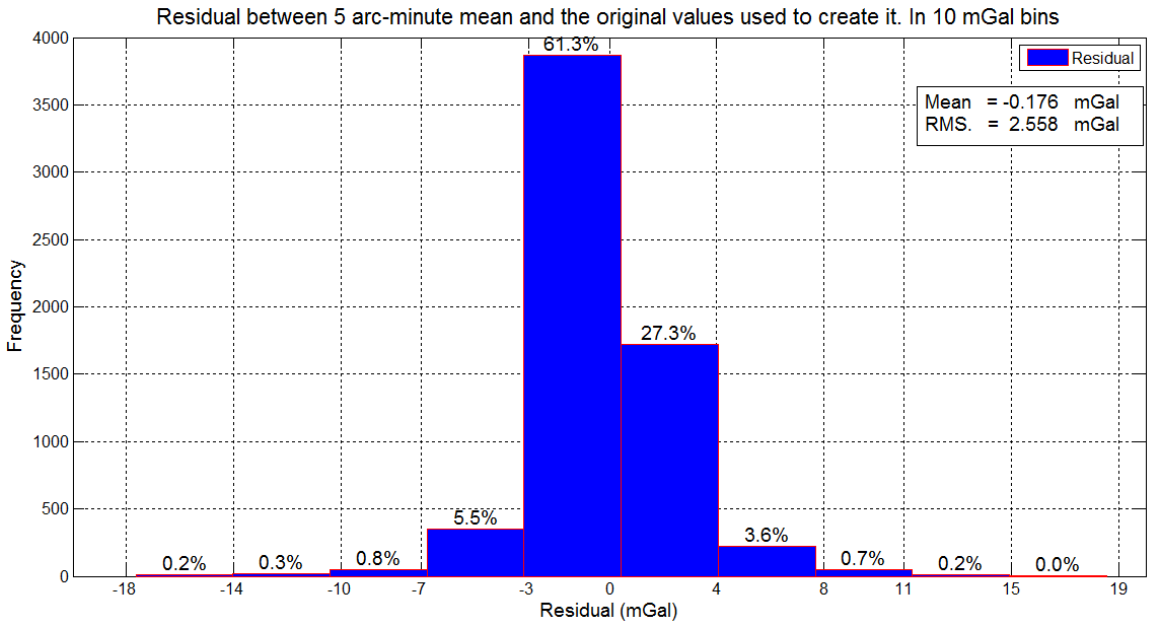

Figure (4.22): Histogram of Residual between The Gravity Anomalies Derived from Original Points and 5 Arc-minute Gravity Anomalies

From Fig. (4.22) the result shows that the grid represents the original data very well.

4.8.4 Preparation of Deflections of the vertical Data

A set of 14 deflections (ξ, η) and 127 is the meridian deflection of the vertical (ξ) were selected Table (4.12) after applying the criterion for rejection of outliers Eq. (4.5) as shown in Fig. (4.23).

Table (4.12): Statistics of The selection Deflections of The vertical.

Deflections of the vertical	NO. of points	Mean	Standard dev.	Minimum	Maximum
		arcsec	arcsec	arcsec	arcsec
Meridian deflection (ξ)	141	1.981	4.926	-9.545	16.508
Prime-vertical deflection (η)	14	-0.679	5.443	-8.044	8.241

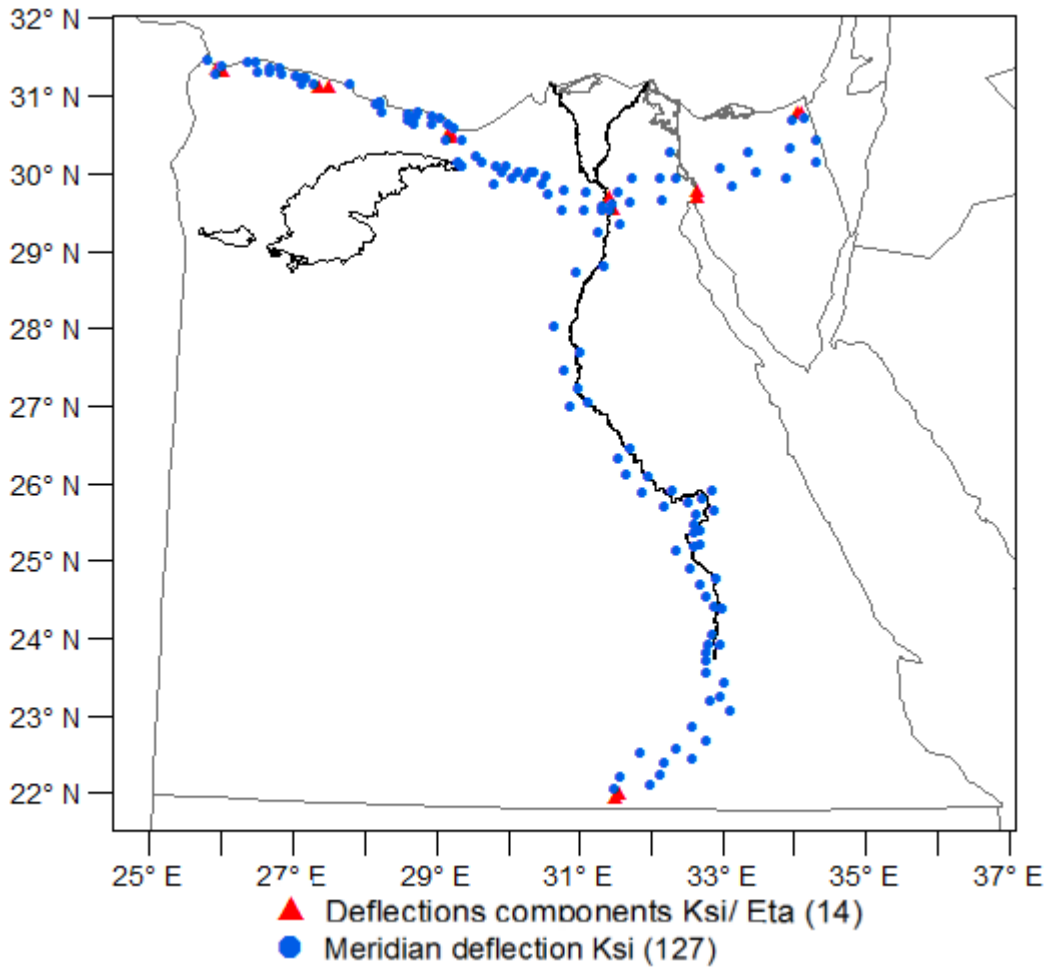

Figure (4.23): Components of Deflections of The Vertical Used for The Computation.

4.8.5 Preparation of GPS/Levelling Data

The geoid heights with respect to the GPS/levelling techniques were computed as follows see Fig. (2.7):

$$N_{GPS/Level} = h_{GPS} - H_{Levelling} \quad (4.8)$$

In practice, the GPS-levelling technique has become quite common and used often erroneously or with a poor understanding of the transformations between reference surfaces and systematic errors involved. As accuracy requirements increase, the incorrect application of Eq. (4.8) has more severe implications. Therefore, it is important to develop proper procedures for combining the heterogeneous height data (Sansò & Sideris, 2013, p.,

524). Thus, from Eq.(4.8), where h_{GPS} is the ellipsoidal height obtained by the GPS observations refer to the tide-free system (cf. section 2.7) and $H_{Levelling}$ denotes the orthometric height estimated at the benchmarks, in this study, refer to mean tide system (cf. section 2.8).

It is now clear that h_{GPS} and $H_{Levelling}$ must be given in a consistent tide system, so the ellipsoidal heights of available GPS stations in Egypt, which described in section (4.6), should be converted to mean tide system such as the vertical datum of Egypt through the formula found in (section 2.7) as follows :

$$\delta h^{Free-Mean} = h_n - \left[h_n + 0.62 \times (9.9 - 29.6 \sin^2 \varphi) \right] \quad (cm) \qquad (4.9)$$

Where h_n is the ellipsoidal height in the non-tidal or tide-free system. Fig. (4.24) show that the differences between tide-free and mean tide system for the ellipsoidal heights of HARN project (17 stations) by using Eq. (4.8).

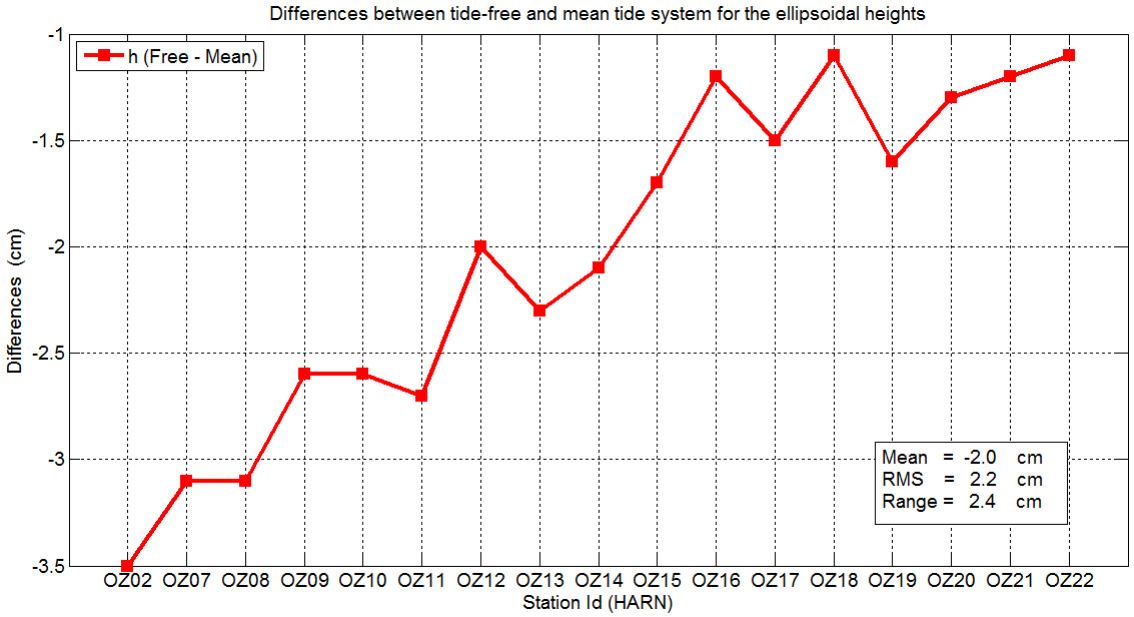

Figure (4.24): Differences between tide-free and mean tide system for the ellipsoidal heights of HARN stations

These differences have an average of -2.0 cm with a Root Mean Square (RMS) about ±2.2 cm. The crudely estimated precision of the geoid heights data assume ~14 cm.

Chapter 5

TAILORED GEOPOTENTIAL MODELS FOR EGYPT

5. TAILORED GEOPOTENTIAL MODELS FOR EGYPT

5.1 Overview

In this chapter, the harmonic coefficients given by integral formulas (Weber & Zomorrodian, 1988) are tailored using an iterative algorithm to improve the accuracy of the obtained harmonic coefficients and decrease the residual field. Moreover, this chapter also briefly presents the following:-

a) The comparisons between the tailored geopotential models in order to determine the best fit for them that would be considered as a reference model for gravity field modelling in Egypt.
b) Geoid models for Egypt have been computed using the harmonic coefficients of the tailored geopotential models.
c) The gravimetric geoid, as well as combined geoid (gravity and astrogeodetic data), has been computed for Egypt using tailored geopotential models in the remove-restore technique through 3D Least-squares collocation (3D LSC).
d) All geoid solutions will be validated to choose the best ones for the determination of orthometric heights above MSL, or more precisely with respect to a vertical geodetic datum in Egypt.

All contour maps in this chapter are plotted by converting grid surface into SURFER format using the GRAVSOFT program G2SUR (cf. Fig. 4.19).

5.2 Tailored Models to Gravity Data in Egypt

Fig. (5.1) illustrates the iteration scheme used for tailored geopotential models, after each iteration a comparison is carried out between observed anomalies (local) and the computed anomalies from the tailored geopotential model (corrected spherical harmonic coefficients)

until two successive iteration steps give practically the same harmonic coefficients, or alternatively, no practical change in the residual field between two successive iteration steps happens.

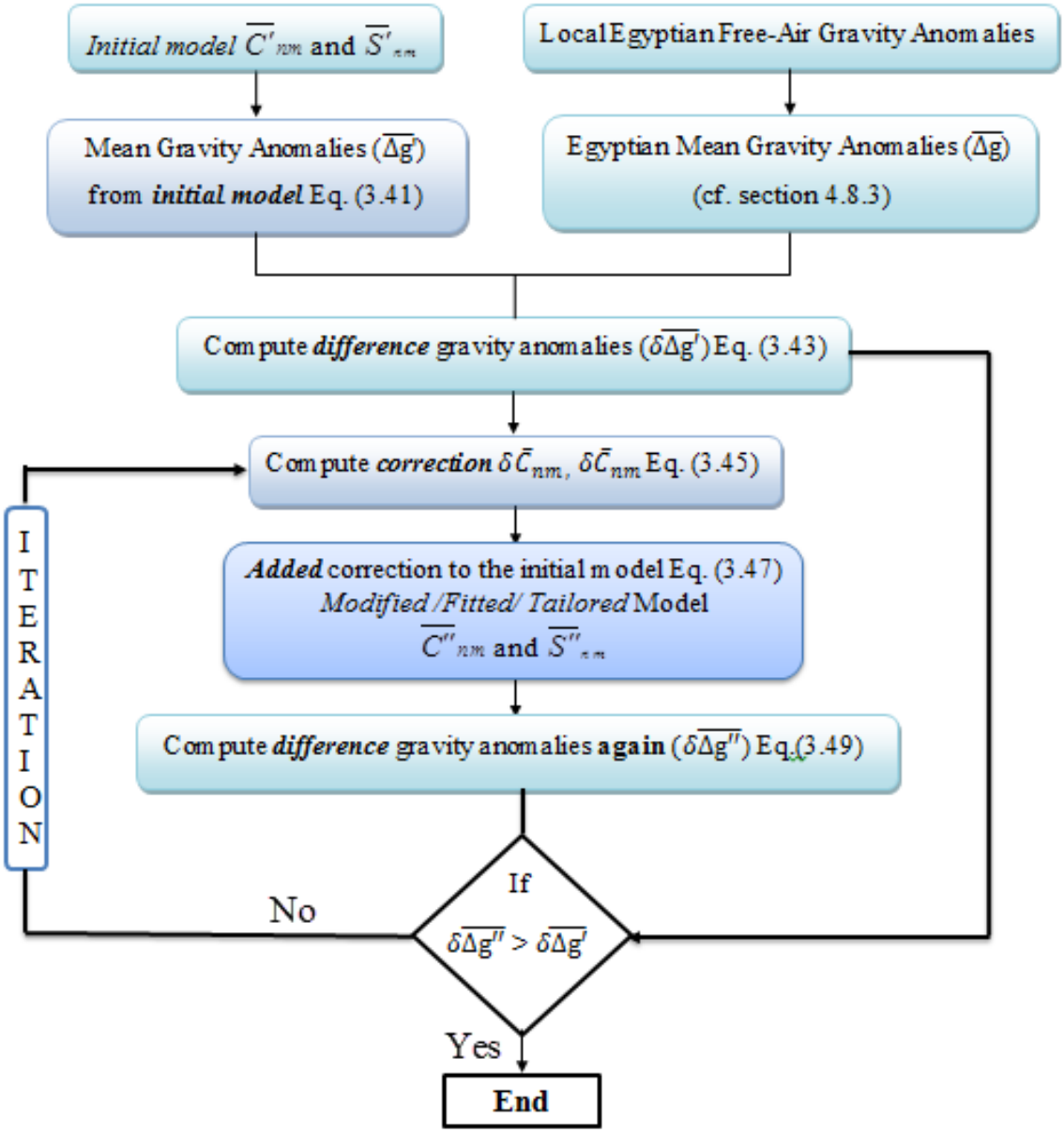

Figure (5.1): Iteration Scheme for Tailored geopotential Model.

We present the results of tests performed on the tailored satellite-only model GOCO05s and high degree reference model EGM2008 for Egyptian territory. This will be done by using a slightly modified version of the program *PMlTES* (cf. section 4.7.2).

5.2.1 Tailored Satellite-only Model GOCO05s

The Egyptian $5' \times 5'$ mean gravity anomaly, described in section (4.8.3), was used to compute the tailored geopotential model GOCO05s denoted as EG1GOC5s till degree and order 280. The harmonic coefficients of tailored geopotential model EG1GOC5s were obtained by integral formulas after five iterations as Table (5.1).

Table (5.1): Statistics of The Differences of The Egyptian 5 Arc-minute Mean Gravity Anomalies with GOCO05s and Tailored Model EG1GOC5s. (Max. degree. 280)

Gravity Anomalies	No. of iterations	Mean	RMS	Minimum	Maximum
		mGal	mGal	mGal	mGal
Mean Free-air ($\overline{\Delta g}$)		5.482	28.891	-216.298	218.099
$\overline{\Delta g}$ - GOCO05s	**0**	**-0.058**	**21.215**	**-214.073**	**188.055**
$\overline{\Delta g}$ - EG1GOC5s	1	0.056	14.562	-139.692	146.786
$\overline{\Delta g}$ - EG1GOC5s	2	0.038	14.371	-137.785	148.127
$\overline{\Delta g}$ - EG1GOC5s	3	0.019	14.288	-137.004	148.669
$\overline{\Delta g}$ - EG1GOC5s	4	0.008	14.237	-136.635	148.894
$\overline{\Delta g}$ - EG1GOC5s	**5**	**0.002**	**14.198**	**-136.448**	**148.952**

The results listed in Table (5.1) show that the tailored geopotential model EG1GOC5s improve the mean differences significantly, decreasing it from - 0.058 to 0.002 mGal. In addition, the Root Mean Square (RMS) show a very dramatic improvement, changing from ± 21.215 mGal to ± 14.562 mGal after only the first iteration. Also, it is cleared that more improvement occurs with successive iterations, where the tailored geopotential model EG1GOC5s has improved by about 33 % compared to GOCO05s in terms of RMS after five iterations.

Fig. (5.2) shows that the decrease of RMS of the differences of the Egyptian 5 arc-minute mean gravity anomalies using tailored geopotential model EG1GOC5s with respect to the iteration number.

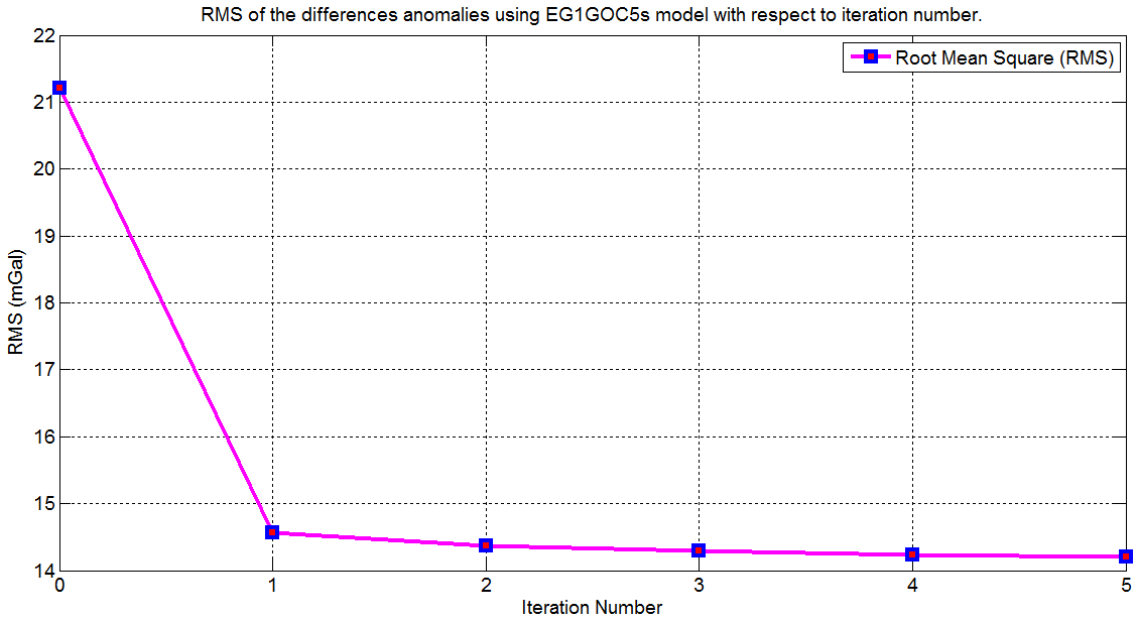

Figure(5.2): RMS of The Differences of The Egyptian 5 Arc-minute Mean Gravity Anomalies Using EG1GOC5s Tailored Model with respect to The Iteration Number.

In order to measure the accuracy of the original and tailored geopotential model at the grid points or a direct comparison between the models all over the Egyptian territory, Fig. (5.3) and Fig (5.4) shown graphically and summarized that the difference between the Egyptian $5' \times 5'$ mean gravity anomalies and the computed gravity anomalies using GOCO05s and EG1GOC5s model, respectively, with regard to iteration number = 0 and 5.

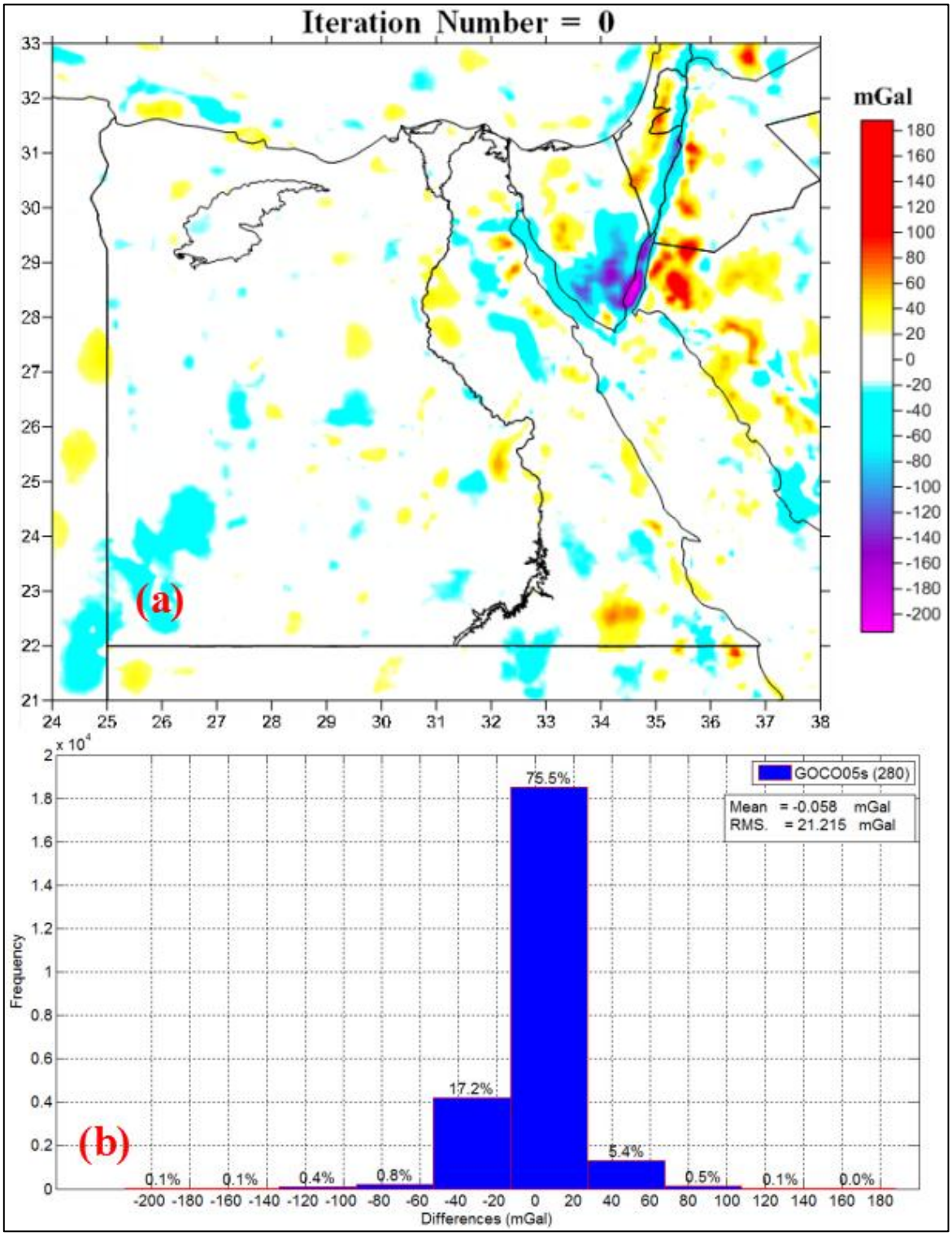

Figure (5.3): (a) Difference between The Egyptian 5′ × 5′ Mean Gravity Anomalies and The Computed Gravity Anomalies Using The Original Model GOCO05s (b) Histogram of These Differences in 10 mGal bins. (Iteration Number =0)

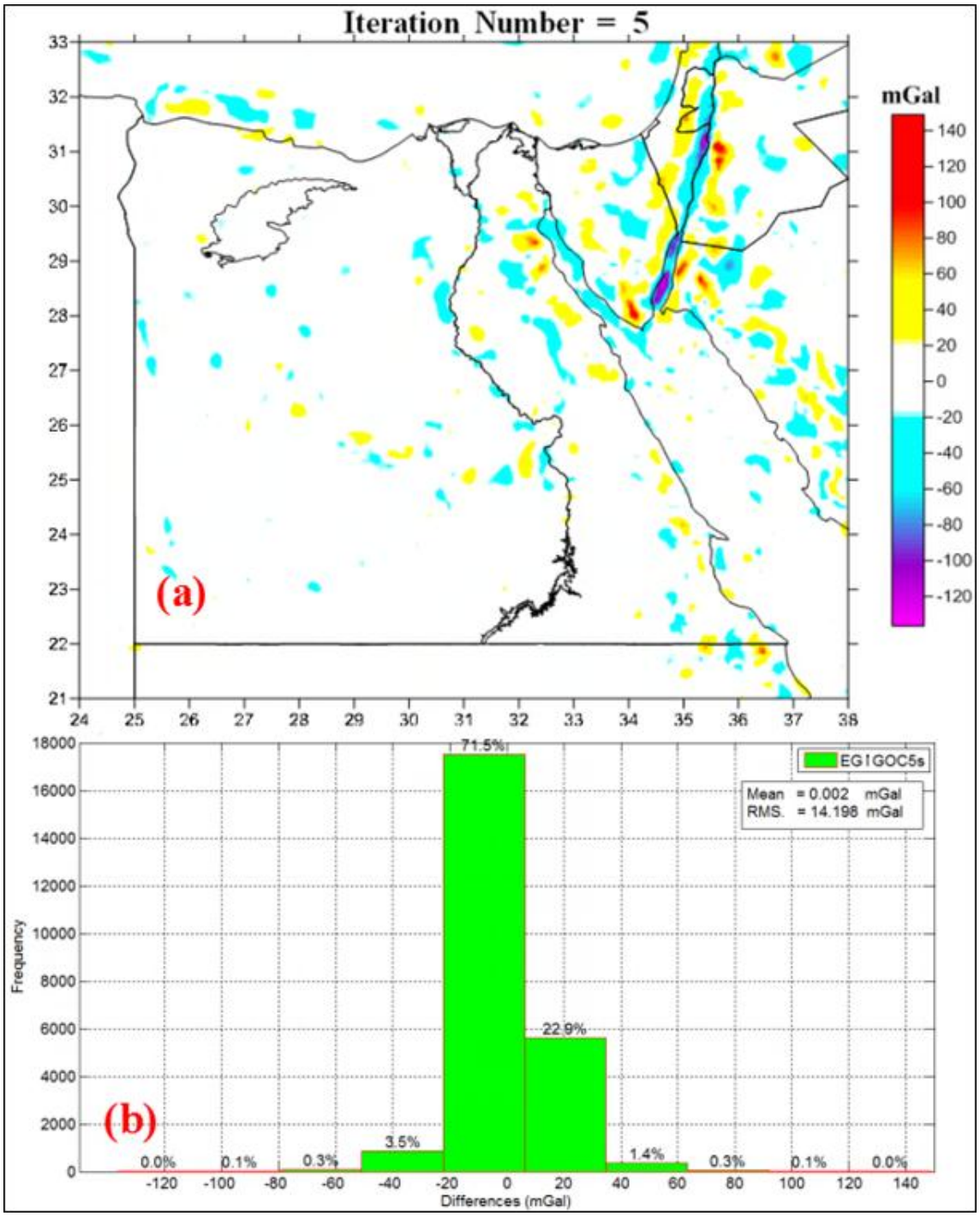

Figure (5.4): (a) Difference between The Egyptian 5′ × 5′ Mean Gravity Anomalies and The Computed Gravity Anomalies Using The EG1GOC5s Tailored Model (b) Histogram of These Differences in 10 mGal bins. (Iteration Number =5)

From Fig.(5.3), one can see that the satellite-only model GOCO05s is able to recover gravity anomalies over 60 % of the Egyptian territory to within ± 20 mGal, which shows a great matching over the Egyptian territory due to a combination of the three gravity field mapping missions (CHAMP, GRACE, and GOCE) (cf. section 4.2.1). In addition, Fig.(5.3) shows the large difference in high topography (mountainous) regions, such as the southern part of Sinai Peninsula.

Similarly, From Fig.(5.4), it can be seen that 83 % of the Egyptian territory has an RMS within ± 20 mGal of difference anomalies for the tailored geopotential model EG1GOC5s, which are quite good and best agreement for Egyptian gravity field than the original model GOCO05s. Thus, the tailored geopotential model EG1GOC5s fits the gravity anomalies in Egypt better than GOCO05s. Fig. (5.5) gives the Egyptian 5′×5′ mean gravity anomalies derived from the tailored geopotential model EG1GOC5s.

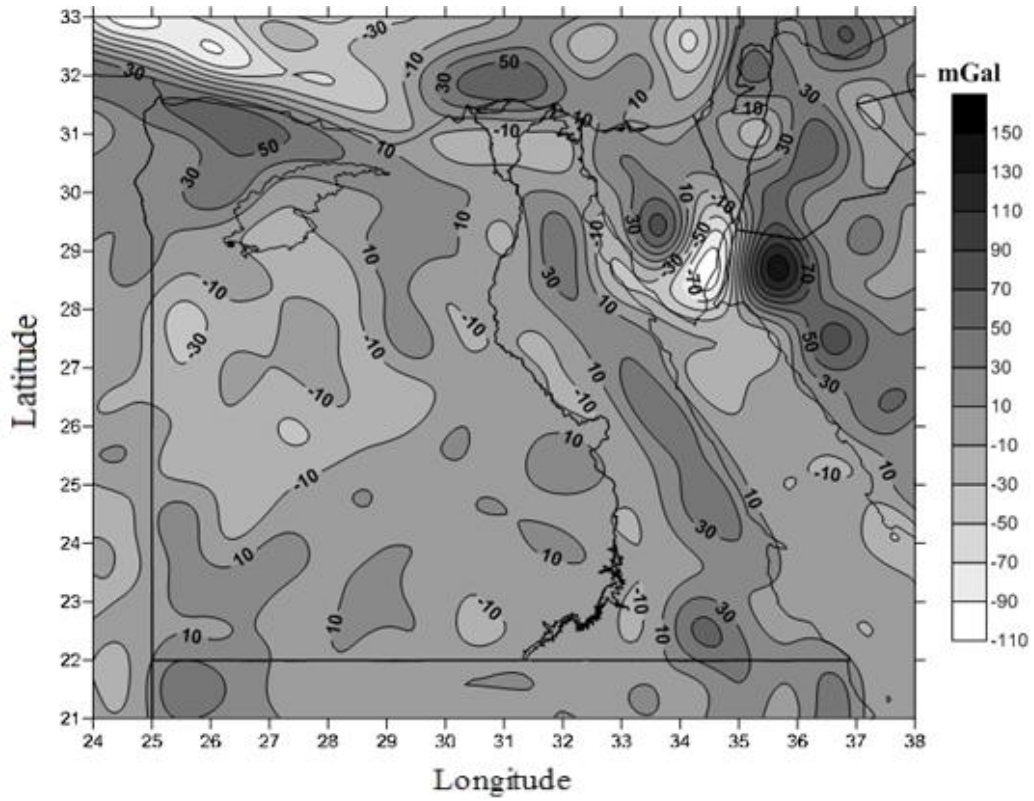

Figure (5.5): The Egyptian 5′×5′ Mean Gravity Anomalies Derived by Using EG1GOC5s Model Completed to Degree and Order 280.

5.2.2 Tailored Ultra-high Degree Model EGM2008

A similar test was performed using the high degree reference model EGM2008. The high degree reference model EGM2008 was tailored to maximum degree 360 as given in Table (5.2), yielding the model denoted as EGM08F.

Table (5.2): Statistics of The Differences of The Egyptian 5 Arc-minute Mean Gravity Anomalies with EGM2008 and Tailored Model EGM08F. (Max. degree. 360)

Gravity Anomalies	No. of iterations	Mean	RMS	Minimum	Maximum
		mGal	mGal	mGal	mGal
Mean Free-air ($\overline{\Delta g}$)		5.482	28.891	-216.298	218.099
$\overline{\Delta g}$ - EGM2008	**0**	**-0.166**	**17.188**	**-159.087**	**143.881**
$\overline{\Delta g}$ - EGM08F	1	-0.031	12.617	-128.411	142.431
$\overline{\Delta g}$ - EGM08F	2	-0.006	12.509	-127.669	142.475
$\overline{\Delta g}$ - EGM08F	3	0.000	12.447	-127.273	142.477
$\overline{\Delta g}$ - EGM08F	4	0.003	12.403	-126.987	142.444
$\overline{\Delta g}$ - EGM08F	**5**	**0.005**	**12.369**	**-126.751**	**142.401**

The results listed in Tables (5.2) show that the tailored geopotential model EGM08F has improved by about 28.0 % compared to EGM2008 (degree and order 360), where the RMS decreased from ±17.188 mGal for EGM2008 to ±12.369 mGal for EGM08F.

Thus, it is clear that the tailored geopotential model EGM08F fits the Egyptian gravity anomalies better than EGM2008. Fig. (5.6) show the RMS of the differences with respect to the iteration number. The results of Tables (5.2) are shown graphically and summarized in Fig. (5.7) and Fig (5.8) with iteration number = 0 and 5, respectively.

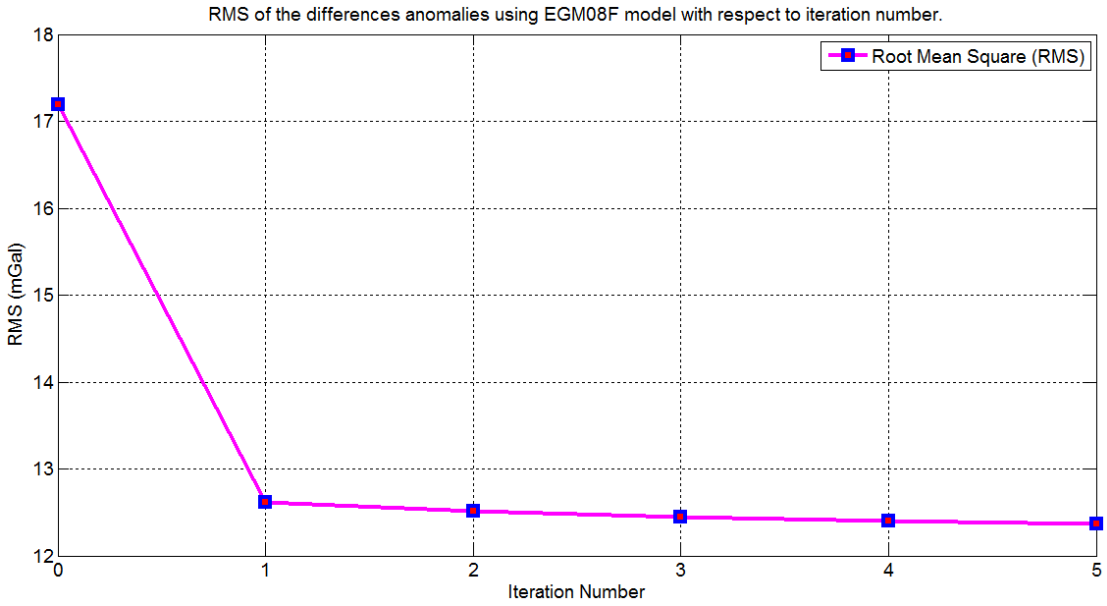

Figure(5.6): RMS of The Differences of The Egyptian 5 Arc-minute Mean Gravity Anomalies Using EGM08F Tailored Model with respect to The Iteration Number.

From Fig. (5.7) and Fig (5.8), It is clear that over 80 % of the Egyptian territory within ± 20 mGal for the EGM2008 and 87% for the tailored geopotential model EGM08F.

For increasing the accuracy of the tailored geopotential model for EGM08F, the higher harmonic coefficients (from n = 361 to n = 2190) of the original geopotential model EGM2008 have been restored, yielding the final tailored geopotential model for Egypt, which was denoted EGTM0818.

Once again, a comparison has been made between the Egyptian 5′×5′ mean gravity anomalies using EGM2008 and EGTM0818 at maximum degree 2190 as shown in Table (5.3). The computations were carried out using GRAVSOFT program GEOCOL (cf. Fig. 4.19).

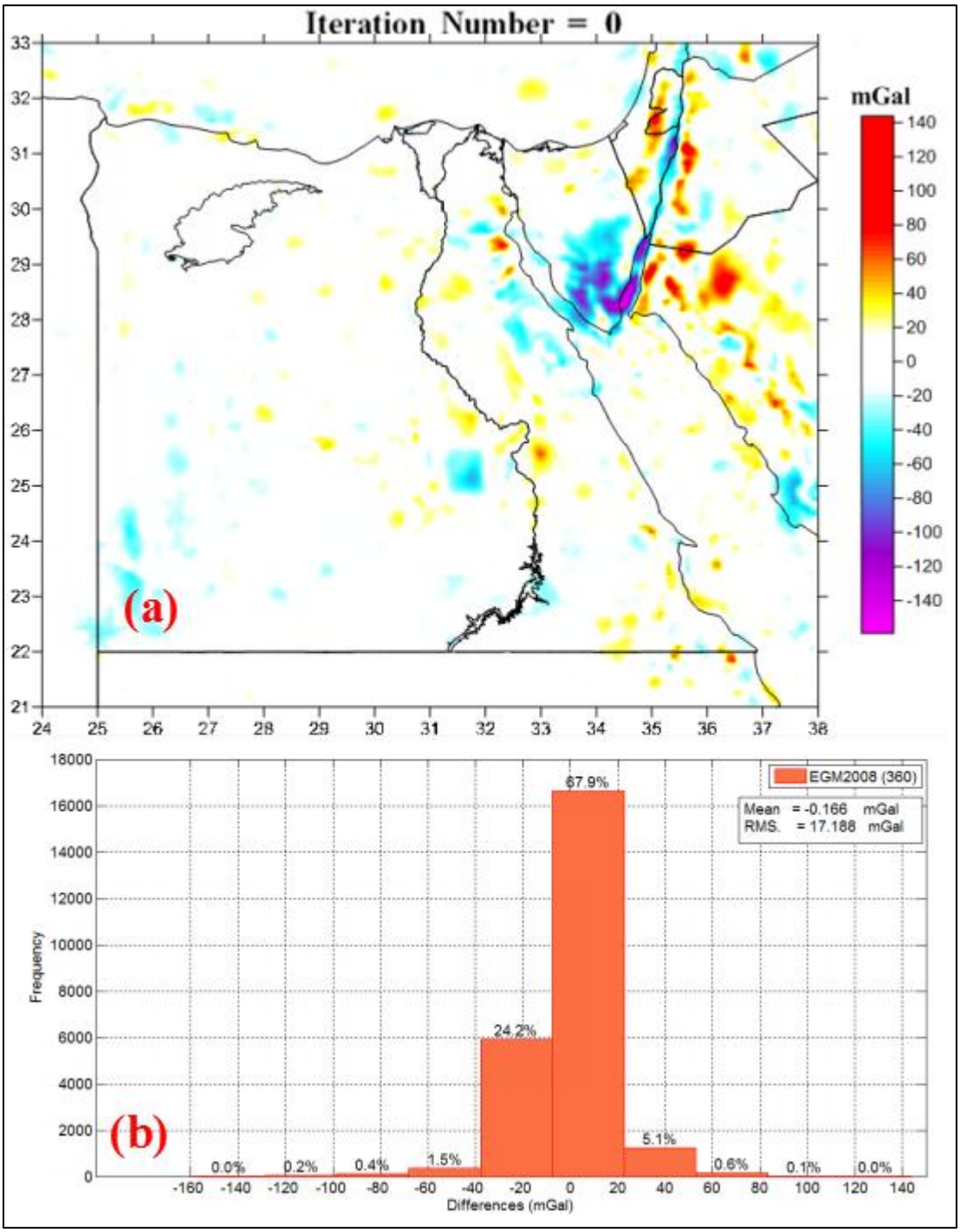

Figure (5.7): (a) Difference between The Egyptian 5′ × 5′ Mean Gravity Anomalies and The Computed Gravity Anomalies Using The Original Model EGM2008 (till degree 360) (b) Histogram of These Differences in 10 mGal bins.(Iteration Number =0)

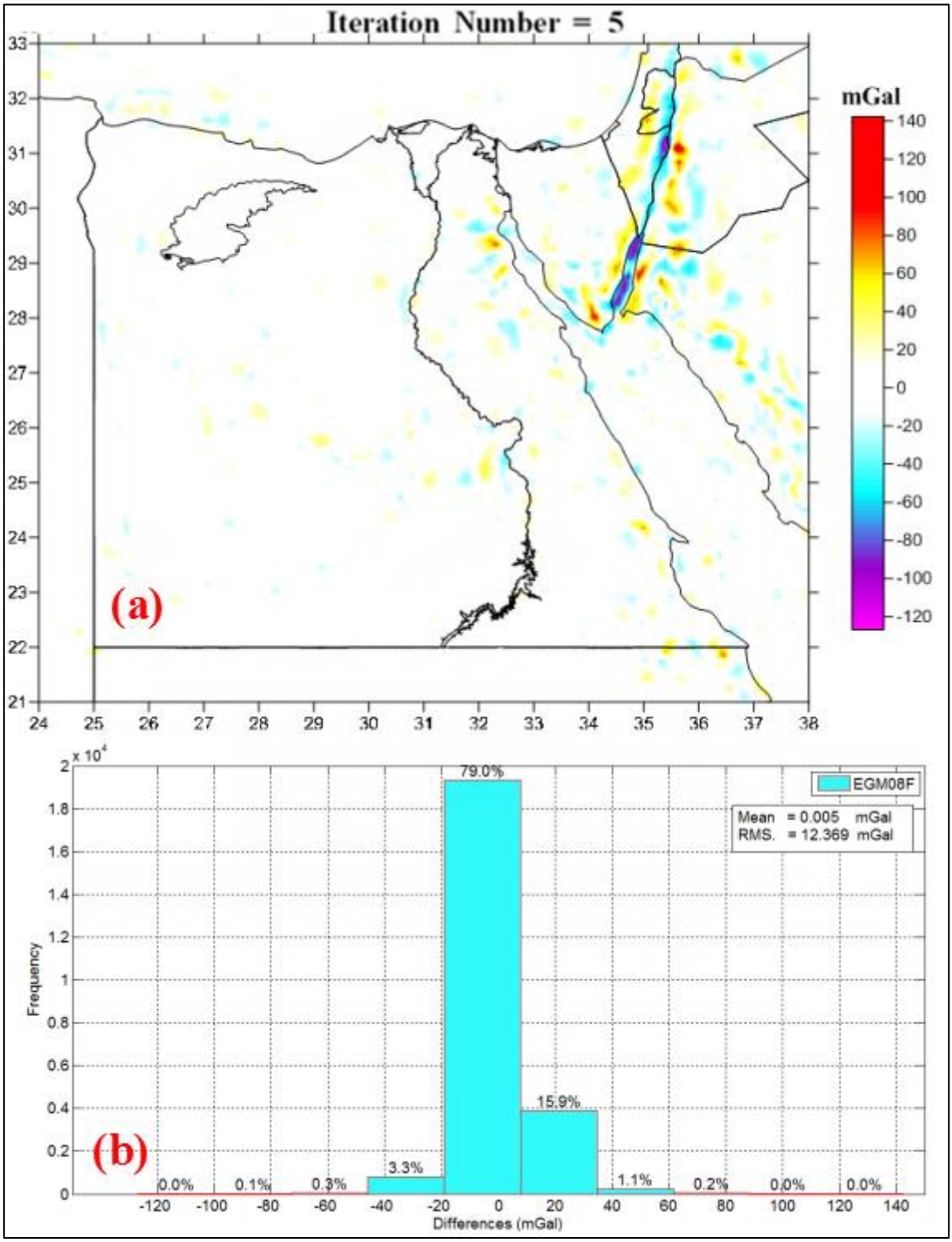

Figure (5.8): (a) Difference between The Egyptian 5′ × 5′ Mean Gravity Anomalies and The Computed Gravity Anomalies Using The EGM08F Tailored Model (b) Histogram of These Differences in 10 mGal bins.(Iteration Number =5)

Table (5.3): Statistics of The Differences of The Egyptian 5′×5′ Mean Gravity Anomalies with EGM2008 and Tailored Model EGTM0818.

Mean Free-air anomalies ($\overline{\Delta g}$)		Max. Degree.	RMS	Minimum	Maximum
NO. of values	24505		mGal	mGal	mGal
$\overline{\Delta g}$ - EGM2008		2190	12.312	-107.965	55.740
$\overline{\Delta g}$ - EGTM0818		2190	5.210	-47.002	50.856

From Tables (5.3), the comparison shows that the RMS of the differences drops from ± 12.312 mGal for EGM2008 to ± 5.210 mGal for EGTM0818 by about 58 %. This reflects that the restore to higher degrees (from n = 361 to n = 2190) increased the accuracy of tailored model EGTM0818. The results list of Tables (5.3) are shown graphically and summarized in Fig. (5.9) and Fig. (5.10).

It can be seen that the tailored geopotential model EGTM0818 gives the best results and great matching over the Egyptian territory than the original geopotential model EGM2008, where over 96 % of the Egyptian territory to within ± 10 mGal and 77 % for EGM2008.

Fig. (5.8) and Fig. (5.9) confirms the conclusion drawn in the previous section that there is the large difference in high topography regions, especially the southern part of Sinai Peninsula.

Finally, from Table (5.1), Table (5.3), and referring to Fig. (5.4) and Fig.(5.10), the comparison between both EG1GOC5s and EGTM0818 tailored geopotential model reveals a greatly better accuracy for the EGTM0818 model, where RMS of the residual mean gravity anomalies has dropped from ± 14.562 mGal for EG1GOC5s to ± 5.210 for EGTM0818 mGal by about 64.0 %. Fig.(5.11) show that the Egyptian 5′×5′ mean gravity anomalies derived by using EGTM0818 model complete to degree and order 2190.

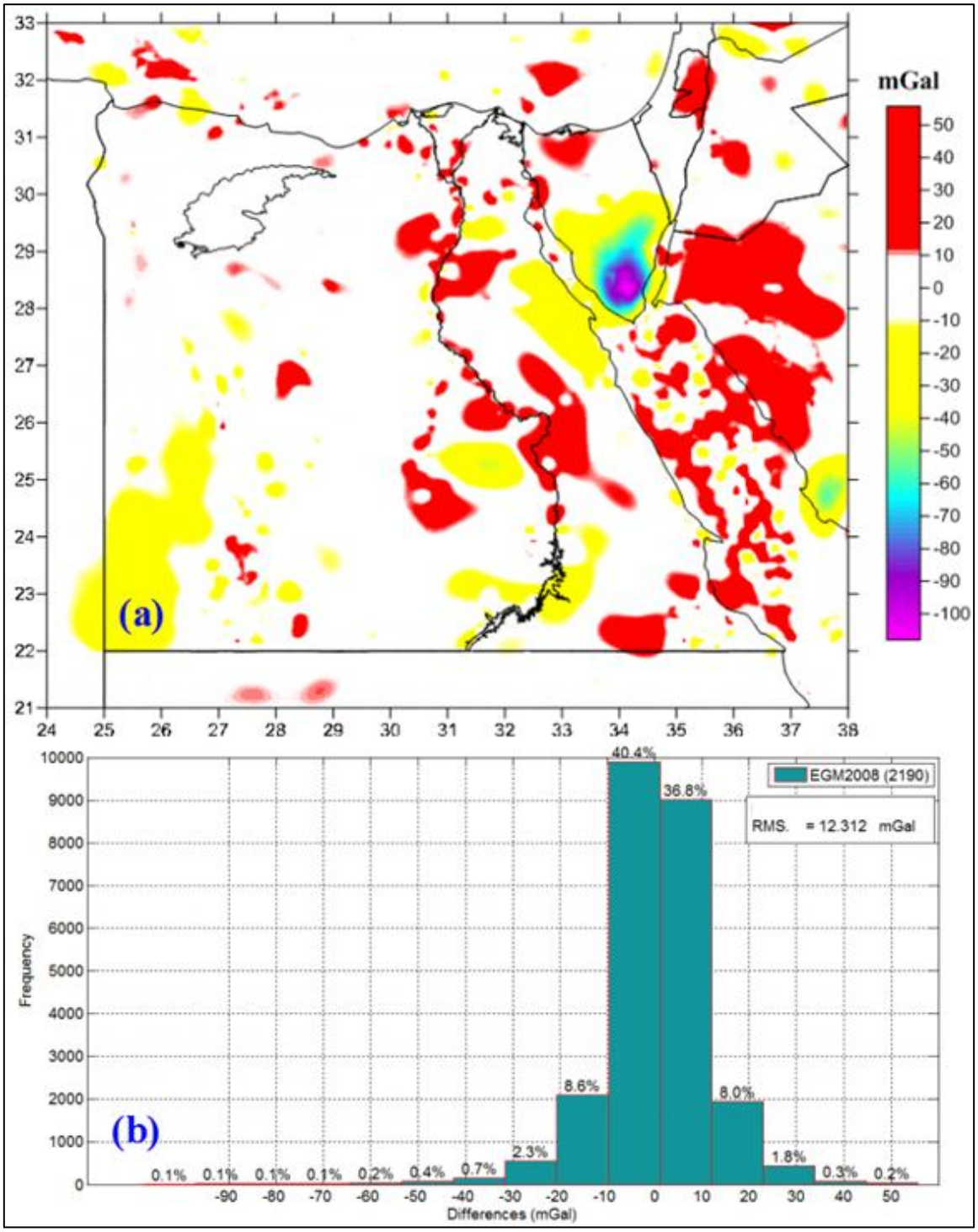

Figure (5.9): (a) Difference between The Egyptian 5′ × 5′ Mean Gravity Anomalies and The Computed Gravity Anomalies Using The Original Model EGM2008 (Max. degree. 2190) (b) Histogram of These Differences in 15 mGal bins.

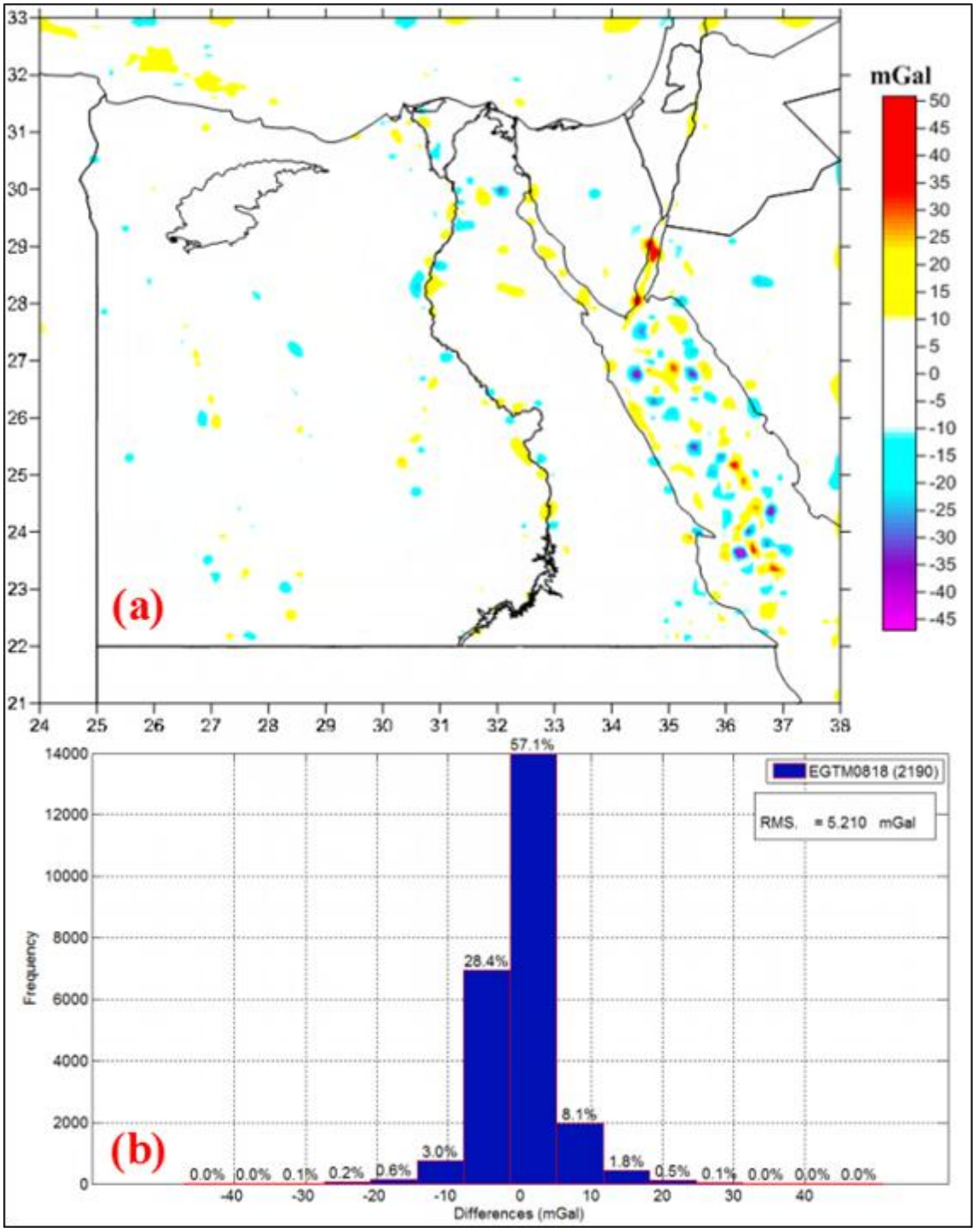

Figure (5.10): (a) Difference between The Egyptian 5′ × 5′ Mean Gravity Anomalies and The Computed Gravity Anomalies Using The EGTM0818 Tailored Model (Max. degree. 2190) (b) Histogram of These Differences in 15 mGal bins.

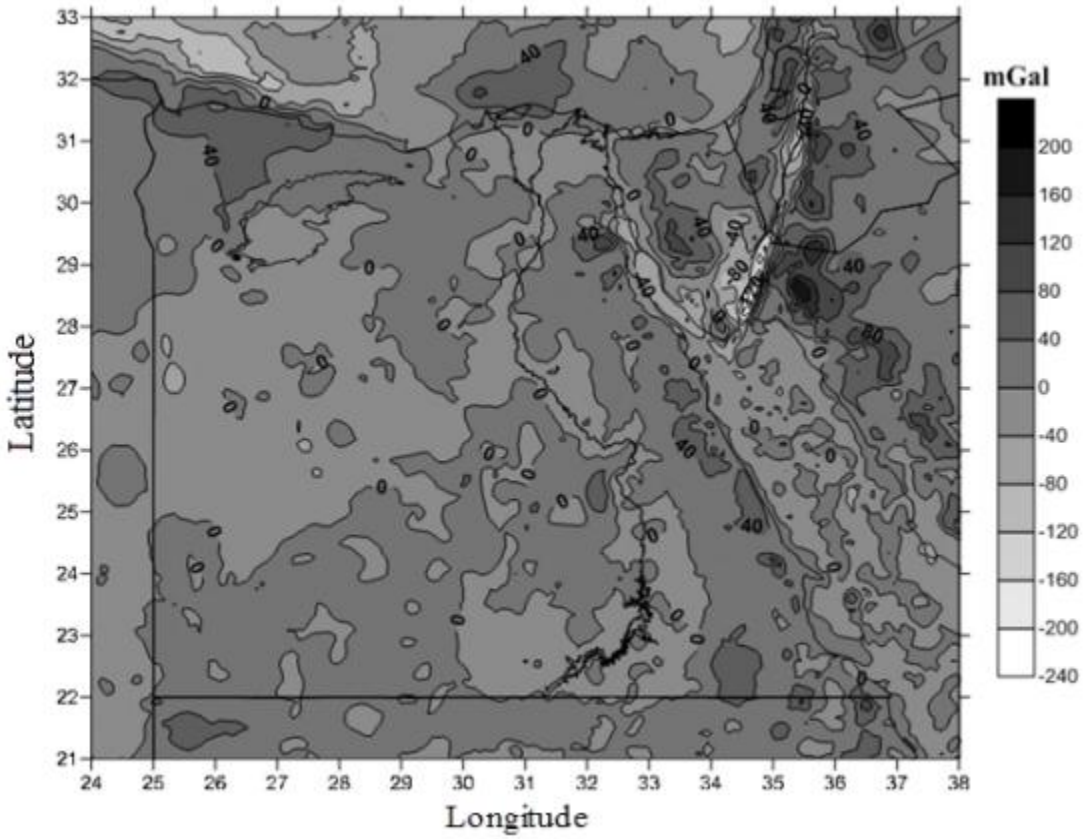

Figure (5.11): The Egyptian 5′×5′ Mean Gravity Anomalies Derived By Using EGTM0818 Model Complete to Degree and Order 2190.

5.3 Assessment of Tailored Models

The assessment of the tailored geopotential models could be made in three ways, firstly by gravity anomalies comparison, secondly by geoid model comparison (derived from the spherical harmonic coefficients of tailored geopotential models) and, thirdly geoid comparisons through GPS/levelling stations as check points.

5.3.1 Gravity Anomalies Comparison

The point gravity anomalies in Egypt (cf. Figure 4.20), 6311 gravity stations (5739 in Land and 572 at Marine), are reduced to all models: GOCO05s, EG1GOC5s, EGM2008, and EGTM0818 as given in Table (5.4). The computations were carried out using the GRAVSOFT program GEOCOL.

Table (5.4): Statistics of Residual Gravity Anomalies (6311 gravity stations) (Max. degree. in brackets)

models	Mean	Standard dev.	Minimum	Maximum	Range
	mGal	mGal	mGal	mGal	mGal
GOCO05s (280)	-1.233	11.131	-77.885	66.881	144.766
EG1GOC5s (280)	-1.603	9.241	-45.549	46.031	91.580
EGM2008 (2190)	-0.606	10.308	-45.365	43.776	89.031
EGTM0818 (2190)	-0.072	7.534	-46.188	46..431	92.619

From Table (5.4), both EG1GOC5s and EGTM0818 tailored geopotential models, give less, and better residual anomalies, reflecting the homogenization of these models on a local gravity data in Egypt.

As a result, it is obvious that the standard deviation and the range of the reduced gravity anomalies to EG1GOC5s compared with GOCO05s have been decreased by about 17% and 37%, respectively, while the standard deviation of the reduced gravity anomalies to EGTM0818 compared with EGM2008 have been dropped by about 27%. In addition, the comparison between both tailored geopotential models reveals a better accuracy for tailored geopotential model EGTM0818, where the mean value and the standard deviation of the reduced gravity anomalies to EGTM0818 have decreased by about 96% and 18%, respectively, compared with EG1GOC5s.

5.3.2 Geoid Comparison

Comparisons, using the original and tailored geopotential models, have been carried out in terms of geoid undulations or geoidal heights (N) through the following formula cf. Eq. (3.20):

$$N_{Model} = \zeta + \frac{\Delta g - 0.1119H}{\overline{\gamma}} H \qquad (5.1)$$

Where H is the elevation of the point above geoid obtained from

DTM2006.0 (cf. section 4.3.1), $\bar{\gamma}$ is the mean normal gravity value above ellipsoid , ζ and Δg corresponds to the height anomaly (quasi-geoid heights) and free-air gravity anomaly relevant to the model that are computed from Eq. (3.12) and Eq. (3.10), respectively, based on the WGS84 normal gravity field parameters.

The spherical harmonic coefficients of both original geopotential models (GOCO05s, EGM2008) and tailored geopotential models (EG1GOC5s, EGTM0818) have been used to create a 5'×5' geoid model for Egypt, as shown in Table (5.5) and (5.6). The numerical computation for Eq. (5.1) has been performed using both GRAVSOFT programs GEOCOL and N2ZETA (cf. Fig. 4.19), where the GEOCOL to defined ζ and Δg, while the program N2ZETA used to convert height anomaly to geoidal heights.

Table (5.5): Statistics of The 5'×5' Geoid Model for Egypt Relevant to Geopotential Model GOCO05s and EG1GOC5s.

Geoid model	Mean	Standard dev.	Minimum	Maximum
	m	m	m	m
N_{GOCO05s}	14.648	3.469	4.047	23.674
N_{EG1GOC5s}	14.613	3.511	4.673	24.709
Difference	0.035	1.103	-3.513	7.081

Table (5.6): Statistics of The 5'×5' Geoid Model for Egypt Relevant to Geopotential Model EGM2008 and EGTM0818.

Geoid model	Mean	Standard dev.	Minimum	Maximum
	m	m	m	m
$N_{EGM2008}$	14.648	3.495	4.065	24.521
$N_{EGTM0818}$	14.458	3.475	3.963	24.716
Difference	0.190	0.982	-3.189	5.546

The difference between both N_{GOCO05s} and N_{EG1GOC5s} geoid models as well as N_{EGM2008} and N_{EGTM0818} are shown graphically in Fig. (5.12) and Fig. (5.13), respectively.

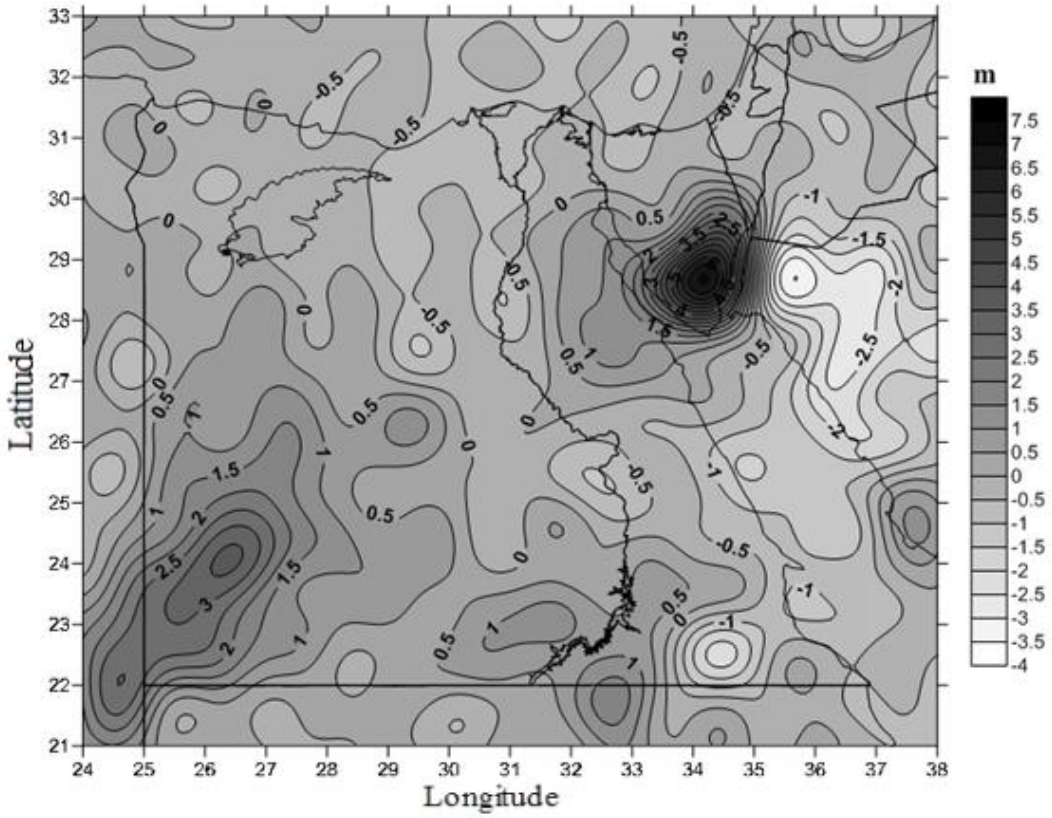

Figure (5.12): Difference between $N_{GOCO05s}$ and $N_{EG1GOC5s}$ Geoid Model for Egypt. Contour interval 0.5 m.

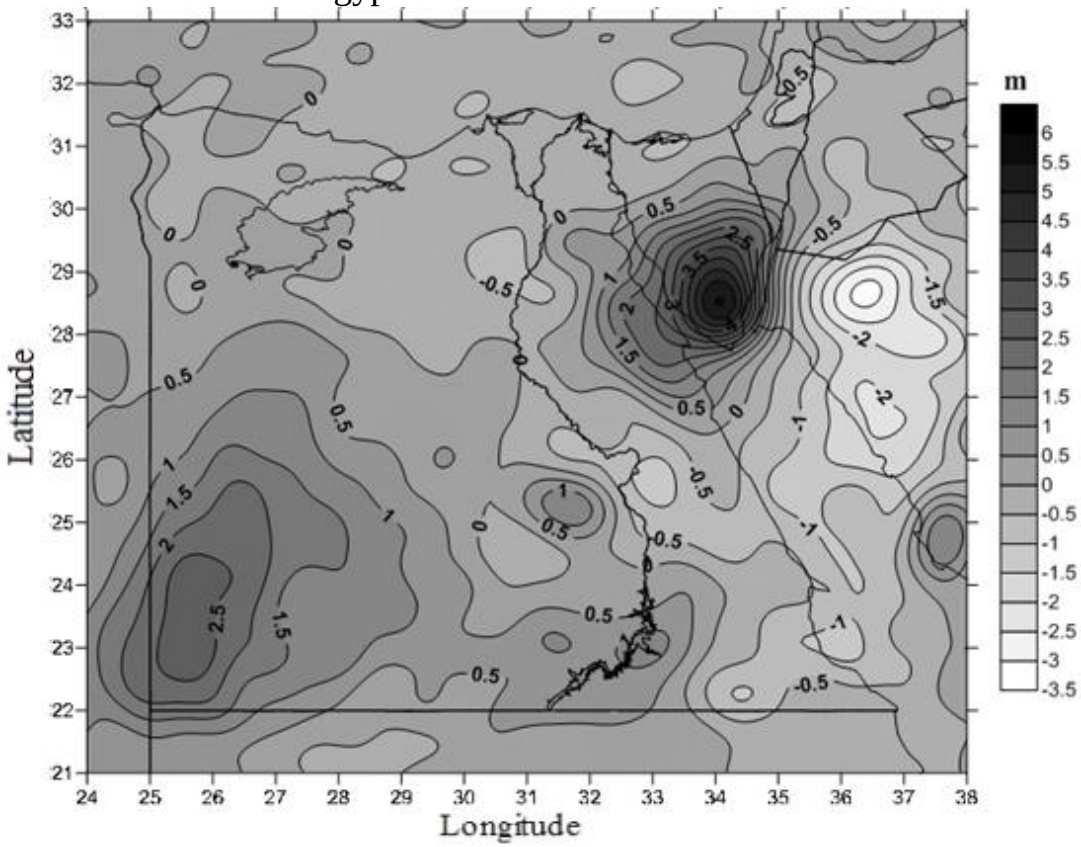

Figure (5.13): Difference between $N_{EGM2008}$ and $N_{EGTM0818}$ Geoid Model for Egypt. Contour interval 0.5 m.

The common characteristics in Fig. (5.12) and Fig. (5.13) are well demonstrated, in the two parts of the greater differences, in the southern part of the Sinai Peninsula and plateau al-Gilf al-Kebir.

These differences are due to the high topography and lack of data in these regions, which may have been affecting the computed mean free-air anomalies used for determining the global geopotential models. This has been confirmed before [cf. section 5.2, Fig. (5.3) and Fig. (5.9)].

5.3.3 GPS/levelling Comparison

The second evaluation of the tailored geopotential models is performed using GPS/leveling stations at certain points, where the geoid heights will be computed from the above geoid models (cf. Table 5.5 and 5.6) at these stations and compared against the geoid heights with respect to the GPS/levelling techniques Eq. (4.7).

This comparison has been performed using the GRAVSOFT program GEOIP (cf. Fig. 4.19) through following formula :

$$\Delta N = N_{GPS/Level} - N_{Model} \tag{5.2}$$

It is now clear that $N_{GPS/Level}$ and N_{Model} must be given in a consistent tide system (cf. section 4.8.1 and 4.8.5). Table (5.7) and Table (5.8) show that the differences (ΔN) of geoid undulations using Eq. (5.2) between the GPS/levelling surveys projects (cf. section 4.6) and those computed using GOCO05s, EG1GOC5s, EGM2008 and EGTM0818 geoid models.

Table (5.7): Differences between The Geoid Models (before and after tailored) $N_{GOCO05s}$, $N_{EG1GOC5s}$, $N_{EGM2008}$ and $N_{EGTM0818}$ to $N_{GPS/Level}$. The Results based on 9 GPS/levelling of ECAA Stations.

ECAA Stations	Differences Geoid Models			
	$\Delta N_{GOCO05s}$	$\Delta N_{EG1GOC5s}$	$\Delta N_{EGM2008}$	$\Delta N_{EGTM0818}$
	m	m	m	m
G25	-1.594	-0.406	-1.423	-0.447
B4	-1.025	-1.843	-0.718	-1.619
27DA	0.168	0.493	0.150	0.794
20CA	0.427	-0.106	0.486	0.175
N7	1.093	0.553	1.043	0.770
2AR	1.028	0.814	1.441	1.067
15CA	0.664	0.175	0.769	0.437
79AX	1.662	0.849	1.376	0.994
69DB	1.415	1.114	1.443	1.261
RMS	**1.118**	**0.868**	**1.082**	**0.942**

Table (5.8): Differences between The Geoid Models (before and after Tailored) $N_{GOCO05s}$, $N_{EG1GOC5s}$, $N_{EGM2008}$ and $N_{EGTM0818}$ to $N_{GPS/Level}$. The Results based on 17 GPS/levelling of HARN Stations.

HARN Stations		Differences Geoid Models			
Old name	New name	$\Delta N_{GOCO05s}$	$\Delta N_{EG1GOC5s}$	$\Delta N_{EGM2008}$	$\Delta N_{EGTM0818}$
		m	m	m	m
O5	OZ02	-1.281	-0.592	-1.268	-0.508
A5	OZ07	-0.671	-0.419	-0.660	-0.517
B19	OZ08	-0.297	-1.068	-0.559	-0.958
B20	OZ09	-0.839	-1.756	-0.896	-1.350
M3	OZ10	-1.212	-1.781	-0.950	-1.492
I15	OZ11	-0.122	0.292	0.071	0.493
OZ11	OZ12	2.259	1.812	2.336	1.910
T2	OZ13	-0.287	-0.480	-0.351	-0.248
B11	**OZ14***	**-4.018**	**-2.437**	**-5.000**	**-2.402**
OZ14	**OZ15***	**-6.414**	**-3.559**	**-4.972**	**-3.010**
B10	OZ16	1.139	0.773	1.591	1.349
A6	OZ17	-0.787	-0.792	-0.226	-0.288
OZ17	OZ18	0.982	0.328	0.592	0.541
E7	OZ19	1.407	0.797	1.180	0.894
D8	OZ20	1.607	1.169	1.758	1.269
X8	OZ21	1.520	1.469	1.307	1.233
Z9	OZ22	0.448	0.092	0.752	0.511
RMS		**2.125**	**1.448**	**2.015**	**1.343**

From Table (5.7) and (5.8), the result shows that, in Egypt, the geoid models N_{EG1GOC5s} and N_{EGTM0818} provide the smallest differences compared to the N_{GOCO05s} and N_{EGM2008} geoids.

Moreover, we can note that the large differences appear in stations OZ14 and OZ15, because of these stations located on in high topography regions, where station OZ14 Located on RAS-GHARIB and station OZ15 Located between the mountains and the hills of TABA. This result can be confirmed in Fig. (5.12) and Fig. (5.13), where there is the large difference at the Sinai Peninsula.

Table (5.9): show gives the statistics of the differences of geoid heights at 24 GPS/levelling of ECAA and HARN stations, after neglected stations OZ14 and OZ15 at 99% level of confidence.

Table (5.9): Statistics of The Differences at the 24 GPS/Levelling Stations of ECAA and HARN project. [Neglected: Stations OZ14 and OZ15]

Geoid model	Mean	RMS	Minimum	Maximum	Range
	m	m	m	m	m
$\Delta N_{\mathrm{GOCO05s}}$	0.321	1.132	-1.594	2.259	3.853
$\Delta N_{\mathrm{EG1GOC5s}}$	0.062	**0.996**	-1.843	1.812	3.655
$\Delta N_{\mathrm{EGM2008}}$	0.385	1.116	-1.423	2.336	3.759
$\Delta N_{\mathrm{EGTM0818}}$	0.261	**0.996**	-1.619	1.910	3.529

Form Table (5.9), it can note that the differences are still having a large offset, where the RMS nearly ± 1.00 m for N_{EG1GOC5s} and N_{EGTM0818} geoid model. The reason for the large offset is mainly from the following:-

a) The defects in the vertical datum of Egypt, where the assumption of zero-level, which is different from the global zero vertical datum due to the sea-surface topography (cf. section 2.8.3).
b) The difference in semi-major axis of the ellipsoid used to derive ellipsoidal heights from the GPS-derived Cartesian coordinates

and that of the "*ideal*" mean-Earth ellipsoid with respect to which our geoid undulations were computed.

In the following, we will describe how to remove this bias towards a precise geoid model for Egypt.

5.3.4 Fitting Geoid Models to GPS/Levelling Data

The most popular and usually best fitting method to remove the bias and tilt is considered to be the classic 4-parameter model, which was used for determining gravimetric geoid models in several countries such as Egypt (Nassar et al., 1993; Shaker et al., 1997a; Ghanem, 2001); Canada (Sideris & She, 1995); Sweden (Nahavandchi & Sjöberg, 2001); Australia (Fotopoulos et al., 2002); Great Britain (Iliffe et al., 2003) and Argentina (Pinon, 2016). The 4-parameter model is given by (Iliffe et al., 2003):

$$\varepsilon = \Delta X \cos\varphi \cos\lambda + \Delta Y \cos\varphi \sin\lambda + \Delta Z \sin\varphi + RS + \varepsilon'^{\,grid} \qquad (5.3)$$

Where the parameters ΔX, ΔY, and ΔZ corresponds to the datum shift between the two datums (Change of origin ~ first-degree term), R is the Earth radius, S is scale factor (~ Zero-degree term) and $\varepsilon'^{\,grid}$ are the residuals surface. The Cholesky decomposition (positive definite symmetric linear equations) will be used to solve the 4-parameters (ΔX, ΔY, ΔZ and S) in order to avoid the complexity of the matrix inversion and to guarantee faster solutions.

The 4-parameter model and the weighted-mean interpolation method were applied to determine the trend surface using a quadrant-based nearest neighbours search technique around a prediction point see Fig. (5.14).

The weighted-mean can be simply expressed as follows (Forsberg & Tscherning, 2008,p. 38):

$$\varepsilon'^{\,grid} = N = \frac{\sum_{i=1}^{n} \frac{N_i}{r^2}}{\sum_{i=1}^{n} \frac{1}{r^2}} \tag{5.4}$$

Where $\widetilde{N}$ denotes the estimated geoid heights at a specified location that results from the weighted sum of *n* adjacent geoid heights observations N_i and *r* is the distance between the interpolation and computation points. The inverse distance $(1/r)$ is the weighting functions.

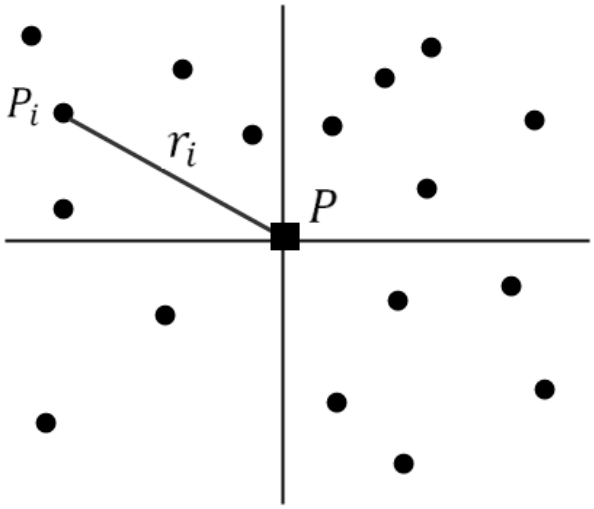

Figure (5.14): Quadrant-based Nearest Neighbours Search Technique.

Finally, the final fitted geoid is obtained by:

$$N^{Fit} = N_{Model} + \varepsilon \tag{5.5}$$

The 4-parameter model and the weighted-mean method (trend surface) are built into the GRAVSOFT program GEOGRID (cf. Fig. 4.19).

Finally, the geoids models are scaled/fitted using only 17 GPS/levelling stations derived geoid ($N_{GPS/Level}$), while 9 GPS/levelling stations were used for an external check see Figure (5.9).

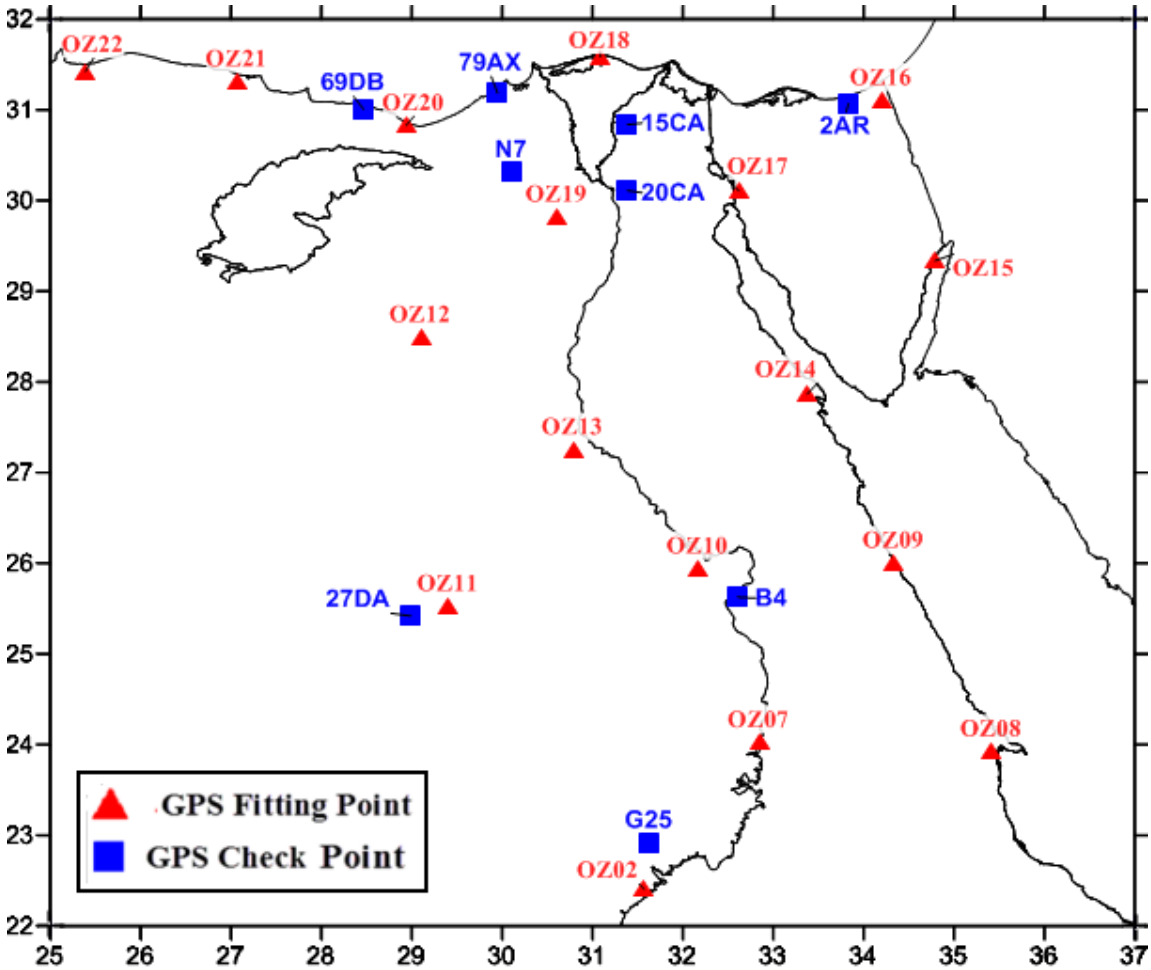

Figure (5.15): Distribution of The GPS Stations with Known Orthometric Height Used for Fitting (Triangle) and Cheek (Square) points.

Table (5.10) shows the differences between the geoid heights derived from 17 GPS/levelling stations of HARN project and those derived from the fitted geoid models after removing trend surface.

From Table (5.10), the results show that the internal precision of the fitted geoids is very good, where the RMS of the differences ± 4 mm for $N_{EG1GOC5s}$ and ± 3 mm for $N_{EGTM0818}$. This reflects that the 4-parameter model and the weighted-mean method for modelling the residuals are very well for fitting geoids to observed geoid heights derived from GPS and levelling.

Table (5.10): Differences between The Geoid Models and The 17 GPS/Levelling of HARN Stations after Removing Trend Surface.

HARN Stations		Differences Geoid Models after Fitting (Internal Accuracy)			
Old name	New name	$\Delta N_{GOCO05s}$	$\Delta N_{EG1GOC5s}$	$\Delta N_{EGM2008}$	$\Delta N_{EGTM0818}$
		m	m	m	m
O5	OZ02	-0.001	0.000	-0.001	0.000
A5	OZ07	0.001	0.002	0.002	0.001
B19	OZ08	0.003	0.003	0.003	0.001
B20	OZ09	0.003	0.001	0.003	0.001
M3	OZ10	-0.001	-0.002	0.000	-0.003
I15	OZ11	-0.001	0.000	0.000	0.001
OZ11	OZ12	0.003	0.003	0.004	0.003
T2	OZ13	0.000	-0.001	-0.001	0.000
B11	**OZ14***	**-0.013**	**-0.008**	**-0.019**	**-0.007**
OZ14	**OZ15***	**-0.017**	**-0.011**	**-0.012**	**-0.007**
B10	OZ16	0.011	0.009	0.012	0.008
A6	OZ17	0.000	-0.001	0.002	-0.001
OZ17	OZ18	0.001	0.001	0.000	0.000
E7	OZ19	0.003	0.002	0.002	0.001
D8	OZ20	0.001	0.001	0.002	0.001
X8	OZ21	0.000	0.000	0.001	0.001
Z9	OZ22	-0.004	-0.004	-0.003	-0.002
RMS		**0.006**	**0.004**	**0.006**	**0.003**

In order to validate an external check of the quality of the fitted geoid models, the 9 GPS/levelling stations were used Table (5.11), which was not used for the geoid fitting in the previous section. In addition, the EGM96 geopotential model (cf. Fig. 4.5), complete to degree and order 360, has also been used to compute geoid model for Egypt for comparison purposes.

Table (5.11): Differences between The Geoid Models and the 9 GPS/Levelling Stations of Check Points after Removing Trend Surface.

ECAA Stations	Differences Geoid Models after Fitting (External Accuracy)				
Stations Id	$\Delta N_{GOCO05s}$	$\Delta N_{EG1GOC5s}$	$\Delta N_{EGM2008}$	$\Delta N_{EGTM0818}$	ΔN_{EGM96}
	m	m	m	m	m
G25	-0.466	0.170	-0.290	0.055	0.211
B4	0.233	-0.240	0.389	-0.264	-0.229
27DA	0.052	0.083	-0.106	0.224	0.122
20CA	0.051	-0.225	0.091	-0.185	0.034
N7	-0.102	-0.188	-0.059	-0.112	-0.085
2AR	0.155	0.213	0.130	-0.082	0.256
15CA	0.221	0.059	0.384	0.060	0.189
79AX	0.574	0.162	0.309	0.129	0.234
69DB	-0.227	-0.110	-0.298	-0.045	-0.158
Mean	**0.055**	**-0.008**	**0.061**	**-0.024**	**0.064**
RMS	**0.287**	**0.172**	**0.260**	**0.149**	**0.183**
Range	**1.040**	**0.453**	**0.687**	**0.488**	**0.485**

The result of check points shows that the geoid models derived from harmonic coefficients of both tailored geopotential models give almost the same external geoid, where the RMS of the residuals ± 17 cm for $N_{EG1GOC5s}$ and ± 15 cm for $N_{EGTM0818}$. The accuracy of both $N_{EG1GOC5s}$ and $N_{EGTM0818}$ geoid models nearly the same as the reference model EGM96, where the RMS ± 18 cm for N_{EGM96}

In addition, the comparison between both $N_{EG1GOC5s}$ and $N_{EGTM0818}$ geoid models and geoid model N_{EGM96} in terms of the mean differences reveals a better accuracy for $N_{EG1GOC5s}$ geoid model, where the mean differences of check points with $N_{EG1GOC5s}$ have decreased by about 60% and 87% compared with $N_{EGTM0818}$ and N_{EGM96} geoids, respectively.

The results of Table (5.11) confirm that the Egyptian gravity data is incorporated in the development of EGM96 geopotential model (cf. section 4.2.3) and the tailored geopotential models EG1GOC5s and EGTM0818 (cf. section 5.2).

Table (5.12) shows the geoid models for Egypt relevant to the satellite-only model GOCO05s, the high degree reference model EGM2008 and their tailored versions after fitted to 17 GPS/levelling stations using the 4-parameter model and the weighted-mean method trend surface.

Table (5.12): Statistics of The 5'×5' Fitted Geoid Models for Egypt.

Fitted Geoid model	Mean	Standard dev.	Minimum	Maximum
	m	m	m	m
N_{GOCO05s}	14.409	4.237	0.959	25.076
N_{EG1GOC5s}	14.344	4.016	1.777	24.437
N_{EGM2008}	14.498	4.258	1.339	25.219
N_{EGTM0818}	14.362	1.134	-4.265	4.029

Finally, Fig. (5.16) and Fig. (5.18) show the geoid model for Egypt derived from harmonic coefficients of both EG1GOC5s and EGTM0818 tailored geopotential models, respectively, while Fig. (5.17) and Fig. (5.19) show their 3D fitted geoid model for both geoid models N_{EG1GOC5s} and N_{EGTM0818}.

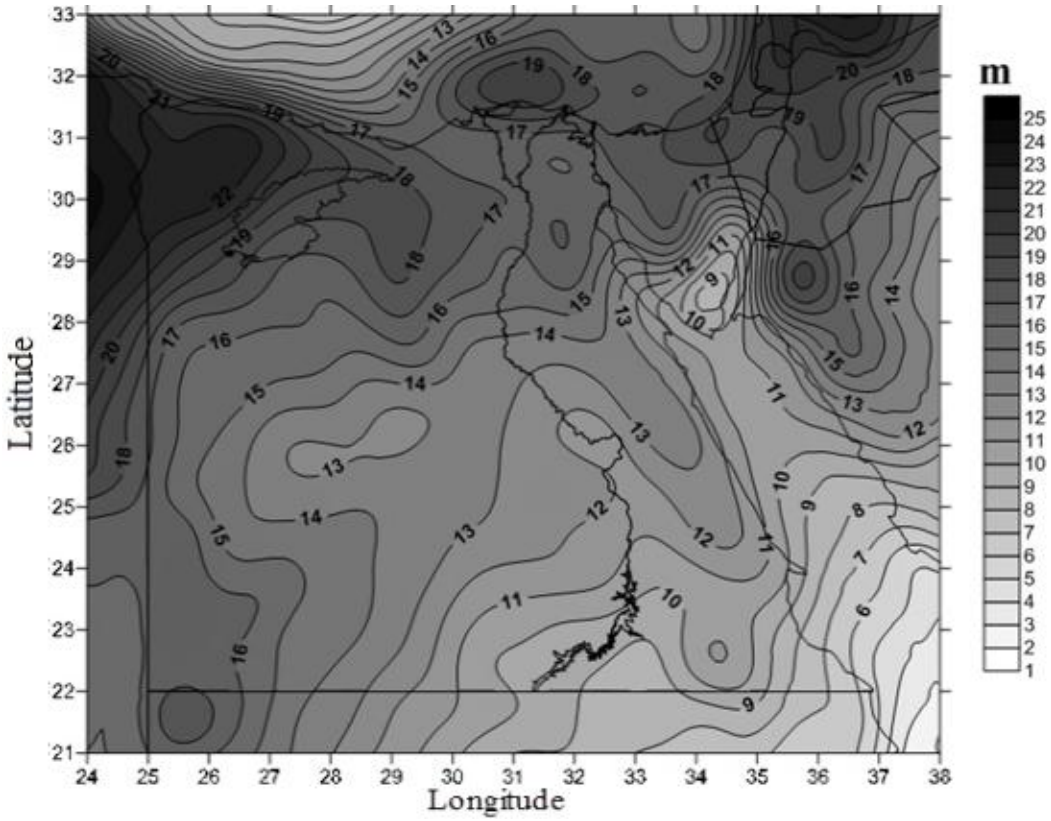

Figure (5.16): Geoid Model for Egypt Derived from Tailored Geopotential Model EG1GOC5s (till degree and order 280) after Removing Trend Surface Using The 4-parameter Model and The Weighted-Mean. Contour interval 1.0 m.

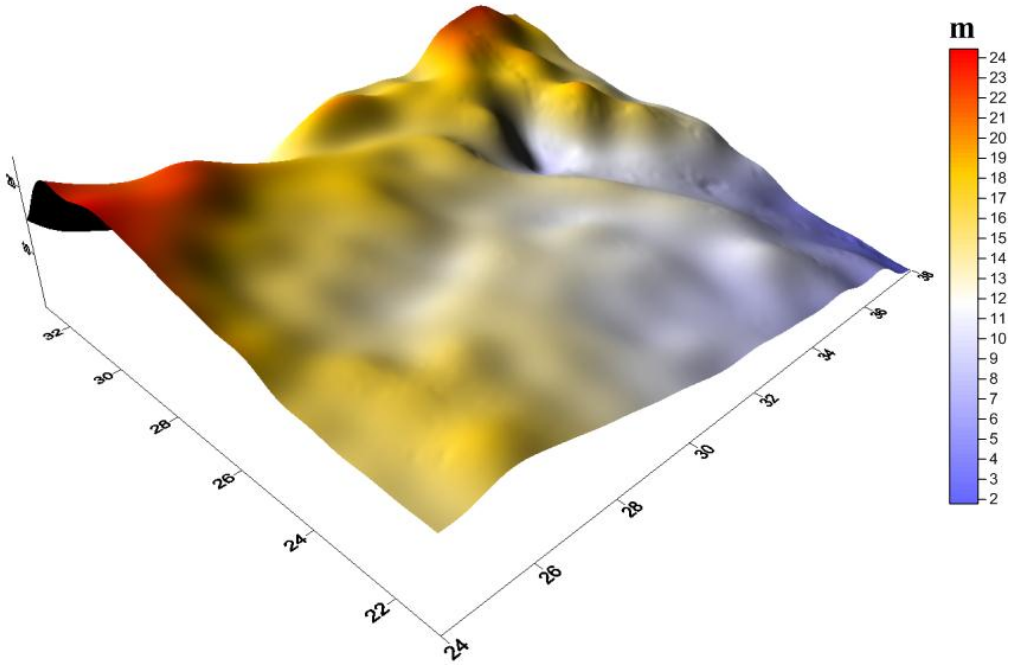

Figure (5.17): 3D - Fitted Geoid Model for Egypt Derived from Tailored Geopotential Model EG1GOC5s.

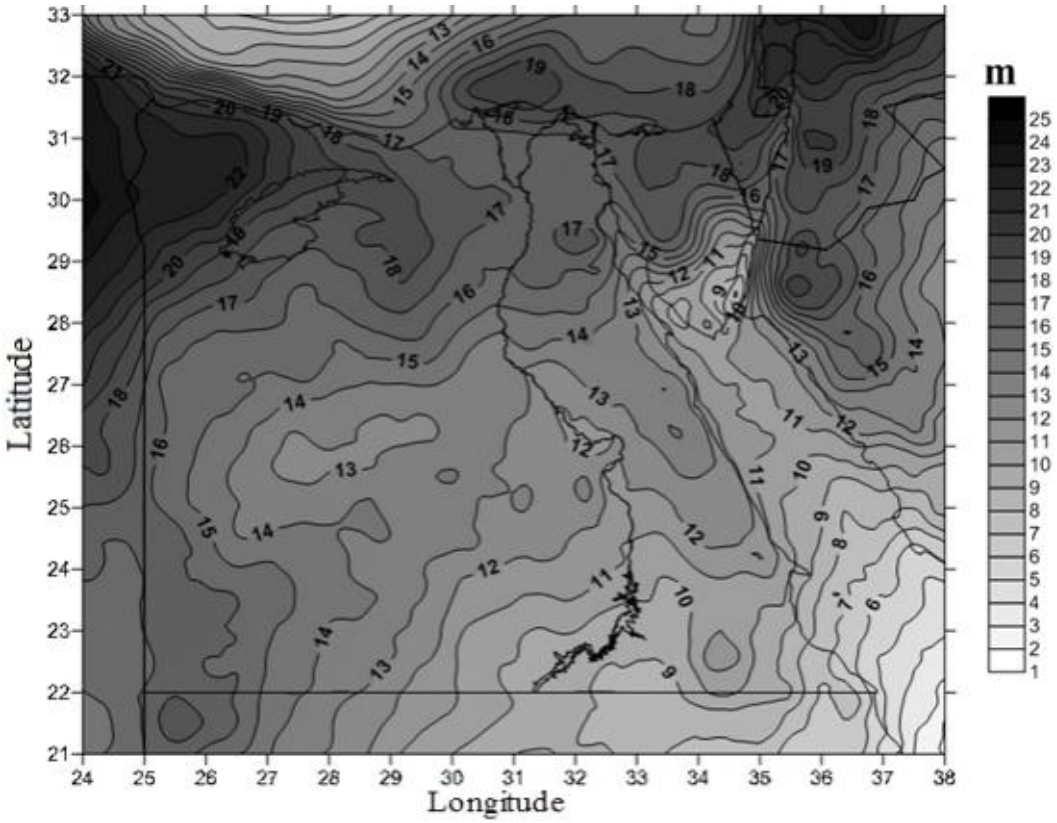

Figure (5.18): Geoid Model for Egypt Derived from Tailored Geopotential Model EGTM0818 (till degree and order 2190) after Removing Trend Surface Using The 4-parameter Model and The Weighted-Mean. Contour interval 1.0 m.

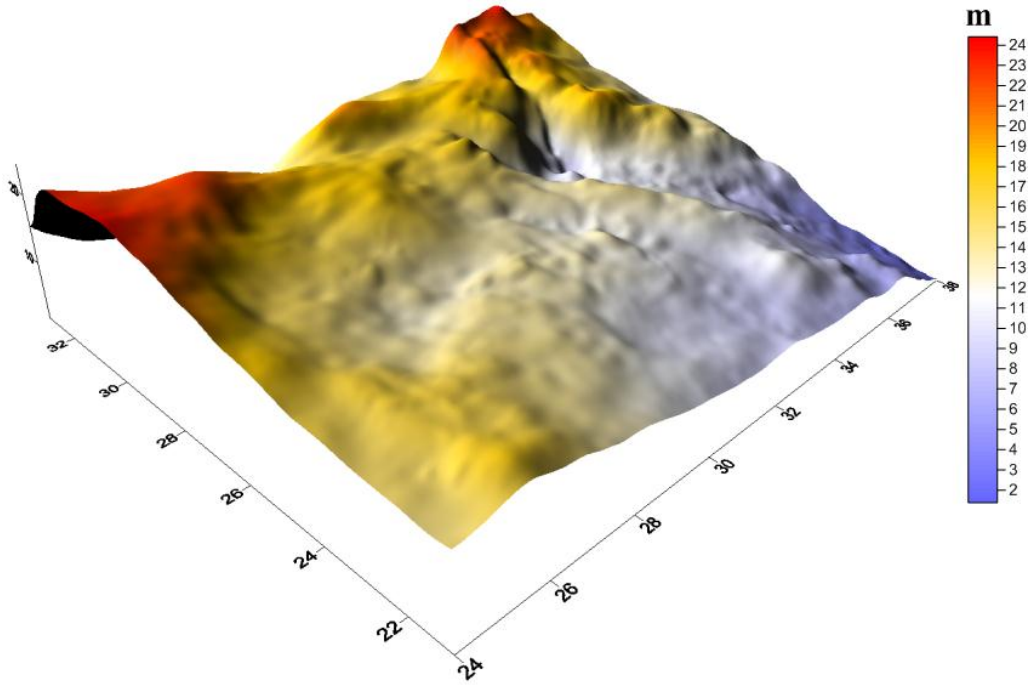

Figure (5.19): 3D - Fitted Geoid Model for Egypt Derived from Tailored Geopotential Model EGTM0818.

The following flowchart Fig. (5.20) summarizes the main procedures performed in the previous section for the generation of the fitted geoid model.

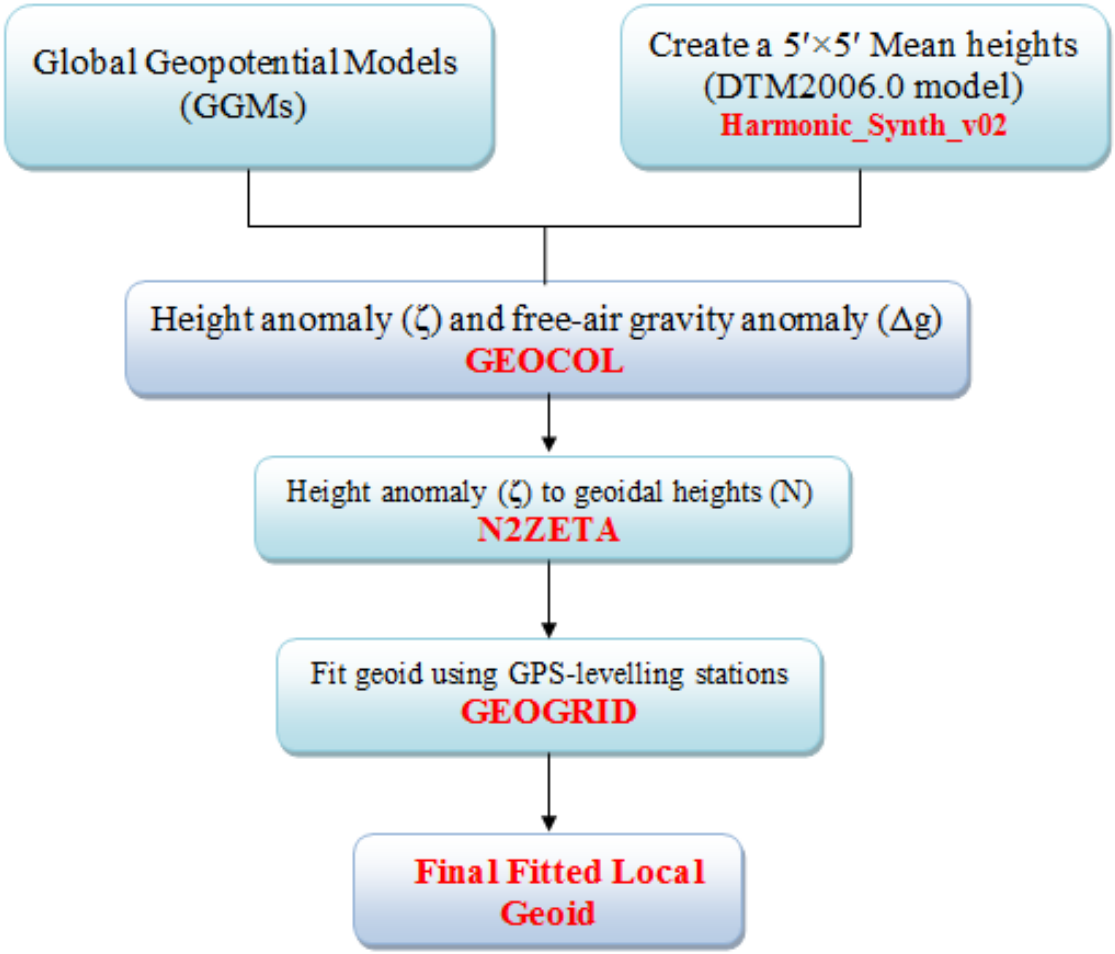

Figure (5.20): The Main Procedure of Geoid Modelling from Global Geopotential Harmonic Models.

5.4 High Precision Geoid Derived from Heterogeneous Data

The following geoid computation is done using gravity data and a combination of gravity and astrogeodetic data for high precision geoid determination of Egypt by using 3D Least-Squares Collocation (3D LSC), where 3D LSC is the most commonly used method for the combination of heterogeneous data. When using the 3D LSC for geoid determination, all quantities must be related to points outside the masses (Molodensky approach). Therefore, the quasi-geoid is to be evaluated at the surface of the Earth and then the quasi-geoid converts to geoid (cf. section 3.3.1).

Thus, the general methodology for geoid determination by 3D LSC is as follows (Tscherning, 2013), after a simple modification:-

a) *Transform* all data to a global geodetic datum (here, WGS84)
b) Make a homogeneous *selection* of the data to be used for geoid determination
c) Use the *remove-restore method*, where to remove the effect of a global Earth gravity field model (EGM) and remove the effect of the topography from the data. This will produce what we will call *residual data*.
d) Estimate the *empirical covariance* function for the residual data in the region in question.
e) Determine an *analytic* representation of the empirical covariance function.
f) Determine using 3D LSC a residual gravity field approximation, and then compute estimates of the residual *height* and *gravity* anomalies and their *errors* at the surface of the Earth. Check for *gross-errors* (make a contour map of data); verify error estimates of residual height anomalies.

g) If the error is too *large*, and more data is available, *add* new data and repeat step (f).
h) *Restore* again the effect of the EGM and of the topography step (c) in terms of residual quantities.
i) *Convert* height anomalies to *geoid heights*.
j) The resulting geoid heights were *scaled/fitted* to GPS/levelling points
k) An external *check* of geoid model, by comparison with data not used to obtain the model.

The first step for geoid solutions is to be select the area (a grid) in which the quasi-geoid is to be computed, where the quasi-geoid is to be evaluated at the surface of the Earth, so the grid must be extracted from a Digital Terrain Model (DTM). Here we will use the 5′ arc-minute of DTM2006.0 (Elevation for marine areas = 0) for the window of $21^{\circ} \leq \varphi \leq 33^{\circ}$ and $24^{\circ} \leq \lambda \leq 38^{\circ}$.

5.4.1 Remove-restore procedure

The gravimetric or a combined geoid solution is done by the well-known remove-restore technique (Forsberg, 1984). For example (remove step), in the case of gravity anomalies (Δg), the residual gravity anomalies (Δg_{res}), which represent a smooth field, are computed by:

$$\Delta g_{res} = \Delta g - \Delta g_{EGM} - \Delta g_{RTM} \tag{5.6}$$

Where Δg_{EGM} is the effect of the reference field (global Earth gravity field model) on the gravity anomalies (*long wavelength part*), and Δg_{RTM} is the terrain correction using the Residual Terrain Model (RTM) (cf. equation 2.23), i.e. the deviations of the topography from a mean height surface, which is a function of the mass (*density*) distribution of the topography (*short wavelength part*).

Since the amount of the terrain correction is usually much less. Even for mountains 3000 m in height, the terrain correction is only of the order of 50 mGal (e.g., Heiskanen & Vening Meinesz, 1958, p. 154). Therefore, in the following geoid solutions, we neglect the short wavelength part, which is due to topography, for the following reasons:-

a) The RTM is depending on whether the topography of an area is above or below the reference elevation surface (cf. section 2.4.4).
b) The topography of Egypt is not high except the Sinai Peninsula and plateau al-Gilf al-Kebir (cf. Figure 4.6).

Hence, both tailored geopotential models were used to compute the short to long wavelength part of the gravity anomalies in the remove-restore procedure. Finally, Eq. (5.6) can be expressed by:

$$\Delta g_{res} = \Delta g - \Delta g_{Tailored\ EGM} \tag{5.7}$$

Thus, the reduced deflections of the vertical can be expressed by:

$$\begin{aligned} \xi_{res} &= \xi - \xi_{Tailored\ EGM} \\ \eta_{res} &= \eta - \eta_{Tailored\ EGM} \end{aligned} \tag{5.8}$$

Note that: when deflections of the vertical are evaluated using a Global Geopotential Model (GGM), they are computed as the spatial angles between the gravity vector computed from GGM model and the normal field gravity vector at the surface of the Earth (Tscherning, 2013). In spherical approximation we obtain the deflections of the vertical from GGM as (Torge, 2001, p. 258):

$$\xi = -\frac{1}{\gamma \cdot r}\frac{\partial T}{\partial \varphi} \qquad \eta = -\frac{1}{\gamma \cdot r \cos\theta}\frac{\partial T}{\partial \lambda} \tag{5.9}$$

For the following geoid solutions only a subset of the terrestrial gravity anomalies Table (4.9), is used. A set of 3587 terrestrial gravity points were selected with a mean distance of 1 km using the GRAVSOFT program *SELECT* (cf. Fig. 4.19). In addition, a set of 572 marine gravity

points, 141 points meridian deflection of the vertical (ξ) and 14 points prime-vertical deflections (η) were added. Tables (5.13) and (5.14) show the statistics for the reduction process (without RTM reductions) for gravity anomalies (3587+572 = 4159 points) and the deflection components, respectively. The computations were carried out using GRAVSOFT program GEOCOL.

Table (5.13): Statistics of Residual Gravity Anomalies Using The Tailored Geopotential Models EG1GOC5s and EGTM0818.

Gravity anomalies		Max. Degree.	Mean	Standard dev.	Minimum	Maximum
NO. of points	4159		mGal	mGal	mGal	mGal
Δg			0.415	16.110	-81.669	76.124
Δg - EG1GOC5s		280	-2.068	9.916	-45.549	46.031
Δg - EGTM0818		2190	-0.077	7.978	-42.857	40.881

Table (5.14): Statistics of Residual Deflection of The Vertical Using The Tailored Geopotential Models EG1GOC5s and EGTM0818.

Meridian deflection (*Ksi*)	Max. Degree.	Mean	Standard dev.	Minimum	Maximum
		arcsec	arcsec	arcsec	arcsec
ξ (141)		1.981	4.926	-9.545	16.508
ξ - EG1GOC5s	280	-0.642	2.675	-8.677	6.724
ξ - EGTM0818	2190	-0.337	1.859	-5.129	4.946
Prime-vertical deflection (*Eta*)	Max. Degree.	Mean	Standard dev.	Minimum	Maximum
		arcsec	arcsec	arcsec	arcsec
η (14)		-0.679	5.443	-8.044	8.241
η - EG1GOC5s	280	-1.464	3.165	-7.617	1.290
η - EGTM0818	2190	-1.458	2.929	-7.077	2.434

After the remove-step, the residual height anomalies, as well as residual gravity anomalies, are estimated at the surface of the Earth from the residual gravity Table (5.13) or a combining between a residual gravity

anomalies and deflections of the vertical Table (5.14). Then, the effects removed are restored again as follows:

$$\zeta^{grid} = \zeta^{grid}_{res} + \zeta^{grid}_{Tailored\ EGM}$$
$$\Delta g^{grid} = \Delta g^{grid}_{res} + \Delta g^{grid}_{Tailored\ EGM} \quad (5.10)$$

Where $\zeta^{grid}_{Tailored\ EGM}$ and $\Delta g^{grid}_{Tailored\ EGM}$ are the contribution of the tailored geopotential models computed using the GRAVSOFT program GEOCOL. Finally, the conversion of height anomalies to geoid heights made by GRAVSOFT program N2ZETA.

In the following, the estimation was done by using 3D LSC, where residual terrestrial gravity anomalies are used to determine the parameters of the covariance function. This covariance function is used to compute a gravimetric geoid as well as a combination of astrogeodetic and gravimetric geoid solution.

5.4.2 Covariance Function Estimation

The residual terrestrial gravity anomalies were used as input to the GRAVSOFT program EMPCOV for empirical covariance function estimation using Eq. (2.37). An optimum spherical distance (ψ) has been considered to be 2.5 arc-minute for better correlation based on the spacing of data. The empirical local covariance function then fitted to analytically model using Eq. (3.58) through the GRAVSOFT program COVFIT.

In the calculations, we have used the error gravity anomaly degree-variances σ_i^{err} (*Express how much gravity anomaly power is left to a certain degree after having subtracted the geopotential model*) for maximal degree 280 and 700 degree for GOCO05s and EGM2008, respectively, according to the *maximal degree for empirical degree-variances*, which may be evaluated approximately using Eq. (2.42).

The error degree-variances are computed by using Eq. (2.35) and the FORTRAN GRAVSOFT program *degv.for*. The output of the program *degv.for* called GOCO05s.edg and EGM2008.edg. In addition, the covariance will be regarded as referring to the mean height, which for the Egyptian gravity data is approximately 360 m using DTM2006.0 (land only).

When using the GRAVSOFT program COVFIT, the three covariance parameters α, A and R_B are given firstly approximate values see Eq. (3.58), and then using an iteration non-linear adjustment to determine the final parameters for covariance function (e.g., Knudsen, 1988). Table (5.15) shows the resulting in the final parameters, after fitting the empirical covariance function to analytic Tscherning /Rapp (1974) model and Fig. (5.21) shows the empirical and analytic fitted covariance functions.

Table (5.15): The Fitted Covariance Function Parameters for The Egyptian Terrestrial Gravity Anomalies minus Tailored Models (3587 points).

Parameters	Residual gravity anomalies		Unit
	EG1GOC5s	EGTM0818	
Scale factor (α)	0.29	1.38	unitless
Radius of Bjerhammar-sphere (R_B)	-0.760	-0.478	km
Variance of gravity at zero height (A)	84.91	51.07	$mGal^2$
Maximal degree	280	700	unitless
Iteration No.	8	4	unitless

Now all tools available for using 3D LSC for geoid solutions; the residual quantities, the covariance function, and the predictions surface area. The rest is to establish the normal equations Eq. (3.52) and compute predictions and error estimates, Eq. (3.53) and (3.56) without parameters (*X*) i.e. the output of 3D LSC called *absolute solution*. This may be done using GRAVSOFT program GEOCOL.

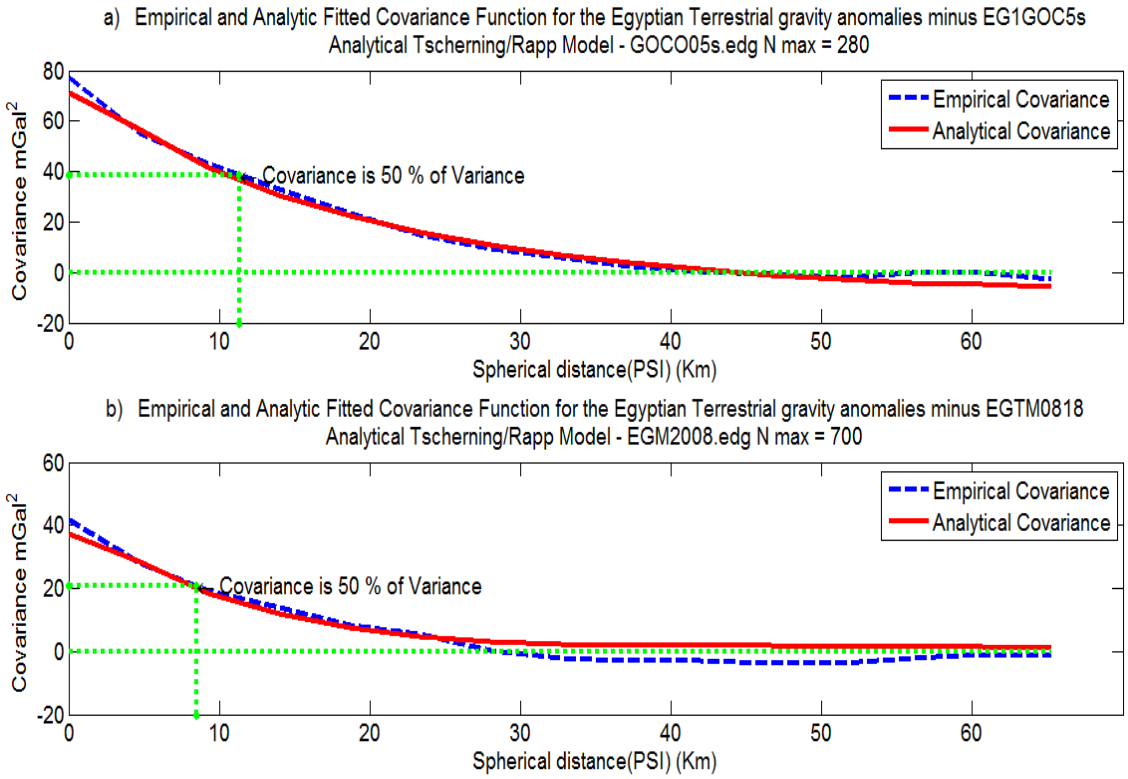

Figure (5.21): Empirical and Analytic Fitted Covariance Function for Egyptian Terrestrial Gravity Anomalies minus Tailored Geopotential Models a) EG1GOC5s and b) EGTM0818.

From Fig. (5.21), it shows that the used fitting technique of the empirical covariance function works best when using the tailored model EG1GOC5s.

5.4.3 Gravimetric Geoid Solution for Egypt

The gravimetric geoids are computed for Egypt using gravity data only. This is obtained by after the following steps:-

a) Estimate, from reduced gravity anomalies to both EG1GOC5s and EGTM0818 tailored geopotential models Table (5.13), the residual height anomalies as well as residual gravity anomalies at the surface of the Earth and their errors. All gravity anomalies were assigned an average standard error about 0.2 mGal with respect to the accuracy given in Table (4.7).

b) Restoring the removing effect of both tailored geopotential models to the predicted residual height/gravity anomalies Eq. (5.10) using the GRAVSOFT program FCOMP (cf. Fig. 4.19).

c) The conversion of height anomalies (ζ) to geoid heights (N) made by using Eq. (3.20) through the GRAVSOFT module N2ZETA.

d) The generated gravimetric geoids for Egypt will be called $N_{\text{GRAV-A}}$ and $N_{\text{GRAV-B}}$ according to use both EG1GOC5s and EGTM0818 tailored geopotential models in remove-restore technique, respectively.

e) Finally, the gravimetric geoids are scaled/fitted using only 17 GPS/levelling stations derived geoid $N_{\text{GPS/Level}}$, while 9 GPS/levelling stations were used for an external check (cf. Figure 5.14). The 4-parameter model and the weighted-mean interpolation approach have been used to remove a trend surface (cf. section 5.3.4).

Table (5.16) shows the comparison between both $N_{\text{GRAV-A}}$ and $N_{\text{GRAV-B}}$ gravimetric geoids and 17 GPS/ levelling Stations. Note that: in general when the gravimetric geoid is compared to a surface constructed from GPS and levelling, one will often note that the two surfaces disagree. Frequently they are related to a height bias or tilt East and West see e.g. (Jiang & Duquenne, 1996; Tscherning, 2002).

Table (5.16): Statistics of The Differences at The 17 GPS Stations Used for The Geoid Fitting before Removing Trend Surface.

Geoid type	Mean	RMS	Minimum	Maximum	Range
	m	m	m	m	m
$\Delta N_{\text{GRAV-A}}$	-0.311	1.354	-3.211	1.829	5.04
$\Delta N_{\text{GRAV-B}}$	-0.154	1.398	-3.254	1.929	5.183

The results lists of Table (5.16) are shown graphically in Fig. (5.22) and Fig. (5.23).

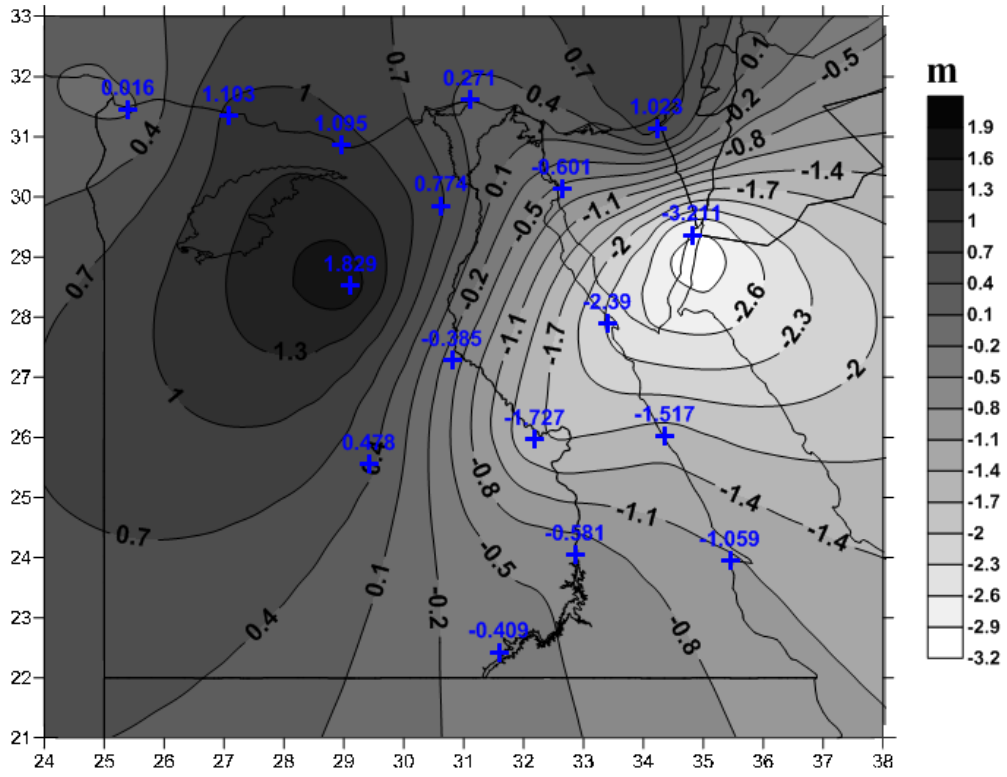

Figure (5.22): Difference in Geoid Heights between The Gravimetric Geoid N_{GRAV-A} and The GPS/Levelling Geoid before Removing Trend Surface. Contour interval = 30 cm.

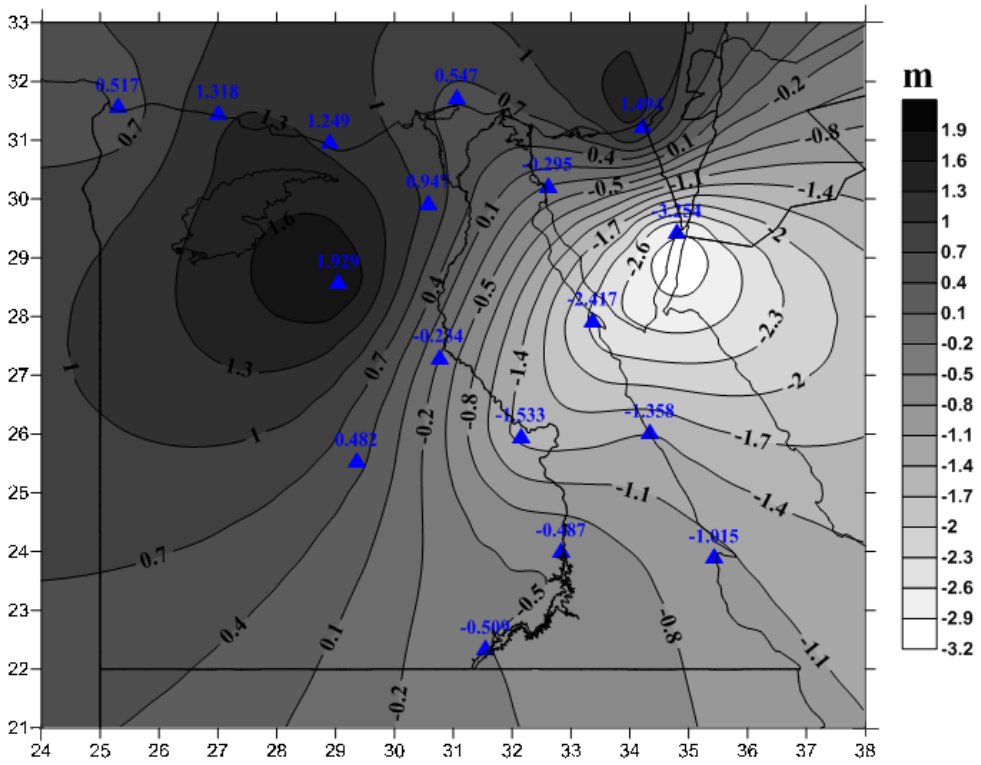

Figure (5.23): Difference in Geoid Heights between The Gravimetric Geoid N_{GRAV-B} and The GPS/Levelling Geoid before Removing Trend Surface. Contour interval = 30 cm.

The common characteristics in Fig. (5.22) and Fig. (5.23) are well demonstrated, where the larger values found in the high East/West parts of Egypt. In addition, the structure of both differences shows non-linear character.

Therefore, these differences are modelled by a four parameter model and the weighted-mean interpolation (cf. section 5.3.4), in order to fits the gravimetric geoids to the vertical datum of Egypt. Table (5.17) shows the statistics of the remaining differences after removing trend surface. This represents an internal check of the quality of the gravimetric geoids. In addition, Table (5.18) shows the statistics of the differences after removing the trend surface at 9 GPS/levelling check points, which were not used for the geoid fitting.

Table (5.17): Statistics of The Differences at The 17 GPS Stations Used for The Geoid Fitting after Removing Trend Surface.

Geoid type	Mean	RMS	Minimum	Maximum	Range
	m	m	m	m	m
$\Delta N_{\mathrm{GRAV-A}/Fit}$	0.000	0.004	-0.008	0.009	0.017
$\Delta N_{\mathrm{GRAV-B}/Fit}$	0.000	0.004	-0.008	0.009	0.017

Table (5.18): Statistics of The Differences at The 9 GPS Stations Used for The External Checking Points after Removing Trend Surface.

Geoid type	Mean	RMS	Minimum	Maximum	Range
	m	m	m	m	m
$\Delta N_{\mathrm{GRAV-A}/Fit}$	-0.034	0.129	-0.191	0.173	0.363
$\Delta N_{\mathrm{GRAV-B}/Fit}$	-0.042	0.152	-0.276	0.217	0.493

Table (5.17) shows that the gravimetric geoids for Egypt have the same trend as shown in Fig. (5.22) and Fig. (5.23). The internal precision of the fitted gravimetric geoids is very good within RMS = ± 4 mm. The comparison between both gravimetric geoids reveals a better accuracy for the gravimetric geoid $N_{\mathrm{GRAV\text{-}A}}$, where the RMS and the range of the

remaining differences have decreased by about 15% and 26%, respectively, compared with the gravimetric geoid $N_{\text{GRAV-B}}$ as given in Table (5.18).

Finally, Table (5.19) and Table (5.20) shows the statistics of both gravimetric geoids for Egypt. The associated error estimates of both gravimetric geoids given by using Eq. (3.56).

Table (5.19): Statistics of Gravimetric Geoid $N_{\text{GRAV-A}}$ for Egypt.

Geoid type	Mean	Standard dev.	Minimum	Maximum
	m	m	m	m
$N_{\text{GRAV-A}}$	14.403	3.945	2.256	24.260
Error-estimates	0.100	0.024	0.011	0.126

Table (5.20): Statistics of Gravimetric Geoid $N_{\text{GRAV-B}}$ for Egypt.

Geoid type	Mean	Standard dev.	Minimum	Maximum
	m	m	m	m
$N_{\text{GRAV-B}}$	14.408	3.978	1.708	24.452
Error-estimates	0.099	0.020	0.022	0.118

In addition, the results listed in Table (5.19) and Table (5.20) is shown graphically in Fig. (5.24) and (5.25), respectively. The error estimates of both gravimetric geoids are too large in the area no coverage gravity data see Fig. (5.26) and Fig. (5.27).

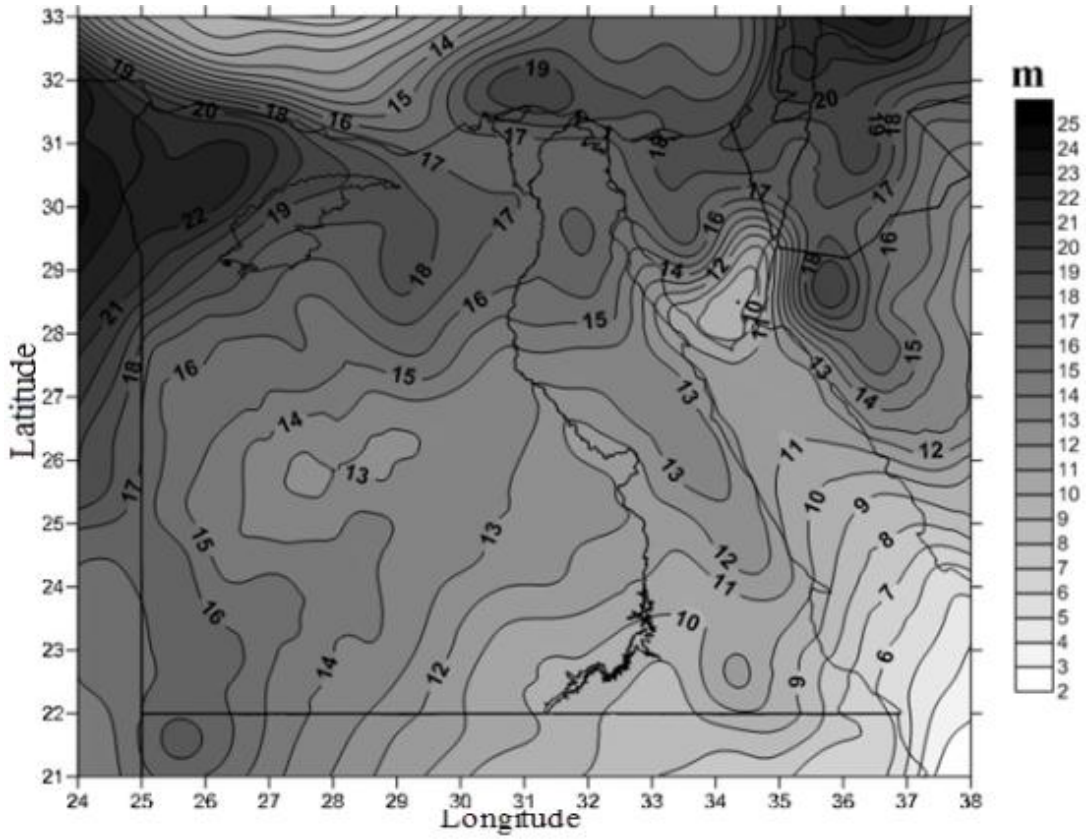

Figure (5.24): Gravimetric Geoid $N_{GRAV\text{-}A}$ for Egypt. Contour interval 1.0 m.

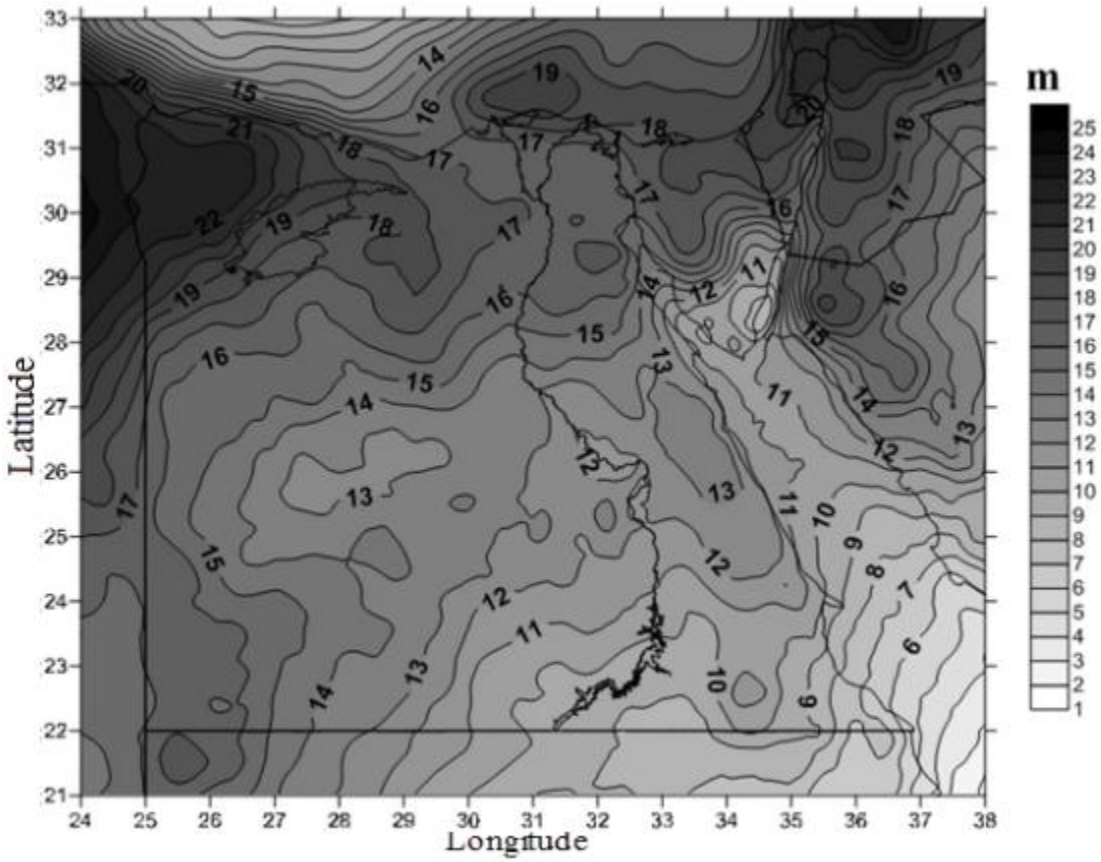

Figure (5.25): Gravimetric Geoid $N_{GRAV\text{-}B}$ for Egypt. Contour interval 1.0 m.

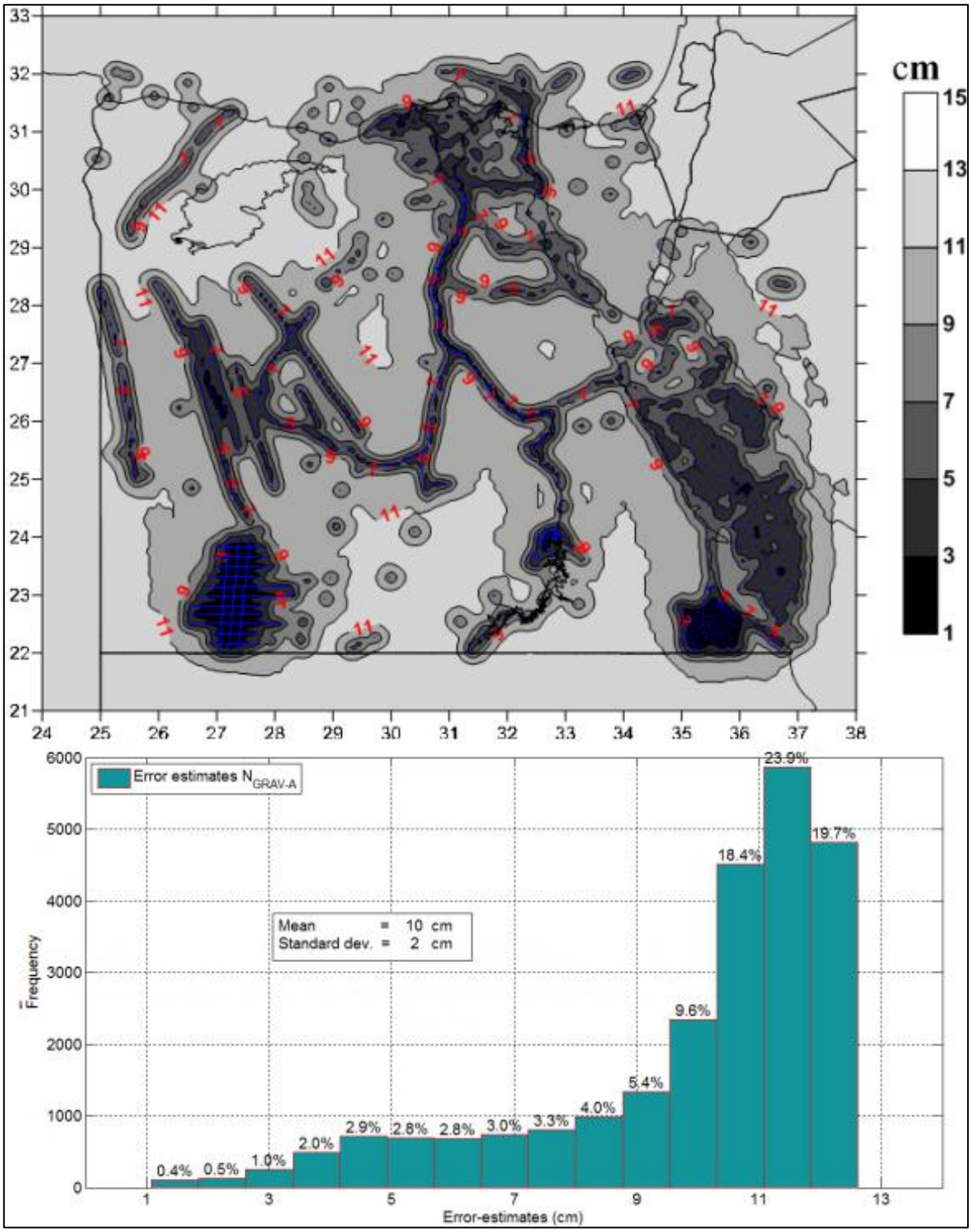

Figure (5.26): Error Estimates of Gravimetric Geoid $N_{\text{GRAV-A}}$

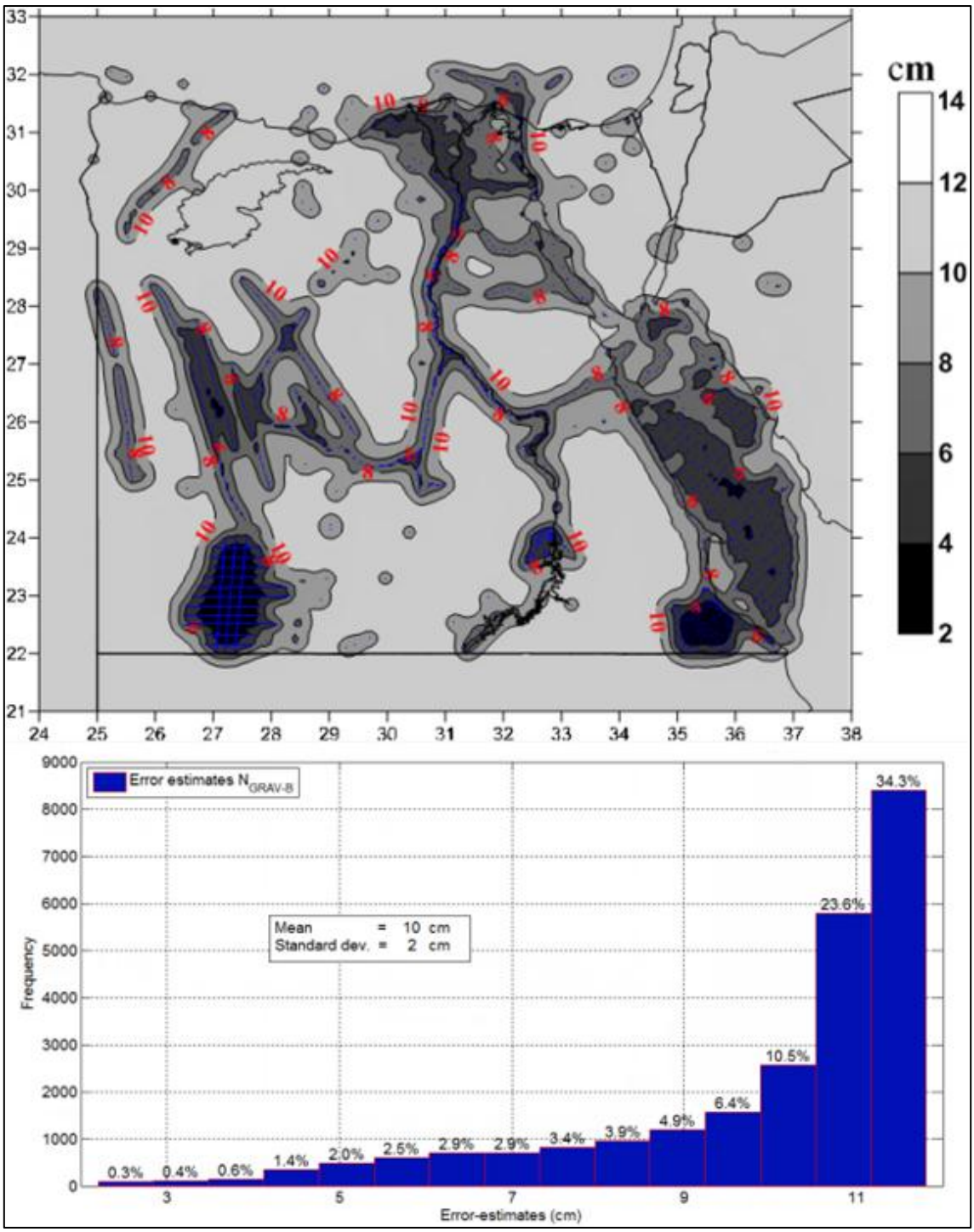

Figure (5.27): Error Estimates of Gravimetric Geoid $N_{\text{GRAV-B}}$

5.4.4 Combined Geoid Solution for Egypt

Now we combined of gravity anomalies Table (5.13) and astrogeodetic data Table (5.14) using 3D LSC for toward high precision geoid determination of Egypt (e.g., Kühtreiber, 2002). The standard error of the deflections components ξ and η were assumed 1.0 arcsec and 1.5 arcsec, respectively, with respect to astronomic and geodetic coordinates. The outcome of these combinations called a combined geoid solution $N_{COMB\text{-}A}$ and $N_{COMB\text{-}B}$ according to both EG1GOC5s and EGTM0818 tailored geopotential models, respectively.

In order to find how the gravimetric fits the combined geoid solution, Figure (5.28) and Figure (5.29) shows the absolute difference between the two solutions.

From Fig. (5.28) and Fig. (5.29), the two geoid solutions are identical within ±5 cm and more than 70 % of the area the agreement is better than ±2 cm. The largest differences occur in the high East/West of Egypt, middle of Egypt and at the components of the deflections of vertical. These largest differences are mostly caused by transforming the geodetic observations of the deflections of vertical from local to global reference system WGS 84. In addition, the lack of deflections of vertical data and the ratio number of deflections to a number of gravity data is very little. Moreover, most of the astrogeodetic data are latitude components of the deflections (Ksi) i.e. in a north-south direction, which further degrades the accuracy of fitted geoids i.e. geoid may be badly distorted.

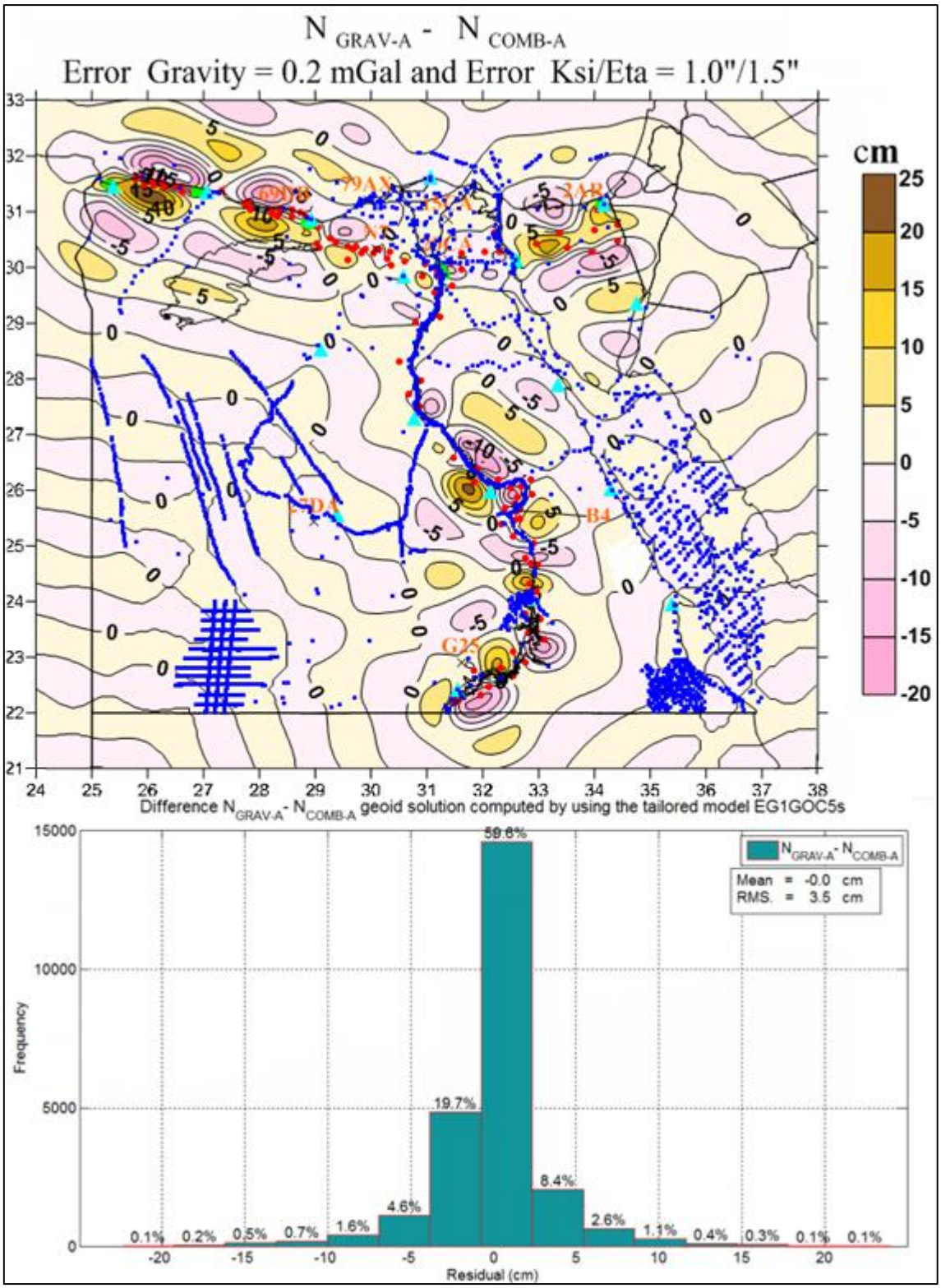

Figure (5.28): Difference Gravimetric minus Combined Geoid Solution Computed by Using Tailored Geopotential Model EG1GOC5s in Remove-Restore Technique. Contour interval 5 cm.

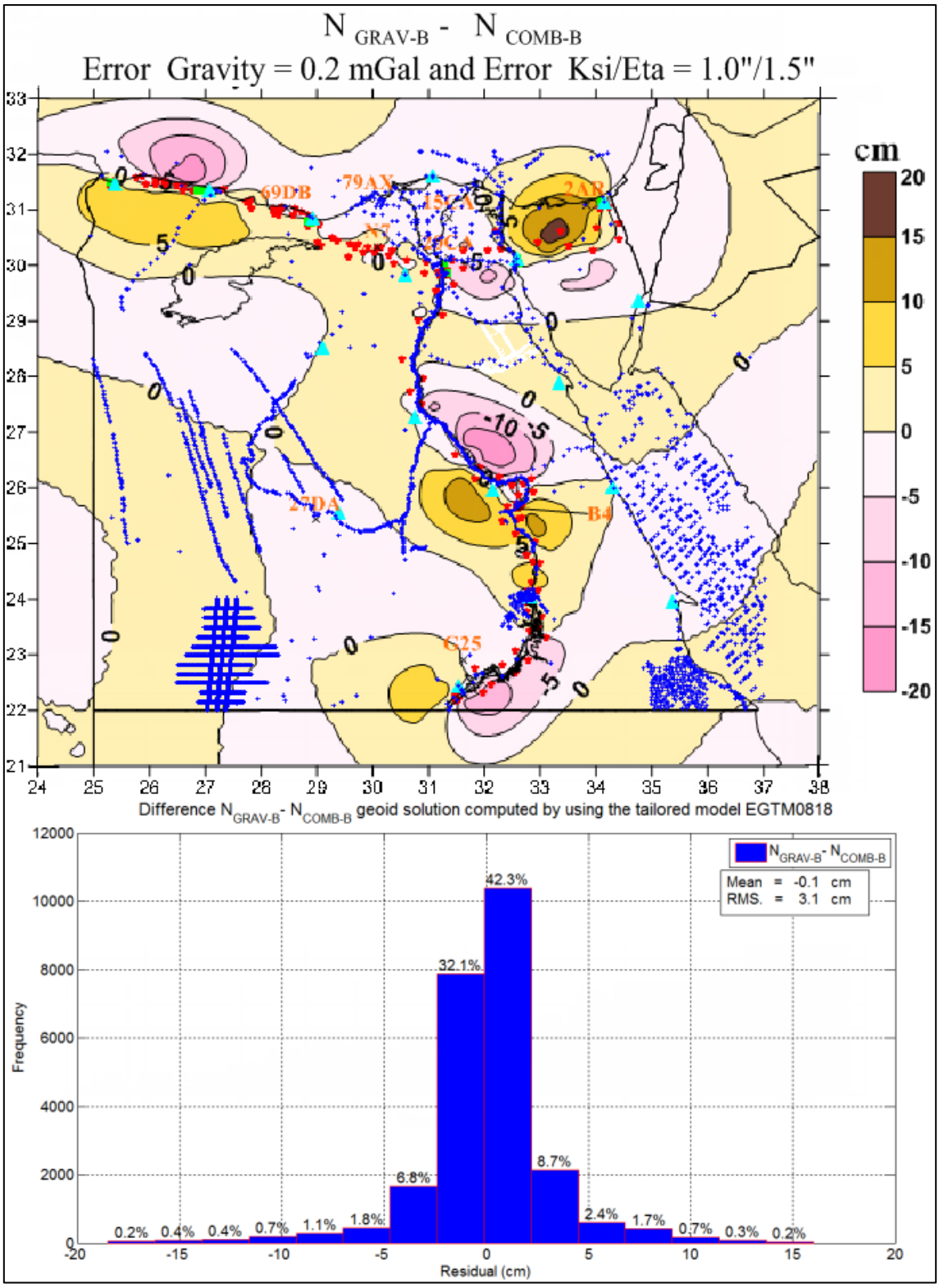

Figure (5.29): Difference Gravimetric minus Combined Geoid Solution Computed by Using Tailored Geopotential Model EGTM0818 in Remove-Restore Technique. Contour interval 5 cm.

Table (5.21) shows the external accuracy of all different combined geoid solutions, after removing trend surface. We have also included a comparison with a gravimetric solution.

Table (5.21): Differences between The Geoid Solutions $N_{\text{GRAV-A}}$, $N_{\text{GRAV-B}}$, $N_{\text{COMB-A}}$ and $N_{\text{COMB-B}}$ to $N_{\text{GPS/Level}}$. Statistics based on 9 Checking Points.

ECAA Stations	Differences Geoid Solutions (External Accuracy)			
	$\Delta N_{\text{GRAV-A}}$	$\Delta N_{\text{GRAV-B}}$	$\Delta N_{\text{COMB-A}}$	$\Delta N_{\text{COMB-B}}$
	m	m	m	m
G25	-0.095	-0.042	-0.098	-0.055
B4	-0.043	-0.276	-0.070	-0.253
27DA	0.170	0.217	0.143	0.213
20CA	-0.121	-0.141	-0.162	-0.189
N7	-0.191	-0.082	-0.209	-0.086
2AR	-0.058	-0.120	-0.068	-0.046
15CA	0.014	0.052	0.015	0.038
79AX	0.173	0.149	0.170	0.139
69DB	-0.156	-0.134	-0.200	-0.143
Mean	**-0.034**	**-0.042**	**-0.053**	**-0.042**
RMS	**0.129**	**0.152**	**0.141**	**0.149**
Range	**0.364**	**0.493**	**0.379**	**0.466**

From Table (5.21), the accuracy of both combined geoids is about the same. In addition, there is no substantial difference in accuracy between the gravimetric and combined geoid solution. Therefore, It can be concluded that the best accuracy is reached for the gravimetric solution using the EG1GOC5s tailored geopotential model, where RMS of differences ± 13 cm.

Finally, in Egyptian territory, so far no official precise geoid model for Egypt that agrees with the Egyptian vertical datum, where it requires a huge effort. Lately, many Egyptian institutes and government authorities have begun cooperating to develop a precise geoid model for Egypt see Dawod (2016) for details.

Chapter 6

CONCLUSIONS AND RECOMMENDATIONS

6. CONCLUSIONS AND RECOMMENDATIONS

6.1 Summary

In this study, satellite-only model GOCO05s versus ultra-high degree reference geopotential model EGM2008 have been tailored to gravity data in Egypt. An integral formulas technique using an iterative algorithm has been used to estimate the harmonic coefficients of the tailored geopotential model to improve the accuracy of the obtained harmonic coefficients and to minimize the residual field.

The Egyptian 5′×5′ mean free-air gravity anomalies, interpolated by Least Squares Collocation (LSC), are used to estimate the harmonic coefficients of the tailored geopotential model GOCO05s denoted as EG1GOC5s complete to degree and order 280. Also, the ultra-high degree reference model EGM2008 was tailored to the maximum degree and order 360. In addition, the higher harmonic coefficients (from n = 361 to n = 2190) of the reference model EGM2008 have then been restored, for increasing the resolution of the tailored model, yielding the EGTM0818 tailored geopotential model complete to degree and order 2190. The results of tailor process show that both EG1GOC5s and EGTM0818 tailored geopotential models, give less, and better residual gravity anomalies than the original models. This reflects that the homogenization of the tailored geopotential models on a local gravity data in Egypt.

The gravimetric and combined geoids solutions for Egypt have been computed using both tailored geopotential models in the remove-restore technique through 3D Least Squares Collocation (3D LSC). The gravimetric and combined solutions are based on gravity data and the combination of gravity with astrogeodetic data, respectively. Furthermore, another solution of geoid models for Egypt has been computed using the

harmonic coefficients of both tailored geopotential models. All geoids solutions have been fitted using only 17 GPS/levelling stations, while 9 GPS/levelling stations were used for an external check.

The results show that the best accuracy is reached when using the tailored geopotential model EG1GOC5s for the gravimetric solution, where it improves the external geoid accuracy by about 15 % compared with the tailored model EGTM0818. In addition, the results of both combined geoids solutions give the same external accuracy.

Finally, the geoid models derived from the spherical harmonic coefficients of both tailored geopotential models give almost the same accuracy, where the RMS of the residuals ± 17 cm for N_{EG1GOC5s} and ± 15 cm for N_{EGTM0818}.

6.2 Conclusions and Major Findings

The major conclusions drawn from the analysis of numerical test results are given below:-

6.2.1 Results of Tailored Models

In this research, satellite-only and high degree geopotential model denoted as GOCO05s and EGM2008, respectively, have been refined to fit the Egyptian gravity field in order to determine the best fit for them that would be considered as a reference model for geoid modeling in Egypt. According to the obtained results of tailor process, the following conclusions could be drawn;

a) The standard deviation of the reduced gravity anomalies to the GOCO05s satellite-only model compared with the EG1GOC5s tailored geopotential model have been decreased from ±11.131 mGal to ± 9.241 mGal, respectively, by about 17%.

b) The EGTM0818 tailored geopotential model has been improved significantly by about 27%, where the standard deviation of the reduced gravity anomalies to reference geopotential model EGM2008 compared with the EGTM0818 model have been decreased from ±10.308 mGal to ± 7.534 mGal, respectively.

c) The comparison between both tailored geopotential models reveals a better accuracy for the EGTM0818 model, where the mean value and the standard deviation of the reduced gravity anomalies to EGTM0818 have decreased by about 96% and 18%, respectively, compared with EG1GOC5s (cf. Table 5.4).

Finally, from the previous analysis, the tailoring process is an efficient way for taking new local gravity data into account when representing local gravity fields if existing GGMs do not appear to fit these data well.

6.2.2 Results of Geoid Models Derived from Tailored Models

The spherical harmonic coefficients of both EG1GOC5s and EGTM0818 tailored geopotential models have been used to create geoid models for Egypt. In addition, the reference model EGM96, complete to degree and order 360, has also been used to compute geoid model for comparison purposes. All geoid models have been fitted to the GPS/levelling station derived geoid by removing a trend surface. According to the obtained results of fitted geoid models, the following conclusions could be drawn;

a) The internal precision of the fitted geoid models by removing a trend surface (cf. Table 5.10), which is derived from the spherical harmonic coefficients of both tailored geopotential models, is very good (where the RMS ± 4 mm for N_{EG1GOC5s} and ± 3 mm for N_{EGTM0818}).

b) The comparison between GPS/levelling derived geoid and the fitted geoid models give almost the same external accuracy, where the RMS of the residuals ± 17 cm for $N_{EG1GOC5s}$, ± 15 cm for $N_{EGTM0818}$ and ± 18 cm for N_{EGM96} (cf. Table 5.11).

c) The results of fitted geoid reflect that the Egyptian gravity data incorporated in the development of the reference geopotential model EGM96 (cf. Fig. 4.5) and both tailored geopotential models.

6.2.3 Results of Gravimetric and Combined Geoid Solutions

Gravimetric and combined (gravity/astrogeodetic data) geoids for Egypt have been computed using both tailored geopotential models in remove-restore technique through 3D LSC. The gravimetric geoids are called N_{GRAV-A} and N_{GRAV-B} were computed by using both EG1GOC5s and EGTM0818 tailored geopotential models, respectively. In addition, the combined geoids solutions are called N_{COMB-A} and N_{COMB-B} were computed based on the combination of gravity and astrogeodetic data using both EG1GOC5s and EGTM0818 tailored geopotential models, respectively. The gravimetric and combined geoids have been fitted to the GPS/levelling derived geoid by removing a trend surface. The major achievements of these solutions are (cf. Table 5.21):

a) The internal precision of the fitted both gravimetric geoids is very good with RMS = ± 4 mm for differences (cf. Table 5.17).

b) The best accuracy is reached when using the EG1GOC5s tailored geopotential model for the gravimetric geoid N_{GRAV-A} , where the RMS and the range of the differences are ± 13 cm and 36 cm, respectively.

c) The comparison between GPS/levelling derived geoid and both $N_{\text{GRAV-A}}$ and $N_{\text{GRAV-B}}$ gravimetric geoids reveal better results for $N_{\text{GRAV-A}}$, where the RMS and the range of the differences have decreased by about 15 % and 26 %, respectively (cf. Table 5.18).

d) The external check for both $N_{\text{COMB-A}}$ and $N_{\text{COMB-B}}$ combined geoids with GPS/levelling points is equal, where the RMS ≈ ± 15 cm for differences (cf. Table 5.18).

Finally, it was believed that the EGTM0818 tailored geopotential model is probably superior; in gravimetric and combined geoids solutions; because of its fits better the Egyptian gravity field than the other tailored geopotential model EG1GOC5s (cf. section 6.2.1). This may be due to the EGM2008 original model does not contain GOCE data (because it has been developed earlier). Furthermore, the EGM2008 reference model is not capable of the representing the high-frequency components of Earth's gravity field. In addition, the error gravity anomaly degree-variances for lower degree portion of EGM2008 (n<180) are larger compare to the satellite-only model GOCO05s (cf. Fig. 2.10), which further degrades the accuracy of covariance function (cf. Eq. 3.58).

6.3 Recommendations

Based on the above-mentioned conclusions, the following recommendations are suggested for future work:-

6.3.1 Gravity Measurements

a) It is recommended to check all datums of all currently available gravity and astrogeodetic data, where this data set has been collected by different organizations and it's likely to be contaminated with several types of errors e.g. datums errors (horizontal, vertical and gravity).

b) Additional gravity observations are recommended for high precision geoid determination of Egypt, where the distributions of the currently available gravity data are very poor and many areas are empty (cf. Fig.4.12). For this reason, these are some of the ways to fill in these gaps are:-

   i. Airborne gravity surveys may suggest to greatly improving the gravity coverage over Egypt, especially in mountainous areas such as plateau al-Gilf al-Kebir and the Sinai Peninsula.

   ii. It is very important that the many Egyptian institutes and government authorities cooperate, in order to facilitate the release of any updated gravity field database, for the encouragement of the geodetic research in Egypt as well as the international organizations, companies, and universities.

   iii. The combination of the observations of three gravity field mapping missions (CHAMP, GRACE, and GOCE) and available gravity data for better gravity field modelling in Egypt.

6.3.2 GPS /levelling Measurements

a) The number of the GPS/levelling stations should be significantly increased for determining a more accurate corrective surface for fitting geoid models to the Egyptian vertical datum, where the distribution of the GPS observations on levelling benchmarks in Egypt is very bad (cf. Fig. 5.15). In addition, these measurements will also contribute to improving the estimation of the accuracy of the future releases of Egyptian geoid models.

b) Practical studies proved that the spacing of the GPS/levelling stations is 50-100 km for best fit geoid (Forsberg & Tscherning 2008, p. 22). Therefore, it is recommended to do so.

6.3.3 Vertical Datum Redefinition

a) It is recommended to redefinition the Egyptian vertical datum by using the recommendations of previous researchers e.g. Saad, A. (1993) and Mohamed, H. F. (2005).
b) Furthermore, according to resolution 16 of the International Association of Geodesy in 1983 (IAG, 1984) endorsed the use of the zero-tide as the preferred tidal system. However, this endorsement has not been adopted in Egypt till now, where the vertical datum of Egypt is a mean- tide system.

6.3.4 Earth Gravity Field Models

a) If future versions of global geopotential models still suffer from the absence of the local Egyptian data, the fitting (or tailoring) principle involved in the current thesis could be carried out, using as much released local data as possible.
b) Several methods of harmonic analysis techniques can be used to estimate the potential coefficients. Hence, a comparison is proposed between the Integral Formulas (Weber & Zomorrodian, 1988), Fast Fourier Transform (Colombo, 1981; Abd-Elmotaal, 2004) and Fast Spherical Collocation (Sanso`& Tscherning, 2003) for choosing the best analysis techniques that minimize the residual field.
c) It is suggested to minimize the residual field from spherical harmonic analysis techniques, by computing the spherical harmonic analysis to a higher degree.
d) All tailored geopotential models in this study, which are fitted to the available Egyptian gravity data, are equally recommended as reference fields for the development of high precision geoid for Egypt.

e) Based on the obtained result of the present research, it is recommended to re-develop the reference geopotential model EGM2008 using complete missions of GOCE data.

f) It is recommended to use the satellite-only models of the GOCO-S series from the Gravity Observation Combination consortium (GOCO, http://www.goco.eu/) for better modelling of the Egyptian gravity field.

REFERENCES

7. REFERENCES

Abd-Elbaky, M.S., (2011). *Tailored High-Degree Geopotential Model for the Egyptian Gravity Field*, (Master Dissertation, M.Sc., Civil Engineering Department, Faculty of Engineering, Minia University, Egypt).

Abd-Elmotaal, H. (2004). An efficient technique for harmonic analysis on a spheroid (ellipsoid and sphere). *VGI*, ***3*(4)**, 126-135.

Abd-Elmotaal, H. (2006). High-Degree Geopotential Model Tailored to Egypt. In *st International Symposium of the International Gravity Field Service (IGFS), Istanbul, Turkey, August*.

Abd-Elmotaal, H. (2008). Gravimetric geoid for Egypt using high-degree tailored reference geopotential model. *NRIAG Journal of Geophysics special issue*, **507-531**.

Abd-Elmotaal, H. (2014). Egyptian geoid using ultra high-degree tailored geopotential model. In *Proceedings of the 25th international federation of surveyors FIG congress, Kuala Lumpur* (pp. 16-21).

Abd-Elmotaal, H. (2015). Egyptian Geoid Using Best Estimated Response of the Earth's Crust due to Topographic Loads. *In IGFS 2014* **(pp. 161-168)**. Springer, Cham.

Abd-Elmotaal, H. , Seitz, K., Abd-Elbaky, M., & Heck, B. (2015). Tailored reference geopotential model for Africa. *In IAG 150 Years (pp. 383-390)*. Springer, Cham.

Abd-Elmotaal, H., Abd-Elbaky, M., Seitz, K., & Heck, B. (2013). Comparison among three harmonic analysis techniques on the sphere and the ellipsoid. *Journal of Applied Geodesy*, ***8*(1)**, 1-20. doi: 10.1515/jag-2013-0008

Al-Krargy, E., (2016). *Development of a national geoid for Egypt using recent surveying data*, (Doctoral Dissertation, Ph. D., Department of Civil Engineering, Faculty of Engineering in Shebin El-Kom, Menoufia University, Egypt).

Alnaggar, D. (1986). *Determination of the geoid in Egypt using heterogeneous geodetic data* (Doctoral Dissertation, Ph. D., Cairo University, Egypt).

Amin, M. M. (2002). Evaluation of Some Recent High Degree Geopotential Harmonic Models in Egypt. *Port-Said Engineering Research Journal PSERJ, Published by Faculty of Engineering, Suez Canal University, Port-Said, Egypt*, ***6*(2)**, 442-458.

Amin, M. M., El-Fatairy, S. M., & Hassouna, R. M. (2003). Two techniques of tailoring a global harmonic model: operational versus model approach applied to the Egyptian territory. *Port-Said Engineering Research Journal PSERJ, Published by Faculty of Engineering, Suez Canal University, Port-Said, Egypt*, ***7*(2)**, 559-571.

Amin, M. M., El-Fatairy, S. M., & Hassouna, R. M. (2005). A precise geoidal map of the southern part of Egypt by collocation: Toshka geoid. In *FIG Working Week 2005 and GSDI-8 Conf., International* Federation of Surveyors, Cairo, Egypt.

Arabelos, D. N., & Tscherning, C. C. (2010). A comparison of recent Earth gravitational models with emphasis on their contribution in refining the gravity and geoid at continental or regional scale. *Journal of Geodesy*, *84*(11), 643-660. doi: http://doi.org/10.1007/s00190-010-0397-z

Balasubramania, N. (1994). Definition and realization of a global vertical datum (Doctoral Dissertation, Ph. D., Department of Geodetic Science and Surveying, Ohio State University, Columbus, USA).

Balmino, G., Sabadini, R., Tscherning, C. C., & Woodworth, P. (1999). Conceptes modernes, objectifs et projects satellitaires pour la determination et ltilisation du champ de gravite terrestre. Tutorial, Bureau Gravimetrique Internationale, Toulouse.

Bašić, T., Denker, H., Knudsen, P., Solheim, D., & Torge, W. (1990). A new geopotential model tailored to gravity data in Europe. In *Gravity, Gradiometry and Gravimetry* (pp. 109-118). Springer, New York, NY.

Bolbol, S. & Saad, A. (2017). Airports Project (Personal Communication, Faculty of Engineering - Shoubra, Surveying Engineering Department, Benha University, Cairo, Egypt)

Bolkas, D., Fotopoulos, G., & Braun, A. (2016). On the impact of airborne gravity data to fused gravity field models. Journal of Geodesy, **90(6)**, 561-571

Bruns, H. (1878). Die Figur der Erde. Publikation des Koniglichen Preussischen Geodetischen Institutes, Berlin.

Cole, J., (1939). Revision of first order levelling Lower Egypt. Survey Department Paper No. 44, Egyptian Survey Authority, Giza, Egypt.

Cole, J., (1944). Geodesy in Egypt, Government Press, Cairo, Egypt.

Colombo, O. L. (1981). *Numerical methods for harmonic analysis on the sphere* **(No. DGS-310)**. OHIO STATE UNIV COLUMBUS DEPT OF GEODETIC SCIENCE AND SURVEYING.

Dawod, G. (1998). *A national gravity standardization network for Egypt* (Doctoral Dissertation, Ph. D., Shoubra Faculty of Engineering, Banha Branch, Zagazig University, Cairo, Egypt).

Dawod, G. (2016). *Towards The Establishment of a Precise Geoid Model for Egypt*. [*Video*] The National Water Research Center (NWRC) Conference on: Research and Technology Development for Sustainable Water Resources Management, Cairo, Egypt. December 4-6. Available at: https://www.youtube.com/watch?v=vpImunwoWGI

Denker, H., & Torge, W. (1998). The European gravimetric quasigeoid EGG97-An IAG supported continental enterprise. In *Geodesy on the move* (pp. 249-254). Springer, Berlin, Heidelberg.

Dimitrijevich, I., (1987). WGS84 Ellipsoidal Gravity Formula and Gravity Anomaly Conversion Equations, Defense Mapping Agency Aerospace Center, 1987.

Ekman, M. (1989). Impacts of geodynamic phenomena on systems for height and gravity. *Journal of Geodesy*, *63*(3), 281-296.

El-Ashquer, M., (2017). *An Improved Habrid Local Geoid model for Egypt*, (Doctoral Dissertation, Ph. D., constructon Eng.&utilites Dep., Faculty of Engineering, Zagazig University, Egypt).

El-Ashquer, M., Elsaka, B., & El-Fiky, G. (2016). On the accuracy assessment of the latest releases of GOCE satellite-based geopotential models with EGM2008 and terrestrial GPS/levelling and gravity data over Egypt. International Journal of Geosciences, 7(11), 1323.

El-Shazly, A.H. (1995). *Towards the Redefinition of the vertical Datum of Egypt: an Analysis of Sea Surface Topography and Levelling by GPS*, (Doctoral Dissertation, Ph. D., Cairo University, Egypt).

El-Tokhey, M. E. (2000). On the Determination of Consistent Transformation Parameters between GPS and the Egyptian Geodetic Reference System. Gravity, Geoid and Geodynamics (GGG2000), Banff, Alberta, Canada.

El-Tokhy, M. E. (1993). *Towards the redefinition of the Egyptian geodetic control networks: geoid and best-fitting reference ellipsoid by combination of heterogeneous data* (Doctoral Dissertation, Ph. D., Ain-Shams University, Cairo, Egypt).

Fairhead, J. D., & Watts, A. B. (1989). The African gravity project: academic, government and commercial data integrated for new map of continent and margins. *Lamont newsletter, summer/1989, Vol 21:6-7, Columbia University.*

Fairhead, J. D., Misener, J. D., Green, C. M., Bainbridge, G., & Reford, S. W. (1997). Large scale compilation of magnetic, gravity, radiometric and electromagnetic data: the new exploration strategy for the 90s. In *Proceedings of Exploration* (Vol. 97, pp. 805-816).

Fashir, H. H., & Kadir, A. M. A. (1998). Gravity Prediction from Anomaly Degree Variances. *Buletin Geoinformasi*, *2*(2), 230-240.

Featherstone, W. E. (2002). Expected contributions of dedicated satellite gravity field missions to regional geoid determination with some examples from Australia. *Journal of Geospatial Engineering*, *4*(1), 1-20.

Featherstone, W. E., & Olliver, J. G. (2001). A review of geoid models over the British Isles: progress and proposals. *Survey Review*, *36*(280), 78-100.

FFG Pty Ltd., (2009). GPS/Gravity Survey, Acquisition and Processing report, Bir Mesaha, Egypt, August 2009, Fugro Ground Geophysics Pty Ltd. JOB NO. G2449

Forsberg, R. (1984). A study of terrain reductions, density anomalies and geophysical inversion methods in gravity field modelling (No. OSU/DGSS-355). Ohio State Univ Columbus Dept of Geodetic Science and Surveying.

Forsberg, R., & Kearsley, A. H. W. (1990). Precise gravimetric geoid computations over large regions. *In Developments in Four-Dimensional Geodesy (pp. 65-83). Springer*, Berlin, Heidelberg.

Forsberg, R., & Tscherning, C.C. (2008). An overview manual for the GRAVSOFT geodetic gravity field modelling programs, 2nd edn. Contract report for JUPEM.

Fotopoulos, G. (2003). *An analysis on the optimal combination of geoid, orthometric and ellipsoidal height data* (Doctoral Dissertation, Ph. D., Faculty of Graduate Studies, Department of Geomatics Engineering, University of Calgary, Calgary, Alberta).

Fotopoulos, G., Featherstone, W. E., & Sideris, M. G. (2002). Fitting a gravimetric geoid model to the Australian Height Datum via GPS data. *Gravity and geoid*, 173-178.

Gauss, C. F. (1828). *Bestimmung des Breitenunterschiedes zwischen den Sternwarten von Göttingen und Altona: durch Beobachtungen am Ramsdenschen Zenithsector*. Bei Vandenhoeck und Ruprecht.

Ghanem, E. (2001). GPS-gravimetric geoid determination in Egypt. *Geo-spatial Information Science*, *4*(1), 19-23.

Goad, C. C., Tscherning, C. C., & Chin, M. M. (1984). Gravity empirical covariance values for the continental United States. *Journal of Geophysical Research: Solid Earth*, *89*(B9), 7962-7968.

Gorten, E., & Tealeb, A. (1995). The first part of repeated relative gravimetry in the active zone of Aswan lake, Egypt. *Bulletin NRIAG, B. Geophysics XI*, 255-263.

Hassouna, R. M. (2003). *Modeling of Outer Gravity Field in Egypt using Recent Available Data* (Doctoral Dissertation, Ph. D., Department of Civil Engineering, Faculty of Engineering in Shebin El-Kom, Menoufia University, Egypt).

Heck, B. (1990). An evaluation of some systematic error sources affecting terrestrial gravity anomalies. *Bulletin Géodésique*, ***64*(1)**, 88-108.

Heck, B., & Rummel, R. (1990). Strategies for solving the vertical datum problem using terrestrial and satellite geodetic data. In *Sea Surface Topography and the Geoid* (pp. 116-128). Springer, New York, NY.

Heck, B., & Seitz, K. (1991). *Harmonische Analyse*. Technical Report, Geodetic Institute, University of Karlsruhe.

Heiskanen WA& Vening Meinesz FA (1958). The earth and its gravity field. Mcgraw-Hill Book Company, Inc. New York, Toronto, London.

Heiskanen, W.A., & Moritz, H. (1967). Physical Geodesy. Freeman, San Francisco.

Heuberger, F. (2005). Validation and Quality Analysis of Gravity Field Models“,Masterarbeit Heuberger, Florian, Institute of Navigation and Satellite Geodesy, Graz University of Technology.

Hofmann-Wellenhof, B., & H. Moritz (2005). Physical geodesy, 2nd ed., Springer, Wien.

Holmes, S. A., & Featherstone, W. E. (2002). A unified approach to the Clenshaw summation and the recursive computation of very high degree and order normalised associated Legendre functions. *Journal of Geodesy*, *76*(5), 279-299.

Holmes, S. A., Pavlis, N. K., & Novák, P. (2006). *A Fortran program for very-high-degree harmonic synthesis*. Version 05/01. http://earthinfo. nga.mil/GandG/wgs84/gravitymod/new egm/new egm.html

IAG. (1971). Geodetic Reference System 1967. International Association of Geodesy, Publi. Spéc. n° 3 du Bulletin Géodésique, Paris.

IAG. (1984). IAG Resolution 16, Geodesists Handbook, International Association of Geodesy, *Bulletin Géodésique*, Vol. 58, No. 3, p. 321, doi: 10.1007/BF02519005.

Iliffe, J. C., Ziebart, M., Cross, P. A., Forsberg, R., Strykowski, G., & Tscherning, C. C. (2003). OSGM02: A new model for converting GPS-derived heights to local height datums in Great Britain and Ireland. *Survey Review*, *37*(290), 276-293.

Jiang, Z., & Duquenne, H. (1996). On the combined adjustment of a gravimetrically determined geoid and GPS levelling stations. *Journal of Geodesy*, *70*(8), 505-514.

Kamal, O., (2010). *Collecting and Unifying the Different Satellite Geodetic Networks in Egypt*, (Master Dissertation, M.Sc., Surveying Engineering Department, Shoubra Faculty of Engineering, Benha University, Egypt).

Kamel, H., & Nakhla, A. (1987). The establishment of the national gravity standard base net of Egypt (NGSBN-77). *Journal of geodynamics*, *7*(3-4), 299-305.

Kaula, W. M. (1966). Tests and combination of satellite determinations of the gravity field with gravimetry. *Journal of Geophysical Research*, *71*(22), 5303-5314.

Kearsley, A. H. W., & Forsberg, R. (1990). Tailored geopotential models–Applications and shortcomings. *Manuscripta geodaetica*, *15*, 151-158.

Kenyon, S. C., & Pavlis, N. K. (1996). The development of a global surface gravity data base to be used in the joint DMA/GSFC geopotential model. In *Global Gravity Field and Its Temporal Variations* (pp. 82-91). Springer, Berlin, Heidelberg.

Kirby, J. F., & Featherstone, W. E. (1997). A study of zero-and first-degree terms in geopotential models over Australia. *Geomatics Research Australasia*, 93-108.

Knudsen, P. (1988). *Determination of local empirical covariance functions from residual terrain reduced altimeter data* (No. OSU/DGSS-395). OHIO STATE UNIV COLUMBUS DEPT OF GEODETIC SCIENCE AND SURVEYING.

Kotsakis, C., Katsambalos, K., & Ampatzidis, D. (2012). Estimation of the zero-height geopotential level W_0^L *VD* in a local vertical datum from inversion of co-located GPS, leveling and geoid heights: a case study in the Hellenic islands. *Journal of Geodesy*, *86*(6), 423-439. doi: 10.1007/s00190-011-0530-7

Kühtreiber, N. (2002, August). High precision geoid determination of Austria using heterogeneous data. In Gravity and Geoid 2002, Proceedings of 3rd meeting of the Int. Gravity and Geoid Commision, Thessaloniki, Greece (pp. 144-149).

Leick, A. (1990). "GPS Satellite Surveying", John Wiley & Sons, New York.

Lemoine, F. G., Kenyon, S. C., Factor, J. K., Trimmer, R. G., Pavlis, N. K., Chinn, D. S., ... & Wang, Y. M. (1998). The development of the joint NASA GSFC and the National Imagery and Mapping Agency (NIMA) geopotential model EGM96, TP-1998-206861, NASA Goddard

Li, Y. C., & Sideris, M. G. (1994). Minimization and estimation of geoid undulation errors. *Journal of Geodesy*, ***68*(4)**, 201-219.

Losch, M., & Seufer, V. (2003). How to Compute Geoid Undulations (Geoid Height Relative to a Given Reference Ellipsoid) from Spherical Harmonic Coefficients for Satellite Altimetry Applications.

Lu, Y., Hsu, H. T., & Jiang, F. Z. (2000). The regional geopotential model to degree and order 720 in China. In *Geodesy Beyond 2000* (pp. 143-148). Springer, Berlin, Heidelberg.

Mäkinen, J., & Ihde, J. (2009). The permanent tide in height systems. In *Observing our changing earth* (pp. 81-87). Springer, Berlin, Heidelberg.

Mayer-Gürr, T., Pail, R., Gruber, T., Fecher, T., Rexer, M., Schuh, W.-D., Kusche, J., Brockmann, J.-M., Rieser, D., Zehentner, N., Kvas, A., Klinger, B., Baur, O., Höck, E., Krauss, S., & Jäggi, A. (2015). The combined satellite gravity field model GOCO05s. *Presentation at EGU 2015*, Vienna, April 2015

McCarthy, D. D., & Petit, G. (2004). *IERS conventions (2003)*. International Earth Rotation and Reference Systems Service (IERS) (Germany).

Meissl, P. (1971). *A study of covariance functions related to the earth's disturbing potential*. Columbus: Ohio State University.

Melbourne, W., Anderle, R., Feissel, M., King, R., McCarthy, D., Smith, D., ... & Vicente, R. (1983). Project MERIT standards. *US Naval Observatory Circulars*, *167*.

Melchior, P (1983). The tides of the planet Earth, *Pergamon Press Oxford, England.*

Melchior, P. (1974). Earth tides. *Geophysical surveys*, *1*(3), 275-303.

Merry, C. L. (2003). The African geoid project and its relevance to the unification of African vertical reference frames. In *2nd FIG Regional Conference, Marrakech, Morocco*.

Merry, C. L., Blitzkow, D., Abd-Elmotaal, H., Fashir, H. H., John, S., Podmore, F., & Fairhead, J. D. (2005). A preliminary geoid model for Africa. In *A Window on the Future of Geodesy* (pp. 374-379). Springer, Berlin, Heidelberg.

Mohamed, H. F. (2005). *Realization and Redefinition of the Egyptian Vertical Datum Based on Recent Heterogeneous Observations*,(Doctoral Dissertation, Ph. D., Surveying Engineering Department, Faculty of Engineering at Shoubra, Zagazig University, Egypt).

Molodenskii, M. S.,Eremeev V.F.&Yurkina M.I. (1962). Methods for study of the external gravitational field and figure of the Earth. *Jerusalem, Israel Program for Scientific Translations*,Jerusalem (Russian original 1960).

Morelli, C., Gantar, C., McConnell, R. K., Szabo, B., & Uotila, U. (1972). *The International Gravity Standardization Net 1971 (IGSN 71)*. Osservatorio Geofisico Sperimentale, Paris, France.

Moritz, H. (1968). On the use of the terrain correction in solving Molodensky's problem (No. DSG-108). OHIO STATE UNIV COLUMBUS DEPT OF GEODETIC SCIENCE.

Moritz, H. (1980). Advanced Physical Geodesy, Herbert Wichmann Verlag, Karlsruhe

Moritz, H. (1990). The figure of the Earth: theoretical geodesy and the Earth's interior. *Karlsruhe: Wichmann, c1990.*

Nahavandchi, H., & Sjöberg, L. E. (2001). Precise geoid determination over Sweden using the Stokes–Helmert method and improved topographic corrections. *Journal of Geodesy*, *75*(2-3), 74-88.

Nassar, M., (1981). Comparative study of rigorous and approximate step-wise techniques of adjusting first-order levelling nets, Scientific Society for Civil Engineering, Al-Azhar University, Cairo, Egypt.

Nassar, M., El-Maghraby, M., El-Tokhey, M., & Issa, M. (2000). Development of a New Geoid Model for Egypt (ASU2000 Geoid) Based on the ESA High Accuracy Reference Network (HARN). *Scientific Engineering Bulletin*, Faculty of Engineering, Ain Shams University, **35(4)**

Nassar, M., Hanafy, M., & El-Tokhey, M. (1993). The 1993 Ain Shams university (ASU93) geoid solutions for Egypt. In *Proceeding of Al-Azhar Third Conference (AEIC), held in Cairo, Egypt*. Sept. 18-21, Volume 4, pp. 395-407.

Nassar, M., Shaker, A., & El-Sayed, M., (1997). Sea surface topography for the Red Sea the eastern part of the Mediterranean Sea based on ERS-1 satellite altimetry data analysis, *Proceedings of Al-Azhar engineering fifth international conference,* Cairo, Egypt, December 19-22.

NIMA. (2004). Department of Defense World Geodetic System 1984. Its Definition and Relationships with Local Geodetic Systems, third Edition, January 3, 2000. United States. National Imagery and Mapping Agency, Technical Report TR8350.2

Paul, M. K. (1978). Recurrence relations for integrals of associated Legendre functions. *Bulletin Geodesique*, *52*(3), 177-190.

Pavlis, N. K., Factor, J. K., & Holmes, S. A. (2007). Terrain-related gravimetric quantities computed for the next EGM. In *Proceedings of the 1st international symposium of the international gravity field service* (Vol. 18, pp. 318-323).

Pavlis, N. K., Holmes, S. A., Kenyon, S. C., & Factor, J. K. (2012). The development and evaluation of the Earth Gravitational Model 2008 (EGM2008). *Journal of Geophysical Research: Solid Earth*, *117***(B4)**.

Petit, G., & Luzum, B. (2010). *IERS Conventions 2010, IERS Technical Note; 36, Frankfurt am Main: Verlag des Bundesamts für Kartographie und Geodäsie*. ISBN 3-89888-989-6.

Pinon, D. (2016). *Development of a precise gravimetric geoid model for Argentina*, (Master Dissertation, M.Sc., School of Mathematical and Geospatial Sciences, College of Science Engineering and Health,, RMIT University, Melbourne, Victoria, Australia).

Poutanen, M., Vermeer, M., & Mäkinen, J. (1996). The permanent tide in GPS positioning. *Journal of Geodesy*, *70*(8), 499-504.

Pugh, D. T. (1987). Tides, surges and mean sea-level: a handbook for engineers and scientists, John Wiley and Sons, Chichester, United Kingdom, 472 pp.

Rapp, R. H. (1967). Analytical and numerical differences between two methods for the combination of gravimetric and satellite data. *Bollettino di geofisica teorica ed applicata*, *11*(41-42), 108-118.

Rapp, R. H. (1977a). The relationship between mean anomaly block sizes and spherical harmonic representations. *Journal of Geophysical Research*, *82*(33), 5360-5364.

Rapp, R. H. (1977b). *Potential Coefficient Determinations from 5 [degree] Terrestrial Gravity Data*. Ohio State University, Research Foundation. Report No. 251

Rapp, R. H. (1982). *A Fortran program for the computation of gravimetric quantities from high degree spherical harmonic expansions* (No. DGS-334). OHIO STATE UNIV COLUMBUS DEPT OF GEODETIC SCIENCE AND SURVEYING.

Rapp, R. H. (1995). A world vertical datum proposal. *Allgemeine Vermessungs-Nachrichten*, *102*(8-9), 297-304.

Rapp, R. H. (1997). Use of potential coefficient models for geoid undulation determinations using a spherical harmonic representation of the height anomaly/geoid undulation difference. *Journal of Geodesy*, *71*(5), 282-289. doi:10.1007/s001900050096

Rapp, R. H., Nerem, R. S., Shum, C. K., Klosko, S. M., & Williamson, R. G. (1991). Consideration of permanent tidal deformation in the orbit determination and data analysis for the Topex/Poseidon mission.

Rapp, R.H. (1981). Geometric Geodesy, Volume I (Basic Principles), the Ohio State University, Columbus,

Saad, A. (1993). *Towards the redefinition of the Egyptian vertical control network* (Doctoral Dissertation, Ph. D., Shoubra Faculty of Engineering, ,Banha Branch, Zagazig University, Cairo, Egypt).

Sadiq, M., Tscherning, C. C., & Ahmad, Z. (2009). An estimation of the height system bias parameter N_0 using least squares collocation from observed gravity and GPS-levelling data. Studia Geophysica et Geodaetica, 53(3), 375-388.

Saleh, J., & Pavlis, N. K. (2002). The development and evaluation of the global digital terrain model DTM2002. *Gravity and Geoid*, 207-212.

Saleh, J., Li, X., Wang, Y. M., Roman, D. R., & Smith, D. A. (2013). Error analysis of the NGS'surface gravity database. *Journal of Geodesy*, ***87*(3)**, 203-221.

Sansò, F., & Sideris, M. G. (Eds.). (2013). *Geoid determination: theory and methods*. Springer Science & Business Media.

Sansò, F., & Tscherning, C. C. (2003). Fast spherical collocation: theory and examples. *Journal of Geodesy*, ***77*(1)**, 101-112. doi: 10.1007/s00190-002-0310-5

Shaker, A. (1986). Selected Topics in Geodesy, Part-II. Surveying Department, Zagazig University, Cairo, Egypt

Shaker, A., (1990). Merits of using inner accuracy theory in adjusting first order levelling network, Proceedings of the Third International Symposium on Recent Crustal Movements in Africa, Aswan, Egypt, Dec. 8-16.

Shaker, A., Alnaggar, D., & Saad, A. A. (2000). Unification of the GPS Work in Egypt. In *Towards an Integrated Global Geodetic Observing System (IGGOS)* (pp. 173-176). Springer, Berlin, Heidelberg. doi: 10.1007/978-3-642-59745-9_33.

Shaker, A., Saad, A., & El Sagheer, A. (1997a). Enhancement of the Egyptian gravimetric geoid 1995 using GPS observations. In *Proceedings of the International Symposium on GIS/GPS, Istanbul, Turkey, Sept* (pp. 15-19).

Shaker, A., El Sagheer, A., & Saad, A., (1997b). Which geoid fits Egypt Better?, *Proceedings of the International Symposium on GIS/GPS*, Istanbul, Turkey, Sept. 15-19.

Sharaf El-Din, S., & Rifat, E., (1968). Variation of sea level at Alexandria, The International Hydrographic Review, V. XLV, No. 2, July.

Sideris, M. G., & She, B. B. (1995). A new, high-resolution geoid for Canada and part of the US by the 1D-FFT method. *Journal of Geodesy*, *69*(2), 92-108.

Sjöberg, L.E. (1980). A recurrence relation for the B_n function. Bulletin Géodésique 54:69–72.

Smith, D. A. (1998). There is no such thing as" The" EGM96 geoid: Subtle points on the use of a global geopotential model. *IGeS Bulletin N. 8, Int. Geoid Service*, 17-27.

Smith, D. A., & Milbert, D. G. (1999). The GEOID96 high-resolution geoid height model for the United States. *Journal of Geodesy*, *73*(5), 219-236.

Smith, W. H., & Sandwell, D. T. (1997). Global sea floor topography from satellite altimetry and ship depth soundings. *Science*, *277*(5334), 1956-1962.Space Flight Cent., Washington, D. C.

Torge W., (1989). Gravimetry. W. de Gruyter, Berlin.

Torge, W. (1980). Geodesy. Walter de Gruyter, Berlin, New York.

Torge, W., (1991). Geodesy. Second Edition, de Gruyter, Berlin, pp. 264

Torge,W. (2001). Geodesy. 3rd. ed.,W. de Gruyter, Berlin-NewYork.

Trimmer, R. G., & Manning, D. M. (1996). The altimetry derived gravity anomalies to be used in computing the joint DMA/NASA earth gravity model. In *Global Gravity Field and its temporal Variations* (pp. 71-81). Springer, Berlin, Heidelberg.

Tscherning, C. C. (1974). *A Fortran IV Program for the Determination of the Anomalous Potential Using Stepwise Least Squares Collocation* (No. DGS-212). OHIO STATE UNIV COLUMBUS DEPT OF GEODETIC SCIENCE.

Tscherning, C. C. (1984). The Geodesist's Handbook. *Bull. Géod, 58*(3).

Tscherning, C. C. (2001). Computation of spherical harmonic coefficients and their error estimates using least-squares collocation. *Journal of Geodesy*, ***75*(1)**, 12-18.

Tscherning, C. C. (2001). Computation of spherical harmonic coefficients and their error estimates using least-squares collocation. *Journal of Geodesy*, *75*(1), 12-18.

Tscherning, C. C. (2002). Datum-shift, error-estimation and gross-error detection when using least-squares collocation for geoid determination. *Lecture notes, IGeS Geoid School, Thessaloniki*.

Tscherning, C. C. (2013). Geoid determination by 3D least-squares collocation. In Geoid Determination (pp. 311-336). Springer Berlin Heidelberg.

Tscherning, C. C., & Rapp, R. H. (1974). Closed Covariance Expressions for Gravity Anomalies, Geoid Undulations, and Deflections of the Vertical Implied by Anomaly Degree Variance Models (No. DGS-208). OHIO STATE UNIV COLUMBUS DEPT OF GEODETIC SCIENCE.

Tscherning, C. C., Radwan, A., Tealeb, A. A., Mahmoud, S. M., El-Monum, M. A., Hassan, R., ... & Saker, K. (2001). Local geoid determination combining gravity disturbances and GPS/levelling: a case study in the Lake Nasser area, Aswan, Egypt. *Journal of Geodesy*, *75*(7-8), 343-348.

Tsoulis, D., & Patlakis, K. (2013). A spectral assessment review of current satellite-only and combined Earth gravity models. *Reviews of Geophysics*, *51*(2), 186-243. *doi:10.1002/rog.20012*

Vanicek, P. (1991). Vertical datum and NAVD 88. *Surveying and Land Information Systems*, *51*(2), 83-86.

Vergos, G. S., Tziavos, I. N., & Sideris, M. G. (2006). On the validation of CHAMP-and GRACE-type EGMs and the construction of a combined model. *Geodezja I Kartografia, Geodesy and Cartography*, *55*(3), 115-131.

Weber, G., & Zomorrodian, H. (1988). Regional geopotential model improvement for the Iranian geoid determination. *Journal of Geodesy*, ***62*(2)**, 125-141.

Wenzel, H. G. (1985). Hochaufl¨osende Kugelfunktionsmodelle f¨ur das Gravitationspotential der Erde. *Habilitationsschrift. Wissenschaftliche Arbeiten der Fachrichtung Vermessungswesen der Universit¨at Hannover*. **No. 137**.

Wenzel, H. G. (1998a). Ultra-high degree geopotential model GPM3E97 to degree and order 1800 tailored to Europe. In *nd Continental Workshop on the geoid in Europe, Budapest, Hungary*.

Wenzel, H. G. (1998b). Ultra-high degree geopotential models GPM98A, B and C to degree 1800. In *joint meeting of the International Gravity Commission and International Geoid Commission* (pp. 7-12).

Werner, M. (2001). Shuttle Radar Topography Mission (SRTM): *Mission overview*, Frequenz, 55(3‑4), 75‑79, doi:10.1515/FREQ.2001.55.3-4.75.

Wolf, P. R., & Ghilani, C. D. (2006). Adjustment Computations Spatial Data Analysis. *New Jersey: John Willey & Sons Inc*.

Youssef, M.F. (1970). Ägyptens Beitrag zur Erdmessung, Dissertation submitted for the Degree of Doktor Ingenieur , Fakultät für Bauingenieur- und Vermessungswesen der Universität Karlsruhe, Karlsruhe, Germany.

جامـــــعة بنـــــها
كلية الهندسة بشبرا
قسم هندسة المساحة

تحسين النماذج التوافقية لجهد الجاذبية العالمية لمصر

رسالة مقدمة كجزء من متطلبات الحصول علي درجة الماجستير في
هندسة المساحة و الجيوديسيا

مقدمه من

المهندس/ عبدالرحيم روبي عبدالحميد حسنين

بكالوريوس هندسة المساحة (2011)

إشـــــراف

أ.د/ أحمد عبدالستار شاكر
أستاذ المساحة والجيوديسيا
كلية الهندسة بشبرا
جامعة بنها

أ.م.د/ ماهر محمد محمد أمين
أستاذ مساعد المساحة والجيوديسيا
كلية الهندسة بشبرا
جامعة بنها

د/ ميرفت محمد رفعت
مدرس المساحة والجيوديسيا
كلية الهندسة بشبرا
جامعة بنها

القاهرة – جمهورية مصر العربية

جامـــــعة بنـــــها
كلية الهندسة بشبرا
قسم هندسة المساحة

القبول النهائى للرسالة

تحسين النماذج التوافقية لجهد الجاذبية العالمية لمصر

رســـــــالة مقدمة من
المهندس/ عبدالرحيم روبي عبدالحميد حسنين
بكالوريوس هندسة المساحة (٢٠١١)

كجزء من متطلبات الحصول علي درجة الماجستير في هندسة المساحة تخصص المساحة والجيوديسيا

وقد تمت مناقشة الرسالة والتوصية بالموافقة علي منح درجة الماجستير في هندسة المساحة تخصص المساحة والجيوديسيا من لجنة الممتحنين

أعضاء لجنة الحكم والمناقشة

أ.د / أحمد عبد الستار شاكر — **التوقيع:** .....

أستاذ المساحة والجيوديسيا بكلية الهندسة بشبرا - جامعة بنها

أ.د / محمد الحسيني عبد الخالق الطوخي — **التوقيع:** .....

أستاذ المساحة والجيوديسيا بكلية الهندسة - جامعة عين شمس

أ.د / علي أحمد الصغير سليمان — **التوقيع:** .....

أستاذ المساحة والجيوديسيا بكلية الهندسة بشبرا - جامعة بنها

أ.م.د / ماهر محمد محمد أمين — **التوقيع:** .....

أستاذ مساعد المساحة والجيوديسيا بكلية الهندسة بشبرا - جامعة بنها

تاريخ المناقشة: ٢٠ / ٢ / ٢٠١٨

إهـــــداء

أهدي هذه الرسالة لوالديّ وصديقي العزيز علاء

وزوجتي الغالية رشا و أبنائي ياسين وجنة

الملخص العربي

ملخص رسالة الماجستير المقدمة

لقسم هندسة المساحة

كلية الهندسة بشبرا

جامعة بنها

من المهندس/ عبدالرحيم روبي عبدالحميد حسنين

المعيد بقسم هندسة المساحة – كلية الهندسة بشبرا – جامعة بنها

عنوان الرسالة

" تحسين النماذج التوافقية لجهد الجاذبية العالمية لمصر"

١. مقدمة:

لا تزال شبكات الثوابت الرأسية المصرية (*Egyptian Vertical Control Networks*) محدودة في الوادي والدلتا ، وحالياً إعادة تكثيف وتدعيم هذه الشبكات لكي تمتد لتغطي كل الأراضي المصرية غير عملي إلي حد ما حيث يتطلب ذلك مجهودات ضخمة وتكلفة باهظة وتستغرق وقت طويل جداً. ومع التطور المتزايد للعلوم و التكنولوجيا في هذا العصر كان لابد لشبكات الثوابت الرأسية أن تتأثر بهذا التقدم.

في الوقت الحاضر أتاح النظام العالمي لتحديد المواقع (*GPS*) دقة تصل إلي بضعة سنتيمترات أو أقل ، ولكن الإرتفاعات التي يتم الحصول عليها من هذا النظام مسندة إلي سطح الإلبسويد (*Ellipsoidal Height*) ولتحويلها إلي إرتفاعات أرثومترية (*Orthometric Height*) مسندة إلي المرجع الجيوديسي الرأسي المصري (*Egyptian Vertical Datum*) يحتاج ذلك إلي نموذج جيوئيد دقيق لمصر.

حالياً يمكن إستخدام نماذج الجيوئيد العالمية (*Global Geoid Models*) المستمدة من النماذج التوافقية لجهد الجاذبية العالمي (*Global Geopotential Models*) مع أرصاد نظام تحديد المواقع العالمي/الميزانية (*GPS/levelling*) لحساب و نمذجة سطح الجيوئيد المصري.

٢. موضوع البحث:

الهدف الرئيسي من هذا البحث هو تطوير نموذج جيوئيد جديد عالي الدقة لمصر، وذلك من خلال تحسين أداء النماذج التوافقية لجهد الجاذبية العالمي ، عن طريق عملية تسمي *Tailoring* ، حيث يتم فيها تحسين المعاملات التوافقية (*Harmonic Coefficients*) لنموذج جهد الجاذبية لكي تتناسب مع مجال الجاذبية المصري إعتماداً علي قيم أرصاد الجاذبية المتوفرة في مصر و يسمي ذلك *Harmonic Analysis* وذلك بواسطة الحل التكاملي (*Integral Technique*). ثم يتم إستخدام النماذج المُحسَنة أو المُعَدَّلة (*Tailored Models*) في حساب و نمذجة سطح الجيوئيد لمصر علي النحو الأتي:-

- **<u>الطريقة الأولي</u>** : حساب تعرجات أو تموجات الجيوئيد (*Geoid Undulation*) من المعاملات التوافقية للنماذج المُحسَنة ويسمي ذلك *Harmonic Synthesis*.
- **<u>الطريقة الثانية</u>** : نمذجة سطح الجيوئيد بإستخدام بيانات شذوذ الجاذبية (Δg) أو دمج أرصاد شذوذ الجاذبية مع أرصاد مركبتي زاوية إنحراف الرأسي (ξ and η) ، وهو ما يعرف بنمذجة الجيوئيد بالبيانات الجيوديسية الغير متجانسة ، من خلال تطبيق أسلوب الحذف - الحساب - الإضافة (*Remove-Restore Technique*) بإستخدام النماذج المُحسَنة مع نظرية أقل مجموع لمربعات الأخطاء *Least-Squares Collocation* (LSC) لانها من النظريات التي أثبتت كفاءتها في دمج الأرصاد الغير متجانسة في آن واحد.

٣. منهجية البحث:

لتحقيق هدف البحث تم عمل مقارنة بين تحسين النموذج *GOCO05s* الذي تم تطوير من قبل إتحاد دمج قياسات الجاذبية (*GOCO*) والنموذج المرجعي عالي الدرجة *EGM2008* الصادر من قبل وكالة الإستخبارات الجغرافية الوطنية الأمريكية (*NGA*) ، من أجل إختيار النموذج الأمثل لإستخدامه كمرجع لنمذجة مجال الجاذبية لنموذج سطح الجيوئيد المصري الجديد.

وقد تم إختيار النموذج الأول *GOCO05s* (تقريباً ٧٢ كيلو متر دقة مكانية) لإنه نموذج لا مثيل له بين نماذج أقمار جهد الجاذبية التي يتم الحصول عليها من المركز العالمي لنماذج سطح الأرض (*ICGEM*) حيث يعتبر أفضل نموذج لتمثيل الطول الموجي الطويل والمتوسط والقصير لمجال الجاذبية الأرضية لإنه يحتوي علي جميع بيانات بعثات أقمار الجاذبية الثلاثة وهي *CHAMP*، *GRACE* و *GOCE* بينما تم أختيار النموذج الثاني *EGM2008* (تقريباً ٩ كيلو متر دقة مكانية) لانه يمثل علامة فارقة ونموذجاً جيداً لنمذجة مجال الجاذبية العالمي بين النماذج الأخري، بالإضافة لذلك تم إختياره من قبل (*NGA*) ليكون بديل للنموذج المرجعي القديم *EGM96* وكمرجع لتحليل البيانات التي سيتم الحصول عليها من بعثة القمر *GOCE*.

❖ وجاءت عملية تحسين النماذج كالأتي (راجع القسم 3.5):

أ. حساب الفروقات (*Differences*) بين قيم الجاذبية المحسوبة من المعاملات التوافقية لنماذج جهد الجاذبية السابقة وقيم الجاذبية المصرية المتوفرة بإستخدام المعادلة التالية:

$$\delta \Delta g = \Delta g_{Local} - \Delta g_{Original\ Model}$$

ب. إستخدام الفروقات (خطوة أ) لحساب *Corrections* للمعاملات التوافقية لنموذج جهد الجاذبية بإستخدام الحل التكاملي المعادلة التالية:

$$\begin{Bmatrix} \delta C_{nm} \\ \delta S_{nm} \end{Bmatrix}_{Corrections} = \frac{1}{4\pi} \iint_{\sigma} \frac{r^2}{GM} \left(\frac{r}{a}\right)^n \frac{1}{\beta_n (n-1)} \delta \Delta g \begin{Bmatrix} \cos m\lambda \\ \sin m\lambda \end{Bmatrix} \bar{P}_{nm}(\cos\theta)\, d\sigma$$

ت. يتم إضافة *Corrections* (خطوة ب) الي معاملات نموذج جهد الجاذبية لإعطاء المعاملات النهائية للنموذج المُعَدَّل كالأتي:

$$\begin{Bmatrix} C_{nm} \\ S_{nm} \end{Bmatrix}_{Tailored\ \ Model} = \begin{Bmatrix} C_{nm} \\ S_{nm} \end{Bmatrix}_{Original\ Model} + \begin{Bmatrix} \delta C_{nm} \\ \delta S_{nm} \end{Bmatrix}_{Corrections}$$

ث. يتم تكرار الخطوات السابقة لتحسين دقة المعاملات التوافقية للنموذج المُعَدَّل وبالتالي تقليل نسبة التباين بين قيم الجاذبية المحسوبة من هذه النماذج مع القيم المصرية.

وجاءت النماذج الناتجة من عملية التحسين السابقة هي *EG1GOC5s* و*EGTM0818* طبقاً للنماذج الأصلية *GOCO05s* و*EGM2008* ، علي الترتيب. حيث أن النموذج *EG1GOC5s* مُعَدَّل حتي ٢٨٠ درجة طبقاً للنموذج الاصلي *GOCO05s*. أما النموذج *EGTM0818* مُعَدَّل حتي أقصي درجة ممكنة وهي ٣٦٠ درجة ، ثم تم إستعادة الدرجات التوافقية العليا من ٣٦١ حتي ٢١٩٠ من النموذج الاصلي *EGM2008* لزيادة الدقة المكانية. ثم جاءت عملية حساب/ نمذجة سطح الجيوئيد المصري كالأتي:-

❖ **<u>الطريقة الأولي</u>**: حساب تموجات الجيوئيد بإستخدام المعادلة التالية (راجع القسم 5.3.2):

$$N_{Model} = \zeta + \frac{\Delta g - 0.1119 H}{\bar{\gamma}} H$$

❖ **<u>الطريقة الثانية</u>**: نمذجة الجيوئيد بإستخدام البيانات الغير متجانسة بأسلوب الحذف – الحساب – الإضافة (حيث تم إستخدام النماذج المحسنة فقط في عملية الحذف/الإضافة وتم إستخدام نظرية LSC في عملية الحساب) (راجع القسم 5.4):

وجاءت أسطح الجيوئيد الناتجة بطريقة LSC السابقة علي النحو المبين في الجدول الأتي:

نموذج جهد الجاذبية المُعَدَّل المستخدم في أسلوب " الحذف – الحساب – الإضافة "	البيانات المستخدمة	نوع الجيوئيد
EG1GOC5s	أرصاد شذوذ الجاذبية "Δg" فقط	N_{GRAV-A}
	أرصاد شذوذ الجاذبية "Δg" + مركبتي زاوية إنحراف الرأسي " ξ/η "	N_{COMB-A}
EGTM0818	أرصاد شذوذ الجاذبية "Δg" فقط	N_{GRAV-B}
	أرصاد شذوذ الجاذبية "Δg" + مركبتي زاوية إنحراف الرأسي " ξ/η "	N_{COMB-B}

ونظراً لإختلاف مستوي الصفر للمرجع الرأسي المصري عن مستوي الصفر للمرجع الرأسي العالمي ، فأن كلا المرجعين لا ينطبقوا علي بعض. ولكي يصبح الجيوئيد الناتج من الطريقة الأولي و الثانية منطبق علي المرجع الرأسي المصري يتم ذلك عن ما يُعرف بتحويل المراجع (*Datum Shift*) من خلال المعادلة التالية (راجع القسم 5.3.4):

$$\varepsilon = \Delta X \cos\varphi \cos\lambda + \Delta Y \cos\varphi \sin\lambda + \Delta Z \sin\varphi + RS + \varepsilon'^{\,grid}$$

تم إستخدام ١٧ محطة أرصاد نظام تحديد المواقع العالمي مع أعمال ميزانية دقيقة مسندة علي المرجع الرأسي المصري في عملية تحويل المراجع (*Datum Shift*) ، بينما تم إستخدام ٩ محطات (*GPS/levelling*) لتحديد مدي دقة نماذج الجيوئيد بعد عملية التحويل ، بالأضافة لذلك تم إستخدام نموذج الجيوئيد العالمي *EGM96* لأعمال المقارنة ، نظراً لأنه يحتوي عن مصر علي بيانات جاذبية أرضية (راجع القسم 4.2.3).

٤. محتويات أبواب الرسالة:-

تحتوي هذه الرسالة علي ستة أبواب بيانها كما ما يلي:

<u>الباب الأول:</u>

يعرض هذا الباب مقدمة عامة عن موضوع البحث. بالإضافة لذلك يعرض بإيجاز الدراسات السابقة ، لعملية نمذجة سطح الجيوئيد عن طريق تحسين نماذج جهد الجاذبية علي المستوي العالمي والقاري والإقليمي (المحلي) ، والمتعلقة بموضوع الدراسة. كما يعرض أيضاً أهداف وأهمية هذا البحث بالنسبة لمصر. كما يتضمن الباب أيضاَ منهجية البحث و يلخص محتوى كل باب فى الرسالة.

الباب الثاني:

في هذا الباب تم تعريف قوة الجاذبية الأرضية والمفاهيم الأساسية لمجال جهد الجاذبية الأرضية والمعاملات التوافقية كحل لمعادلة لابلاس. كما يستعرض الأنواع المختلفة لشذوذ الجاذبية وبعض الطرق الإحصائية المستخدمة في تقييم نماذج جهد الجاذبية وأنواع المراجع الرأسية. وعلاوة علي ذلك يعرض هذا الباب بالتفصيل تأثير المد والجزر علي الأرصاد الجيوديسية. كما يصف في النهاية المرجع الجيوديسي الرأسي لمصر وكذلك يعطي نبذة مختصرة عن شبكات الثوابت الراسية المصرية.

الباب الثالث:

يعرض هذا الباب المعادلات الأساسية المستخدمة في حساب عناصر مجال جهد الجاذبية والمعاملات التوافقية لنماذج جهد الجاذبية. كما يشرح بالتفصيل الطريقة المستخدمة في هذا البحث لتحسين أداء النماذج التوافقية لجهد الجاذبية العالمي وهي الحل التكاملي مع التكرار. وكذلك تم عرض الخلفية الرياضية لنظرية أقل مجموع لمربعات الأخطاء (LSC).

الباب الرابع:

يصف هذا الباب البيانات المصرية المتاحة المستخدمة في هذا البحث بالتفصيل وهي بيانات شذوذ الجاذبية وأرصاد مركبتي زاوية إنحراف الرأسي بالإضافة إلي ذلك أرصاد نظام تحديد المواقع العالمي/الميزانية. علاوة علي ذلك بعض نماذج جهد الجاذبية المستخدمة في الرسالة ، كما يصف أيضاً البرامج الأساسية المستخدمة في هذه الدراسة. كما يشرح بالتفصيل كيفية تم التحضير لهذه البيانات قبل أستخدامها.

الباب الخامس:

يحتوي هذا الباب علي الجزء العملي من الرسالة و هو تحسين نماذج جهد الجاذبية العالمية لمصر وكيف تم إستخدامها لنمذجة سطح الجيوئيد المصري. بالإضافة لذلك تم عرض مدي دقة ونتائج عملية تحسين نماذج جهد الجاذبية وكذلك عملية نمذجة الجيوئيد. أيضاً تم عمل التحليل الإحصائي لجميع النتائج.

الباب السادس:

يتضمن هذا الباب ملخص للبحث وأهم النتائج والإستنتاجات المستخلصة من هذه الدراسة و التوصيات المقترحة للحصول علي نتائج أفضل في المستقبل لنموذج الجيوئيد في مصر.

٥. إستنتاجات ونتائج البحث الرئيسية

تم تقسيم نتائج البحث الرئيسية إلي ثلاثة أجزاء: هم نتائج عملية تحسين نماذج جهد الجاذبية لمصر ونتائج عملية حساب تموجات الجيوئيد المصري من المعاملات التوافقية لهذه النماذج وكذلك نتائج عملية نمذجة الجيوئيد المصري بإستخدام البيانات الغير متجانسة. وفيما يلي الإستنتاجات الرئيسية لهذه النتائج:-

أولاً : نتائج تحسين نماذج جهد الجاذبية العالمية لمصر

ووفقاً لنتائج عملية تحسين النماذج، يمكن إستخلاص الإستنتاجات التالية :-

١. الإنحراف المعياري للفرق بين قيم شذوذ الجاذبية المحسوبة من النموذج *GOCO05s* و٦٣١١ نقطة شذوذ جاذبية مصرية هو ± 11.131 مللي جال ، في حين أن قيمته للنموذج المُعَدَّل *EG1GOC5s* هو ± 9.241 مللي جال (أي إنخفض بنسبة 17 %).

٢. النموذج المُعَدَّل *EGTM0818* أظهر تحسن ملحوظ بنسبة 27 % عن النموذج الأصلي *EGM2008* ، حيث تقلص الإنحراف المعياري للفرق بين قيم شذوذ الجاذبية المحسوبة من النموذج *EGM2008* و٦٣١١ نقطة شذوذ جاذبية مصرية من ± 10.308 مللي جال للنموذج *EGM2008* إلي ± 7.534 مللي جال للنموذج *EGTM0818*.

٣. المقارنة بين كلا النموذجين المُعَدَّلين تكشف عن دقة أفضل الي حد ما للنموذج *EGTM0818* ، حيث إنخفض الإنحراف المعياري للفروقات شذوذ الجاذبية بنسبة حوالي ١٨٪ مقارنة بالنموذج المُعَدَّل *EG1GOC5s*.

نستنتج من تحليل النتائج السابقة ، إن النماذج المُعَدَّلة هي وسيلة فعالة لإدخال بيانات الجاذبية المحلية في النماذج التوافقية لجهد الجاذبية العالمي وخاصة إذا لم تظهر هذه النماذج تناسب مع هذه البيانات بشكل جيد.

ثانياً : نتائج حساب تموجات الجيوئيدالمصري المستمدة من المعاملات التوافقية للنماذج المحسنة

ووفقا للنتائج التي تم الحصول عليها من تحويل نماذج الجيوئيد المستمدة من المعاملات التوافقية للنماذج المحسنة الي المرجع الرأسي المصري يمكن إستخلاص الإستنتاجات التالية:

١. الجذر التربيعي لمتوسط مربعات الخطأ (*RMS*) بين تموجات الجيوئيد الناتجة من $N_{EG1GOC5s}$ ، $N_{EGTM0818}$ ، N_{EGM96} و ٩ محطات أرصاد نظام تحديد المواقع العالمي/الميزانية (*GPS/levelling*) هو ± ١٧ سم ، ± ١٥ سم و± ١٨ سم علي الترتيب.

٢. تعكس النتائج السابقة للجيوئيد أن بيانات الجاذبية المصرية تم إدماجها في تطوير النموذج *EGM96* والنماذج المُحسَنة في هذا البحث.

ثالثاَ : نتائج نمذجة الجيوئيد المصري بطريقة LSC بإستخدام البيانات الغير متجانسة

ووفقا للنتائج التي تم الحصول عليها من نمذجة الجيوئيد بطريقة LSC يمكن إستخلاص الإستنتاجات التالية:-

١. نموذج الجيوئيد N_{GRAV-A} هو الأفضل من حيث الدقة ، حيث كان الجذر التربيعي لمتوسط مربعات الخطأ (*RMS*) و المدي (*Range*) للفروقات " بين تموجات الجيوئيد الناتجة من هذا النموذج و ٩ محطات أرصاد نظام تحديد المواقع العالمي/الميزانية " هما ± ١٣ سم و ٣٦ سم علي الترتيب.

٢. المقارنة بين كلا النموذجين N_{GRAV-A} و N_{GRAV-B} تكشف عن دقة أفضل الي حد ما للنموذج N_{GRAV-A} ، حيث إنخفض *RMS* و *Range* للفروقات بنسبة حوالي ١٥٪ و ٢٦٪ علي الترتيب.

٣. المقارنة بين كلا النموذجين N_{COMB-A} و N_{COMB-B} تعطي تقريباً نفس الدقة حيث كان ال *RMS* للفروقات هو ± ١٥ سم.

نلاحظ من النتائج السابقة أن لا يوجد تباين كبير بين نماذج حلول الجيوئيد المبنية علي أرصاد الجاذبية و نماذج حلول الجيوئيد المبنية علي دمج أرصاد الجاذبية مع أرصاد مركبتي زاوية إنحراف الرأسي، نظراً لإن نسبة عدد أرصاد مركبتي زاوية إنحراف الرأسي لعدد أرصاد الجاذبية قليلة جداً.

كما نلاحظ أيضاً أن النموذج *المُعَدَّل EGTM0818* لم يظهر نتائج أفضل في نمذجة الجيوئيد المصري بطريقة LSC علي الرغم من تناسبه لمجال الجاذبية المصري بشكل أفصل وربما يرجع ذلك للأسباب الأتية:-

- النموذج العالمي *EGM2008* تم تطويره من قبل إطلاق القمر *GOCE* وبذلك لا يحتوي علي بياناته. حيث يعتبر القمر *GOCE* أفضل أقمار الجاذبية لتمثيل الطول الموجي القصير لمجال الجاذبية الأرضية نظراً للإرتفاعه القليل عن مستوي سطح الأرض مقارنة بالأقمار الأخري.

- كما أن دقة المعاملات التوافقية للنموذج *EGM2008* أقل من النموذج *GCOO05s* حتي ١٨٠ درجة (راجع الشكل 2.10) ، وهو ما يوثر علي دقة وظيفة دالة التباين *Covariance Function* (راجع المعادلة 3.58).

٦. توصيات البحث:-

يتطلع العديد من الباحثين المصريين للوصول إلى نموذج جيوئيد دقيق لمصر يتفق مع المسند الرأسي المصري ، لمزيد من المعلومات حول الجهود المبذولة لنمذجة الجيوئيد في مصر يمكن الإطلاع علي هذا الرابط:
https://sites.google.com/site/gomaadawod/geoidofegypt

وحتى الآن لا يوجد نموذج جيوئيد عالي الدقة لمصر، حيث يتطلب ذلك جهداً كبيراً. إلي أن في الآونة الأخيرة ، بدأت العديد من المعاهد والهيئات المصرية علي رأسهم معهد بحوث المساحة تتعاون لإنشاء نموذج جيوئيد دقيق لمصر بالتعاون مع بعض الجامعات المصرية مثل جامعة بنها لمزيد من التفاصيل حول هذا المشروع والجهات المشاركة فيه يمكن الإطلاع علي هذا الرابط:
https://www.youtube.com/watch?v=vpImunwoWGI

إستناداً إلى الإستنتاجات السابقة ، نقترح التوصيات التالية للوصول إلي سطح جيوئيد عالي الدقة لمصر في المستقبل:-

أولاَ: بالنسبة لقياسات الجاذبية

١. نوصي بمراجعة جميع أسطح الإسناد (*Datums*) لبيانات الجاذبية و مركبتي زاوية إنحراف الرأسي الحالية قبل إستخدامها مرة أخري ، حيث تم الحصول عليها من عدة منظمات وهيئات وشركات مختلفة ، ولذلك من المحتمل أن تكون ملوثة بعض الأخطاء علي سبيل المثال أخطاء في المسند الأفقي والرأسي ومسند الجاذبية.
٢. نوصي بزيادة كثافة بيانات الجاذبية وخاصة في المناطق التي تخلو من البيانات حيث أن توزيع بيانات الجاذبية الحالية غير جيد. وفيما يلي بعض المقترحات لملء الفجوات في المناطق التي تخلو من البيانات :-

أ. إستخدام تقنية قياس الجاذبية من الجو (*Airborne gravity*) ،حيث تتميز هذه التقنية بأنها أرخص وأسرع من القياسات الأرضية وتغطي مساحات كبيرة و خاصة في المناطق عالية التضاريس مثل شبه جزيرة سيناء وهضبة الجلف الكبير.
ب. التنسيق مع المنظمات و الشركات والجامعات الدولية والهيئات المحلية لإتاحة أي أرصاد حديثة وفتح قواعد البيانات أمام أبحاث الجيوديسيا في مصر مثل شركة جيتيش (*GETECH*) وجامعة ليدز (*Leeds University*) و المكتب العالمي للجاذبية الأرضية (*BGI*) و مركز المعلومات بالهيئة المصرية العامة للبترول (*EGPC*) و الهيئة المصرية العامة للموارد المعدنية (*EGSMA*) والمعهد القومى للبحوث الفلكية والجيوفيزيقية بحلوان (*NRIAG*) و الهيئة المصرية للطاقة الذرية (*EAEA*).
ت. إستخدام أرصاد بعثات أقمار الجاذبية (*CHAMP، GRACE* و*GOCE*) ودمجها مع بيانات الجاذبية المصرية المتاحة لتحسين نمذجة مجال الجاذبية في مصر.

ثانياَ: بالنسبة لأرصاد نظام تحديد المواقع العالمي/الميزانية الدقيقة

في هذه الدراسة، تم إستخدام ١٧ محطة أرصاد نظام تحديد المواقع العالمي مع أعمال ميزانية دقيقة (*GPS/levelling*) لتحويل المراجع الرأسية العالمية الي المرجع الرأسي المصري بمسافات بينية تقريباً ٢٠٠ كيلو متر مع توزيع غير جيد. ولذلك يوصي بالأتي:-

أ. يوصي بزيادة كثافة محطات أرصاد نظام تحديد المواقع العالمي مع أعمال ميزانية دقيقة.

ب. نوصي بأن المسافات البينية تكون من ٥٠ الي ١٠٠ كيلو متر مع التوزيع الجيد لنقاط (*GPS/levelling*) المستخدمة في لتحويل المراجع الرأسية العالمية الي المرجع الرأسي المصري (Forsberg & Tscherning 2008, p. 22).

ثالثاَ: إعادة تعريف المرجع الرأسي المصري

أ. أخذ توصيات الباحثين السابقين ، مثل أ.د/ عبدالله أحمد سعد (١٩٩٣) و د/ هدي فيصل محمد (٢٠٠٥) ، في ضرورة إعادة تعريف المرجع الرأسي المصري وبالتالي إعادة ضبط الثوابت الرأسية المصرية لتأثيرهما الشديد علي دقة ونمذجة الجيوئيد في المستقبل.

ب. يجب الأخذ في الإعتبار التأثير الغير مباشر الناتج عن المد والجزر علي جميع الأرصاد الجيوداسية المختلفة وكما ينبغي توحيد هذه الأرصاد علي نظام الصفر *Zero-Tide* ووفقاً لتوصيات الأتحاد العالمي للجيوديسيا عام ١٩٨٣ القرار رقم ١٦، ومع ذلك لم يتم إعتماد هذا القرار في مصر حتى الآن.

رابعاَ: النماذج التوافقية لجهد الجاذبية العالمية

بناءاً علي النتائج التي تم الحصول عليها من إستخدام نماذج جهد الجاذبية لنمذجة الجيوئيد لمصر يوصي بالأتي:-

١. يوصي بإستخدام مبدأ التحسين المطبق في هذا البحث، إذا إستمر خلو نماذج جهد الجاذبية من البيانات المصرية في المستقبل (وخاصة في المناطق عالية التضاريس مثل شبه جزيرة سيناء) ، مع الأخذ في الإعتبار إدخال بيانات حديثة ذات كثافة عالية بقدر الإمكان.

٢. يوصي بإستخدام طرق أخري لتحسين دقة المعاملات التوافقية لنماذج جهد الجاذبية مثل:

- *Fast Fourier Transform* (Colombo, 1981; Abd-Elmotaal, 2004).
- *Fast Spherical Collocation* (Sanso`& Tscherning, 2003).

ومقارنتها بطريقة الحل التكاملي (*Integral Technique*) المستخدمة في هذه الدراسة وأختيار أفضل طريقة تقلل نسبة التابين بين قيم الجاذبية المحسوبة من هذه النماذج مع القيم المحلية.

٣. يوصي بحساب قيم المعاملات التوافقية لنماذج جهد الجاذبية حتي أعلي درجة ممكنة.

٤. يوصي بإستخدام النماذج المحسنة في هذا البحث كنماذج مرجعية أثناء نمذجة الجيوئيد المصري في المستقبل.

٥. يوصى بإعادة تطوير النموذج المرجعي *EGM2008* بإضافة بيانات القمر *GOCE* .

٦. يوصي بإستخدام نماذج جهد الجاذبية المنتجة من قبل اتحاد دمج قياسات الجاذبية. (*GOCO*) في المناطق عالية التضاريس ، حيث أظهرت نتائج جيدة.